

Some pages of this thesis may have been removed for copyright restrictions.

If you have discovered material in AURA which is unlawful e.g. breaches copyright, (either yours or that of a third party) or any other law, including but not limited to those relating to patent, trademark, confidentiality, data protection, obscenity, defamation, libel, then please read our [Takedown Policy](#) and [contact the service](#) immediately

**LOW SEVERITY FISCHER-TROPSCH SYNTHESIS FOR THE PRODUCTION
OF SYNTHETIC HYDROCARBON FUELS**

TAMER PANAGIOTIS DOSS

Doctor of Philosophy

Chemical Engineering and Applied Science

ASTON UNIVERSITY

January 2012

© Tamer Panagiotis Doss, 2012

Tamer Panagiotis Doss asserts his moral right to be identified as the author of this thesis

This copy of the thesis has been supplied on condition that anyone who consults it is understood to recognise that its copyright rests with its author and that no quotation from the thesis and no information derived from it may be published without proper acknowledgement.

Aston University

Low Severity Fischer-Tropsch Synthesis for the Production of Synthetic Hydrocarbon Fuels

Tamer Panagiotis Doss

Doctor of Philosophy, 2012

Summary

Currently, the main source for the production of liquid transportation fuels is petroleum, the continued use of which faces many challenges including depleting oil reserves, significant oil price rises, and environmental concerns over global warming which is widely believed to be due to fossil fuel derived CO₂ emissions and other greenhouse gases. In this respect, lignocellulosic or plant biomass is a particularly interesting resource as it is the only renewable source of organic carbon that can be converted into liquid transportation fuels. The gasification of biomass produces syngas which can then be converted into synthetic liquid hydrocarbon fuels by means of the Fischer-Tropsch (FT) synthesis. This process has been widely considered as an attractive option for producing clean liquid hydrocarbon fuels from biomass that have been identified as promising alternatives to conventional fossil fuels like diesel and kerosene. The resulting product composition in FT synthesis is influenced by the type of catalyst and the reaction conditions that are used in the process. One of the issues facing this conversion process is the development of a technology that can be scaled down to match the scattered nature of biomass resources, including lower operating pressures, without compromising liquid composition.

The primary aims of this work were to experimentally explore FT synthesis at low pressures for the purpose of process down-scaling and cost reduction, and to investigate the potential for obtaining an intermediate FT synthetic crude liquid product that can be integrated into existing refineries under the range of process conditions employed. Two different fixed-bed micro-reactors were used for FT synthesis; a 2cm³ reactor at the University of Rio de Janeiro (UFRJ) and a 20cm³ reactor at Aston University. The experimental work firstly involved the selection of a suitable catalyst from three that were available. Secondly, a parameter study was carried out on the 20cm³ reactor using the selected catalyst to investigate the influence of reactor temperature, reactor pressure, space velocity, the H₂/CO molar ratio in the feed syngas and catalyst loading on the reaction performance measured as CO conversion, catalyst stability, product distribution, product yields and liquid hydrocarbon product composition. From this parameter study a set of preferred operating conditions was identified for low pressure FT synthesis.

The three catalysts were characterized using BET, XRD, TPR and SEM. The catalyst selected was an unpromoted Co/Al₂O₃ catalyst. FT synthesis runs on the 20cm³ reactor at Aston were conducted for 48 hours. Permanent gases and light hydrocarbons (C₁-C₅) were analysed in an online GC-TCD/FID at hourly intervals. The liquid hydrocarbons collected were analyzed offline using GC-MS for determination of fuel composition.

The parameter study showed that CO conversion and liquid hydrocarbon yields increase with increasing reactor pressure up to around 8 bar, above which the effect of pressure is small. The parameters that had the most significant influence on CO conversion, product selectivity and liquid hydrocarbon yields were reactor temperature and catalyst loading. The preferred reaction conditions identified for this research were: T = 230°C, P = 10 bar, H₂/CO = 2.0, WHSV = 2.2 h⁻¹, and catalyst loading = 2.0g. Operation in the low range of pressures studied resulted in low CO conversions and liquid hydrocarbon yields, indicating that low pressure BTL-FT operation may not be industrially viable as the trade off in lower CO conversions and once-through liquid hydrocarbon product yields has to be carefully weighed against the potential cost savings resulting from process operation at lower pressures.

Keywords: Biomass-to-liquids (BTL), influence of pressure, FT diesel

To Amber

Acknowledgments

First of all I want to thank GOD, without whom drawing even a single breath is not possible, let alone going through this doctorate degree.

I would like to express my gratitude to my supervisor, Professor Tony Bridgwater, for his valuable guidance and advice, as well as his support throughout this project. I also gratefully acknowledge Supergen Bioenergy II for the financial support provided.

My gratitude and appreciation are also extended to Professor Victor Teixeira da Silva (at the Department of Chemical Engineering at the University of Rio de Janeiro, or UFRJ, in Brazil), without whose advice and assistance this work would not have been possible. I would also like to thank him and his research group (COPPE) for making me feel very welcome and like a member of the group during my research exchange visit to their laboratories and facilities at UFRJ, and generally making my experience in Brazil very pleasant and one that I will always remember.

I would like to also extend my gratitude and appreciation to past and present members of the Bioenergy Research Group at Aston University. I would like to thank Dr John Brammer and Dr James Titiloye for taking the time to see me during my “surprise” visits to their offices and for their valuable advice whenever I needed it. A word of thanks to BERG technician Surila Darbar (a.k.a. ‘Chuck Norris’), whose help in the laboratory with the analytical work is greatly appreciated. Special thanks also to Dr Romani Fahmi and my PhD colleagues, including Antonio ‘Billiardo’ Oliveira, Charles Greenhalf (with whom I shared my office in the CEAC “dungeon”), Angela Fivga, Yianna Dimitriou, Abba Kalgo and Allan Harms for all the good times we’ve had together, the great scientific (and non-scientific!) conversations, their advice and help in the laboratory, as well as their moral support and encouragement when things were looking gloomy at times.

I am in deep gratitude to my family in Greece, my ‘in-law’ family in North Wales, as well as my church family at “Bethel” in Birmingham for their love and support through this degree. Last but definitely never, ever least I wish to express my love and gratitude to my wife, Amber, to whom I have also dedicated this thesis, for her understanding, support, encouragement, patience, (and the list could go on...) during this work!

The Unknown God

“I perceive that in all things you are very religious, for as I passed by and beheld your devotions, I found an altar with this inscription: TO THE UNKNOWN GOD. Whom therefore you ignorantly worship, Him declare I unto you.

God that made the world and all things therein, seeing that he is Lord of heaven and earth, does not dwell in temples made with hands. Neither is worshipped with men's hands, as though he needed any thing, seeing he gives to all life, and breath, and all things. He has made of one blood all nations of men for to dwell on all the face of the earth, and has determined the times before appointed, and the bounds of their habitation; that they should seek the Lord, if haply they might feel after him, and find him, though he is not far from every one of us. For in him we live, and move, and have our being; as certain also of your own poets have said, ‘for we are also His offspring’.

Forasmuch then as we are the offspring of God, we ought not to think that the Godhead is like unto gold, or silver, or stone, graven by art and man's device. The times of this ignorance God overlooked; but now commands all men every where to repent, because he has appointed a day, in which he will judge the world in righteousness by that Man whom He has ordained; whereof He has given assurance unto all men, in that he has raised Him from the dead.”

The Apostle Paul's address to the people of Athens

(Acts 17:22-31, the Holy Bible)

List of Contents

Summary.....	2
Acknowledgments	4
Table of Contents.....	6
List of Figures.....	11
List of Tables.....	14
1 INTRODUCTION.....	15
1.1 Background.....	15
1.2 BTL via FT Synthesis	15
1.3 Project Aims and Objectives	17
1.4 Structure of the Thesis.....	17
2 LITERATURE REVIEW ON FISCHER-TROPSCH SYNTHESIS	19
2.1 Introduction	19
2.2 Theoretical Background	20
2.2.1 Reaction Mechanism	21
2.2.2 Operating Modes	23
2.2.3 Product Characteristics	24
2.3 Product Distribution	25
2.4 Influence of FT Catalysts on the Product Distribution.....	26
2.4.1 Iron Catalysts	27
2.4.2 Cobalt Catalysts	28
2.4.3 Catalyst Deactivation	29
2.4.4 Catalysts used in this Project	29
2.5 Influence of Operating Conditions on the Product Distribution	30
2.5.1 Operating Temperature.....	30
2.5.2 Operating Pressure	31
2.5.3 Space Velocity	33
2.5.4 Synthesis Gas Composition (H ₂ /CO Molar Ratio)	35
2.6 Previous Studies on the Influence of Operating Conditions on FT Product Distribution	36
2.6.1 Studies using Iron Catalysts.....	37
2.6.2 Studies Using Cobalt Catalysts	43
2.6.3 Summary of Findings from Parameter Studies found in the Literature.....	50
2.6.4 Research Gaps.....	52
2.7 BTL-FT – Process Technology.....	53
2.7.1 Step 1 – Biomass Pretreatment	55
2.7.2 Step 2 – Gasification	55
2.7.2.1 BTL-FT Gasifiers.....	56
2.7.2.2 Syngas Composition	57
2.7.3 Step 3 – Syngas Cleaning and Conditioning.....	58
2.7.3.1 Syngas Cleaning	58
2.7.3.2 Syngas Conditioning.....	60

2.7.4	Step 4a – FT Synthesis	61
2.7.4.1	HTFT Operation	62
2.7.4.2	LTFT Operation	62
2.7.4.3	Choice of FT Reactor	64
2.7.5	Step 4b – Product Recovery and Upgrading	65
2.7.5.1	C ₁ -C ₄ Fraction	65
2.7.5.2	Naphtha Fraction	65
2.7.5.3	Diesel and Waxes Fraction	66
2.7.6	Step 5 – Optional Power Generation	67
2.8	Status of BTL-FT Processing	67
3	EXPERIMENT PLAN, EQUIPMENT AND METHODOLOGY	69
3.1	Experiment Plan	69
3.1.1	Catalyst Selection Procedure	70
3.1.1.1	Catalyst Characterization	70
3.1.1.2	FT Synthesis Catalyst Screening Tests	71
3.1.2	FT Synthesis Parameter Study	71
3.1.3	Product Analysis	71
3.1.3.1	Online Gas Analysis	71
3.1.3.2	Offline Liquid Analysis	72
3.2	Gases Required	72
3.3	2cm ³ Reactor at UFRJ	72
3.4	20cm ³ Fixed-Bed Reactor System at Aston	73
3.4.1	20cm ³ Reactor Sub-Systems	75
3.4.1.1	Reactant Preparation	76
3.4.1.2	Reactor	76
3.4.1.3	Gas Liquid Separators	77
3.4.1.4	Back Pressure Regulator	77
3.4.1.5	GC Sampling Valve	77
3.4.1.6	Transfer Line	79
3.4.1.7	BTRS Oven	79
3.4.2	20cm ³ Reactor Commissioning	79
3.4.3	20cm ³ Reactor System Limitations	79
3.4.3.1	Nitrogen Flow Rate	80
3.4.3.2	Pneumatic Air Supply	80
3.4.3.3	Reactor Temperature Control	81
3.5	Product Analysis Equipment	81
3.5.1	2cm ³ Reactor Product Analysis at UFRJ	81
3.5.2	20cm ³ Reactor Online Gas Product Analysis at Aston	82
3.5.2.1	Permanent Gas Analyzer Channel	82
3.5.2.2	Light Hydrocarbon Analyzer Channel	83
3.5.2.3	Gas Calibration	83

3.5.2.4	Reactant Conversion and Product Distribution.....	84
3.5.3	20cm ³ Reactor Offline Liquid Product Analysis.....	85
3.5.3.1	Liquid Hydrocarbon Product Analysis.....	85
3.5.3.2	Aqueous Product Analysis	88
3.5.3.3	Liquid Hydrocarbon Calorific Value Determination	88
3.6	Catalyst Characterization Techniques	89
3.6.1	Morphological Studies.....	89
3.6.1.1	Specific Surface Area, Porosity, Particle Size and Bulk Density	89
3.6.1.2	Scanning Electron Microscopy (SEM).....	90
3.6.2	X-Ray Diffraction (XRD).....	90
3.6.3	Temperature Programmed Reduction.....	90
3.6.4	Thermo-Gravimetric Analysis (TGA).....	91
3.7	FT Synthesis Experiment Procedure	91
3.7.1	Stage 1 – Reactor Loading.....	91
3.7.1.1	2cm ³ Reactor Loading.....	92
3.7.1.2	20cm ³ Reactor Loading.....	92
3.7.2	Stage 2 – Catalyst Pre-Treatment.....	93
3.7.2.1	2cm ³ Reactor Catalyst Activation Procedure (UFRJ)	94
3.7.2.2	20cm ³ Reactor Catalyst Activation Procedures (Aston)	94
3.7.3	Stage 3 – FT Synthesis	96
3.7.4	Stage 4 – Product Sampling.....	96
3.7.4.1	2cm ³ Reactor Product Sampling (UFRJ).....	96
3.7.4.2	20cm ³ Reactor Product Sampling (Aston).....	96
4	CATALYST SELECTION	97
4.1	Introduction	97
4.2	Catalyst Characterization.....	98
4.2.1	Catalyst Morphological Studies – Results	98
4.2.2	X-Ray Diffraction Results	99
4.2.2.1	XRD of Co/Al ₂ O ₃ Catalyst.....	100
4.2.2.2	XRD of Co/TiO ₂ Catalyst.....	100
4.2.2.3	XRD of Fe/Al ₂ O ₃ Catalyst.....	101
4.2.3	Catalyst Reducibility – TPR Results	101
4.2.3.1	TPR of Co/Al ₂ O ₃ Catalyst	102
4.2.3.2	TPR of Co/TiO ₂ Catalyst.....	102
4.2.3.3	TPR of Fe/Al ₂ O ₃ Catalyst.....	104
4.3	Catalyst Screening – FT Synthesis Tests.....	104
4.4	Catalyst Screening – 2cm ³ Reactor Tests (at UFRJ)	105
4.4.1	Product Analysis: GC-TCD Results.....	106
4.4.2	Product Analysis: GC-FID Results	106
4.4.2.1	Hydrocarbon Product Composition.....	107
4.5	Catalyst Screening – 20cm ³ Reactor Tests (at Aston)	108

4.5.1	Criteria for Selection of Specific Reaction Conditions	109
4.5.2	Catalyst Activity and Stability	110
4.5.3	Catalyst Product Profile.....	113
4.5.3.1	Product Yields	113
4.5.3.2	Product Selectivity	114
4.5.3.3	Product Physical Characteristics	114
4.5.3.4	Liquid Hydrocarbon Product Composition	115
4.6	Results Summary and Chapter Conclusions	117
5	FT SYNTHESIS PARAMETER STUDY	119
5.1	Introduction	119
5.1.1	Temperature Profile.....	119
5.1.2	Pressure Profile	120
5.1.3	Space Velocity Profile.....	121
5.1.4	H ₂ /CO Molar Ratio Profile	121
5.1.5	Catalyst Loading Profile	122
5.1.6	Experiment Outline and Summary	122
5.2	Performance Criteria for Selection of Preferred Conditions.....	123
5.2.1	CO Conversion and Product Selectivity Criteria	124
5.2.2	Product Yields Criterion	124
5.2.3	Liquid Hydrocarbon Product Composition Criterion.....	124
5.2.4	Catalyst Stability Criterion	125
5.3	Results and Discussion.....	125
5.3.1	Influence of Reactor Temperature.....	125
5.3.1.1	CO Conversion	125
5.3.1.2	CO ₂ Selectivity	127
5.3.1.3	CH ₄ and C ₂ -C ₅ Selectivity	128
5.3.1.4	C ₆₊ Selectivity.....	129
5.3.1.5	Product Yields	131
5.3.1.6	Energy Content and Composition of Liquid Hydrocarbon Products ..	132
5.3.1.7	Catalyst Stability	135
5.3.1.8	Reactor Temperature Selection for Further Experiments	137
5.3.2	Influence of Reactor Pressure	138
5.3.2.1	CO Conversion	138
5.3.2.2	CO ₂ Selectivity	140
5.3.2.3	CH ₄ and C ₂ -C ₅ Selectivity	141
5.3.2.4	C ₆₊ Selectivity.....	144
5.3.2.5	Product Yields	145
5.3.2.6	Energy Content and Composition of Liquid Hydrocarbon Products ..	147
5.3.2.7	Catalyst Stability.....	150
5.3.2.8	Reactor Pressure Selection for Further Experiments	152
5.3.3	Influence of Space Velocity.....	153

5.3.3.1	CO Conversion	153
5.3.3.2	CO ₂ Selectivity	154
5.3.3.3	CH ₄ and C ₂ -C ₅ Selectivity	155
5.3.3.4	C ₆₊ Selectivity	157
5.3.3.5	Product Yields	158
5.3.3.6	Energy Content and Composition of Liquid Hydrocarbon Products ..	160
5.3.3.7	Catalyst Stability	163
5.3.3.8	Space Velocity Selection for Further Experiments	164
5.3.4	Influence of H ₂ /CO Molar Ratio in Syngas	165
5.3.4.1	CO Conversion	165
5.3.4.2	CO ₂ Selectivity	166
5.3.4.3	CH ₄ and C ₂ -C ₅ Selectivity	167
5.3.4.4	C ₆₊ Selectivity	169
5.3.4.5	Product Yields	170
5.3.4.6	Energy Content and Composition of Liquid Hydrocarbon Products ..	172
5.3.4.7	Catalyst Stability	175
5.3.4.8	H ₂ /CO Molar Ratio Selection for Further Experiments	176
5.3.5	Influence of Catalyst Loading	177
5.3.5.1	CO Conversion & Product Selectivity	177
5.3.5.2	Product Yields	178
5.3.5.3	Mass and Energy Balances	179
5.3.5.4	Energy Content and Composition of Liquid Hydrocarbon Products ..	180
5.3.5.5	Catalyst Stability	182
5.3.5.6	Selection of Preferred Catalyst Loading	183
5.3.6	Comparison of Effect of Parameters on Performance Criteria	184
5.3.6.1	CO Conversion Criterion	184
5.3.6.2	Product Selectivity Criterion	185
5.3.6.3	Liquid Hydrocarbons – Yields and Composition Criteria	186
5.3.7	Summary of Results	186
5.4	Economic Impact	188
5.5	Chapter Conclusions	190
6	CONCLUSIONS	192
6.1	Evaluation and Comparison of Available Catalysts	192
6.2	Parameter Study	192
7	RECOMMENDATIONS FOR FUTURE WORK	195
	References	197
	APPENDIX A - Gas Mixtures for Online GC Calibration	208
	APPENDIX B – Scanning Electron Microscopy (SEM) Micrographs	209
	APPENDIX C – Catalyst Preparation Methods	211
	APPENDIX D – GC-MS: Liquid Hydrocarbon Product Analysis Method Development	213
	APPENDIX E – Calculations	215

APPENDIX F – GC/MS Chromatograms of Standard Saturated C ₇ -C ₄₀ Alkane Solution versus FT Liquid Hydrocarbons	219
APPENDIX H – FT Synthesis Experiments Lab Record Sheet	220
APPENDIX I – Publications	222

List of Figures

Figure 2.1 – FT polymerization steps (left) and carbon chain growth and termination sequences (right) (derived from [21, 43, 53])	22
Figure 2.2 – Product distribution as a function of chain growth probability (α)	23
Figure 2.3 – Typical compositions of LTFT and HTFT products (derived from [35])	24
Figure 2.4 – Typical composition of FT cobalt catalysts (A) and iron catalysts (B) (derived from [5, 31, 43, 71])	27
Figure 2.5 – Influence of reactor pressure on FT product yields	32
Figure 2.6 – Influence of reactor pressure on FT mass percentage product composition using a typical cobalt catalyst (adapted from [70])	33
Figure 2.7 - Basic steps in a BTL-FT process	54
Figure 2.8 – HTFT reactors: A) circulating fluidized bed, and B) fixed fluidized bed	62
Figure 2.9 – LTFT reactors: A) multi-tubular fixed bed, and B) slurry phase	63
Figure 3.1 – 2cm ³ fixed-bed reactor (UFRJ, Brazil)	72
Figure 3.2 – Automated 20cm ³ fixed-bed micro-reactor system at Aston	73
Figure 3.3 – 20cm ³ fixed-bed micro-reactor inside open oven chamber	73
Figure 3.4 – Schematic of 20cm ³ automated fixed-bed reactor set-up at Aston	74
Figure 3.5 – Screenshot of software program used for controlling the 20cm ³ fixed-bed reactor at Aston	75
Figure 3.6 – External volumetric flow meter arrangement on 20cm ³ reactor system at Aston	76
Figure 3.7 – OLD GC Sampling Valve connections	78
Figure 3.8 – NEW GC Sampling Valve connections	78
Figure 3.9 – Chromatogram obtained from GC-TCD calibration of permanent gases at Aston	84
Figure 3.10 – Chromatogram obtained from GC-FID calibration of C ₁ -C ₅ hydrocarbon gases at Aston	84
Figure 3.11 – GC-MS chromatogram of standard saturated C ₇ -C ₄₀ alkane solution	87
Figure 3.12 – GC-MS chromatogram: comparison of standard versus liquid hydrocarbon product from FT synthesis test FT4 (at 210°C)	88
Figure 3.13 – Stages in FT experiment procedure	91
Figure 3.14 – 2cm ³ reactor loading method	92
Figure 3.15 – 20cm ³ reactor loading method	93
Figure 4.1 – SEM micrographs of the three catalysts prior to FT synthesis reaction	99
Figure 4.2 – XRD diffractogram of Co/Al ₂ O ₃ catalyst	100
Figure 4.3 - XRD diffractogram of Co/TiO ₂ catalyst	100
Figure 4.4 – XRD diffractogram of Fe/Al ₂ O ₃ catalyst (a) compared to MS library identity patterns for haematite (b) and aluminium oxide (c)	101
Figure 4.5 – TPR spectrum of Co/Al ₂ O ₃ catalyst used in present study	102
Figure 4.6 – TPR spectrum of a Co/TiO ₂ catalyst reported by Li <i>et al.</i> [163]	103
Figure 4.7 – TPR spectrum of Co/TiO ₂ catalyst used in present study	103
Figure 4.8 – TPR spectrum of Fe/Al ₂ O ₃ catalyst used in present study	104
Figure 4.9 –GC-FID chromatogram from 2cm ³ reactor catalyst screening test B2 (using Co/Al ₂ O ₃ at 210°C, 10 bar, WHSV = 7.5 h ⁻¹ , H ₂ /CO = 2.0, and m _{cat} = 0.1g)	107
Figure 4.10 – GC-FID chromatogram from 2cm ³ reactor catalyst screening test B3 (using Fe/Al ₂ O ₃ at 300°C, 10 bar, WHSV = 15 h ⁻¹ , H ₂ /CO = 2.0, and m _{cat} = 0.1g)	107
Figure 4.11 – 2cm ³ reactor catalyst screening tests (B1-B4) performed at UFRJ: composition of hydrocarbon products	108
Figure 4.12 – 20cm ³ reactor catalyst screening tests (FT4-FT6): Total CO conversion	111

Figure 4.13 – 20cm ³ reactor catalyst screening tests (FT4-FT6): Catalyst performance (CO conversion versus time on stream)	112
Figure 4.14 – Chromatogram of liquid hydrocarbon products (Test FT4 using Co/Al ₂ O ₃ at 210°C, 10 bar, H ₂ /CO = 2.0, WHSV = 8.8 h ⁻¹ , and m _{cat} = 0.5g)	115
Figure 4.15 – Chromatogram of liquid hydrocarbon products (Test FT5 using Co/TiO ₂ at 230°C, 10 bar, H ₂ /CO = 2.0, WHSV = 8.8 h ⁻¹ , m _{cat} = 0.5g).....	116
Figure 4.16 – Test FT4 and FT5: Relative composition of liquid hydrocarbon products (at 210°C, 10 bar, H ₂ /CO = 2.0, WHSV = 8.8 h ⁻¹ , and m _{cat} = 0.5g)	116
Figure 5.1 – Influence of reactor temperature on CO conversion in the present study	126
Figure 5.2 – Influence of reactor temperature on CO ₂ selectivity in the present study (at 10 bar, H ₂ /CO = 2.0, WHSV = 8.8 h ⁻¹ , and m _{cat} = 0.5g) in comparison to similar studies by Xu <i>et al.</i> [83] and Das <i>et al.</i> [111]	127
Figure 5.3 – Influence of reactor temperature on CH ₄ selectivity in the present study (at 10 bar, H ₂ /CO = 2.0, WHSV = 8.8 h ⁻¹ , and m _{cat} = 0.5g) in comparison to similar studies by Xu <i>et al.</i> [83], Woo <i>et al.</i> [115], and Das <i>et al.</i> [111]	128
Figure 5.4 – Influence of reactor temperature on C ₂ -C ₅ selectivity in the present study (at 10 bar, H ₂ /CO = 2.0, WHSV = 8.8 h ⁻¹ , and m _{cat} = 0.5g) in comparison to similar studies by Woo <i>et al.</i> [115], de la Osa <i>et al.</i> [89].....	129
Figure 5.5 – Influence of reactor temperature on C ₆₊ selectivity in the present study (at 10 bar, H ₂ /CO = 2.0, WHSV = 8.8 h ⁻¹ , and m _{cat} = 0.5g) in comparison to similar studies by Xu <i>et al.</i> [83], de la Osa <i>et al.</i> [89] and Woo <i>et al.</i> [115]	130
Figure 5.6 – Influence of reactor temperature on the ratio of liquid products to product gases (at 10 bar, H ₂ /CO = 2.0, WHSV = 8.8 h ⁻¹ , and m _{cat} = 0.5g).....	132
Figure 5.7 – FT liquid products collected at the end of experiment FT7	132
Figure 5.8 – GC-MS chromatogram of liquid hydrocarbons collected from temperature profile test FT4 at 210°C	133
Figure 5.9 – GC-MS chromatogram of liquid hydrocarbons collected from temperature profile test FT7 at 230°C	134
Figure 5.10 – GC-MS chromatogram of liquid hydrocarbons collected from temperature profile test FT8 at 250°C	134
Figure 5.11 – Influence of reactor temperature on liquid hydrocarbon product composition (at 10 bar, H ₂ /CO = 2.0, WHSV = 8.8 h ⁻¹ , and m _{cat} = 0.5g).....	135
Figure 5.12 – Influence of reactor temperature on catalyst stability: CO conversion versus time on stream (at 10 bar, H ₂ /CO = 2.0, WHSV = 8.8 h ⁻¹ , and m _{cat} = 0.5g)	136
Figure 5.13 – Influence of reactor pressure on CO conversion in the present study	139
Figure 5.14 – Influence of reactor pressure on CO ₂ selectivity in the present study	141
Figure 5.15 – Influence of reactor pressure on CH ₄ selectivity in the present study	142
Figure 5.16 – Influence of reactor pressure on C ₂ -C ₅ selectivity in the present study.....	142
Figure 5.17 – Influence of reactor pressure on C ₆₊ selectivity in the present study	144
Figure 5.18 – Influence of reactor pressure on the ratio of liquid products to product gases (at 230°C, H ₂ /CO = 2.0, WHSV = 8.8 h ⁻¹ , and m _{cat} = 0.5g)	147
Figure 5.19 – GC-MS chromatogram of liquid hydrocarbons collected from pressure profile test FT10 at 5 bar	148
Figure 5.20 – GC-MS chromatogram of liquid hydrocarbons collected from pressure profile test FT11 at 8 bar	149
Figure 5.21 – GC-MS chromatogram of liquid hydrocarbons collected from pressure profile test FT7 at 10 bar	149
Figure 5.22 – Influence of reactor pressure on liquid hydrocarbon product composition (at 230°C, H ₂ /CO = 2.0, WHSV = 8.8 h ⁻¹ , and m _{cat} = 0.5g)	150
Figure 5.23 – Influence of reactor pressure on catalyst stability: CO conversion versus time on stream (at 230°C, H ₂ /CO = 2.0, WHSV = 8.8 h ⁻¹ , and m _{cat} = 0.5g).....	151
Figure 5.24 – Influence of space velocity on CO conversion in the present study	154
Figure 5.25 – Influence of space velocity on CO ₂ selectivity in the present study.....	155
Figure 5.26 – Influence of space velocity on CH ₄ selectivity in the present study.....	156
Figure 5.27 – Influence of space velocity on C ₂ -C ₅ selectivity in the present study	156
Figure 5.28 – Influence of space velocity on C ₆₊ selectivity in the present study	158

Figure 5.29 – Influence of space velocity on the ratio of liquid products to product gases (at 230°C, 10 bar, H ₂ /CO = 2.0, and m _{cat} = 0.5g).....	160
Figure 5.30 – GC-MS chromatogram of liquid hydrocarbons collected from space velocity profile test FT7 at WHSV = 8.8 h ⁻¹	161
Figure 5.31 – GC-MS chromatogram of liquid hydrocarbons collected from space velocity profile test FT12 at WHSV = 10.5 h ⁻¹	161
Figure 5.32 – GC-MS chromatogram of liquid hydrocarbons collected from space velocity profile test FT13 at WHSV = 11.5 h ⁻¹	162
Figure 5.33 – Influence of space velocity on liquid hydrocarbon product composition (at 230°C, 10 bar, H ₂ /CO = 2.0, and m _{cat} = 0.5g).....	162
Figure 5.34 – Influence of space velocity on catalyst stability: CO conversion versus time on stream (at 230°C, 10 bar, H ₂ /CO = 2.0, and m _{cat} = 0.5g).....	163
Figure 5.35 – Influence of the H ₂ /CO molar ratio on CO conversion in the present study.....	165
Figure 5.36 – Influence of the H ₂ /CO molar ratio on CO ₂ selectivity in the present study.....	166
Figure 5.37 – Influence of the H ₂ /CO molar ratio on CH ₄ selectivity in the present study.....	168
Figure 5.38 – Influence of the H ₂ /CO molar ratio on C ₂ -C ₅ selectivity in the present study.....	168
Figure 5.39 – Influence of the H ₂ /CO molar ratio on C ₆₊ selectivity in the present study.....	169
Figure 5.40 – Influence of the H ₂ /CO molar ratio in the feed syngas on the ratio of liquid products to product gases (at 230°C, 10 bar, WHSV = 8.8 h ⁻¹ , and m _{cat} = 0.5g).....	172
Figure 5.41 – GC-MS chromatogram of liquid hydrocarbons collected from H ₂ /CO molar ratio in the feed syngas profile test FT14 at H ₂ /CO = 1.6.....	173
Figure 5.42 – GC-MS chromatogram of liquid hydrocarbons collected from H ₂ /CO molar ratio in the feed syngas profile test FT15 at H ₂ /CO = 1.8.....	173
Figure 5.43 – GC-MS chromatogram of liquid hydrocarbons collected from H ₂ /CO molar ratio in the feed syngas profile test FT7 at H ₂ /CO = 2.0.....	174
Figure 5.44 – Influence of the H ₂ /CO molar ratio in the feed syngas on liquid hydrocarbon product composition (at 230°C, 10 bar, WHSV = 8.8 h ⁻¹ , and m _{cat} = 0.5g).....	174
Figure 5.45 – Influence of the H ₂ /CO molar ratio in the feed syngas on catalyst stability: CO conversion versus time on stream (at 230°C, 10 bar, WHSV = 8.8 h ⁻¹ , and m _{cat} = 0.5g).....	175
Figure 5.46 – Influence of catalyst loading on the ratio of liquid products to product gases (at 230°C, 10 bar, H ₂ /CO = 2.0, and WHSV = 8.8 h ⁻¹).....	179
Figure 5.47 – GC-MS chromatogram of liquid hydrocarbons collected from catalyst loading profile test FT7 at 0.5g.....	181
Figure 5.48 – GC-MS chromatogram of liquid hydrocarbons collected from catalyst loading profile test FT16 at 2.0g.....	181
Figure 5.49 – Influence of catalyst loading on liquid hydrocarbon product composition (at 230°C, 10 bar, H ₂ /CO = 2.0, and WHSV = 8.8 and 2.2 h ⁻¹ , respectively).....	182
Figure 5.50 – Influence of catalyst loading on catalyst stability: CO conversion versus time on stream (at 230°C, 10 bar, H ₂ /CO = 2.0 and WHSV = 8.8 and 2.2 h ⁻¹ , respectively).....	182
Figure 5.51 – Comparison of influence of parameters investigated on CO conversion.....	184
Figure 5.52 – Comparison of influence of parameters investigated on C ₆₊ selectivity.....	185
Figure 5.53 – Comparison of influence of parameters on liquid hydrocarbon yields.....	186

List of Tables

Table 2.1 – Names used for FT fuels and their equivalent carbon chain lengths	24
Table 2.2 – Comparison of typical FT diesel with standard diesel specifications	25
Table 2.3 – Summary of cited parameter studies using iron-based catalysts	38
Table 2.4 – Summary of cited parameter studies using cobalt-based catalysts	44
Table 2.5 – Problems caused by syngas contaminants and FT contaminant tolerance levels	59
Table 2.6 – Syngas cleaning methods (derived from [8, 125]).....	59
Table 3.1 – 2cm ³ reactor: GC column specifications	81
Table 3.2 – 20cm ³ reactor: online GC column specifications	82
Table 3.3 – GC method used for permanent gases and C ₁ -C ₅ hydrocarbon analysis.....	83
Table 3.4 – GC-MS liquid hydrocarbon analyzer column specifications	85
Table 3.5 – GC method used for C ₇ -C ₄₀ liquid hydrocarbon analysis	86
Table 3.6 – Summary of catalyst pre-treatment procedures followed for catalyst screening test runs on 20cm ³ reactor.....	95
Table 4.1 – Available catalysts: composition and preparation methods	97
Table 4.2 – Results of catalyst morphological studies	98
Table 4.3 – 2cm ³ reactor FT synthesis catalyst screening tests: Reaction conditions	106
Table 4.4 – 20cm ³ reactor FT synthesis catalyst screening tests: Reaction conditions	109
Table 4.5 – 20cm ³ reactor catalyst screening tests (FT4-FT6): Mass balance	113
Table 4.6 – 20cm ³ reactor catalyst screening tests (FT4-FT6): Product selectivities	114
Table 4.7 – 20cm ³ reactor catalyst screening tests: Physical characteristics of liquid and wax products collected	114
Table 5.1 – Parameter study tests: Summary of reaction conditions used in the 20cm ³ reactor.....	123
Table 5.2 – Influence of reactor temperature on FT gas and liquid product yields	131
Table 5.3 – Influence of reactor temperature on the energy content of liquid hydrocarbon products (at 10 bar, H ₂ /CO = 2.0, WHSV = 8.8 h ⁻¹ , and m _{cat} = 0.5g)	133
Table 5.4 – Influence of reactor temperature on the extent of carbon and wax deposition on the catalyst surface (TGA results).....	137
Table 5.5 – Influence of reactor pressure on FT gas and liquid product yields.....	146
Table 5.6 – Influence of reactor pressure on the energy content of liquid hydrocarbon products (at 230°C, H ₂ /CO = 2.0, WHSV = 8.8 h ⁻¹ , and m _{cat} = 0.5g).....	148
Table 5.7 – Influence of reactor pressure on the extent of carbon and wax deposition on the catalyst surface (TGA results)	152
Table 5.8 – Influence of space velocity on FT gas and liquid product yields	159
Table 5.9 – Influence of space velocity on the energy content of liquid hydrocarbon products (at 230°C, 10 bar, H ₂ /CO = 2.0, and m _{cat} = 0.5g)	160
Table 5.10 – Influence of space velocity on the extent of carbon and wax deposition on the catalyst surface (TGA results)	164
Table 5.11 – Influence of the H ₂ /CO molar ratio in the feed syngas on FT gas and liquid product yields (at 230°C, 10 bar, WHSV = 8.8 h ⁻¹ , and m _{cat} = 0.5g).....	171
Table 5.12 – Influence of the H ₂ /CO molar ratio in the feed syngas on the energy content of liquid hydrocarbon products (at 230°C, 10 bar, WHSV = 8.8 h ⁻¹ , and m _{cat} = 0.5g)	172
Table 5.13 – Influence of the H ₂ /CO molar ratio in the syngas on the extent of carbon and wax deposition on the catalyst surface (TGA results).....	176
Table 5.14 – Influence of catalyst loading on CO conversion, product selectivity and energy content of liquid hydrocarbon products (at 230°C, 10 bar, H ₂ /CO = 2.0, and WHSV = 8.8 h ⁻¹)	177
Table 5.15 – Influence of catalyst loading on FT gas and liquid product yields	178
Table 5.16 – Mass and energy balances over 20 cm ³ reactor at Aston	180
Table 5.17 – Influence of catalyst loading on the extent of carbon and wax deposition on the catalyst surface (TGA results)	183
Table 5.18 – Parameter study results	187
Table 5.19 – Parameter study results summary: Influence of increasing reaction parameters on CO conversion, product selectivity and yield of liquid hydrocarbons.....	188

1 Introduction

Fischer-Tropsch (FT) synthesis is an industrially important chemical process that converts synthesis gas or syngas, a mixture of mainly CO and H₂, into a wide spectrum of products, consisting primarily of hydrocarbons that range from C₁-C₆₀₊, as well as oxygenated compounds [1-3]. Historically, coal and natural gas have been used as feedstocks in producing hydrocarbon fuels via FT synthesis. Security of fuel supply and environmental concerns over the past years, however, have driven research in the direction of renewable fuels, where biomass can be used as a substitute to produce synthetic liquid transport fuels by means of the FT synthesis.

1.1 Background

The energy consumed for transportation accounts for a significant, and continuously increasing, proportion of the total global energy demand. Currently, the main source for the production of liquid transportation fuels is petroleum, the supplies of which have been abundant and relatively low-cost [4, 5]. Its continued use, however, faces many challenges. These include depleting oil reserves, which has raised concerns for the security of fuel supply and has led to significant rises in the price of oil (both currently and anticipated for the future), as well as environmental concerns over global warming, the main causes of which are widely believed to be fossil fuel derived CO₂ emissions and other greenhouse gases [6].

In order to meet the increasing demand for transportation fuels, as well as comply with continuously more stringent environmental policies and legislation, alternative sources must be implemented for the purpose of developing more sustainable means of production of fuels and chemicals. This makes lignocellulosic or plant biomass a particularly interesting resource as it is the only renewable source of organic carbon that can be converted into liquid fuels and chemicals (also known as biomass-to-liquids or BTL) [7, 8]. The resulting carbon dioxide emissions from the combustion of biomass fuels are commonly regarded as neutral because carbon dioxide is fixed by photosynthesis in the original plant or tree [9]. As a result, biomass is considered as the only sustainable route to synthetic transport fuels and many organic chemicals [10, 11].

1.2 BTL via FT Synthesis

There are three main routes for the conversion of biomass into liquid biofuels. These include thermal conversion (gasification and pyrolysis), biological conversion (digestion and fermentation) and mechanical extraction (oilseed extraction) [8]. Biological processes can be extremely slow and give specific products such as ethanol, whereas thermal conversion processes are rapid in comparison, offering higher conversion efficiencies, scalability and giving a number of products

[8]. Gasification of biomass produces synthesis gas or syngas, which can be converted into synthetic liquid hydrocarbon fuels by means of the Fischer-Tropsch synthesis. This process has been widely considered as an attractive option for producing clean liquid hydrocarbon fuels from biomass [12, 13]. These synthetic fuels have been identified as promising alternatives to conventional fossil fuels like diesel and kerosene [9, 14-16]. When compared to conventional crude oil derived products, FT liquid fuels have an environmental superiority, because they are free from sulphur, nitrogen and heavy metal contaminants, and have a very low aromatic content resulting in lower engine emissions [17-20]. In addition, FT diesel fuels originating from biomass are compatible with contemporary vehicle engines and can also be used for blending with conventional diesel fuels in any proportion [12]. This means that they can be refined to current fuel standards and specifications in conventional refineries, and are therefore able to offer economies of scale and access to state-of-the-art processing. Moreover, while separate distribution systems may be required for a number of alternative fuels, FT fuels can be easily managed by the existing fuel infrastructure.

However, as FT plants are both capital and energy intensive, the viability of the FT process has been very dependent on crude oil prices, which have gone through dramatic fluctuations over the last three decades (current prices in 2012 exceeding \$100/bbl) [20, 21]. A recent economic study on FT fuel production plants conducted by van Vliet *et al.* [22] in 2009, reported that the production costs of BTL via FT synthesis (or BTL-FT, as it will be referred to in the remainder of the thesis) break even when oil prices rise above \$75/bbl. The steep increase in the price of crude oil, and more importantly, recent environmental legislation demands, have reignited the interest in the well established, century old technology of FT synthesis in recent years [5, 9, 23, 24]. FT synthesis is typically carried out at pressures in the range of 25-60 bar [19, 25]. One way of potentially reducing the capital and operating costs in a BTL-FT process, therefore, is by operation at lower pressures which implies lower expenditure on the energy consumed for gas compression and lower investment costs that are associated with plant equipment operation at higher pressures.

There are currently very few commercial-scale FT plants in existence globally, with main operations by Sasol in South Africa and Qatar, and by Shell in Malaysia and Qatar [26]. These, however, are based on either coal (CTL) or natural gas (GTL) [27-29]. FT synthesis using biomass feedstocks (BTL) is still at a very early stage of development, and to date, there are no industrial-scale FT operations based on biomass [30]. The main hindrances to the application of BTL-FT technology appear to be in the biosyngas clean-up steps and the limitations of economy of scale imposed by the availability and cost of biomass as a feedstock. There are, nonetheless, a number of laboratory scale BTL-FT studies, as well as planned pilot plant studies that aim to commercialize the technology, and these will be discussed in section 2.8. Some of the issues that need to be addressed in developing and implementing BTL-FT technology include the following:

- Developing a technology that can be scaled down to match the scattered nature of biomass resources, including lower operating pressures, without compromising liquid composition.
- Producing a lower specification product for upgrading in conventional refineries.
- Considering the co-production of higher value chemicals such as SNG and C₂-C₄ olefins or the co-production of liquid fuels and electricity.
- Managing the contaminants that are peculiar to biomass derived syngas (or biosyngas) including more tolerant catalysts that can handle alkali metals and tars. The contaminants that are present in biosyngas may or may not be similar to those found in coal or natural gas-derived syngas. Hence, it is this uncertainty in the composition of biosyngas that poses one of the greatest challenges in BTL operations.

1.3 Project Aims and Objectives

In response to some of the above challenges facing BTL-FT technology, the main aims of this project are to:

1. Experimentally explore the de-severetisation of the FT synthesis process for down-scaling and cost reduction.
2. Investigate the potential for obtaining an intermediate FT synthetic crude liquid product that can be integrated into existing refineries under the range of process conditions employed.

The specific objectives of this work are to:

1. Evaluate and compare the standard FT catalysts that are available for this project and determine their suitability both for operation on the fixed-bed micro-reactor system at Aston University and for fulfilment of the main aims of the work, as outlined above.
2. Determine the relationship between the product distribution and yields, and the processing conditions employed in the FT synthesis reaction (syngas composition, operating pressure, operating temperature, space velocity, etc.) using a standard FT catalyst at low pressures (down to 2 bar).
3. Determine a set of operating conditions for low pressure FT synthesis on the fixed-bed micro-reactor at Aston University that would give maximum yields of a lower specification liquid hydrocarbon product. Ideal characteristics of this product would be a high diesel composition, low wax and low naphtha contents, therefore reducing the need for product up-grading operations which are commercially capital intensive to integrate on site.

1.4 Structure of the Thesis

The arrangement of the remaining chapters within this thesis is as follows:

Chapter 2 – Literature Review on Fischer-Tropsch Synthesis: A literature review is carried out in this chapter which encompasses the historical context and the theoretical background of FT

synthesis, including the main FT reactions, the reaction mechanism, FT products and the factors that influence the product composition. Studies in the available literature that have investigated the influence of FT synthesis reaction conditions on the catalyst activity and performance, the product distribution, and the product yield, using standard iron and cobalt-based FT catalysts similar to those used in this project, are critically reviewed. The different steps in BTL-FT processes are also discussed from feedstock to final fuel products, including the various technologies that are employed in FT processing, such as syngas generation, syngas cleaning, syngas conversion, FT reactors, and product recovery and upgrading. In addition, the status of BTL-FT processing is discussed, and recent developments aiming towards the commercialisation of the technology are highlighted.

Chapter 3 – Experiment Plan, Equipment and Methodology: the experiment plan that is followed is presented, and the laboratory equipment that is used for the FT synthesis experiments and product analyses is described. The experimental methodologies and procedures that are followed are also outlined. Fischer-Tropsch synthesis is conducted in two different stainless steel fixed-bed micro-reactors: a 2cm³ reactor at the University of Rio de Janeiro (UFRJ) and a 20cm³ reactor at Aston University. Online analysis of the products is carried out using gas chromatographs equipped with thermal conductivity detectors (TCDs) and flame ionisation detectors (FIDs). Offline analysis of liquid hydrocarbon products from the 20cm³ reactor are analysed on a gas chromatograph equipped with a mass spectrometer (GC-MS).

Chapter 4 – Catalyst Selection: this is the first of two chapters that contain the results of the experimental work that is carried out during this project. The catalyst selection procedure is outlined and the results of the catalyst characterization studies, including BET surface area determination and pore size, XRD, TPR and TGA are presented and discussed. These are followed by the results obtained for the FT synthesis catalyst screening experiments and their discussion.

Chapter 5 – FT Synthesis Parameter Study: this is the second of the two chapters that discuss the results of the experimental work carried out on the 20cm³ reactor at Aston. The details of the FT synthesis parameter study that is carried out are provided, and the results that are obtained for each parameter investigated are presented and discussed. The impact of the results found on process investment costs is also discussed.

Chapter 6 – Conclusions: provides a summary of the major findings of the work carried out and the conclusions that are drawn.

Chapter 7 – Recommendations for Future Work: provides recommendations for future research and development to complement on the work carried out in this project.

2 Literature Review on Fischer-Tropsch Synthesis

The FT process converts syngas into a wide range of hydrocarbons, as well as some oxygenated compounds such as alcohols. The literature review in this chapter encompasses the historical context and the theoretical background of FT synthesis, which includes the main FT reactions, the reaction mechanism, FT products and the factors that influence the product composition. Studies that have investigated the influence of FT synthesis reaction conditions on the catalyst activity and performance, the product distribution, and the product yield, using standard iron and cobalt-based FT catalysts similar to those used in this project, are critically reviewed. The different steps in BTL-FT processes are also discussed from feedstock to final fuel products, including the various technologies that are employed in FT processing, such as syngas generation, syngas cleaning, syngas conversion, FT reactors, and product recovery and upgrading. In addition, the status of BTL-FT processing is discussed, and recent developments aiming towards the commercialisation of the technology are highlighted.

2.1 Introduction

The synthesis reaction was implemented for methane synthesis as early as the beginning of the 1900s. However, it wasn't until the 1920s when the initial major FT work was carried out in Germany by Franz Fischer and Hans Tropsch, who obtained a liquid product that consisted mainly of hydrocarbons [31, 32] from the hydrogenation of CO over iron and cobalt catalysts, leading to their famous patent of the FT synthesis process in 1925 [33]. Their research greatly contributed to the later development of the synthesis process, establishing, for example, that Fe, Co and Ni are the most effective catalysts for producing hydrocarbons (Co being the most active for hydrocarbon production and Ni for methane), that alkali additives or promoters improve liquid hydrocarbon yields, and that sulphur permanently poisons these catalysts [34].

The process was first commercialized in 1936 by Ruhrchemie AG in Germany [31, 35] and the technology became valuable when Germany became isolated due to its war effort, which made it dependent on coal that was readily available in Germany [20, 36]. The technology implemented at the early stages of development after the war, however, was too expensive to compete with crude oil [20], the prices of which were extremely low in the post-war period due to the discovery of the large oil reserves in the Middle East [5, 20, 36]. This led to the minimal interest in FT synthesis during this time period, and development of the process continued almost exclusively at SASOL (South African Synthetic Oil Limited) in South Africa which was formed in 1950 [20, 37]. This

was attributed to the fact that South Africa faced an oil embargo sanctioned by the international community, and relied on its vast coal deposits for the production of liquid fuels and higher value chemicals [37].

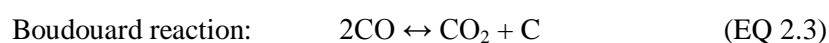
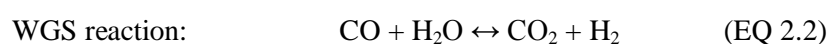
Interest in FT synthesis revived, however, in the 1970s and 1980s due to alarming forecasts at the time about depleting crude oil reserves, as well as international politics which included oil boycotts by major oil producing nations [5]. The attention towards FT processing further increased in the 1990s when it was realised that the technology could be used to take advantage of remotely located sources of natural gas, which would be too expensive to transport in pipelines but could either be liquefied and then transported as liquefied natural gas (LNG) or gasified and processed via FT synthesis to produce synthetic transport fuels [20]. Consequent to this rich history, a wealth of published papers and patents exist, a significant amount of which can be accessed on a recently developed web site sponsored by Syntroleum, Inc., known as the Fischer-Tropsch Archive [38]. This website contains a comprehensive bibliography of FT synthesis literature from as early as the 1920s, holding over 7000 references and citations including journal and conference articles, books, government reports and patents [39, 40]. Today, with continuously depleting oil reserves, and the added factors of environmental concerns, as well as the recent improvements to the technology used in FT processing, the research focus in FT synthesis has turned towards BTL technologies for the production of clean and sustainable synthetic fuels.

2.2 Theoretical Background

Irrespective of the operating conditions used, and contrary to thermodynamic expectations [41, 42], the FT synthesis reaction always yields an array of products consisting mainly of hydrocarbons that range from methane and C_2 compounds to high molecular weight waxes (C_{60+}) [21, 42]. These products can be a mixture of alkanes, alkenes, aromatics, ring compounds and oxygenated compounds [43]. Typically, the oxygenated compounds are comprised of mainly alcohols as well as some acids, ketones and aldehydes [44]. Other products of the reaction include water (which is a primary product of the reaction), and carbon dioxide (which is a secondary product formed via the water gas shift reaction, Equation 2.2 below) [45]. The lower molecular weight oxygenated compounds that are formed during FT synthesis are mainly dissolved in the water phase, those with higher molecular weight are dissolved in the oil or liquid hydrocarbon phase, whereas usually negligible amounts of oxygenated compounds are reported to be present in the wax phase [44]. The composition or distribution of all these products in the mixture varies depending on the type of catalyst that is used as well as the reaction conditions that are implemented. These reaction parameters are discussed in more detail in section 2.5.

The FT synthesis reaction is commonly represented by Equation 2.1 below, and industrially, it takes place over iron or cobalt-based catalysts [20]. The reasons for the choice of these particular catalysts are discussed in detail in section 2.4. Equation 2.1 shows that, stoichiometrically, the FT

synthesis reaction requires two hydrogen molecules to react with one molecule of carbon monoxide, thus requiring a H₂/CO molar ratio of 2.0 in the feed syngas. Equations 2.2 and 2.3 represent the water gas shift (WGS) reaction and the Boudouard reaction, respectively. These are two equilibrium reactions that also take place during FT synthesis and are important as they are responsible for the disproportionation of CO in the reactor and can, therefore, influence the stoichiometry of the FT synthesis reaction. In the WGS reaction, the CO is disproportionated towards the formation of carbon dioxide and hydrogen, whereas in the Boudouard reaction, the carbon product remains on the catalyst surface, and only CO₂ is formed, but no hydrocarbons [46]. Reactions 2.2 and 2.3, therefore, are mainly responsible for high CO₂ selectivities during FT synthesis.



A H₂/CO molar composition ratio of two is usually recommended in the syngas when the reaction takes place over cobalt-based catalysts, whereas lower H₂/CO ratios (in the range of 0.5-1.5) can be used over iron-based catalysts [20]. The reasons for this relate to the different WGS (Equation 2.2) activity of these catalysts and are discussed in more detail in section 2.4. As opposed to cobalt-based catalysts, which display a very low WGS activity, iron-based catalysts exhibit a very high WGS activity, shifting the reaction equilibrium towards the production of hydrogen [43]. This makes it possible for the syngas fed to the FT reactor using iron catalysts to have a H₂/CO ratio lower than two, as this ratio is increased by the WGS reaction [43]. This is important when using biomass as a feedstock, as the H₂/CO ratio in the syngas derived from its gasification is usually low (0.5-1.8) [21, 47].

2.2.1 Reaction Mechanism

There are numerous reaction mechanisms and variations of these mechanisms that have been proposed for the FT synthesis reaction and examples of these can be found in work published by Dry [48], Claeys and van Steen [49], and Davis [50, 51]. Some of the differences have to do with the chain initiation step. A number of these theories support that the CO molecules are adsorbed on to the catalyst surface either by, 1) first dissociating into the individual comprising atoms and then becoming hydrogenated, or 2) becoming directly hydrogenated and then taking part in the chain-growth reaction, or 3) directly taking part in the reaction and then becoming hydrogenated [21]. Despite the differences, what is common between all the proposed mechanisms is the assumption that the carbon chain grows in steps like a polymerisation process [43, 52], and this is depicted in Figure 2.1 below. This figure summarizes the FT mechanism polymerisation steps, and illustrates the different reaction paths that these monomers can follow.

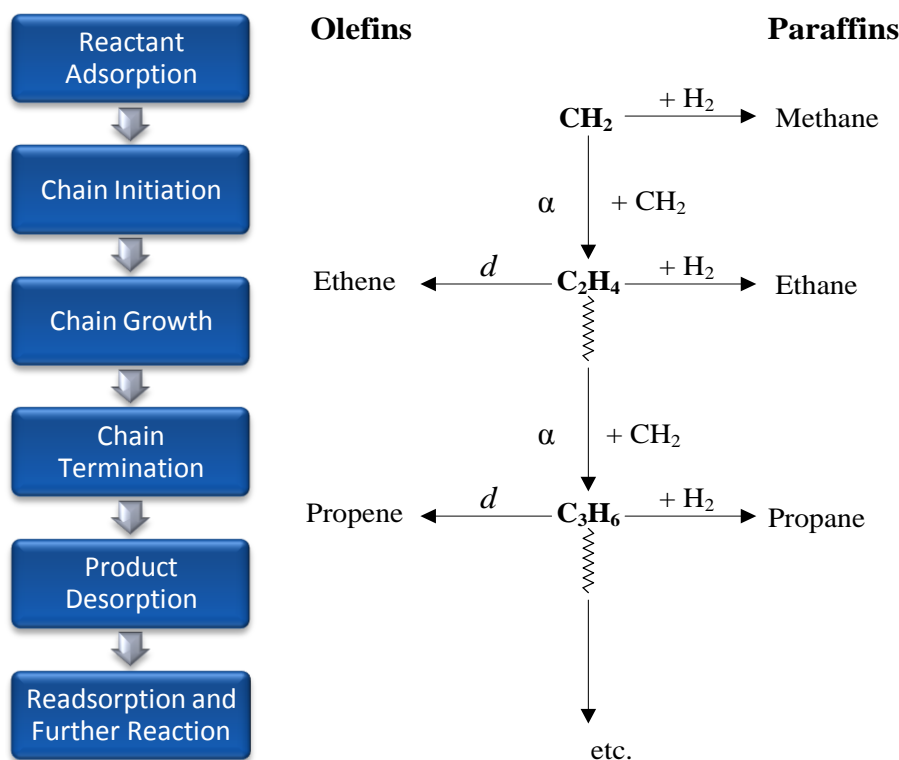


Figure 2.1 – FT polymerization steps (left) and carbon chain growth and termination sequences (right) (derived from [21, 43, 53])

The monomers, or basic building blocks, in this process are presumed to be $-\text{CH}_2-$ units [52]. For these units to form, the CO molecules in the reacting syngas dissociate into carbon and oxygen (chain initiation). The H_2 molecules then adsorb on to the carbon molecules, resulting in the CH_2 monomers, as well as on the oxygen molecules, giving water [54]. The CH_2 monomer has the option to either react with H_2 , forming methane, and then desorb from the catalyst surface (known as chain termination [39]), or attach to another $-\text{CH}_2-$ monomer, forming a C_2H_4 species. This species, in turn, can either desorb to give ethene, react with H_2 to give ethane, or attach to another $-\text{CH}_2-$ monomer to produce an adsorbed C_3H_6 unit, and so forth. The CO molecules are also in competition with H_2 , CO_2 and H_2O for adsorption on to the catalyst surface [55]. Other products in the FT synthesis, like alcohols, can be formed from various combinations of other species giving different monomers, such as CO species with H species giving CHOH monomers.

The latter route option of attachment of further $-\text{CH}_2-$ monomers, explained above, is referred to as the probability of chain growth or the α (alpha) value of the synthesis reaction [43, 56, 57]. Rather than the chain terminating, it can continue to grow with more CH_2 units, increasing the likelihood of particular products being formed. The reaction sequences can continue giving rise to hydrocarbon products ranging from methane to high molecular weight waxes [43]. Therefore, as the alpha value increases so does the length of the hydrocarbon chains [43]. This probability of chain growth or α value has been modelled according to the Anderson-Schulz-Flory (ASF) chain polymerization kinetics model [42], which can be used as an arbitrary approximation for the

distribution of the hydrocarbon products. This model is graphically illustrated in Figure 2.2 below, which shows that between the two carbon number extremes, the FT products go through a maximum point as the alpha value increases.

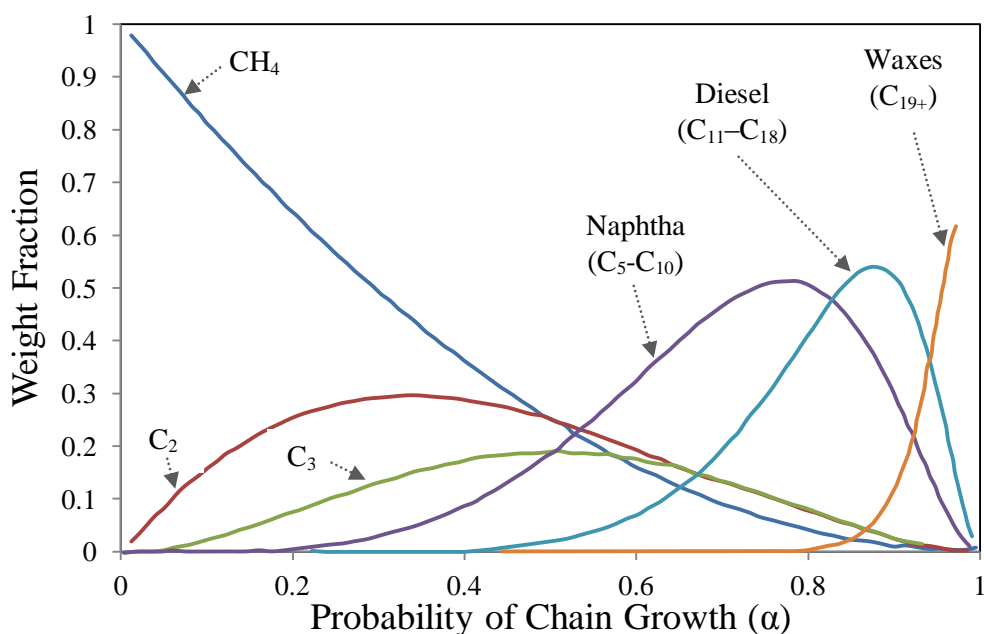


Figure 2.2 – Product distribution as a function of chain growth probability (α)
(adapted from [43])

Hence, the ASF model also sets theoretical limits to the maximum possible yields of specific products from the process [55], e.g. the maximum yield of diesel (C₁₁-C₁₈) is theoretically 55 wt.%. This shows that in order to maximize the yields of diesel further product upgrading, such as wax hydro-cracking, is required downstream. [55]. In practise, however, FT synthesis reactions can deviate from this model [58], and it cannot be used to predict the actual product distribution, but is helpful in determining the interrelation between all the hydrocarbon products.

2.2.2 Operating Modes

FT processes are technically divided into two categories according to the operating temperature of the synthesis – low temperature FT (LTFT) and high temperature FT (HTFT). Typical LTFT processes operate in the temperature range of 200-250°C and pressures of 25-60 bar using cobalt or iron-based catalysts [19], whereas HTFT processes operate in the temperature range of 300-350°C and at similar pressures to LTFT using iron-based catalysts [59]. FT reactor operating temperatures do not normally exceed 350°C, as at higher temperatures mainly methane would be produced [20]. The main steps involved in a typical FT commercial process are discussed in section 2.7, which deals with the industrial technology implemented.

The mode of FT operation has a significant influence on the nature and composition of the products obtained from the synthesis reaction. HTFT products are mainly composed of naphtha (low-grade gasoline) and low molecular weight hydrocarbons, whereas LTFT products contain mainly diesel

and waxes (which are usually hydro-cracked to maximize the yields of diesel) [35]. The differences in product composition, arising from the different modes of operation, are illustrated in Figure 2.3 below, which compares the typical compositions of LTFT and HTFT products, obtained from a fixed-bed and a circulating fluidized bed reactor, respectively (discussed in section 2.7.4).

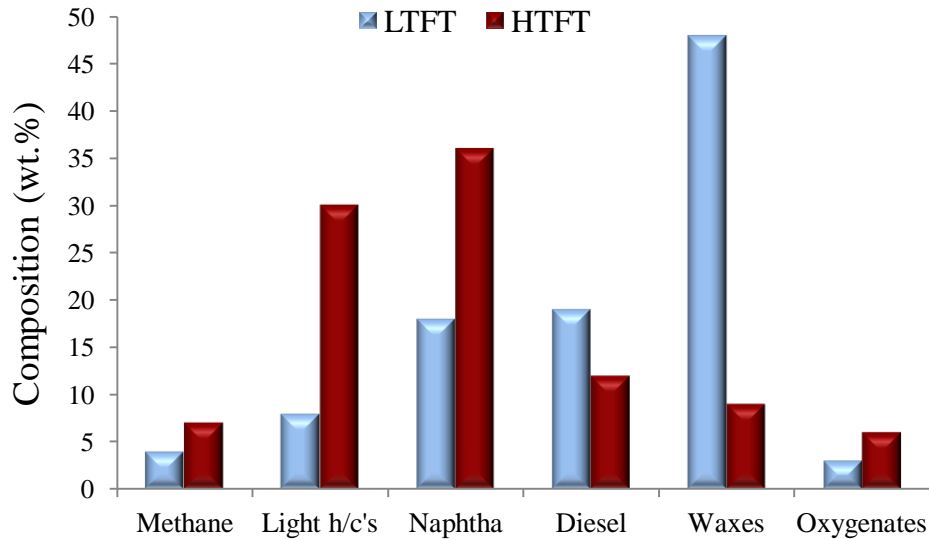


Figure 2.3 – Typical compositions of LTFT and HTFT products (derived from [35])

2.2.3 Product Characteristics

Due to their predominantly hydrocarbon nature, FT products are regarded as an alternative to crude oil for producing synthetic liquid fuels (such as gasoline, diesel and kerosene) and higher-value chemicals (such as 1-alkenes) [60]. Hence, the names adopted for FT fuels are equivalent to those used in the petroleum industry as listed in Table 2.1 below. The options for the recovery and upgrading of these hydrocarbon fuels in a BTL-FT complex are discussed in more detail in section 2.7.5. FT liquid fuels are considered to be environmentally superior to petroleum derived fuels, as they contain no sulphur, nitrogen, heavy metal contaminants, or aromatics [17-20]. Hence, the resulting emissions contain significantly lower amounts of SO_x , NO_x and particulates.

Table 2.1 – Names used for FT fuels and their equivalent carbon chain lengths (derived from [35, 61])

Names	Carbon Chain Length
Fuel Gas	$\text{C}_1\text{-C}_2$
LPG	$\text{C}_3\text{-C}_4$
Naphtha	$\text{C}_5\text{-C}_{10}$
Kerosene	$\text{C}_{11}\text{-C}_{13}$
Diesel	$\text{C}_{11}\text{-C}_{18}$
Soft Wax	$\text{C}_{19}\text{-C}_{23}$
Medium Wax	$\text{C}_{24}\text{-C}_{35}$
Hard Wax	C_{35+}

The quality of a diesel fuel is usually rated by assignment of a cetane number. This is a measure of its combustion quality during compression ignition; the higher the cetane number, the easier the fuel ignites when it is injected into the engine [9]. Some of the properties of a typical FT diesel are contrasted against standard diesel specifications in Table 2.2 below.

Table 2.2 – Comparison of typical FT diesel with standard diesel specifications
(derived from [62])

Property	US Diesel (ULSD) US07	FT Diesel
Cetane number	53.90	79.00
Sulfur (mg/m ³)	46.00	0.05
Aromatics (wt%)	24.40	0.30
Density at 15°C (kg/m ³)	827.10	784.60
Viscosity at 40°C (mm ² /s)	2.47	3.50
Calorific Value (MJ/kg)	42.70	43.90

Table 2.2 above, shows that conventional diesel has a significantly lower cetane number than that of the straight-run diesel fraction (C₁₁-C₁₈) produced from FT processes. This is because FT diesel has a low aromatics content and low degree of branching [63]. This high cetane number makes it possible to use FT diesel for blending with low cetane petroleum diesel for upgrading purposes in order to meet the increasingly strict transportation fuel specifications [20]. Moreover, this requires no extra modifications to be made in diesel engines or the existing fuel distribution framework. The low aromatics content and low degree of branching in FT diesel result in a lower density than conventional diesel and poor cold properties [63], which are disadvantages of FT diesel as this results in a lower power output in diesel engines [60]. However, on account of the typical efficiency of diesel engines (which is reported to be approximately 44% as opposed to 24% for gasoline engines) the use of diesel is more advantageous from an environmental perspective and merits preference as the fuel of choice [60]. In addition, during combustion diesel produces less CO₂ and more H₂O than gasoline as diesel is more hydrogenated than gasoline thus contributing to lower greenhouse gas emissions [42].

2.3 Product Distribution

The distribution of the resulting carbon containing products in FT synthesis is commonly referred to as the product selectivity [43]. The product selectivity is a particularly valuable way of presenting the product composition in FT synthesis as it represents the molar composition of the total products formed. Hence, product selectivities are used in the experimental work (which will be discussed in chapters 4 and 5) in order to evaluate the influence of reaction conditions on the distribution of FT products. The methods used to calculate the product selectivities are discussed in section 3.5.2.4. FT product selectivity or distribution can be altered through modification of key process variables, which relate to either the operating conditions (reactor temperature, reactor pressure, space velocity and H₂/CO molar ratio in the feed syngas) [43, 53, 64-66], or the FT

catalyst (such as the type of metal, supports and promoters used, as well as preparation methods) [67, 68]. These influencing factors are discussed in sections 2.4 and 2.5 below.

2.4 Influence of FT Catalysts on the Product Distribution

Only the four transition metals iron, cobalt, nickel and ruthenium are sufficiently active for application in the FT synthesis reaction [43, 69]. The relative cost of these four metals can be expressed as Fe:1, Ni:250, Co:1,000 and Ru:48,000 [43]. From these four metals, Ru is the most active for FT synthesis. Ni, Co and Fe form volatile carbonyls to varying extents during the FT reaction, however, those formed by Fe and Co are volatile at 500-600°C (temperatures that are higher than those used in typical FT conditions), whereas those formed by Ni are volatile at 200-300°C (within the range used in typical FT conditions) [20]. In the case of Ni, this causes the continuous loss of the metal during the reaction [43]. In addition, Ni is considered more as a methanation catalyst as it produces mainly methane and gives the lowest yield of higher molecular weight compounds at typical FT conditions [69]. Ru does not oxidise or carburise under normal FT conditions, and it gives high yields of oils and waxes [69]. However, because of its very high cost and low availability, large scale application of Ru as a catalyst is not viable for the production of low value chemicals and/or synthetic fuels, but could potentially be used in the production of higher value chemicals [43].

Hence, only iron and cobalt catalysts are used commercially for FT synthesis [43, 44, 70] and for this reason only these two types of catalysts are considered in this research project. The mode of operation in the FT process usually dictates which of these two industrially applicable catalysts is selected, as different operating conditions are more suited to either type of catalysts. Fe catalysts are used for HTFT processes, whereas both Fe and Co are suitable for LTFT processes [21]. The type of feedstock that is used, as well as the type of products that are desired (i.e. gasoline versus diesel and waxes) also play a significant role in the choice of catalyst. The reasons for the choice of catalyst to suit the operating mode, feedstock and desired products are discussed in sections 2.4.1 to 2.4.3.

The differences in the compositions of typical iron and cobalt-based catalysts are illustrated in Figure 2.4 below. The general compositional trend for typical cobalt and iron-based industrial catalysts comprises of the metal (in its oxide form), a support or carrier material, and promoters (other metals and metal oxides) [31]. Some of the common support materials and promoters used in both iron and cobalt-based catalysts are discussed in sections 2.4.1 and 2.4.2, respectively. The iron or cobalt oxide phases in the catalyst require reduction prior to the FT reaction (typically using hydrogen), as they both need to be reduced to the equivalent metallic phase which is the phase that actually possesses the necessary activity for the FT reaction.

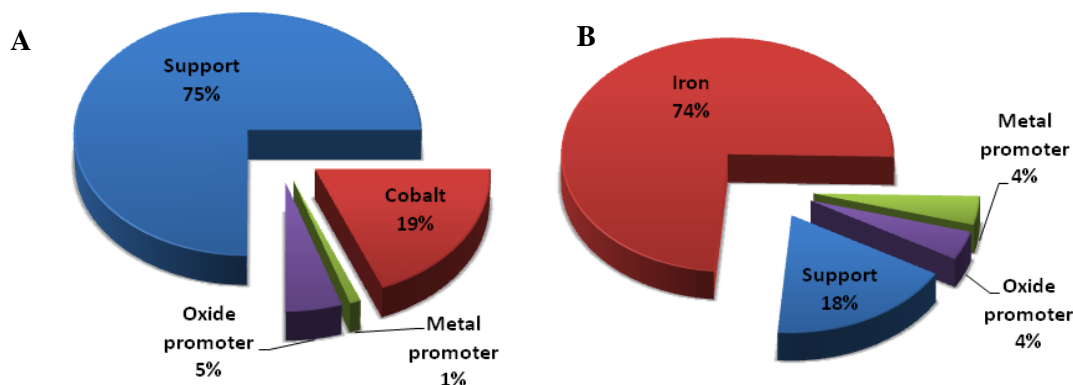


Figure 2.4 – Typical composition of FT cobalt catalysts (A) and iron catalysts (B)
(derived from [5, 31, 43, 71])

Research on both cobalt and iron-based catalysts has focused on a number of aspects in an effort to improve catalyst reducibility and activity, tailor and enhance the selectivity to certain products and by the same token, decrease the selectivity to undesired products like methane, as well as increasing their resistance to catalyst poisons, such as sulphur compounds. These aspects include the influence of physical and chemical properties, the support or carrier materials, promoters and other additives, the preparation techniques and the catalyst pre-treatment or activation procedures implemented. A small number of these studies have also explored catalyst suitability for FT applications that use biomass as a feedstock [72-75]. This is important as FT catalysts are very sensitive to syngas contaminants (section 2.7.3), and therefore have intensive syngas cleaning requirements. Any design improvements in catalyst resistance to syngas or biosyngas poisons, therefore, could lead to potential savings in capital and operating costs as the cleaning requirements may be reduced.

2.4.1 Iron Catalysts

Iron-based catalysts are used both in LTFT and HTFT processes. The catalyst preparation techniques, supports and promoters used, however, differ depending on this operational mode. For example, added mechanical strength is required for HTFT processes that take place in fluidized-beds (discussed in section 2.7.4.1) hence fused iron catalysts are used instead of those prepared by precipitation for LTFT processes. Typical iron support materials include silica and/or alumina, and promoters include copper and alkali metals like sodium and potassium [43]. Compared to cobalt, iron is reported to be more responsive to promoters, and the more alkaline the promoter is the higher the average carbon chain length of the hydrocarbon products [69]. This is because CO surface adsorption and subsequent decomposition into C and O atoms (chain initiation in section 2.2.1) has been reported to be enhanced by surface alkalinity [21].

Since iron is so much cheaper than cobalt, the degree of dispersion of the metal on the catalyst surface is not as important. Hence, as shown in Figure 2.4 above, typical iron catalyst compositions comprise of mainly the iron phase and a much lower proportion of the support material. This

significantly higher metal surface area in typical iron catalysts compared to that in typical cobalt catalysts has been reported to give iron-based catalysts a higher initial intrinsic activity [66]. However, according to Espinoza *et al.* [66], this activity decreases as the reactant conversion increases, making iron catalysts suitable for a given range of conditions, such as high space velocities and operating pressures, whereas the opposite has been reported for cobalt catalysts [66].

An advantage of iron catalysts is that they display high water gas shift activity (reportedly due to the iron carbides and re-oxidised Fe_3O_4 that are formed during the FT reaction [53]). This means that the carbon dioxide produced in the synthesis reaction is hydrogenated into more FT products (Equation 2.2 in section 2.2). This water gas shift activity also implies that iron is more versatile as an FT catalyst, as syngas with low H_2/CO molar ratios (below 2.0) and/or high CO_2 content can be used [69]. This allows for more flexibility in industry for using hydrogen-poor syngas, such as biomass derived syngas (with H_2/CO molar ratios typically in the range of 0.5-1.5) to be used with less or no conditioning and adjustment of H_2/CO molar ratios to higher values [69]. The main reported disadvantage of using iron-based catalysts is that they deactivate faster due to oxidation and coke deposition and have a much shorter process life than cobalt-based catalysts (~2-3 months) [69].

2.4.2 Cobalt Catalysts

Cobalt-based catalysts are used in LTFT processes only as, due to their high activity, it has been reported that they would produce mainly methane at higher temperatures [21, 76]. At LTFT conditions, cobalt-based catalysts have been reported to be more stable than iron-based catalysts, have a much higher resistance to deactivation by water and therefore have much longer process lives than iron catalysts (~5 years in LTFT fixed-bed reactors) [67, 69]. In addition, they have been reported to exhibit a high activity and selectivity towards linear hydrocarbons (paraffins), which is favourable for diesel and wax products [21]. The differences in catalyst compositions illustrated in Figure 2.4 above, are mainly due to the relative cost of both metals. The very high price of Co means that, ideally, more of the metal needs to be exposed on the catalyst surface [21]. For this reason, cobalt-based catalysts are usually supported on carriers that are stable (during catalyst calcination, activation and reaction) and that have a high surface area such as alumina, silica and titania [71]. This is usually done by impregnation of these support materials with aqueous cobalt salt solutions. These support materials can also have an influence on the catalyst activity and performance (in terms of CO conversion versus time on stream) and the product distribution.

Promoters like boron, ruthenium, rhenium and CaO are commonly used in order to improve the reducibility of the catalyst prior to FT reaction, as well as enhancing the catalyst activity and C_{5+} selectivity by keeping the metal surface clean from carbon deposition during the reaction [31, 77, 78]. This has been shown in studies by Bao, Liew and Li [79], Khodakov [80] and de la Osa *et al.* [68]. The cobalt oxide phase in the catalyst usually reduces at temperatures above 300°C, which are

higher than those used in LTFT conditions. Hence, the ease of catalyst reducibility is quite significant, as the catalyst has to be reduced before it is loaded into the reactor, adding extra costs and process stages. The main reported disadvantage of using cobalt-based catalysts is that they require H_2/CO ratios in the syngas greater than or equal to 2.0, as they are not very active water gas shift catalysts [69, 81]. Therefore, if syngas derived from biomass is used, which contains low H_2/CO molar ratios, an external shift reactor would be required to adjust this ratio in the syngas prior to entering the FT reactor.

2.4.3 Catalyst Deactivation

What is common between both cobalt and iron catalysts are the means by which their deactivation occurs. Some of these means include sintering of the metal, re-oxidation of the active metal phase by water and poisoning by syngas contaminants, especially sulphur compounds which are permanent poisons [17] (typical FT syngas requirements for sulphur content are below 0.05 ppm [69]). In comparison, iron has been reported to be more easily deactivated by water, whereas cobalt is more sensitive to sulphur compounds [66]. Despite these differences, sulphur removal from the syngas is vital for the success, longevity and viability of the FT process when either type of catalyst is used. Typical syngas contaminants and gas cleaning requirements are discussed in section 2.7.3.

Other deactivation mechanisms that have been reported to occur during the reaction include catalyst pore plugging and fouling due to mainly wax (heavy hydrocarbons), as well as coke deposition or accumulation inside the catalyst pores [82, 83]. These mechanisms are speculated to be partly responsible for the declining CO conversion with time on stream which have also been reported to potentially contribute to intra-particle diffusion limitations [83]. The occurrence and extent of these deactivation mechanisms can be examined by using catalyst characterization techniques such as BET specific surface area determination (discussed in section 3.6.1) as these deposits would decrease the total surface area of the catalyst. The technique that is used in this work is thermo-gravimetric analysis (TGA, discussed in section 3.6.4) which can also be used to examine the occurrence and extent of this mechanism by monitoring the weight loss profile as the deposits are burned off with increasing temperature.

2.4.4 Catalysts used in this Project

Three catalysts are available to work with in this project; two cobalt-based catalysts and one iron-based catalyst. Their compositions and characteristics are discussed in detail in chapter 4. With regard to the catalyst, FT synthesis work can be carried out according to three different approaches [84] as listed below:

1. Catalyst intrinsic chemistry – this relates to the science involved in the preparation of the catalyst, including the type of metal, promoters and support used.

2. Engineering the catalyst pellet – this has to do with the catalyst performance on stream and involves the design of a catalyst pellet that will help to maintain this desired performance in operation and particularly in up-scaling.
3. Methods of operating the catalyst pellet – this involves the careful selection of the right conditions for process operation, including factors such as reactor pressure, syngas composition, reactant conversion, etc. which have been reported to have a significant influence on the catalyst performance and product selectivity [44, 85].

The first two approaches that are listed above are beyond the scope of this project as their executions require dedicated catalysis research, the equipment and expertise for which are not available for this work. The work that is carried out, therefore, follows the third approach listed above. The three available catalysts are first evaluated and compared, and the most suitable catalyst is selected for further exploration on the effects of operating conditions on its activity (reactant conversion), product distribution and product yields. The catalyst selection procedure is detailed in chapter 4, whereas the parameter study which examines the influence of operating conditions is discussed in chapter 5.

2.5 Influence of Operating Conditions on the Product Distribution

The reaction conditions that have an effect on the synthesis process and that will be examined in the experimental work (discussed in chapters 4 and 5) include the operating temperature, operating pressure, space velocity, and the H₂/CO molar ratio in the feed syngas. These parameters are discussed in sections 2.5.1 to 2.5.4 below.

2.5.1 Operating Temperature

Temperature is one of the most important variables in FT processing due to the highly exothermic nature of the FT reaction. Therefore, the temperature needs to be carefully controlled and maintained within a constant range in order to avoid temperature runaways that can lead to the predominant formation of methane and rapid catalyst deactivation [43]. Overall, in the FT reaction, an increase in temperature has been reported to increase the reaction rate and, therefore, the reactant conversion and product formation. However, as the temperature increases the product composition shifts towards the production of methane and low molecular weight compounds, i.e. the average chain length of the products decreases [55]. This is true for both iron and cobalt-based catalysts and has been widely reported in the literature [86-90]. This can be explained by the increased rate of chain termination reactions (discussed previously in section 2.2.1), where the ‘CH₂’ monomers are hydrogenated to CH₄ [91]. Lower C₅₊ selectivity at higher temperatures has also been attributed to thermal cracking of the heavier compounds [91]. The operating temperature can also adversely affect the catalyst life. Increasing operating temperature favours catalyst deactivation mechanisms, such as sintering or carbon deposition and wax deposition (discussed previously in section 2.4.3), which inhibit the activity of the catalyst by occupying or ‘blocking’ the

catalyst active sites. The rate of these deactivation mechanisms has been found to increase excessively at elevated temperatures [91]. Previous work investigating the effects of operating temperature on FT catalyst activity, product distribution, etc. is discussed in section 2.6.

As discussed previously in sections 2.4.1 and 2.4.2 above, the optimum operating temperature range for cobalt is reported to be in the LTFT range (200-250°C), whereas iron-based catalysts could be used in either the LTFT or HTFT (300-350°C) ranges, depending on their preparation methods and formulation. The operating temperature range recommended by the manufacturer for the iron-based catalyst used in this project (section 4.1) is in the range of 300-350°C. Hence, depending on the type of each catalyst used in this work, these are the temperature ranges that will be implemented in the FT synthesis work discussed in chapters 4 and 5.

2.5.2 Operating Pressure

Pressure is an important parameter as it has a significant effect on capital cost and can require additional expenditure on energy and equipment for compression, either for gas compression or from the higher capital cost of a pressurized gasifier. A sensitivity analysis on product value carried out in a techno-economic assessment by Swanson *et al.* [92] on BTL-FT plant scenarios showed that the capital cost of gas compression significantly influences the product value. Conversely, the equipment sizes become less as the pressure increases. The overall effect of a 25 bar working pressure compared to 5 bar is approximately a 150% increase in capital cost [93]. Thus operation at 5 bar compared to 25 bar would reduce capital costs by around 60%. These assumptions could be drawn from a review of the costs of biomass gasification technologies by Bridgwater [93], where the installed plant costs for gasification plants from across Western Europe were collected and compared and showed a clear difference in the capital costs between atmospheric and pressurized systems. The capital cost data that was collected encompassed each system from the reception of the biomass feedstock to a final, clean syngas ready for the generation of electricity [93]. For plants of the same capacity, this data showed that a pressurized gasification system accounts for an increase of approximately 150% in capital costs over those of an atmospheric gasification system [93].

Cost reduction estimates for operation at lower pressures could also be drawn from step count estimating procedures, such as those put forward by Zevnik and Buchanan [94] and Wilson [95], to which adjusted UK plant cost indexes are included for more current costs (year 2000 basis) [96]. These capital cost estimation models relate basic process parameters like plant capacity, pressure, temperature, and construction materials to total plant cost by considering the number of main plant items or functional units in the process [96]. Using these process step capital cost estimation procedures shows that for plants of the same capacity (and assuming that the same number of process units is involved and that they remain unchanged) a reduction in working pressure from 25 bar to 5 bar would reduce capital costs by 15%. A reduction of 20% in capital cost could be

achieved instead, however, if the syngas compression step is eliminated (accounting for one less process unit). An example of the calculations for estimating these capital costs is provided in APPENDIX E. Hence, combining the data from installed gasification systems and the values calculated using step count estimation procedures, it can be assumed that potential savings of 20-60% in capital costs could be realised if lower working pressures are implemented in a BTL-FT plant. The influence of these lower operating pressures on FT synthesis product distribution, product yields, etc. therefore requires investigation, as these are also important considerations that affect the process both from technical and economic perspectives.

The general consensus in the available literature is that an increase in FT reactor pressure results in an increase in both CO conversion and selectivity towards higher molecular weight hydrocarbon products (C_{5+}) [43, 87]. Wax formation is reported to increase considerably with increasing pressure, whereas a less marked influence on liquid fuel formation (naphtha and diesel) has been observed, particularly at pressures above 10 bar. Moreover, operation at increased pressures (≥ 30 bar) has been found to have a negative effect on the catalyst life as these conditions promote deactivation at a faster rate than operation at low pressures [70]. The influence of reactor pressure on the FT product yields as reported in a review on the selectivity in FT synthesis by Caldwell [97] is illustrated in Figure 2.5 below.

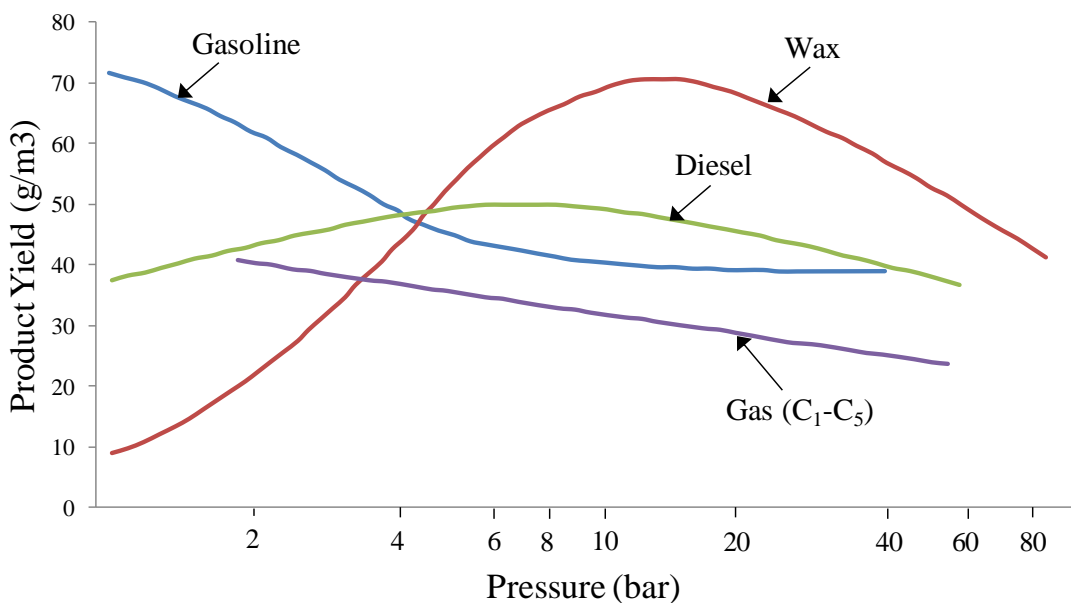


Figure 2.5 – Influence of reactor pressure on FT product yields
(adapted from [97])

The results taken from the above review do not give an overall view of the total products obtained as they are not expressed in weight percentage yields, but still serve in showing the differences and trends in the yields of hydrocarbon products as influenced by increasing pressure. For example, an increase in pressure up to 15 bar results in increased wax yields, whereas these yields are lowered as the pressure is further increased above 15 bar. Further evidence on the influence of operating pressure on FT product distribution (using cobalt catalysts) is provided in Figure 2.6 below, which

is adapted from a review by Davis [70]. Both figures show that the most significant effect of operating pressure on the product yields and distribution is observed at lower pressures (1-10 bar).

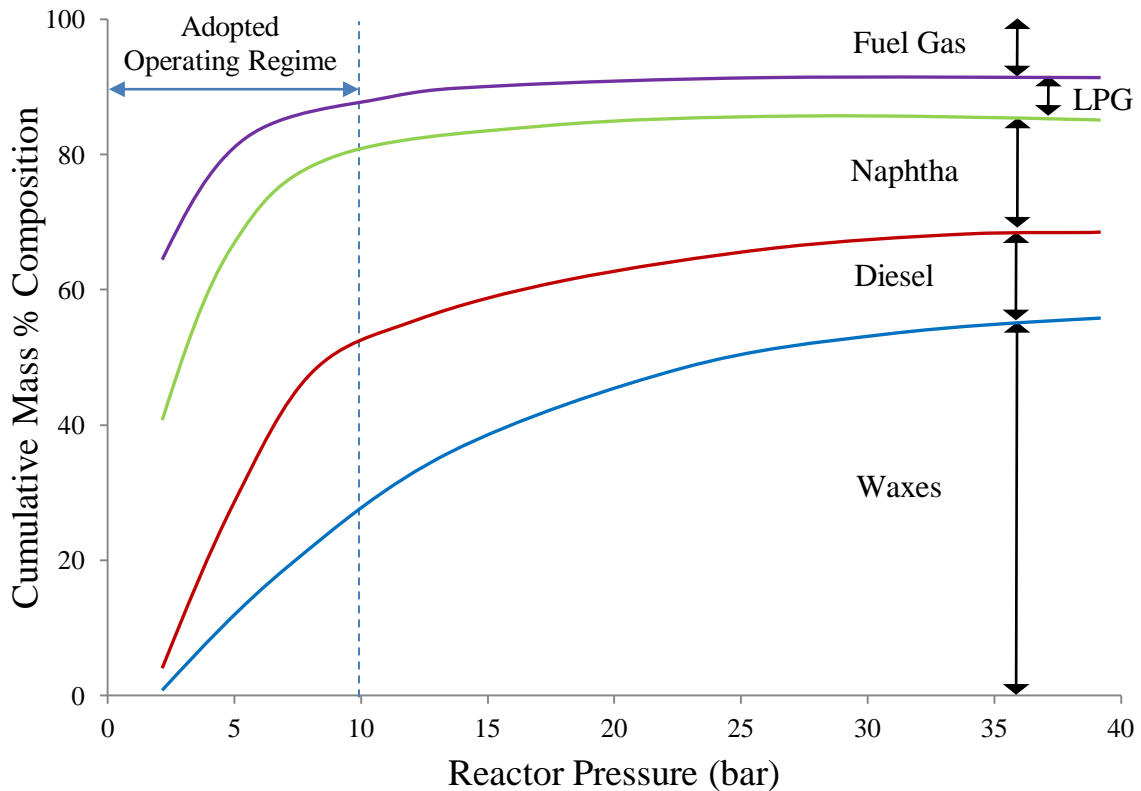


Figure 2.6 – Influence of reactor pressure on FT mass percentage product composition using a typical cobalt catalyst (adapted from [70])

Commercial FT processing is usually carried out at pressures in the range of 20-40bar, and therefore the majority of the available literature on FT synthesis deals with experimental studies within this range. Work performed at lower pressures is not as common, but the influence of these milder conditions on the FT synthesis process is of interest from an economic perspective as previously discussed above. Hence, operating pressures in the lower pressure range of 1-10 bar will be implemented for the FT synthesis work discussed in chapters 4 and 5. Previous work investigating the effects of operating pressure on FT catalyst activity, product distribution, etc. is discussed in section 2.6.

2.5.3 Space Velocity

Space velocity is the inverse of residence time, τ , and is usually defined as the ratio of the feed gas flow rate to the size of the reactor (units = h^{-1}). The space velocity can be defined in terms of gas hourly space velocity (GHSV, which is more commonly expressed in the following units in research publications: $\text{L}_{\text{gcat}}^{-1}\text{h}^{-1}$), or weight hourly space velocity (WHSV), and calculated using Equations 2.4 and 2.5 below, respectively.

$$\text{GHSV} = \frac{\text{Feed Gas Volumetric Flow Rate}}{\text{Reactor (or Catalyst) Volume}} \quad (\text{EQ 2.4})$$

$$\text{WHSV} = \frac{\text{Feed Gas Mass Flow Rate}}{\text{Catalyst Mass}} \quad (\text{EQ 2.5})$$

Hence, space velocity can also be used for rating the approximate size of the reactor. Since higher space velocities correspond to shorter reactor residence times, catalyst activity and C₅₊ hydrocarbon selectivity are expected to decline with increasing space velocity and these phenomena have been reported by several authors including de la Osa *et al.* [89], and Liu *et al.* [44]. This is not always the case in the available literature, however, where the relationship of increasing space velocity to catalyst activity and product distribution using different catalysts and reactor set-ups can be more complex. An example of this is seen in the work carried out by Mohanty *et al.* [91] who reported CO conversion increasing to a maximum point as the space velocity was increased, but thereafter declining as the space velocity was further increased. The step-wise growth nature of the FT reaction mechanism (discussed previously in section 2.2.1) that has been reported to potentially occur in series, parallel or in a cyclic arrangement means that definite trends for conversion or product selectivity with changing space velocity are not necessarily observed [46].

The implications of varying the syngas space velocities in commercial FT applications is of interest, as the relationship of space velocity to the size of the FT reactor vessel is inversely proportional, i.e. the higher the space velocities or syngas flow rates, the smaller the reactor vessel required and the lower the capital cost of the FT processing plant. If low FT reactor operating pressures are desired, this would mean that larger FT reactor vessels are necessary to handle the larger gas volumes. Potentially, therefore, a balance could be achieved between having higher space velocities and lower operating pressures that would lead to potential capital cost savings. These cost implications could be checked from the scaling relationship given in Equation 2.6 below [96], where C is the capital cost, Q is the capacity, and X is the scaling factor (typically ranging from 0.6-0.7). For instance, if the capital cost of an industrial fixed-bed FT reactor is taken as \$16.7 million (according to the techno-economic review carried out by Tijmensen *et al.* [9]), and if the scaling factor, X, is assumed to be 0.67, then a 200% increase in the feed flow rate or capacity lowers the capital cost to \$10.5 million, a cost reduction of approximately 30%.

$$\frac{C_2}{C_1} = \left(\frac{Q_2}{Q_1} \right)^X \quad (\text{EQ 2.6})$$

In order to investigate the influence of increasing space velocity the values of space velocity (WHSV) that will be investigated in the FT synthesis work discussed in chapter 5 are in the range of 8.8 to 11.5 h⁻¹. The minimum value of 8.8 h⁻¹ is selected due to equipment limitations that will be discussed in section 3.4.3. Previous work investigating the effects of space velocity on FT catalyst activity, product distribution, etc. is discussed in section 2.6.

2.5.4 Synthesis Gas Composition (H_2/CO Molar Ratio)

As the molar ratio of H_2/CO changes in the feed syngas so does the stoichiometry of the FT reaction. This affects the partial pressure and, therefore, the concentration of each species (CO and H_2) on the catalyst surface. The widely accepted ‘alkyl’ reaction mechanism (discussed previously in section 2.2) proposed that the CO adsorbed on the catalyst surface is hydrogenated to form the CH_2 monomers which can propagate the reaction, whereas H_2 is more responsible for chain termination reactions. Hence, the likelihood of this chain growth is dependant on the H_2/CO ratio in the feed syngas [55]. An increasing H_2/CO in the feed syngas has been reported to favour the formation of lighter hydrocarbon compounds, whereas, the C_{5+} hydrocarbon selectivity increases with decreasing H_2/CO molar ratio [91, 98, 99]. In addition, an increasing H_2/CO molar ratio has been reported to improve the exothermic heat removal in the reactor and enhance the catalyst life and activity as carburisation (or coke formation) on the catalyst surface is minimized [91, 100]. Previous work investigating the effects of the H_2/CO molar ratio in the feed syngas on FT catalyst activity, product distribution, etc. is discussed in section 2.6.

As discussed previously in section 2.4.2, a H_2/CO molar ratio in the syngas of 2.0 is generally recommended for cobalt catalysts in order to achieve a good activity in the FT synthesis reaction, whereas iron catalysts can handle a much lower H_2/CO ratio due to their high WGS activity [20]. The syngas produced in BTL processing via biomass gasification tends to have a low H_2/CO ratio (0.45-1.8, depending on the means of gasification employed) [9]. The biosyngas has to therefore be conditioned in order to adjust this ratio to a higher value before entering the FT reactor. Due to their higher activity than iron catalysts and heavier hydrocarbon product yields, cobalt catalysts have been mainly considered so far for BTL-FT applications, assuming that the syngas is sufficiently cleaned prior to the FT reactor [73]. If H_2/CO molar ratios lower than 2.0 could be used with cobalt catalysts this could potentially lower the syngas conditioning requirements in the process and lead to potential savings.

The possibility of using iron-based catalysts is also examined in this work (chapter 4), as iron catalysts can be used with hydrogen deficient biosyngas. In addition, iron catalysts have been reported to display a much higher resistance to typical biosyngas contaminants (section 2.7.3.1), and can therefore potentially be applied in BTL-FT processing [73]. These two advantages of iron-based catalysts, which imply the removal of the syngas conditioning step and less stringent gas cleaning requirements, in combination with their much lower price than cobalt catalysts, could also potentially lead to significant cost savings. The values for the H_2/CO molar ratios in the feed syngas that will be implemented in the FT synthesis work discussed in chapter 4 and 5 are in the range of 1.5 to 2.0.

2.6 Previous Studies on the Influence of Operating Conditions on FT Product Distribution

The three catalysts that are available for this project (which will be described in chapter 4) not only differ in the type of active metal phase used, but also in the type of support materials and promoters implemented in their formulation. The influence of support materials and promoters in these three catalysts on the catalyst activity and performance, the product distribution, and the product yield, therefore, can not be accurately compared, neither is it within the scope of this work. As discussed previously in section 2.4.4, this project focuses on methods of operating the catalyst in the reactor for FT synthesis, and therefore, similar studies that have examined the influence of operating conditions on FT catalyst performance in terms of activity, product distribution, etc. are reviewed and discussed in this section.

In relation to the wealth of published material available on FT synthesis, only a small number of studies have investigated the influence of reaction conditions on the activity, stability (in terms of reactant conversion versus time on stream), and product distribution (or selectivity) of either iron or cobalt-based catalysts. The studies which are reviewed in this section are relevant to the FT synthesis parameter study carried out in this project and span mainly the last few decades. These studies have mainly concentrated on the effects of reactor temperature, reactor pressure, syngas space velocity and the H₂/CO molar composition in the feed syngas. As commercial FT processing is typically carried out at pressures in the range of 20-40 bar, the majority of these studies deal with experimental investigation on the influence of operating conditions within this conventional range of FT reactor pressures. As the work aims to explore the influence of less severe FT operating conditions, studies that specifically address the influence of lower operating pressures (in the range of 1-20 bar) on catalyst activity and stability, and product distribution using either iron or cobalt-based catalysts are of particular interest. These specific studies, however, are very limited in number.

As previously discussed in sections 2.2.2 and 2.4, there are fundamental differences in FT synthesis when using either iron or cobalt-based catalysts, and these relate to the operating conditions that are used and the type of products that are obtained. Cobalt catalysts are selective towards the formation of straight-chain diesel range hydrocarbons and waxes, whereas iron catalysts are more selective towards naphtha grade products and lower molecular weight hydrocarbons. The type of reactor that is implemented, such as a fixed bed or slurry (CSTR) reactor that are discussed in section 2.7.4, also plays an integral role in the final product distribution. On account of these differences, therefore, the literature review of the parameter studies is divided into two parts; studies carried out using iron-based catalysts are discussed in section 2.6.1, whereas those using cobalt-based catalysts are discussed in section 2.6.2. Important findings of these studies that are closely related to this work, including the influence of reaction conditions on reactant conversion, liquid and wax yields, C₅₊ hydrocarbon product selectivity, etc. are reviewed. For convenience, the shorthand format that is adopted for reference to the set of process conditions that were implemented in each of the

studies that are discussed below, as well as in the remainder of the thesis, is the following: (T, P, GHSV or WHSV, H₂/CO, and m_{cat}, if applicable).

2.6.1 Studies using Iron Catalysts

Research on FT synthesis using iron-based catalysts has been quite extensive owing to the development of HTFT technology since the 1950s mainly by Sasol in South Africa (section 2.1), for which iron-based catalysts are more suitable for the reasons discussed previously in section 2.4.1. This research has primarily focused on the development of reactor technology, and catalyst design including its preparation, structural supports and promoters. Studies that have addressed the influence of reaction conditions, and FT reactor pressure in particular, on the catalyst activity, catalyst stability and the product distribution using iron-based catalysts are relatively few. Studies that specifically address the influence of low pressure (1-20 bar) are even less. These studies have been carried out at a laboratory-scale in both fixed-bed reactors [86, 88, 101-104] and slurry reactors [44, 90, 98, 105-107] and are reviewed below. Some earlier studies carried out just over two decades ago [98, 104] are also included. From these particular studies, only a few specifically examine the influence of low operating pressures (within the range of 1-20 bar) on FT synthesis [86, 98, 103]. The reaction conditions investigated in all the studies using iron-based catalysts reviewed in this section are summarized in Table 2.3 below.

The effects of temperature and H₂/CO molar ratio, as well as the influence of alkali promoters using commercial Ruhrchemie iron-based catalysts (Fe-Cu-K-Na/SiO₂, which was representative of typical industrial catalysts implemented at the time) were investigated by Donnelly and Satterfield (1989) [98] in a slurry reactor (one litre CSTR) under the following reaction conditions: (230-265°C, 8-30 bar, GHSV = 0.6-2.4 h⁻¹, H₂/CO = 0.5-2.0, and m_{cat} = 25g). The influences of reactor pressure and space velocity were not reported, as these specific parameters were kept constant (at different values) for each of the catalysts tested. As opposed to the unpromoted catalyst which displayed rapid deactivation over the reaction test period, the promoted catalyst was reported to have displayed a stable activity over a 1300 hour reaction period. However, the average molecular weight of the products was reported to decrease with both increasing reactor temperature and time on stream, which is in general agreement with other contemporary work at the time, as well as with the more recent studies that are reviewed in this section. The product distribution was reported to be unaffected by the H₂/CO molar ratio in the feed syngas, an observation which is contrary to the findings of Mirzaei, Vahid and Feyzi [86] and Liu *et al.* [44] which are reviewed further down. This trend, however, is presented in terms of the α -value of the synthesis reaction, which is an arbitrary value (section 2.2.1), and individual product or product group selectivities, which are commonly reported in more recent publications, are not reported by Donnelly and Satterfield thus not allowing for accurate comparison.

Table 2.3 – Summary of cited parameter studies using iron-based catalysts

	Catalyst	Reactor Type	T (°C)	P (bar)	H₂/CO	GHSV (h⁻¹)	m_{cat} (g)	Reference	Year
1	Fe-Cu-K-Na/SiO ₂	Slurry (1L CSTR)	230-265	8-30	0.5-2.0	0.6-2.4	25	Donnelly and Satterfield [98]	1989
2	Fe-Cu-K/SiO ₂	1) Fixed-bed (ID =10mm, L = 36cm) 2) Slurry (1L CSTR)	235-250	15	0.7-1.0	1.0-4.0	3.5	Bukur, Patel and Lang [104]	1990
3	Fe/Cu/K	Fixed-bed (ID = 18mm, L = 30cm)	220-270	11-31	1.0-3.0	4.0-10.0	-	Wang <i>et al.</i> [101]	2003
4	Fe-Mn	CSTR	260-290	9-30	1.0	0.46-1.85	4.75	Liu <i>et al.</i> [44]	2007
5	Fe-Cu-K/SiO ₂	1L CSTR	240-270	20-30	1.0	-	10	Farias <i>et al.</i> [105]	2007
6	Fe/SiO ₂	1) 0.1 L CSTR 2) 1 L CSTR	240-280	10-29	0.4-2.0	-	15	Hayakawa, Tanaka and Fujimoto [90]	2007
7	Fe-Mn	Fixed-bed (ID = 9mm, L = 110cm)	280-450	1-15	1.0-3.0	2.7	1.0	Mirzaei, Vahid and Feyzi [86]	2009
8	Fe	Fixed-bed	260-300	30	1.0	1.3	-	Kumabe <i>et al.</i> [102]	2010
9	Fe-Cu-K/SiO ₂	Slurry (3.6 L)	245-265	25	1.0	2.6-3.9	720	Jung <i>et al.</i> [106]	2010
10	Fe-Mn	Fixed-bed (ID = 7mm, L = 30cm)	230-300	1-20	2.0	1.0-1.6	0.5	Feyzi, Irandoust, and Mirzaei [103]	2011
11	1) Fe-Zn-K/Al ₂ O ₃ 2) Fe-Co	Fixed-bed	250-300	14-24	2.0	0.135-1.20	20	Dasgupta and Wiltowski [88]	2011

The performance of a similar type of Ruhrchemie catalyst to those used by Donnelly and Satterfield above was also compared by Bukur, Patel and Lang [104] in a fixed-bed reactor (I.D. = 10mm, L = 36cm) and a slurry reactor (one litre CSTR) under the following reaction conditions: (235-250°C, 15 bar, GHSV = 1.0-4.0 h⁻¹, H₂/CO = 0.7-1.0, and m_{cat} = 3.5g). The results concurred with the other literature findings reviewed in this section in that CO conversion increases with increasing temperature. In addition, it was reported that both the activity and the C₅₊ hydrocarbon product selectivity declined over time in both reactors. The study also demonstrated that fixed bed reactors are easier to use and require smaller amounts of catalyst than slurry reactors. In addition, it was concluded that it is feasibly possible to use the same catalyst for evaluation in either type of reactor as the results obtained from both reactors were comparable.

The influence of the following operating conditions (280-450°C, 1-15 bar, GHSV = 2.7 h⁻¹, H₂/CO = 1.0-3.0 and m_{cat} = 1.0g) on an unpromoted Fe-Mn/Al₂O₃ catalyst were investigated by Mirzaei, Vahid and Feyzi [86] in a fixed-bed micro-reactor (I.D. = 9mm, L = 110cm). In line with the aims of the work conducted in this particular study, this catalyst emerged as the most suitable for optimum production of light olefins out of a number of catalysts supported on different materials (TiO₂, SiO₂ and Zeolites) and containing different promoters (Rb, Mg, K and Li) that were screened in their work. Hence, the optimum operating conditions that were determined at 360°C, 6 bar and H₂/CO = 1.0 did not target high C₅₊ hydrocarbon selectivities. Despite this, their results still illustrated that the temperature, pressure and H₂/CO molar ratio have a considerable effect on FT synthesis. The reactant conversion was significantly influenced by all these parameters, whereas product distribution was most influenced by variation in H₂/CO molar ratio in the feed syngas and reactor pressure. For example, an increase in pressure from 2-15 bar resulted in a 43% increase in the C₅₊ hydrocarbon selectivity. Both CO conversion and methane selectivity increased with an increasing H₂/CO molar ratio and an increasing temperature, whereas the opposite trend was observed for the C₅₊ selectivity; similar results were also reported by Liu *et al.* [44]. When the temperature was increased above 360°C, this resulted in excessive coke formation and deposition on the catalyst surface, leading to faster deactivation of the catalyst; an observation which was also made by Feyzi, Irandoust, and Mirzaei [103]. An increase in pressure from 1-15 bar resulted in the decrease of both CO conversion and methane selectivity, but favoured C₅₊ selectivity. As will be discussed in the other studies, reviewed below, the general agreement is that an increase in pressure results in higher C₅₊ hydrocarbon selectivity and yields. The influence of pressure on reactant conversion reported by Mirzaei, Vahid and Feyzi, however, is not conclusive as opposing results are reported in the literature. An accurate comparison is difficult to make, though, as different reaction conditions, catalysts and reactors are implemented in each study.

Another study which also aimed towards obtaining high selectivities to C₂-C₄ olefin compounds, rather than high C₅₊ hydrocarbon selectivity was carried out by Feyzi, Irandoust, and Mirzaei [103], who explored the effect of reactor temperature, reactor pressure and space velocity using a

potassium promoted Fe-Mn catalyst in a fixed-bed reactor (I.D. = 7mm, L = 30cm) under the following reaction conditions (230-300°C, 1-20 bar, GHSV = 1.0-1.6 h⁻¹, H₂/CO = 2.0, and m_{cat} = 0.5g). Once again, despite the main aims that were outlined, their study serves in shedding further light on the influence of key operating conditions on the FT synthesis reaction. In accordance with the other studies reviewed in this section, an increase in temperature from 230-300°C resulted in significantly higher catalyst activity (CO conversion), lower C₆₊ hydrocarbon selectivity and an increased rate of coke formation [86]. In contrast, an increase in pressure from 1-20 bar resulted in a significant increase in the C₆₊ hydrocarbon selectivity. This was also observed by Mirzaei, Vahid and Feyzi [86] also working in a similar range of pressures, as well as by other groups working at higher pressures that are discussed further down in this section [88, 90, 101]. A similar trend for CO conversion as that observed for increasing temperature was also reported for increasing pressure from 1-20 bar. Interestingly, however, only in this study by Feyzi, Irandoust, and Mirzaei [103], is it reported that the product distribution was not significantly influenced by pressure in the range from 1-3 bar. An increase in space velocity resulted in lower CO conversions, which was also observed by Liu *et al.* [44] and Jung *et al.* [106]. However, contrary to these two studies, a more complex relationship was observed for the selectivity of C₆₊ hydrocarbons; C₆₊ selectivity decreased as the space velocity was increased from 1.0-1.2 h⁻¹, but thereafter increased as the space velocity was increased to 1.6 h⁻¹. This shows that space velocity is also an important consideration in FT synthesis, and optimum values for this parameter cannot be simply predicted and must be determined experimentally on different reactor systems and under different operating conditions.

The influence of temperature, pressure and space velocity were also examined by Dasgupta and Wiltowski [88], in a fixed-bed micro-reactor under the following reaction conditions (250-300°C, 14-24 bar, GHSV = 0.135-1.20 h⁻¹, H₂/CO = 2.0, and m_{cat} = 20g). Fe and Fe-Co hybrid or co-catalysts were used in an attempt to improve FT catalyst design and make them more versatile in handling syngas from a variety of feedstocks. As expected, CO conversion was found to increase as the reactor temperature was raised, and overall, an increase in reactor pressure and a decrease in temperature gave heavier hydrocarbon products. In comparison to the hybrid catalysts, the formation of these heavier hydrocarbon products was higher using Fe catalysts, indicating that Fe catalysts are more likely to be suitable for BTL-FT applications aiming to maximize the yields of liquid and/or wax hydrocarbons.

The influence of reactor temperature and reaction time (or time on stream) on the selectivity of an unpromoted 100% Fe catalyst, specifically towards kerosene grade-products (C₁₁-C₁₃), was examined by Kumabe *et al.* [102] in a fixed-bed reactor under the following reaction conditions (260-300°C, 30 bar, WHSV = 13 h⁻¹, and H₂/CO = 1.0). CO conversion and C₆₊ hydrocarbon selectivity were found to increase as the temperature was increased (in agreement with the other studies reviewed in this section, as discussed above), and the maximum kerosene selectivity was observed at 280°C. Optimum catalyst stability (a measure of CO conversion versus time on stream)

was observed at 280°C and above. Ideally, however, longer reaction durations than the five to six hours used in these experiments are necessary in order to more accurately determine the stability of any catalyst during FT synthesis. Nevertheless, this study did show that FT synthesis over a 100% Fe catalyst is feasible for the production of hydrocarbons in the range of C₁-C₁₃, indicating that pure iron could potentially be used for the production of liquid hydrocarbon fuels. Due to the relatively low cost of iron as a material, in comparison to cobalt-based catalysts and other conventional FT catalysts, this could potentially offer significant process savings, and therefore further investigation into this topic can be recommended for future investigation.

The effects of temperature, pressure and space velocity were studied by Liu *et al.* [44] using an Fe-Mn catalyst in a CSTR under the following FT synthesis reaction conditions (260-290°C, 9-30 bar, H₂/CO ratio = 1.0, GHSV = 0.46-1.85 h⁻¹, and m_{cat} = 4.75g). Their results showed that CO conversion increased with increasing temperature, increasing pressure and decreasing space velocity, whereas the C₅₊ hydrocarbon selectivity was reported to decrease with both increasing temperature and space velocity; all in agreement with the findings of Feyzi, Irandoust, and Mirzaei [103] and Jung *et al.* [106]. Contrary to the findings of these two other research groups, however, Liu *et al.* report that the C₅₊ hydrocarbon selectivity was relatively unaffected by variation in pressure. The influence of the H₂/CO molar ratio was also separately investigated by Liu *et al.* in the same publication, using the same CSTR, as well as a fixed-bed reactor, under the following reaction conditions (300°C, 20 bar, GHSV = 1300 h⁻¹, and H₂/CO = 0.8-2.5). In agreement with the findings of Mirzaei, Vahid and Feyzi [86], CO conversion was observed to increase with increasing H₂/CO molar ratio in both reactors, whereas the opposite trend was reported for the C₅₊ selectivity. However, significantly higher CO conversions and C₅₊ selectivities were achieved in the fixed bed reactor (15-20% higher, on average) than in the CSTR for the same H₂/CO molar ratios. From these results it can be seen that the selection of the appropriate H₂/CO molar ratio also plays a significant role in the FT synthesis reaction, and can significantly improve the catalyst performance, irrespective of the reactor type used. It could also be deduced that the fixed-bed reactor used in this study was more favourable for the production of liquid hydrocarbons than its CSTR counterpart.

The influence of pressure and temperature on the production of diesel range hydrocarbons and heavy waxes was investigated by Farias *et al.* [105] in a one litre CSTR using a Cu and K promoted Fe catalyst supported on SiO₂ under the following reaction conditions (240-270°C, 20-30 bar, H₂/CO = 1.0, and m_{cat} = 10g). The products obtained in this study were reported to be mainly n-paraffins, and their results showed that the relationship of temperature and pressure to the liquid product distribution was not straight-forward for the Fe catalyst implemented. At lower temperatures (~240°C), an increase in pressure resulted in the increased formation of lower molecular weight compounds as opposed to heavy waxes. At higher temperatures (~270°C) a decrease in pressure gave higher yields of C₂₁-C₂₅. Wax formation was favoured at pressures between 24-27 bar, whereas variation in temperature at these pressures did not significantly

influence wax formation. Higher pressures and temperatures, however, resulted in the formation of heavier waxes (C_{35+}). The results of this study indicate that reaction conditions can be adjusted in order to selectively narrow the product distribution and maximize the yields of targeted products, such as diesel.

Although specific hydrocarbon products were not targeted it was also shown in a study by Wang *et al.* [101] that liquid hydrocarbon (and wax) yields could be maximized with increasing pressures. These results were found using a fixed-bed micro-reactor (I.D. = 18mm, L = 30cm) and an industrial Fe/Cu/K catalyst under the following conditions: (220-270°C, 11-31 bar, GHSV = 4.0-10.0 h^{-1} , and $H_2/CO = 1.0-3.0$). However, no reactant conversion or product selectivity data was provided in this study by Wang *et al.* for comparison with other studies or with the work carried out in this project.

The influence of temperature, pressure and H_2/CO molar ratio using both unsupported and silica-supported Fe catalysts was studied by Hayakawa, Tanaka and Fujimoto [90] in both a 0.1 litre CSTR and a one litre CSTR under the following conditions (240-280°C, 10-29 bar, $H_2/CO = 0.4-2.0$, and $m_{cat} = 3.0$ and 15g, respectively). At lower temperatures (< 260°C), CO conversion and C_{5+} selectivity were found to both increase as the pressure was increased, but the results were more pronounced in the case of the silica-supported Fe catalyst. At higher temperatures (> 260), higher C_{5+} selectivities were obtained with the unsupported catalyst as the pressure was increased, resulting in significantly higher liquid hydrocarbon yields. The trends in CO conversion and C_{5+} selectivity resemble those reported by Feyzi, Irandoust, and Mirzaei [103] and Dasgupta and Wiltowski [88]. Higher CO conversions were also achieved as the H_2/CO molar ratio was increased, which was also observed by Mirzaei, Vahid and Feyzi [86] and Liu *et al.* [44]. However, contrary to the findings of these two other research groups, Hayakawa, Tanaka and Fujimoto report that an increasing H_2/CO molar ratio resulted in higher C_{5+} selectivities. The silica-free catalyst, however, displayed the highest activity (CO conversion) between H_2/CO molar ratios of 0.4-1.0, whereas further increases to the H_2/CO molar ratio did not influence the catalyst activity or the C_{5+} selectivity. Different catalyst supports and promoters were used in each of these studies, in different types of reactors and therefore accurate comparisons are difficult to make. However, what can be drawn from the study by Hayakawa, Tanaka and Fujimoto is that the catalyst support also significantly influences the activity and selectivity of iron catalysts. For instance, the silica support enhanced the catalyst activity and the C_{5+} selectivity at lower H_2/CO molar ratios. These results indicate that silica supported iron catalysts are potentially more suitable for H_2 deficient syngas, which is commonly generated in BTL applications.

The influence of temperature and space velocity using a Cu and K promoted Fe catalyst supported on SiO_2 was examined by Jung *et al.* [106] in a slurry reactor under the following conditions (245-265°C, 25 bar, GHSV = 2.6-3.9 h^{-1} , $H_2/CO = 1.0$, and $m_{cat} = 720g$). Their results showed that higher

temperatures favoured CO conversion and the selectivity to methane and light hydrocarbons, but not the liquid hydrocarbon (C₆₊) yields. An increase in space velocity was reported to result in decreasing CO conversions and higher C₆₊ selectivities, amounting to a higher liquid hydrocarbon or oil production rate. Similar results were also reported by Feyzi, Irandoust, and Mirzaei [103] and Liu *et al.* [44].

2.6.2 Studies Using Cobalt Catalysts

Research on the product distribution in FT synthesis using cobalt-based catalysts goes back to the time of the discovery of the process in Germany (discussed previously in section 2.1). The results from these early studies in Germany, as well as other studies carried out at later dates, were summarized in a review by Storch *et al.* [108]. The work performed on the Co/ThO₂/MgO/Kieselguhr catalysts used in these studies reported that wax selectivity increased with decreasing H₂/CO molar ratios and increasing reactor pressure. Optimum wax selectivity was reported at reactor pressures between 5-9 bar. Since this early research, studies on cobalt-based catalysts have primarily focused on catalyst preparation techniques, as well as catalyst structural supports and promoters and their influence on catalyst activity and product selectivity. However, studies that have addressed the influence of reaction conditions, and reactor pressure in particular, on the catalyst activity, catalyst stability, the product distribution and the product yields using cobalt-based catalysts are relatively few. Studies that specifically address the influence of low reactor pressures (1-20 bar) are even less. The influence of reaction conditions using cobalt-based catalysts in these particular studies have been investigated at a laboratory-scale in mainly fixed-bed reactors (and some in slurry reactors). Some earlier studies have also been included in the review below [87, 109]. From these studies, only a small number expressly examine the influence of low reactor pressures (within the range of 1-20 bar) on catalyst activity and FT product distribution [46, 83, 109, 110], and are also reviewed below. The reaction conditions investigated in all the studies using cobalt-based catalysts reviewed in this section are summarized in Table 2.4 below.

Table 2.4 – Summary of cited parameter studies using cobalt-based catalysts

	Catalyst	Reactor Type	T (°C)	P (bar)	H₂/CO	GHSV (h⁻¹)	m_{cat} (g)	Reference	Year
1	Co/Kieselguhr	Fixed-bed	157-240	1,6 and 11	0.5-2.0	0.93-6.25	-	Gibson and Hall [87]	1954
2	Co/Rurchemie	1 L CSTR	220-240	5-15	1.5-3.5	0.008-0.085	-	Yates and Satterfield [109]	1992
3	Co-Ni/ZrO ₂	Fixed-bed (I.D. = 4mm, L = 23cm)	240-260	1-31	1.0	5-25 (WHSV)	0.1	Sethuraman <i>et al.</i> [46]	2001
4	Co-Re/Al ₂ O ₃	1 L CSTR	220	20	2.0	1.0-8.0	20.0	Das <i>et al.</i> [111]	2003
5	Co/SiO ₂	Fixed-Bed (I.D. = 6.35mm)	200-220	1 and 9	1.0-3.0	-	2.0	Sharifnia, Mortazavi and Khodadadi [112], [113]	2005, 2008
6	Co-Pt-ZrO ₂ /Al ₂ O ₃	Fixed-bed	200-220	5-35	2.0	0.5 and 1.0	1.0	Xu <i>et al.</i> [83]	2006
7	Co/SiO ₂	Fixed-bed (I.D. = 20mm, L = 60cm)	230	2-20	2.0	2.0	6.0	Zheng <i>et al.</i> [110]	2007
8	1) Co/γ-Al ₂ O ₃ 2) Co-Re/γ-Al ₂ O ₃	Fixed-bed (I.D. = 9.3mm)	210	20	1.0-2.1	0.85-1.2	1.0	Tristantini <i>et al.</i> [114]	2007
9	CuO–CoO–Cr ₂ O ₃ (+ MFI Zeolite)	Fixed-bed (I.D. = 13mm, L = 29cm)	225-325	28-38	1.0-2.0	0.457-0.850	3.0-5.0	Mohanty <i>et al.</i> [91]	2010
10	1) Co/Al ₂ O ₃ 2) Ru- Co/Al ₂ O ₃	Slurry (I.D. = 50mm, L = 150cm)	210-250	10-30	2.0	1.0-6.0	-	Woo <i>et al.</i> [115]	2010
11	1) Co/Al ₂ O ₃ 2) Ca–Co/Al ₂ O ₃	Fixed-bed (I.D. = 18mm, L = 100cm)	210-300	20	0.5-2.0	4.0-12.0	5.0	de la Osa <i>et al.</i> [89]	2011
12	Co/Al ₂ O ₃	Fixed-bed (I.D. = 27mm, L = 200cm)	200	20	-	0.037-0.180	-	Rafiq <i>et al.</i> [116]	2011

Later work on the influence of reaction conditions on the product distribution in FT synthesis using cobalt catalysts includes a study by Gibson and Hall [87] in 1954. According to the claims of these authors, the majority of the FT research and process development up to and at the time of their publication concentrated on iron catalysts, with very little work investigating the effects of reaction conditions on the nature of the products. The experiments in their study were carried out in laboratory-scale fixed-bed reactors using eleven different Co/Kieselguhr catalysts (representative of industrial catalysts and support materials used at the time), under the following reaction conditions (157-240°C, 1 and 11 bar, GHSV = 0.93-6.25 h⁻¹, and H₂/CO = 0.5-2.0). Their work investigated the effects of reactor temperature, reactor pressure, and the H₂/CO molar ratio in the feed syngas on the olefin and alcohol content of liquid and wax products (C₅₊) and the molecular weight distribution of the products. The results of this early FT work pointed out that these reaction parameters did not influence the reaction independently of each other, revealing more complex relationships than had initially been anticipated at the time. For instance, wax production decreased with increasing reactor temperature at a pressure of one bar, whereas an increase in reactor temperature at 11 bar resulted in a rapid increase of wax formation. Overall, the average molecular weight of the products was reported to decrease with increasing temperature and increasing H₂/CO molar ratio in the feed syngas. A similar observation at similar pressures (1 and 9 bar) was also made by Sharifnia, Mortazavi and Khodadadi [112, 113]. An increase in pressure was reported to result in higher reactant conversions and a higher average molecular weight of the products. This can be considered equivalent to a high C₆₊ hydrocarbon product selectivity and is therefore in agreement with the findings of more recent studies carried out at low reactor pressures (1-20 bar), which are reviewed further down, by Xu *et al.* [83], Zheng *et al.* [110], and Sharifnia, Mortazavi and Khodadadi [112, 113]. Other investigations, including those by Sethuraman *et al.* [46] and Woo *et al.* [115], conducted at higher pressures (15-30 bar), however, report that an increase in pressure resulted in lower C₆₊ hydrocarbon product selectivities. The results from all these studies indicate that an optimum C₆₊ hydrocarbon selectivity, and therefore optimum liquid hydrocarbon yields, can be achieved at low pressures in the range of 5-15 bar, as discussed previously in section 2.5.2.

Interestingly, the findings from a different investigation on the effects of low reactor pressures (as well as reactor temperature, space velocity and H₂/CO molar ratio) on FT product distribution by Yates and Satterfield [109] showed that variation in both reactor temperature and reactor pressure did not have a significant effect on the C₆₊ hydrocarbon product distribution. This observation is in opposition to the findings of more recent studies, but this may be attributed to the differences in formulation of the catalyst used by Yates and Satterfield in comparison to that of the more modern cobalt catalysts used in the other studies. The intent of their study was to obtain optimal yields of diesel range products and waxes using a Co-Mg/diatomaceous earth catalyst in a one litre CSTR

reactor under the following reaction conditions: (220C-240°C, 5-15 bar, GHSV = 0.008-0.085 h⁻¹, and H₂/CO = 1.5-3.5). The yield of C₆₊ hydrocarbon products was reported to increase with increasing space velocity and decreasing H₂/CO molar ratio; an observation which was also made by Tristantini *et al.* [114]. Their work, however, fails to report a set of process conditions for obtaining optimal yields of diesel and/or waxes.

More recent work on the influence of reactor pressure (covering a wider range of values from 1-31 bar), as well as reactor temperature and the space velocity on reactant conversion and product distribution was performed by Sethuraman *et al.* [46] in a fixed-bed micro-reactor (ID = 4mm, L = 23cm) over a Co-Ni/ZrO₂ catalyst under the following reaction conditions: (240-260°C, 1-31bar, WHSV = 5-25 h⁻¹, and m_{cat} = 0.1g). The work concentrated on mainly improving the yields of C₄ hydrocarbons (such as iso-butane), which are important in polymer manufacture, and therefore incorporated the use of a secondary catalyst bed or follow bed in the experiments (using a C₄ hydrocarbon selective sulphated-ZrO₂ catalyst), and compared the yields with a single-bed containing the Co-Ni/ZrO₂ catalyst. Thus only the results of the single-bed experiments are relevant for comparison and are, therefore, discussed here. In agreement with the other studies reviewed in this section, Sethuraman *et al.* report that an increase in temperature resulted in lower C₅₊ hydrocarbon selectivities and this was attributed to an increased rate of thermal cracking at higher temperatures. The CO conversion was also reported to increase as the space velocity was increased; the CO₂ selectivity also increased, but at the expense of the weight fraction of C₆₊ hydrocarbons, for which the opposite trend was observed. The trends reported by Sethuraman *et al.* for the weight fraction of C₆₊ hydrocarbons are in agreement with the other literature findings reviewed below; those observed for CO conversion are in opposition to these other studies. However, this may be due to the ZrO₂ supported catalysts used by Sethuraman *et al.* as opposed to the alumina supported catalyst mainly used in the other studies. As discussed previously in section 2.4, the catalyst support can have a significant influence on the catalyst activity and product distribution. An increase in pressure from 1-31 bar was reported by Sethuraman *et al.* to result in significantly higher CO conversions and methane formation. A different trend was reported for the weight fraction of C₆₊ hydrocarbon selectivity which decreased significantly as the pressure was increased from 1 to 11 bar, was then relatively unaffected by a further increase from 11 to 21 bar, but then decreased markedly as the pressure was further increased from 21 to 31 bar. These results do not agree with those reported in other investigations, such as those by Xu *et al.* [83], Zheng *et al.* [110], and Mohanty *et al.* [91], where an increase in pressure (up to 20-25 bar) resulted in higher C₅₊ selectivities. This may be due to the lower H₂/CO ratio of 1.0 used in this particular study by Sethuraman *et al.* [46], as opposed to the ideal molar ratio of 2.0 used in the other studies that is generally recommended for cobalt-based catalysts (as discussed previously in section 2.4.2).

Sethuraman *et al.* report that the highest weight fraction of C₆₊ hydrocarbon products (52%) were obtained at the following reaction conditions: (250°C, 1 bar, WHSV = 5 h⁻¹, and H₂/CO = 1.0).

The influence of a wide range of reactor pressures, as well as reactor temperature, on the FT product distribution were also investigated by Xu *et al.* [83] over a Co/Al₂O₃-Pt/ZrO₂ catalyst in a fixed-bed reactor under the following reaction conditions: (200-220°C, 5-35 bar, GHSV = 1.0 h⁻¹, and H₂/CO = 2.0). This study mainly concentrated on the influence of nitrogen content in the feed syngas (10-50%), however, both temperature and pressure were reported to have a significant effect on CO conversion and product selectivity. As expected [43, 87], an increase in temperature was reported to result in higher CO conversions, CH₄ selectivities and CO₂ selectivities, but lower C₅₊ hydrocarbon selectivities. An increase in pressure from 5-15 bar was reported to result in increasing CO conversion, however, further increases in pressure had very little influence on CO conversion. The selectivity of C₅₊ hydrocarbons was also reported to increase with increasing reactor pressure, whereas that of CH₄ decreased as expected. Similar trends for the performance of cobalt-based catalysts with increasing temperature were reported by Bechara, Ralloy and Vanhove [117], and with increasing reactor pressure by Das *et al.* [111] using unpromoted and Re-promoted Co/Al₂O₃ catalysts. The trends reported for the influence of reactor pressure are important as they indicate that pressure has a significant effect only in the low range of 1-15 bar, as discussed previously in section 2.5.2, which further favours the case for exploring FT synthesis operation at lower reactor pressures in this project.

A study that exclusively explored the effects of reactor pressure on the FT product distribution was carried out by Zheng *et al.* [110] in a fixed-bed reactor (I.D. = 20mm, L = 60cm) over a Co/SiO₂ catalyst under the following reaction conditions: (230°C, 2-20 bar, GHSV = 2.0 h⁻¹, H₂/CO = 2.0 and m_{cat} = 6.0g). Similar to the results reported above by Xu *et al.* [83], both the CO conversion and the C₅₊ selectivity were reported to increase as the pressure was increased, whereas the opposite trend was reported for the selectivity of CH₄ and light hydrocarbon compounds (C₂-C₄). Once again, at reactor pressures above 15 bar little change was reported in both CO conversion and product distribution, providing further evidence that the operating pressure has a significant influence on the FT synthesis product distribution only at values below 15 bar.

The influence of reactor temperature, reactor pressure and space velocity on CO conversion and the selectivity of C₁₁₊ hydrocarbon products (diesel and waxes) were investigated by Woo *et al.* [115] using a Co/Al₂O₃ and a Ru/Co/Al₂O₃ catalyst in a slurry bed reactor under the following reaction conditions: (210-250°C, 10-30bar, GHSV = 1.0-6.0 h⁻¹, and H₂/CO = 2.0). Optimum C₁₁₊ hydrocarbon product selectivity and yields were reported at reactor temperatures between 220-230°C and a reactor pressure of 20 bar. The promoted catalyst was reported to display a better and higher stability in CO conversion than its unpromoted counterpart. The selectivity of C₁₁₊

hydrocarbons was reported to decrease with increasing reactor temperature and increasing reactor pressure (above 20 bar) in agreement with other studies reviewed in this section, such as those by Sethuraman *et al.* [46] and Xu *et al.* [83], whereas an increase space velocity resulted in higher C₁₁₊ selectivities. Opposing results for the influence of space velocity on the FT product distribution are found in the literature, with some investigations, such as those by Sethuraman *et al.* [46], and Mohanty *et al.* [91] reporting the opposite trend. This demonstrates that the effect of the space velocity on the product distribution is difficult to predict and must be determined experimentally for each specific reactor system, reaction conditions and catalyst used.

The influence of reactor temperature, reactor pressure, space velocity and H₂/CO molar ratio in the feed syngas on the catalyst activity and FT product distribution were investigated by Mohanty *et al.* [91] over a CuO–CoO–Cr₂O₃ catalyst mixed with MFI Zeolite in a fixed-bed reactor (I.D. = 13mm, L = 29cm) under the following reaction conditions: (225-325°C, 28-38 bar, GHSV = 0.457-0.85 h⁻¹, H₂/CO = 1.0-2.0 and m_{cat} = 3.0-5.0g). Overall, reactor temperature and pressure were found to be the most influential parameters on the yield and selectivity of C₅₊ hydrocarbons. Their results showed that CO conversion increased with increasing reactor temperature, reaching a maximum value at 275°C, and thereafter decreasing as the temperature was raised further. This can be attributed to excessive -CH₂- monomer hydrogenation at higher temperatures, as well as increased sintering of the catalyst as the temperature exceeds 275°C (as discussed previously in section 2.5.1). This observation has not been made by other investigations that were carried out over similar temperature ranges, reviewed in this section, but a similar behaviour was noted by Mirzaei, Vahid and Feyzi for iron-based catalysts in section 2.6.1. Optimum C₅₊ hydrocarbon selectivity was reported at temperatures in the range between 240 and 260°C, which is within the optimum range for operation with cobalt-based catalysts as commonly recommended in the literature [60]. An increase in H₂/CO molar ratio was reported to result in lower CO conversions and higher C₅₊ hydrocarbon selectivities, an observation which differs from the findings of other investigations on the influence of the H₂/CO ratio on the catalyst activity and product distribution, such as those by de la Osa *et al.* [89] and Tristantini *et al.* [114]. However, these other studies were conducted at lower reactor pressures (20 bar) and over Al₂O₃ supported cobalt catalysts which may significantly influence the outcome of the synthesis reaction. An increase in space velocity was reported by Mohanty *et al.* to result in lower CO conversions, whereas the overall hydrocarbon selectivity increased with space velocity, peaking at GHSV = 0.585 h⁻¹, but thereafter decreasing as the space velocity was further increased. The formation of liquid hydrocarbons (C₈₊), however, was reported to decrease steadily with increasing space velocity. An increase in pressure was found to favour CO conversion and to significantly influence the product distribution favouring the formation of heavier hydrocarbons (C₈₊), whereas the opposite trend was reported for gaseous hydrocarbons (C₁-C₃). However, no data on the influence of reactor pressure on the product selectivity was provided

by Mohanty *et al.* for comparison of results with other studies or the work carried out in this project.

Similar trends for the influence of space velocity on CO conversion and C₅₊ hydrocarbon selectivity were also reported by Rafiq *et al.* [116] using a Co/Al₂O₃ catalyst in a fixed-bed reactor (I.D. = 27mm, L = 200cm) under the following reaction conditions: (200°C, 20 bar, GHSV = 0.037-0.18 h⁻¹, and H₂/CO = 2.0). It was reported that with increasing space velocity, CO conversion decreased, C₅₊ selectivity increased and, overall, the hydrocarbon productivity increased. The C₅₊ selectivity was found to reach a maximum value as the space velocity was increased from 0.037-0.111 h⁻¹ and thereafter declined with further increase in the space velocity. Their results demonstrated yet again that the relationship that exists between the space velocity and the product distribution is not straight forward and may be unique for specific reactor systems, catalysts and reaction conditions.

The influence of the H₂/CO molar ratio in the feed syngas and the space velocity on the product distribution were studied by Tristantini *et al.* [114] in a fixed-bed reactor (I.D. 9.3mm) over a Co/Al₂O₃ and a Re-Co/Al₂O₃ catalyst under the following reaction conditions: (210°C, 20 bar, GHSV = 0.85-1.20 h⁻¹, H₂/CO = 1.0-2.1, and m_{cat} = 1.0g). The space velocity was adjusted in the case of each catalyst in order to achieve similar CO conversions and allow fairer comparison. An increase in space velocity was reported to result in lower CO conversions and higher C₅₊ hydrocarbon selectivities for both catalysts. As discussed above, the results reported in the literature cited in this section are not conclusive, as similar trends for the C₅₊ hydrocarbon selectivity were observed by Woo *et al.* [115] and Rafiq *et al.* [116] (who worked at similar reactor temperatures and pressures of ~20 bar, but at either lower or higher space velocities), whereas the opposite trends are reported by other research groups, including de la Osa *et al.* [89], Mohanty *et al.* [91] and Sethuraman *et al.* [46]. Tristantini *et al.* also report that an increase in the H₂/CO molar ratio in the feed syngas resulted in higher CO conversions and lower C₅₊ selectivities, which was also observed by Sharifnia, Mortazavi and Khodadadi [112, 113], whereas the opposite trends were reported by de la Osa *et al.* [89] and Mohanty *et al.* [91]. Interestingly, in this particular study by Tristantini *et al.* [114], the hydrocarbon selectivities were similar at H₂/CO ratios of 1.5 and 2.1, which may be of particular interest when applied to a BTL-FT concept implying lower syngas conditioning requirements, as will be discussed later in section 2.7.3.2. It was also reported that the variation in the H₂/CO ratio had a much more marked effect on the Re promoted Co/Al₂O₃ catalyst than the unpromoted CoAl₂O₃ catalyst, although the Re-Co/Al₂O₃ catalyst displayed a higher activity and selectivity towards C₅₊ hydrocarbons than its counterpart at all the H₂/CO molar ratios examined. An assumption that can be drawn from the study by Tristantini *et al.*, therefore, is that if low reactant conversions are acceptable in the FT process using the same catalysts, then lower H₂/CO molar ratios in the feed syngas could potentially be used in order to achieve higher C₅₊

hydrocarbon selectivities. This would imply avoiding the use of a WGS (shift) reactor prior to the FT reactor in order to adjust the H₂/CO ratio of a typical biosyngas. However, in a BTL-FT complex where maximum liquid fuel yields are desirable, the option of eliminating the shift reactor step has to be weighed against the cost of syngas conditioning and cleaning, as well as the cost of FT reactor off-gas recycling and conditioning (as will be discussed later in section 2.7.3.2).

The influence of space velocity and the H₂/CO molar ratio, as well as the reactor temperature, on the distribution of hydrocarbon products (particularly diesel range products) was also investigated by de la Osa *et al.* [89], using a Co/Al₂O₃ and a Ca-Co/Al₂O₃ catalyst in a fixed-bed reactor (I.D. = 18mm, L = 100cm) under the following reaction conditions: (210-242°C, 20 bar, GHSV = 6.0-12.0h⁻¹, H₂/CO = 0.5-2.0 and m_{cat} = 5.0g). Their results showed that the unpromoted catalyst was more markedly influenced by reaction conditions than its promoted counterpart. CO conversion was found to increase with increasing temperature, decreasing space velocity and increasing H₂/CO molar ratio for both catalysts. In contrast, the selectivity of C₅₊ hydrocarbons was reported to decrease with increasing reactor temperature and increasing space velocity. No definite trend was reported for the C₅₊ selectivity with increasing H₂/CO molar ratio, although, the results still point towards higher C₅₊ selectivity at low H₂/CO molar ratios (0.5-1.0), which can lead to the same assumption made in the previous paragraph.

The influence of the same parameters, reactor temperature and H₂/CO molar ratio, on the activity and product distribution, this time using a Co/SiO₂ catalyst were examined by Sharifnia, Mortazavi and Khodadadi [112, 113] using a fixed bed reactor (I.D. = 6.35mm) under the following conditions: (200-220°C, 1 and 9 bar, H₂/CO = 1.0-3.0 and m_{cat} = 2.0g). As expected, it was reported that higher CO conversions and lower C₅₊ hydrocarbon selectivities resulted from an increase in both reactor temperature and the H₂/CO molar ratio in the feed syngas. This was also reported by Tristantini *et al.* above. Although reactor pressure was not a parameter that was examined more extensively by Sharifnia, Mortazavi and Khodadadi, higher CO conversions and C₅₊ selectivities were reported at the higher pressure of 9 bar they investigated.

2.6.3 Summary of Findings from Parameter Studies found in the Literature

The studies using iron and cobalt-based catalysts reviewed in sections 2.6.1 and 2.6.2 above, illustrated the influence of reaction conditions on catalyst activity and FT product distribution, and highlighted the importance of the selection of the appropriate conditions for achieving a narrow distribution of products or, in other words, targeting a particular grade(s) of products, such as diesel or waxes. The following conclusions can be drawn from the studies that were reviewed in sections 2.6.1 and 2.6.2 above:

- In comparison to the wealth of literature available on FT synthesis, publications that are related to the investigation of the influence of reaction conditions (reactor temperature, reactor pressure, space velocity and the H₂/CO molar ratio in the feed syngas) on the catalyst activity, catalyst stability, product distribution and product yields are relatively few in number. In addition, the majority of the studies that do examine the influence of reactor pressure are carried out at pressure ranges used in typical FT processes (20-40 bar). Studies that specifically address the influence of low operating pressures (1-20 bar) on catalyst activity, product selectivity, etc., using either iron or cobalt-based catalysts, are actually very limited in number.
- The general consensus in these studies appears to be that the most influential parameters on the catalyst activity, the product distribution and the product yields in FT synthesis are the reactor temperature and reactor pressure.
- The most commonly studied iron-based catalysts appear to be promoted with Cu and/or K and supported on silica (SiO₂) or alumina (Al₂O₃), whereas the most commonly studied cobalt-based catalysts seem to be supported on alumina, with a lot of research focusing on the influence of various promoters, including, Ca, Re and Ru. The supports and promoters used were found to have a significant influence on the FT synthesis by enhancing the catalyst reducibility, catalyst activity and could also be used to tailor the product selectivity or distribution.
- It was also widely agreed that an increase in reactor temperature results in higher reactant conversions, and favours the formation of lighter hydrocarbon products for FT synthesis over both iron and cobalt-based catalysts. The C₆₊ hydrocarbon product selectivity decreases, whereas the selectivity of CH₄ and light hydrocarbons (C₂-C₅) increases with increasing reactor temperature. Optimum C₆₊ hydrocarbon selectivities and, therefore, optimum liquid hydrocarbon yields are typically obtained at 250-300°C and 200-250°C using iron-based and cobalt-based catalysts, respectively.
- In general, it appears that reactor pressure has the most significant effect on the product distribution (particularly the C₆₊ hydrocarbon product selectivity) in the low pressure range of 1-20 bar. The C₆₊ selectivity and the liquid hydrocarbon yields have been reported to generally decline as the reactor pressure is increased above pressures in the range of 10-15 bar. As mentioned previously, for both iron and cobalt-based catalysts only a few studies on the influence of low reactor pressures (1-20 bar) have been carried out, but the results that are reported are not always in agreement. Thus, a conclusive trend in the relationship between

reactor pressure and the FT product distribution cannot be presumed from the findings of these studies and, therefore, further investigation is required.

- Different trends are reported in the literature for the influence of space velocity on the catalyst activity and product distribution (using either iron and cobalt-based catalysts), and sometimes a more complex behaviour is observed, depending on the reactor system, operating conditions and catalyst composition implemented. Optimum values for this parameter cannot be simply predicted, therefore, and must be determined experimentally for each study accordingly.
- It would be expected that an increasing H_2/CO molar ratio in the feed syngas would favour the formation of lighter hydrocarbon compounds [91, 98, 99]. However, as discussed previously in section 2.5.4, what is true for space velocity above for both iron and cobalt-based catalysts, is also the case for the influence of the H_2/CO molar ratio in the feed syngas on the product distribution, as contrary C_{6+} selectivity trends are also reported in the reviewed literature. Nevertheless, what can be concluded from the findings of the studies reviewed in sections 2.6.1 and 2.6.2 is that iron-based catalysts can be used with hydrogen deficient syngas (low H_2/CO molar ratios) giving high C_{6+} selectivities. Moreover, it appears that H_2/CO molar ratios in the feed syngas lower than the recommended 2.0 can be used for cobalt-based catalysts to achieve higher C_{6+} selectivities, although this does not necessarily also imply high liquid hydrocarbon yields. Hence, optimum values for this parameter must also be determined experimentally to suit the needs of individual studies undertaken.

2.6.4 Research Gaps

The review of the available literature on the influence of reaction conditions on the product distribution in FT synthesis (sections 2.6.1 and 2.6.2 above) pointed out that only a relatively small number of studies have investigated the influence of reaction conditions on the catalyst activity and product distribution using iron and cobalt-based catalysts. As discussed in section 2.6.3 above, some of the findings from the parameter studies reviewed, related to reactor pressure, space velocity and the H_2/CO molar ratio in the feed syngas, are not always in agreement. This emphasizes the need for further investigation into this area of FT synthesis. The influence of reactor pressure, in particular, has been mainly studied at conventional FT process ranges (20-40 bar). As was concluded in the section 2.6.3 above, reactor pressure appears to have the most significant effect on the product distribution at lower pressures, but its influence at these lower pressures (1-15 bar) is not well documented and therefore requires further exploration. Moreover, studies with the specific intent of maximizing the yields of liquid hydrocarbons, such as diesel, at these lower pressures have not been found, but may have been undertaken in earlier FT work.

In addition to the influence of lower reactor pressures (1-15 bar) on the catalyst activity and product distribution, it would be of interest to incorporate some additional information, as well as some supplementary studies that may not have been previously included or performed in combination as part of one single investigation. This information includes the following:

- The product yields obtained – these are not usually reported in FT synthesis research publications. What is commonly presented is the product distribution or selectivity, which provides information on the molar composition of the hydrocarbon products that are formed, but does not give an overall picture of all the products that are formed during the synthesis reaction and their physical quantities.
- Analyses of the liquid hydrocarbon products that are collected – analyses of their fuel composition (naphtha, diesel and wax content), energy content (or calorific value) and, in the case of the aqueous product, for water content, are very rarely reported in the literature.
- The catalyst stability (in terms of the CO conversion versus time on stream) – this reflects on the performance of the catalyst and provides information on its activity or effectiveness in the synthesis process, as well as how quickly or slowly it deactivates. This is important as, industrially, high and steady catalyst performance over long periods of time are desirable in order to lower the requirement of periodical FT catalyst regeneration or replacement which results in the loss of production and profits.

2.7 BTL-FT – Process Technology

As discussed previously in chapter 1, FT synthesis is a well established technology already commercialized by Sasol and Shell [26]. Hence, it is assumed that the commercial technology used for conventional FT processes can be applied in a BTL-FT plant. The application of FT technology consists of basic steps that begin with the pre-treatment of the biomass feedstock and generation of the syngas via biomass gasification. The syngas (or bio-syngas) is then cleaned and conditioned in order to modify or adjust the H₂/CO molar composition to the specifications necessary in the FT reactor. This is followed by FT synthesis in the FT reactor, and finally, the recovery and/or upgrading of the products [17, 20], as illustrated in Figure 2.7 below. Each of these process stages is discussed in more detail in sections 2.7.1 to 2.7.5.

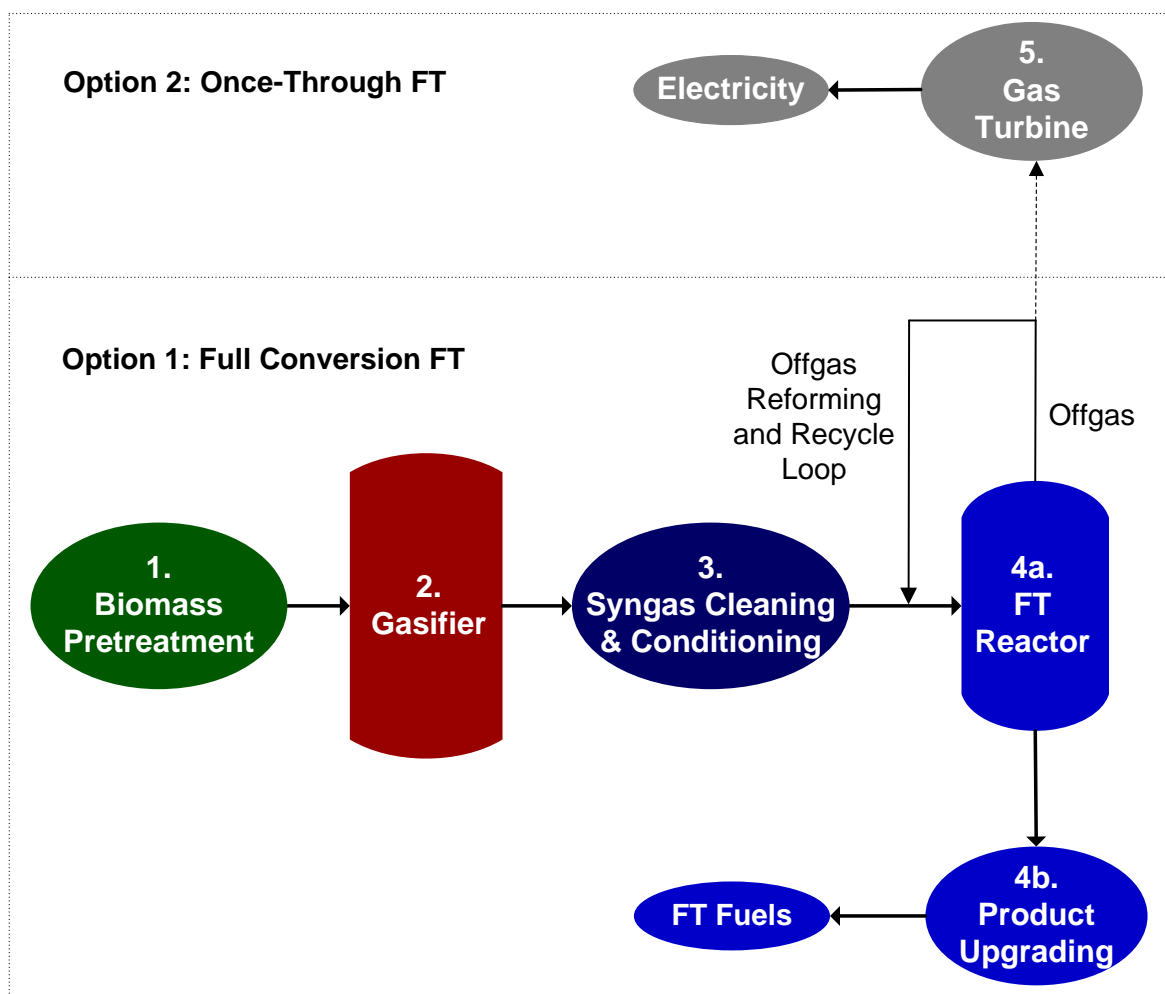


Figure 2.7 - Basic steps in a BTL-FT process

A short review of the status of BTL-FT processing is provided in section 2.8, highlighting the recent developments in the field aiming towards the commercialisation of the technology. There can be a number of possible process configurations for converting biomass to FT liquids. These options relate to the choice of gasifier, gas cleaning and conditioning considerations, FT process (reactor and mode of operation), and the type of products (or by-products, such as SNG and power generation) that are desired [9]. All these different configurations, however, can be divided into two general process schemes [9], as illustrated in Figure 2.7 above:

1. **Full conversion FT** – aimed at maximizing the yields of FT liquid fuels where the FT reactor off-gas (containing methane and C₂-C₄ hydrocarbon gases) is reformed back into syngas and recycled back into the FT reactor (Option 1 in Figure 2.7 above).
2. **Once-through FT** – aimed towards achieving maximum energy efficiency where the FT reactor off-gas is completely combusted in gas turbines for power generation (Option 2 in Figure 2.7 above).

2.7.1 Step 1 – Biomass Pretreatment

The first stage in the overall FT process has to do with preparation of the biomass feedstock, so as to enable steady feeding into the gasifier. This involves several steps that begin with receiving the biomass, storage and handling, as well as some pre-treatment processes such as drying, screening and size reduction [8, 12, 118], or even torrefaction [119]. Drying is a vital pre-treatment process as biomass can contain high levels of moisture (30-45%) which needs to be reduced significantly (down to 10-15%) in order to improve the efficiency of the gasifier [9, 118, 120]. This is an energy intensive step, but the energy required can be recovered from the excess process heat, or the steam produced during FT synthesis in order to improve overall process economics [9, 120].

2.7.2 Step 2 – Gasification

The integration of biomass gasification with downstream syngas conversion into liquid transport fuels via FT synthesis is currently at a very early stage in its commercial development, despite the fact that both biomass gasification and syngas conversion technologies separately exist at commercial scales in industry. The main hindrances to the commercialisation of BTL-FT have to do with the gas clean-up, as well as economies of scale which are important in biomass applications because, as opposed to capital costs, feedstock costs increase with increasing plant capacity and are, therefore, the limiting factor to higher BTL plant capacities [12, 92]. Research is still needed for more efficient biomass pre-treatment, biosyngas generation, and the subsequent gas cleaning and conditioning, as these operations have been commonly reported to pose the most difficulties and comprise the majority of the capital and plant running costs in a typical commercial FT complex. According to several authors [21, 55, 119, 121] these process steps account for approximately 60-70% of the total plant costs. The gasification pressure, as well as the gasification medium that is implemented, significantly influence the capital and operating costs of the gasifier as well as other downstream equipment [12], making the gasification step vital in the BTL-FT process. Operation of the gasifier (as well as other downstream equipment) at lower pressures than those used in conventional FT processes could potentially offer significant cost reductions which would improve the overall plant economics. These potential cost reductions were discussed previously in section 2.5.2.

Once the biomass feedstock is pre-treated, the second process step involves the generation of the syngas that is necessary for FT synthesis. To do this, the pre-treated biomass feedstock has to undergo gasification. This is a thermal conversion technology in which the biomass is completely broken down into syngas, volatiles, char and ash in a gasifier [122]. Syngas is a gas mixture comprised mainly of carbon monoxide, hydrogen, methane and carbon dioxide as well as other minor components [8] (section 2.7.2.2, below). Gasification is an endothermic process which involves three steps. As the biomass is heated in the gasifier (at 100-150°C), first the moisture

content is driven off. This is then followed by pyrolysis, in which the volatile components in the biomass are vaporized (at 250-550°C), producing volatile vapours (including CO, H₂, CO₂, hydrocarbon gases, water and tar), as well as char and ash which are not vaporized during the pyrolysis step [122, 123]. In the last step, the volatile vapours and the char are gasified through partial oxidation with oxygen (direct or autothermal gasification at <1000°C) or steam (indirect or allothermal gasification at >1200°C) [8, 25].

Although air is the most commonly used gasification agent in biomass gasification [123], it would not normally be used as a gasification agent in BTL-FT applications as this would result in a syngas containing high concentrations of nitrogen [122]. Hence, when oxygen or steam are used as the gasification agent the amount of nitrogen within the system is brought down to a minimum. Firstly, this ensures that the syngas produced contains high concentrations of H₂ and CO, which is important for maintaining a high reaction rate in the FT reactor as well as high C₅₊ hydrocarbon selectivity [9]. Secondly, this reduces the equipment size that is used, and therefore capital costs, as much lower gas volumes are handled [8]. Thirdly, the lack of inert gas dilution in the syngas contributes to the much higher heating values of syngas derived from oxygen or steam gasification [8]. Moreover, in the case of full conversion FT (Figure 2.7 above), where reforming and recycling of the FT reactor off-gas (which contains unreacted syngas, methane and hydrocarbon gases) are carried out for maximum production of biofuels, the level of inert gases must also be kept at a minimum in order to avoid their accumulation within the system. Conversely, there have been a few laboratory-scale studies investigating the use of nitrogen-rich syngas (up to 50 vol.%) in FT synthesis that concluded on its suitability for the conversion process [83, 116]. Despite the suitability of nitrogen-rich syngas for the FT synthesis reaction at a laboratory scale, however, industrial gasification using air would result in a significant increase in gasifier and downstream equipment size and capital costs [12, 120]. For full conversion FT, therefore, oxygen and steam blown gasifiers (and CO₂ removal units which are discussed in section 2.7.3.2) would be more suitable.

2.7.2.1 *BTL-FT Gasifiers*

There are a number of atmospheric and pressurized gasifier designs that are commercially available for syngas production, operating at temperatures in the range of 800–1500°C [124]. These gasifiers can be categorized according to the gasification agent (steam or oxygen), the pressure, temperature, fluid dynamics and the mode of heat supply that are used (direct or indirect) [125]. These parameters, the type of feedstock and gasifier that are used, as well as the final application of the syngas all define the specifications of the syngas that is produced [25]. Generally, there are three types of gasifier designs and these include fixed-bed, fluidized-bed and entrained-flow reactors [122, 126].

As discussed previously, full conversion FT applications require a minimum concentration of inert gases, like nitrogen, in the syngas and therefore oxygen and steam are the preferred gasification agents. Oxygen-blown entrained-flow gasifiers (direct or autothermal gasification) have been considered as one of the most suitable reactor technologies for BTL-FT applications [123]. These types of gasifiers operate at high temperatures ($>1200^{\circ}\text{C}$) and allow for pressurized operation. The syngas produced from this type of gasification processes contains almost no tars (as they are completely cracked during operation at these elevated temperatures) and low levels of methane (less than 1%), allowing for simpler gas cleaning requirements prior to the FT reactor and making the syngas more suitable for FT synthesis [25, 123]. However, direct or autothermal gasification with oxygen requires an air separation unit, which is an energy and cost intensive operation to integrate on site that could become more economical in large scale BTL-FT applications [25]. In comparison, steam-blown fluidized-bed gasifiers (indirect or allothermal gasification), which operate at lower temperatures ($< 1000^{\circ}\text{C}$) and also allow for pressurized operation, can also potentially be used for BTL-FT applications [25]. The syngas produced from these types of gasification processes, however, would contain higher levels of tars (due to the lower operating temperatures) and methane ($\sim 10\%$), requiring additional tar cleaning operations prior to the FT reactor [25]. One of the main advantages of this type of gasification process, though, is that it does not require an air separation unit on site [25].

As opposed to atmospheric gasification, pressurized gasifier operation would be more suitable for BTL-FT applications because the FT reactor operates at higher pressures (typically 25-60 bar), and therefore, if the syngas is already pressurized, this potentially removes the costs of syngas compression prior to the FT reactor. This would be true even at the lower FT reactor pressures investigated in this project (2-10 bar), where pressurized gasification would need to take place at a few bar higher than the pressure in the FT reactor. A pressurized gasifier would also mean higher capacities and a reduced gasifier size due to the lower gas volumes processed and therefore lower capital costs. In addition, Tijmensen *et al.* [9] report that a pressurized gasifier in a BTL-FT application would contribute to a higher overall energy efficiency, because of the higher energy consumption that would otherwise be required for syngas compression after an atmospheric gasifier.

2.7.2.2 Syngas Composition

The composition of the syngas produced depends on several factors which include the gasification conditions that are employed, such as reactor type and operating temperature [125, 126], as well as the properties of the feedstock that is used. These properties include the carbon, hydrogen and oxygen content (ultimate analysis) of the biomass, its moisture content, its volatile matter and ash content (proximate analysis), its energy content, as well as physical properties like the particle size

and bulk density [124]. For instance, when compared to natural gas, biomass contains less hydrogen and more oxygen, which lowers the gasification conversion efficiency as more carbon is released as CO₂, carrying a lot of excess heat [127]. As a result of this elemental composition in the biomass feedstock, biosyngas has a lower H₂/CO ratio (0.5-1.8, as opposed to 2.0 or higher in the case of natural gas-derived syngas) [47]. A typical biosyngas is a mixture of compounds containing mainly hydrogen, carbon monoxide and carbon dioxide, as well as other minor constituents. This is because during gasification, elements that are normally found in biomass, like carbon, hydrogen, nitrogen, oxygen, sulphur, and chlorine are turned into CO, H₂, H₂O, CO₂, CH₄ and C₂₊ gases, N₂, NH₃, H₂S, HCl, COS, HCN, and various other contaminants [47] which are discussed in section 2.7.3 below.

2.7.3 Step 3 – Syngas Cleaning and Conditioning

In addition to a low H₂/CO molar ratio composition, as discussed in section 2.7.2.2 above, the resulting biosyngas also contains many impurities, and therefore it must be cleaned and conditioned before it can be used in the FT reactor. This is because FT catalysts are extremely sensitive and can be easily poisoned or deactivated by syngas pollutants [9]. These contaminants can also potentially lead to other process problems such as blockages, and equipment fouling and corrosion, as well as environmental problems due to harmful emissions [125].

Commercially, regeneration or replacement of the FT catalysts occur periodically and, hence, the additional investment costs for gas cleaning are weighed against the costs incurred by process down-time due to catalyst poisoning, or maintenance due to equipment fouling and corrosion, in order to achieve the right economic balance [25]. The acceptable levels of contaminants, therefore, may be different for each plant and FT catalyst. Notably, it has been identified by Boerrigter *et al.* [26] that there are no syngas contaminants that are specific to biomass and, therefore, conventional gas cleaning approaches can be adopted. This may or may not be true, however, as operational experience in biomass gasification applications is relatively small in comparison to that of coal and natural gas gasification, and it is this uncertainty in knowledge of the exact contents and contaminants of biosyngas that poses one of the greatest challenges in the commercialization of BTL-FT operations [125]. The various typical syngas contaminants and conventional methods used for their removal are discussed in section 2.7.3.1 below, whereas the methods used for syngas conditioning are discussed in section 2.7.3.2.

2.7.3.1 Syngas Cleaning

Raw or unprocessed syngas typically contains tars (high molecular weight hydrocarbons), particulates, alkali compounds, nitrogen and chlorine compounds (such as NH₃, HCl, HCN) and sulphur compounds, such as H₂S and COS, which can permanently poison the FT catalyst by adhering to the active sites [9, 18, 128]. The impurities present in the syngas are not easily avoided

and the amounts present depend on the type of gasification process and feedstock used [8]. Biomass feedstocks generally contain very low amounts of sulphur, nevertheless, minuscule levels are sufficient to poison the catalyst [8]. Some of the potential problems that can be caused by these impurities are listed in Table 2.5 below. This table also gives their corresponding tolerance levels, which are representative of the typical requirements for FT synthesis.

Table 2.5 – Problems caused by syngas contaminants and FT contaminant tolerance levels

Contaminant	Examples [8, 125]	Potential Problems Caused [8, 125]	FT Tolerance Levels (ppb) [9]
Particulates	Dust, ash, char, and bed material	<ul style="list-style-type: none"> • Erosion of metallic components • Environmental pollution 	0
Alkali metals	Sodium, and potassium compounds	<ul style="list-style-type: none"> • High-temperature metal corrosion • Reactor bed de-fluidisation • Deposits on catalyst • Product contamination 	10
Nitrogen compounds	Ammonia and HCN	<ul style="list-style-type: none"> • NO_x formation • FT catalysts deactivation 	20
Sulphur and chlorine compounds	HCL and H ₂ S	<ul style="list-style-type: none"> • Corrosive emissions • Acid corrosion of metals • Permanent poisoning of FT catalysts 	10
Tars	Condensable organic compounds with boiling points in the range of 80-350°C [18].	<ul style="list-style-type: none"> • Clogging of filters and valves • Produce metallic corrosion • Internal reactor deposits • Difficult to burn • Deposits on catalyst • Product contamination 	10

Consequently, the syngas must undergo an intensive cleaning process prior to taking part in FT synthesis [125]. Biosyngas is reported to be similar to other more conventionally derived types of syngas, like those produced from coal, and therefore the same gas cleaning technologies can be used [129]. Some of these cleaning methods are listed in Table 2.6 below.

Table 2.6 – Syngas cleaning methods (derived from [8, 125])

Contaminant	Cleaning Methods
Particulates Alkali metals HCl	<ul style="list-style-type: none"> • Cyclones, filters, scrubbers and packed beds with sorbents (such as lime or dolomite). • Alkali metals condense at 550°C on the particulates and are removed together
Acid gases Inorganics	<ul style="list-style-type: none"> • Scrubbers and conventional gas removal processes with physical or chemical solvents
Sulphur compounds (H ₂ S and COS)	<ul style="list-style-type: none"> • Scrubbers, adsorbers • Catalyst guard beds (ZnO and activated carbon)
Tars	<ul style="list-style-type: none"> • Tar cracking (catalytic or thermal reforming) • Tar removal (e.g. water scrubbing)

2.7.3.2 Syngas Conditioning

As mentioned previously in section 2.7.2, the main syngas constituents include CO, H₂, CO₂ and CH₄. For the syngas to be used for conversion in FT synthesis the inert gas concentration needs to be as low as possible (< 2 vol. %) [25]. The methane composition is commonly reduced by reforming with steam, whereas the carbon dioxide can be removed using conventional separation technologies [130]. The composition of the carbon monoxide and hydrogen (H₂/CO molar ratio) also needs to be adjusted to the specific requirements of the FT synthesis process. This is usually done by means of the water-gas shift (WGS) reaction in a shift reactor [131]. The water present in the syngas is also removed prior to the FT reactor by cooling the gas and knocking the water out [12]. This is because water would shift the WGS equilibrium reaction (Equation 2.2 in section 2.2) and lower the partial pressures of CO and H₂. The above syngas conditioning process steps are discussed in the following paragraphs.

Methane Reforming

Methane and low molecular weight hydrocarbon gases (C₂₊) present in the syngas can reduce the conversion efficiency of the FT synthesis reaction, as well as possibly deactivate the FT catalyst [47]. The composition of these gases can be adjusted to meet the requirements of the FT process by methane reforming over a nickel catalyst. This method uses steam to convert methane (as well as other light hydrocarbon gases) into carbon monoxide and hydrogen (Equation 2.7 below) [12].



Water-Gas Shift Reaction

Stoichiometrically, FT reactions need an H₂/CO molar ratio in the feed syngas of approximately 2.0 (recommended for cobalt catalysts) or lower (for iron catalysts). Typically, the H₂/CO molar ratio of the biosyngas produced are lower than 2.0 [131], and this must then be adjusted using the WGS equilibrium reaction (Equation 2.2 in section 2.2). Using steam, this turns carbon monoxide into carbon dioxide and hydrogen. In the case of FT synthesis using cobalt catalysts, the WGS reaction is carried out in an external shift reactor, which is usually operated between 15-25 bar and around 300°C [131] over copper-promoted catalysts [25]. When using iron catalysts, however, they are WGS active and the WGS reaction occurs in the FT reactor with no need for an external shift reactor [121]. This means that the FT reactor would be able to handle syngases with a high CO content (low H₂/CO ratio) by producing more hydrogen. The costs associated with adding a shift reactor, though, are small in comparison to the total FT plant capital and operational costs [121], and any costs are usually outweighed by using cobalt catalysts which display higher catalytic activity and C₅₊ hydrocarbon selectivity and have a much longer process life than iron catalysts (section 2.4).

Removal of Carbon Dioxide

The CO₂ in the syngas is generally regarded as un-reactive during FT synthesis and can therefore lower the conversion efficiency of the process, particularly to C₅₊ products, as it dilutes the syngas [12, 131]. Moreover, this CO₂ content can also be further raised by the WGS reaction (Equation 2.2 in section 2.2). Carbon dioxide can be removed from the syngas using conventional separation technologies such as adsorption with solid absorbents (e.g. silica gel and zeolites), chemical or physical absorption with a washing liquid (e.g. amine treatment) or by using cryogenic membranes [25, 125, 130].

2.7.4 Step 4a – FT Synthesis

After the syngas is cleaned and conditioned, it is then ready to take part in the next stage of the industrial process where the FT synthesis reaction is carried out. As discussed previously in section 2.5.2, if pressurized gasification is carried out at a slightly higher pressure than the desired operating pressure in the FT reactor, there would be no need for a syngas compression step prior to the FT reactor. The fundamentals of the FT synthesis process, including the reactions that take place and the factors that influence the products that are formed, were discussed previously in sections 2.2 to 2.5.

A major consideration in the design of FT reactors is the highly exothermic nature of the synthesis reactions. This requires reactor technology with rapid heat removal from the catalyst bed. Isothermal temperature control within the reactor or catalyst bed is crucial because, firstly, higher temperatures in FT synthesis favour the production of methane and lower molecular weight hydrocarbons, which are not the desired products in full conversion FT (Figure 2.7 in section 2.7). Secondly, if the catalyst overheats this could lead to a higher catalyst deactivation rate due to sintering and other deactivation mechanisms [21, 55] (discussed previously in section 2.4.3). Industrially, high heat exchange rates are ensured by using high gas space velocities (and therefore turbulent gas flows) through narrow catalyst-packed tubes in fixed bed reactors [21]. Alternatively, fluidized bed reactors are used, in which the catalyst is dispersed within the liquid phase and therefore very efficient heat transfer is achieved resulting in good isothermal temperature control [21].

The exact reactor technology used depends on the two modes of process operation (discussed previously in section 2.2.2) and the products that are desired. Detailed reviews on the fundamentals and development of FT reactors can be found in the literature by Dry [21, 55], Steynberg *et al.* [132], Davis [133], Guettel *et al.* [36], Sie and Krishna [134], and Jager [135]. There are three main types of reactors that are used in commercial FT applications. These include multi-tubular fixed-bed reactors, gas/solid fluidized bed reactors (fixed fluidized bed and circulating fluidized bed) and slurry phase reactors [132]. Circulating fluidized bed reactors and fixed fluidized bed reactors are

usually used in HTFT processes (Figure 2.8 below) for producing gasoline and higher-value chemicals, whereas multi-tubular fixed-bed reactors and slurry phase reactors are commonly used in LTFT processes (Figure 2.9 below) for the production of diesel and waxes (section 2.2.2) [35].

2.7.4.1 HTFT Operation

As shown in Figure 2.8 below, the type of reactors used in HTFT processes are fluidized bed reactors because their design enables more efficient heat exchange, when compared to multi-tubular fixed beds, and more isothermal conditions due to the high gas circulation rates.

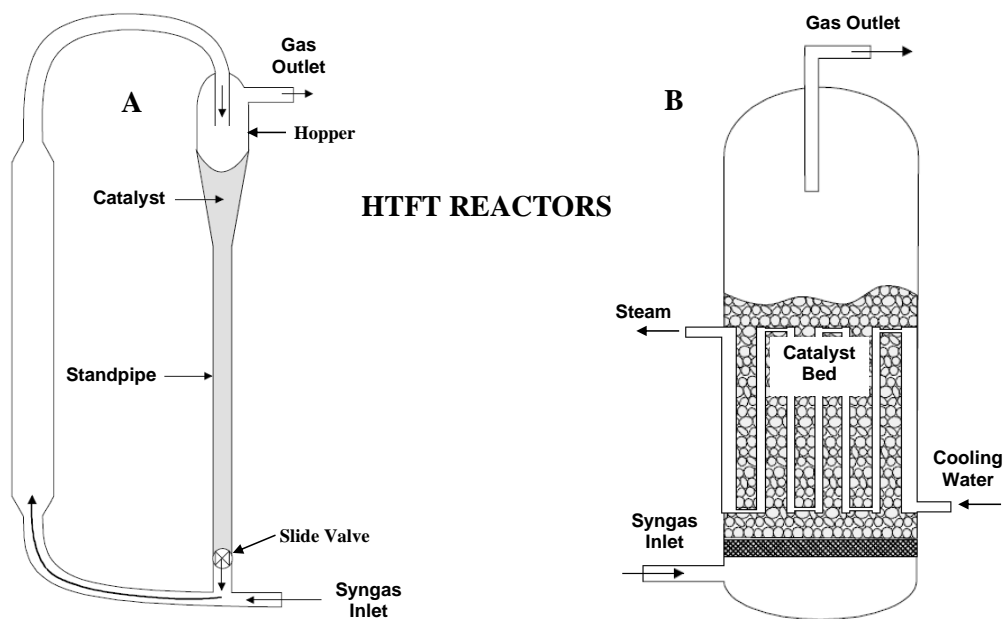


Figure 2.8 – HTFT reactors: A) circulating fluidized bed, and B) fixed fluidized bed
(adapted from [39])

At HTFT conditions within the reactor, all the products are in the gas-phase, and hence only two phases exist within the system (the catalyst being the solid phase) [134]. These reactors can only be used with two phases (gas/solid) as any liquid or wax deposits on the catalyst would lead to agglomeration of the catalyst and subsequent loss of the fluid phase [133]. Therefore, the heaviest hydrocarbons that are produced using these types of reactors are naphtha grade products [132]. As BTL-FT processes would usually aim for maximum yields of liquid fuels and diesel in particular, HTFT operations using fluidized beds have not been investigated for BTL-FT applications.

2.7.4.2 LTFT Operation

LTFT processes employ multi-tubular fixed bed and slurry phase reactors, as shown in Figure 2.9 below. Both types of reactors are described below and their main advantages and disadvantages are also discussed. At these conditions, within both of these types of reactors, three phases exist; the gas phase (containing the reactants, water vapour and hydrocarbon gases), the liquid phase (which is composed of the higher molecular weight hydrocarbons), and the catalyst as the solid phase

[134]. The main types of catalysts used in LTFT reactors are cobalt-based catalysts, which have a high selectivity towards diesel and high molecular weight waxes [20]. Iron-based catalysts can also be used in LTFT reactors, however, it has been reported that the operating temperature cannot exceed 260°C, as the reactor will be blocked from carbon deposition [55]. The waxes produced are usually further upgraded or hydro-cracked in order to maximize the yield of diesel. As mentioned in section 2.7.4.1 above, BTL-FT operations typically aim to obtain high yields of liquid fuels and it is therefore, this mode of operation that is receiving attention for application in BTL-FT.

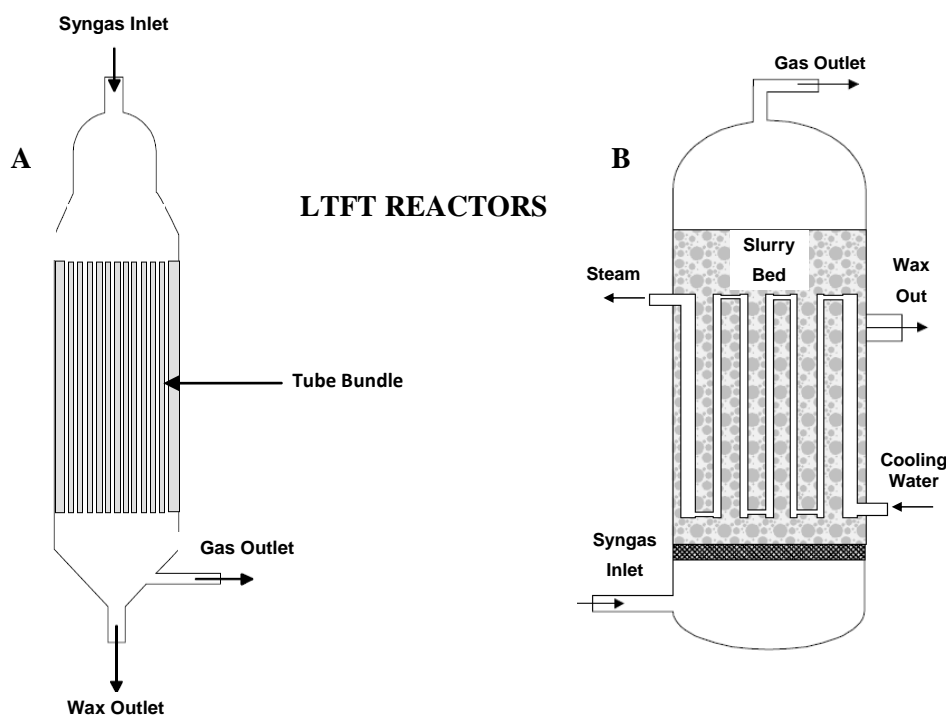


Figure 2.9 – LTFT reactors: A) multi-tubular fixed bed, and B) slurry phase
(adapted from [39])

Multi-Tubular Fixed Bed Reactors

Multi-tubular fixed bed reactors consist of catalyst-filled narrow tubes surrounded by cooling water (Figure 2.9 above). Temperature control and efficient heat exchange are reportedly achieved by the combination of narrow tubes, high space velocities and sufficiently large catalyst particle sizes (which also significantly reduce the pressure drop across the catalyst bed) [55]. The heat given off by the synthesis reaction generates high pressure steam [136] which can be used within the same complex for other operations, such as biomass drying, in order to improve the overall process economics.

The waxes and liquids produced are easily extracted as they trickle down to the bottom of the reactor, therefore making the reactor design suitable for wax production at LTFT conditions. The operation and scale-up of these types of reactors is simple and they are quite versatile with regards to the range of temperatures and pressures that can be used [55]. Furthermore, any contaminants

present in the syngas after gas cleaning are absorbed by the top layers in the catalyst bed, therefore leaving the rest of the bed contaminant free [55]. This allows for flexibility in the choice of raw materials used, and to a certain extent, the leniency of the gas cleaning requirements. The main disadvantages of multi-tubular fixed-bed reactors are mainly associated with process economics. This is because their construction is expensive, the high pressure drops within the bed necessitate higher gas compression, and catalyst replacement is time and labour intensive [9].

Slurry Phase Reactors

Slurry phase reactors are composed of an outer shell with cooling water coils immersed in the slurry bed. The syngas flows up the slurry bed, which contains mainly FT waxes and liquid products, as well as the suspended catalyst, making it a three-phase system [66]. This makes these reactors suitable for LTFT operation as the waxes produced also serve as the liquid phase within the reactor [55]. The main advantages that fixed slurry beds have over the multi-tubular fixed beds include the following [21, 55, 135]:

- Lower capital cost for the equivalent capacity.
- Much lower pressure drop in the reactor vessel, and therefore lower gas compression costs.
- Lower catalyst related costs – less catalyst loading and consumption, and longer reactor runs are possible, as the catalyst can be removed and replaced online.
- Isothermal bed operation (no hot spots), which allows for higher temperatures to be used giving higher syngas conversions.

Despite the above advantages of slurry phase beds, they have a few reported drawbacks [21, 55]. Firstly, the wax that is produced needs to be separated from the slurry and suspended catalyst, requiring additional equipment so as not to lose any of the catalyst. Secondly, if a contaminant like H₂S enters the reactor, then unlike the poisoning of only the top layers that would occur in multi-tubular fixed bed reactors, the entire amount of catalyst used would be poisoned in the slurry phase reactor. For this reason, gas cleanliness requirements are stricter when operating slurry phase beds.

2.7.4.3 Choice of FT Reactor

From the preceding sections on the different types of reactors, the modes of reactor operation, and targeted products, it can be said that the LTFT mode, in which either multi-tubular fixed-bed or slurry phase reactors are implemented to produce diesel and heavy hydrocarbon waxes, is more suitable for application in a BTL-FT scenario, where maximum yields of liquid fuels are typically desired (full conversion FT). Both types of LTFT reactors have advantages and drawbacks which were discussed in the previous sections. Even though the advantages of slurry phase reactors seem to outweigh those of multi-tubular fixed-bed reactors, successful large-scale, natural gas based FT

operations carried out by Shell in Malaysia using multi-tubular fixed bed reactors and a proprietary catalyst [135, 137], illustrate that both reactor technologies are commercially viable.

2.7.5 Step 4b – Product Recovery and Upgrading

Product recovery and/or upgrading comprise the last stage of the FT synthesis process. In order for the products to meet market specifications they need to be refined or up-graded and, typically, the same refining processes that are used in the petroleum industry can be used in treating FT products [43]. Some of these refining processes include: i) isomerisation (branching of straight hydrocarbons) and aromatisation for improving octane value and density, ii) oligomerisation for shifting light molecular weight products to higher products, iii) hydrocracking for converting heavy hydrocarbon products (waxes) to lighter products, and iv) hydrogenation for removing any oxygenates or olefins that are not desired [63]. Sections 2.7.5.1 to 2.7.5.3 below, outline the options that can be followed for further product processing or upgrading and recovery. The products from the FT reactor can be divided into four general categories: C₁-C₄ (hydrocarbon gases), naphtha (C₅-C₁₀), diesel (C₁₁-C₁₈) and waxes (C₁₉₊). The C₅₊ products are usually separated by condensation and then recovered and/or upgraded [12].

2.7.5.1 C₁-C₄ Fraction

Methane is not normally a desired product in FT synthesis and is, therefore, usually reformed back to syngas using steam and recycled into the FT reactor (as discussed previously in section 2.7.3.2). The olefins in the C₂-C₄ product fraction, such as ethylene and propylene, can potentially be recovered as higher-value chemicals because they can be used as raw materials in the polymer industry (e.g. for the production of polyethylene and polypropylene) [138]. Other hydrocarbons in the C₂-C₄ product fraction can be oligomerized into diesel or gasoline [138]. However, the energy requirements for the recovery of this small fraction of C₂-C₄ products in the mix are high [12], and therefore these product gases are usually also reformed, along with methane, back into syngas and recycled back into the FT reactor in order to maximize the liquid hydrocarbon fuel yields [138].

2.7.5.2 Naphtha Fraction

Gasoline and other fuels are usually rated by assignment of an octane number. This is a rating method that indicates the measure of the resistance of the fuel to explosive pre-ignition, also known as knocking, within an internal combustion engine in comparison to a mixture of iso-octane and heptane [9]. Conventional gasoline has an octane number of 87-89 [9], whereas the naphtha fraction (C₅-C₁₀ hydrocarbons) in the FT product has a significantly lower octane number than this due its low aromatic content and low degree of branching [63]. In its unrefined condition, therefore, naphtha cannot be used directly in gasoline engines and cannot be used for blending with conventional gasoline [136].

The naphtha fraction can be upgraded to gasoline by isomerisation of the C₅-C₆ hydrocarbons and catalytic reforming (over a Pt catalyst) of the C₇-C₁₀ hydrocarbons, as carried out by Sasol [138]. Before this can be done, however, the naphtha must first be hydro-treated in order to make it compatible with conventional technologies used for isomerisation and reforming [136]. Hence, naphtha upgrading requires additional processing steps that increase capital and operating costs and process complexity, and the viability of which need to be weighed against the value that the upgraded gasoline product would add to the BTL-FT operation [136]. Ideally, therefore a low composition of naphtha-grade products is desired within the liquid fuel mix. However, in a decentralized BTL-FT process scheme where an intermediate or synthetic crude FT liquid fuel product is transported to a conventional refinery, the naphtha content of this product is not a major issue, as the technology for its recovery, upgrading or further processing for the production of higher-value chemicals would be more readily available.

2.7.5.3 Diesel and Waxes Fraction

The properties and characteristics of FT diesel and its advantages and disadvantages over conventional petroleum diesel were discussed previously in section 2.2.2. As previously discussed in section 2.2.1, and according to the Anderson-Schulz-Flory distribution model (Figure 2.2 in section 2.2.1), theoretically there is a maximum amount of straight-run diesel (typically around 20%) that can be obtained from FT synthesis [60]. For example, it was reported by Boerrigter and den Uil [18] that the equivalent of 1kg of woody biomass produces 175ml of FT wax, finally giving 150ml of diesel after hydro-cracking. In an energy analysis conducted by Manganaro *et al.* [139], the diesel yields obtained from biomass (containing 30wt.% moisture) are reported to be around 13wt.%. Their modelling also showed that significant energy densification is achieved, as 42% of the original energy content of the biomass is contained in the diesel produced.

It is generally accepted in the literature that the highest yields of diesel are obtained by producing waxes and then hydro-cracking them into diesel [136]. Wax hydro-cracking is commonly carried out in LTFT processes, which aim for high yields of waxes and use conventional crude oil refinery technology [136]. This is usually carried out over catalysts like Pt or NiMo on alumina or zeolite carriers at pressures above 100 bar and temperatures of 350°C or higher [136]. This process route is followed in the operations carried out by Shell in Malaysia [135, 137] which are geared towards maximum wax yields. Presumably, wax hydrocracking allows for more control over the final product range, and the middle distillate or diesel range of fuels can be maximized. The energy demands of this upgrading step in a BTL-FT process, therefore, would be high. In a decentralized BTL-FT process scheme, however, the energy dense intermediate or synthetic crude liquid product (containing naphtha, diesel and C₁₉₊ waxes) would be transported to a dedicated, central refinery and the upgrading costs would not be incurred on site.

2.7.6 Step 5 – Optional Power Generation

From experimental demonstrations at ECN, in The Netherlands [26], maximum overall energy efficiency of syngas to liquid fuels via FT synthesis of about 70% are reported, with about a quarter of the energy given off as heat. The remainder of the energy, with potential for power generation, is carried by the unreacted syngas and the C₁-C₄ fraction [26]. Alternatively therefore, this C₁-C₄ gas product fraction can be combusted, along with the FT off-gas (containing unreacted syngas), for the purpose of co-producing power, as in the case of once-through FT (section 2.7) [9]. However, generating power as a co-product in BTL-FT processing may not be an economically viable solution. This is because of the high cost of the syngas cleaning and conditioning process steps, which are vital for the FT synthesis downstream, but are not necessary for power generation. Ideally therefore, in a BTL-FT process aiming to maximize liquid fuel yields, a high reactant conversion and a low selectivity towards the formation of this light hydrocarbon fraction are desired. As discussed previously in section 2.5, this selectivity is also influenced by process conditions, such as reactor temperature and pressure, which will be investigated in the parameter study discussed in chapter 5.

2.8 Status of BTL-FT Processing

As mentioned previously in section 1.2, existing large-scale commercial applications that combine gasification and syngas conversion technologies are either coal or natural gas based and include operations by Sasol in South Africa [26] and Qatar [140], and those by Shell in Malaysia [26] and Qatar [141]. As already pointed out in section 1.2, the synthesis of FT liquids from biomass feedstocks is a relatively new development in the field of FT synthesis and, to-date, there are no BTL-FT applications that have been commercialized [30]. There are, nonetheless, a number of lab-scale studies, as well as planned pilot plant studies that aim to commercialize BTL-FT technology.

The very first lab-scale application of BTL-FT was run successfully by ECN in 2001, where FT liquids were produced for the first time using syngas derived from biomass (willow) using an oxygen-blown circulating fluidized bed gasifier combined with an oxygen-blown tar-cracker (resulting in H₂/CO ratios between 0.8-2.1) [26]. FT synthesis was successfully run for 150 hours on a small fixed-bed reactor using a proprietary cobalt-based catalyst made by Shell, achieving C₅₊ hydrocarbon selectivities around 90% [26]. Following this, the first BTL-FT pilot plant was initiated in a joint project by Choren and SüdChemie in Freiburg, Germany, in 2005 producing 7.5 bbl/day of FT diesel [142]. The success of this project later led to the planning of the world's first demonstration BTL-FT plant in partnership with Shell, which was under construction in Freiberg, Germany, with an expected capacity of 1.5 million bbl/year [143-145]. This would have qualified this particular BTL-FT technology as the closest to becoming commercialized. Unfortunately, however, this venture is no longer going forward due to financial difficulties.

Two pilot plants (planned to produce diesel and kerosene based on biomass gasification) are currently under construction in France, and scheduled to start operating in 2012 [146]. This is part of a demonstration project, called BioTFuel, involving the industrial plant technology company, Uhde, and five French partners, aiming to integrate and commercialize all the stages of the BTL process chain (from biomass reception to FT fuels).

Another BTL-FT pilot plant aiming to produce gasoline type fuels at Karlsruhe, Germany, known as Bioliq, is under construction and apparently due for completion in 2016 [147]. The process is planned to consist of three stages involving flash pyrolysis, entrained-flow gasification and synfuel production. This project is being carried out by Forschungszentrum Karlsruhe GmbH in partnership with LURGI GmbH.

A BTL demonstration plant making biofuels from wood residues is claimed to exist at Stora Enso's Varkaus Mill in Finland, known as NSE Biofuels Oy, and is a joint venture between the Finnish Neste Oil and Stora Enso (a paper, packaging and forestry products company) [148]. This plant has a capacity of approximately 5000 bbl/year using a 12 MW gasifier. Future plans by NSE Biofuels (partnering with Foster Wheeler and VTT) include using the gained experience and data for the development of a commercial production plant with a capacity of 740,000 bbl/year by 2016 at one of Stora Enso's mills.

Small amounts of FT liquids are also produced by Repotec in Güssing, Austria, where a 8MW CHP demonstration plant is operated in combination with FT liquids production in a lab-scale slurry bed reactor, using wood as the primary feedstock [142, 149]. Repotec intends to up-scale the process and planning for the construction of a 30MW plant combined with FT diesel production (31,000 bbl/year) is apparently underway [142].

3 Experiment Plan, Equipment and Methodology

This chapter outlines the plan that was devised for the experimental work and describes the experimental equipment and the work that is carried out, as well as the methodology and procedures that are followed. Two fixed-bed reactor systems are used for FT synthesis work – a 2cm³ reactor at the Federal University of Rio de Janeiro, in Brazil (UFRJ), and a 20cm³ reactor at Aston University. Both of these reactor systems, as well as the equipment used for analytical work and catalyst characterization studies are described.

3.1 Experiment Plan

The primary objective of this project entailed the experimental exploration of the influence of lower FT synthesis pressures for the potential production of an intermediate synthetic crude or syncrude liquid product that can be integrated into existing refineries. To do this, the catalysts that are available are first evaluated and compared in order to determine their suitability for fulfilling this aim, as well as for operation on the 20cm³ fixed-bed micro-reactor system at Aston University. Using the most suitable catalyst, the relationships between the catalyst activity and stability, product distribution (or selectivity) and product yields, and the process parameters (discussed previously in section 2.5) are then studied in order to identify the preferred set of operating conditions on the 20cm³ fixed-bed micro-reactor at Aston University. The two different fixed-bed, down-draft reactors that are used for carrying out FT synthesis work in this project include:

- A single stainless steel shaft, 2cm³ (total volume) fixed-bed micro-reactor at the Federal University of Rio de Janeiro (UFRJ), Brazil. This reactor system uses syngas that is ready-mixed in a standard gas cylinder and is described in section 3.3.
- A single stainless steel shaft, 20cm³ (total volume) fixed-bed micro-reactor at Aston University, that is fully integrated into an automated bench-top reactor system (BTRS) manufactured by Autoclave Engineers. This reactor system uses syngas that is mixed inside the reactor system and is described in section 3.4.

The gases that are required for this project are discussed in section 3.2. Both reactors are used in the catalyst selection procedure, whereas only the 20cm³ reactor is used in the FT synthesis parameter study. The equipment used for product analysis is described in section 3.5. The techniques and equipment used to characterize the catalysts are described in section 3.6. Finally, section 3.7 outlines the experimental procedures followed, from start to finish, for the FT synthesis

tests on both fixed-bed reactors. The devised experiment plan is comprised of three main items, which are listed below and discussed in sections 3.1.1 to 3.1.3 below.

1. **Catalyst selection procedure** – Evaluation and comparison of the catalysts that are available for this project. This includes catalyst characterization and initial FT synthesis experiments that assess the performance of the catalysts. The most promising catalyst candidate is selected for further study.
2. **FT synthesis parameter study** – This is the main part of the work and is comprised of an investigation on the influence of important process parameters on the selected catalyst activity and stability, product selectivity, product yields, etc. during FT synthesis.
3. **Product analysis** – Analysis of the gaseous, liquid and solid reaction products. This is achieved by means of various gas chromatography techniques, as well as other techniques for the determination of the energy content of the hydrocarbon products and water content of the aqueous phase.

3.1.1 Catalyst Selection Procedure

As discussed previously in section 2.4.4, three catalysts (representative of those typically used in industry) are available for the FT synthesis experiments. The compositions and preparation methods of these catalysts are discussed in the beginning of chapter 4. One of the catalysts was prepared in collaboration with the University of Rio de Janeiro and is an un-promoted cobalt-based catalyst supported on γ -alumina (Al_2O_3). However, only approximately 10g of this cobalt/alumina catalyst formulated in the laboratory is available for use in this work. This type of catalyst is commonly used in FT synthesis, albeit with added promoters, on the merit of its high activity and resistance towards re-oxidation by water [5, 21, 89], as well as the mechanical properties of the alumina support due to the strong cobalt oxide interactions with the alumina (discussed in section 4.2.3). The other two catalysts are provided by Catal International Ltd. The first one is a ruthenium promoted cobalt-based catalyst supported on titania (TiO_2) which was recommended by BP for its high C_{10+} hydrocarbon selectivity [84], and the second one is an iron-based catalyst promoted with various transition metals and supported on γ -alumina. All three catalysts are compared and subjected to a screening procedure (chapter 4) that will decide on the most suitable catalyst which will take part in the parameter study (chapter 5). This procedure includes a combination of characterization studies on the three catalysts and a number of FT synthesis screening experiments to evaluate their performance during reaction. These studies are explained in sections 3.1.1.1 and 3.1.1.2 below.

3.1.1.1 Catalyst Characterization

The characterization studies are performed in order to determine catalyst properties such as the surface area and pore size, active phase in the catalyst, moisture retention, suitable reduction

temperatures for the catalyst activation procedures, extent of coke and wax deposition during reaction, etc. A variety of techniques are used which include morphological studies (BET surface area, pore diameter and volume determination, and scanning electron microscopy or SEM), X-ray diffraction (XRD), temperature programmed reduction (TPR), and thermo-gravimetric analysis (TGA). These techniques are discussed in more detail in section 3.6.

3.1.1.2 FT Synthesis Catalyst Screening Tests

The initial FT synthesis experiments are designed to evaluate each catalyst under fixed and representative conditions from which the most promising catalyst is selected for further study. Their catalytic activity and selectivity (or product composition) are contrasted. The catalyst yielding a product composition with the most potential for achieving the main aims of this work (section 1.3) is selected for continued use in the parameter study tests that involves process parameter profiling. The screening tests are carried out on both reactors and the reaction conditions implemented are discussed in chapter 4.

3.1.2 FT Synthesis Parameter Study

This study comprises the main series of FT synthesis tests that are performed using the selected catalyst to investigate the influence of important process parameters on the performance of the catalyst in terms of its activity and stability (i.e. CO conversion versus time on stream), product distribution, product yields and liquid hydrocarbon product composition. These parameters include the reactor temperature, reactor pressure, syngas space velocity, syngas composition (H_2/CO molar ratio) and catalyst loading (i.e. catalyst mass). The experiments in this parameter study are carried out on the 20cm^3 fixed-bed reactor, which is described in detail in section 3.4. The results obtained will then aid in identifying a set of preferred conditions for operation on this reactor. The details of this parameter study, including a summary of the planned experiments and the reaction conditions employed, are presented in chapter 5.

3.1.3 Product Analysis

Analysis of the FT synthesis products are carried out online as well as offline as summarized in sections 3.1.3.1 and 3.1.3.2 below. The equipment used and the analysis methods employed are described in detail in section 3.5.

3.1.3.1 Online Gas Analysis

Product gases (from both reactors) are analysed online using gas chromatographs (GCs) equipped with thermal conductivity (TCD) and flame ionisation (FID) detectors. The TCDs are used for the detection and quantification of permanent gases (CO , H_2 , N_2 , CO_2 and CH_4), whereas the FIDs aid in the detection and quantification of hydrocarbons and other volatiles.

3.1.3.2 *Offline Liquid Analysis*

The hydrocarbon liquids collected from the experimental runs on the 20cm³ reactor are analysed offline on a gas chromatograph coupled with a mass spectrometer (GC-MS). The calorific values of these hydrocarbon liquids are also determined by ultimate analysis (section 3.5.3.3). The aqueous products are also analyzed for water content using a volumetric titrator, as this serves as an indication to the percentage of oxygenated compounds present.

3.2 Gases Required

The gases required for FT synthesis, as well as for the 20cm³ reactor and analysis equipment operation are supplied by BOC Gases in standard gas cylinders for use in the laboratory. These include FT feed gases (pure carbon monoxide, hydrogen and nitrogen), GC sample carrier gas (argon), GC operational gas (pure helium for pneumatic operation of the detectors and mass flow controllers), and air (for automated pneumatic valve operation in the reactor system). These cylinders are connected via high pressure lines to the equipment, fitted with pressure regulators and, in the case of H₂ and CO, connected to automatic safety alarms and trips, which are designed to shut off the main gas supply in the case of gas leaks above the maximum allowable levels.

3.3 2cm³ Reactor at UFRJ

This fixed-bed, downdraft micro-reactor (Figure 3.1) was used during a researcher exchange visit at UFRJ, Brazil. Only a picture of the disassembled reactor shaft is provided (courtesy of UFRJ, Brazil) as the entire reactor system set-up used was confidential. The reactor consisted of a single stainless steel tube (L = 10cm, ID = 5mm) with a total volume of 2cm³.



Figure 3.1 – 2cm³ fixed-bed reactor (UFRJ, Brazil)

The syngas flows through a coiled tube wrapped around the outside of the reactor shaft and then into the top of the vessel. The reactor shaft is mounted onto a metal framework and is surrounded by a well insulated ceramic heating jacket that controls the reactor temperature and heats the syngas before it enters the reactor.

3.4 20cm³ Fixed-Bed Reactor System at Aston

This fixed bed micro-reactor is integrated within a fully automated reactor system, which is completely encased within one bench top unit, as shown in Figure 3.2 below.



Figure 3.2 – Automated 20cm³ fixed-bed micro-reactor system at Aston

Figure 3.3 below, shows a close-up of the reactor assembly within the oven chamber. A schematic process diagram of this system is also presented in Figure 3.4 below. This reactor system is also used in the catalyst screening procedure, where all three available catalysts are compared, as well as the parameter study tests that are discussed in section 3.7.3.

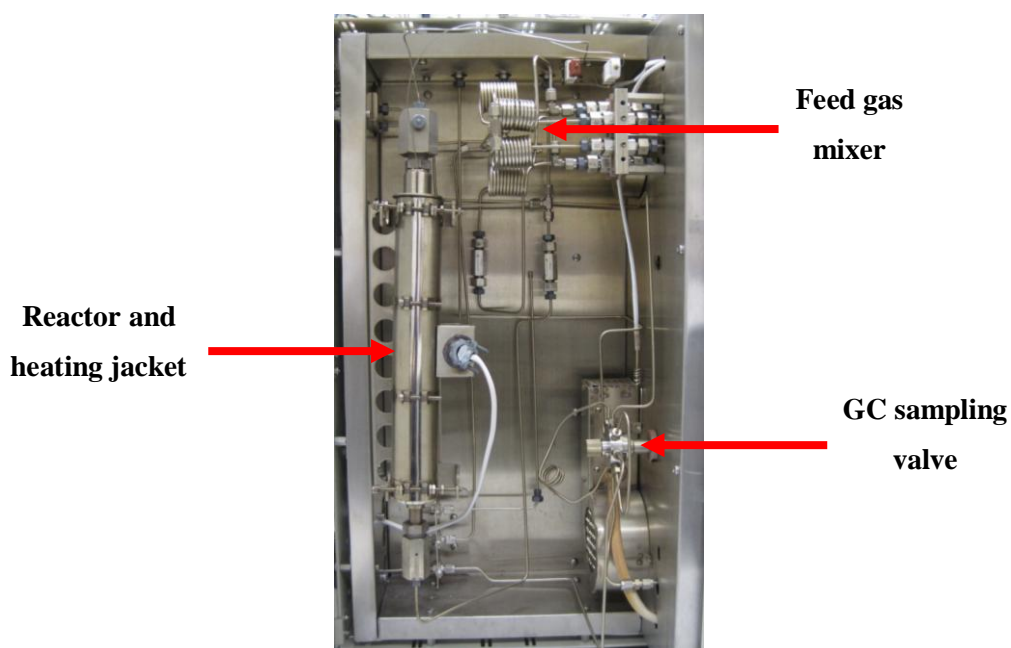


Figure 3.3 – 20cm³ fixed-bed micro-reactor inside open oven chamber

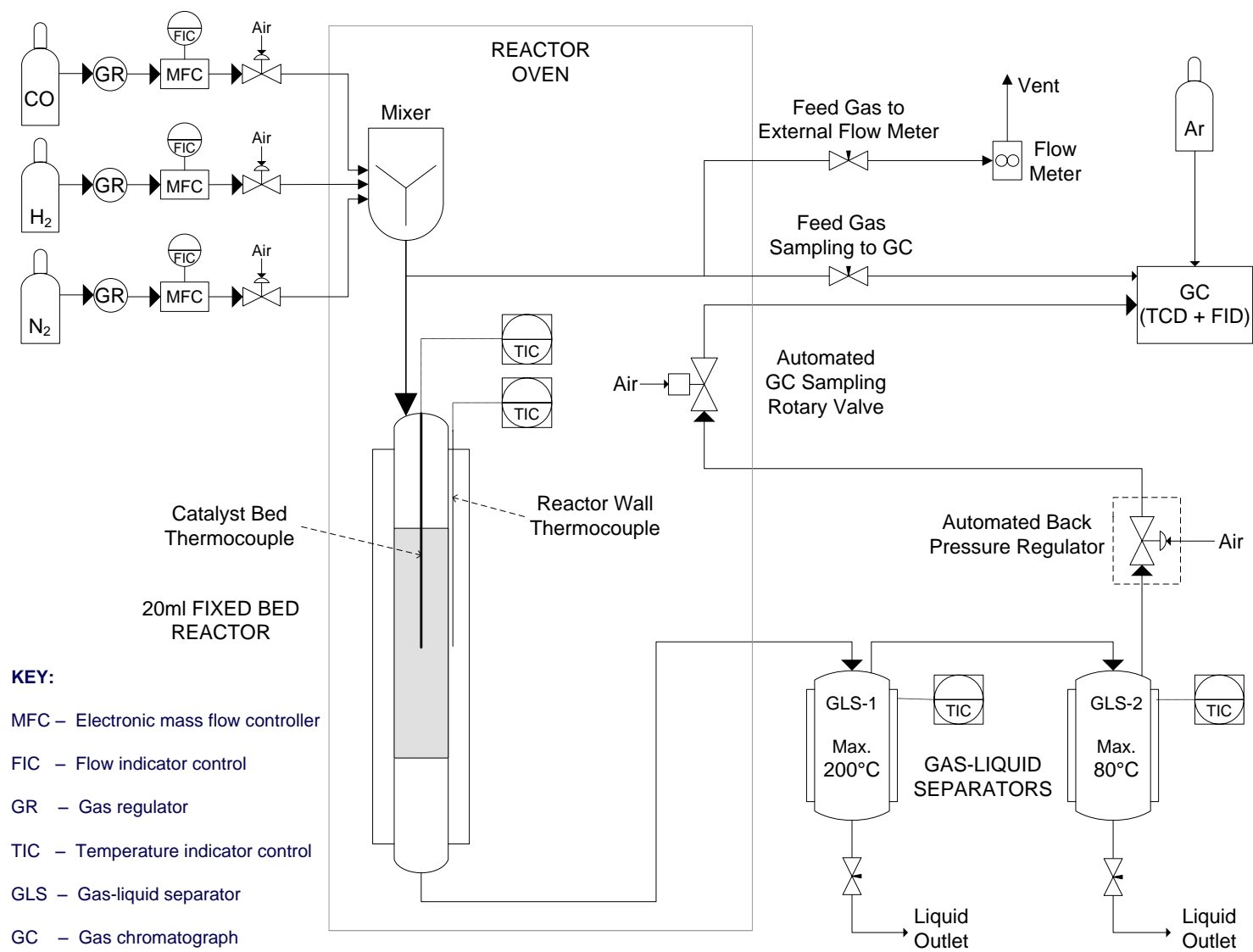


Figure 3.4 – Schematic of 20cm³ automated fixed-bed reactor set-up at Aston

3.4.1 20cm³ Reactor Sub-Systems

The overall system can be divided into the following four major subsystems:

- Reactant preparation (feed mixing and heating)
- Reactor
- Product handling (gas liquid separation vessels, GC sampling valve and GC transfer line)
- Reactor pressure control (back pressure regulator)

These different sub-systems are described in sections 3.4.1.1 to 3.4.1.7 in the order that they are met by the stream path of the reactant and product gases in the overall system. All pipelines to and from the reactor are 1/16 inch stainless steel tubes. The digital outputs from the system are connected to a computer from which all the settings (temperatures, pressure, gas flow rates, etc.) are controlled via a customized software package. A screenshot of this software program is shown in Figure 3.5 below.

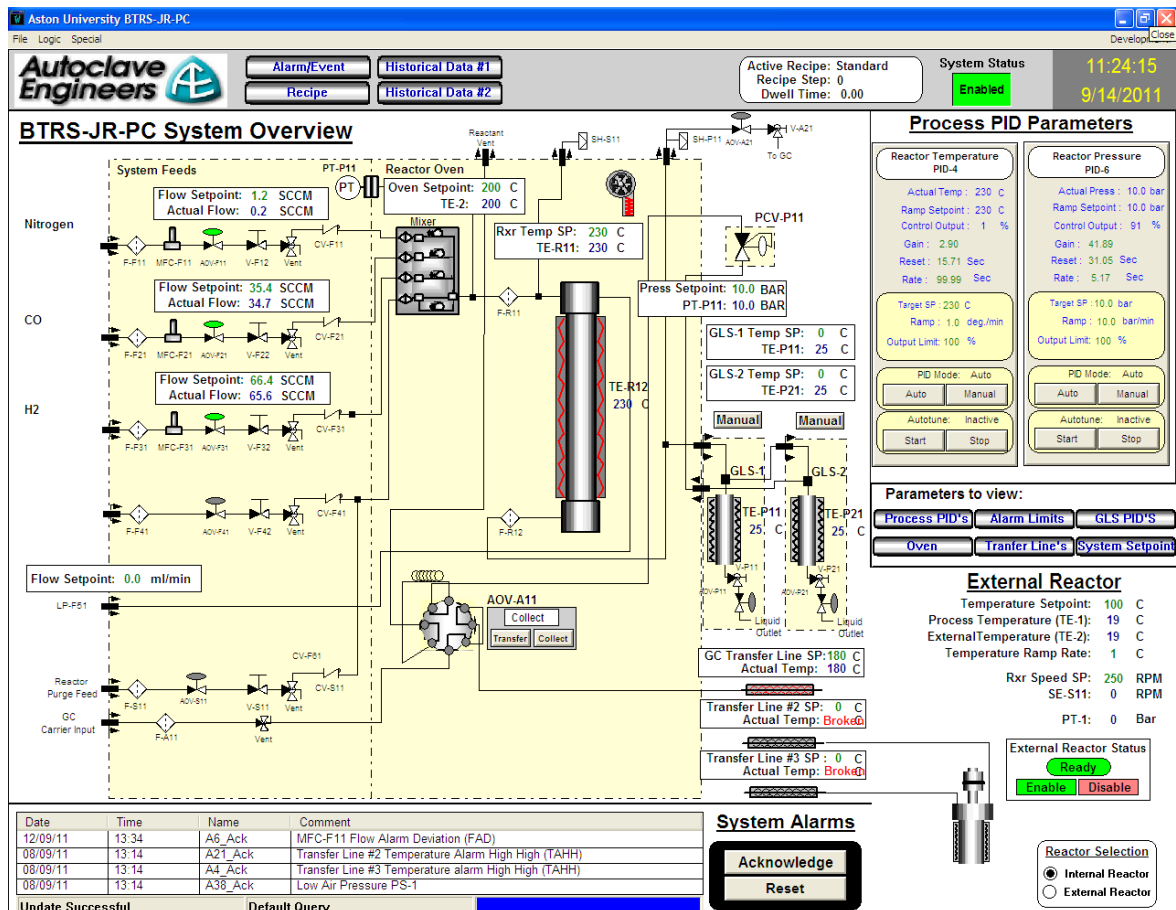


Figure 3.5 – Screenshot of software program used for controlling the 20cm³ fixed-bed reactor at Aston

3.4.1.1 Reactant Preparation

Three gas inputs (hydrogen, carbon monoxide and nitrogen) are connected to the reactor system, and the gas delivery rate is controlled by three mass flow controllers (Brooks Instrument Model number 5850TRG); one for each gas input (Figure 3.4). For verification purposes, the gas delivery rates (controlled by these mass flow controllers) are checked and adjusted by means of an external glass volumetric flow meter, using soapy water and a stopwatch as shown in Figure 3.6 below. The gas flow rates are calculated by measuring the time taken for a soap bubble to travel the equivalent distance of 5ml up the glass tube in order to work out the volumetric flow per minute. For instance, if 5ml are travelled upwards by the soap bubble in 2 seconds, then the flow rate would be calculated to be 150ml/min. The maximum standard deviation in these measurements was 0.56%.

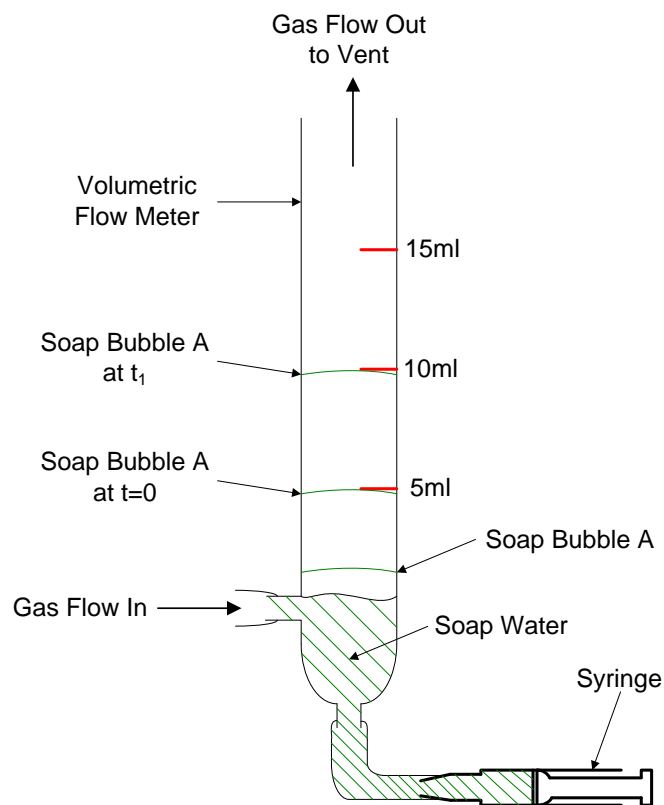


Figure 3.6 – External volumetric flow meter arrangement on 20cm³ reactor system at Aston

Next, the feed gases enter the mixer which is located inside the reactor oven chamber (Figure 3.4). Here they are mixed and heated to the desired temperature before entering the reactor.

3.4.1.2 Reactor

After being mixed and heated, the gas stream then flows in through the top of the reactor (Figure 3.4). The reactor assembly consists of:

- A type 316 stainless steel tube (7.65 mm I.D. x 14.05 mm O.D. x 43.5 cm, V= 20cm³)
- A ceramic heating jacket

- An internal catalyst bed thermocouple
- An external reactor wall thermocouple

3.4.1.3 Gas Liquid Separators

After leaving the reactor, the gases then flow into the Gas Liquid Separators (GLS-1 and GLS-2) or knock-out pots, which are 150 ml cylindrical vessels located outside of the oven (Figure 3.2 and Figure 3.4 above). The product gases enter the GLSs through a dip tube at the top of each vessel and then exit through a tee at the top of each vessel. An air operated valve and a metering valve are connected in series to the bottom of each GLS vessel to drain the condensed liquids and waxes. The knock-out pots are each surrounded by ceramic heating jackets that could heat GLS-1 and GLS-2 to maximum temperatures of 200 and 80°C, respectively. This makes the option for specific product separation available if required, e.g. soft waxes in GLS-1 at 200°C, and lighter hydrocarbons at 80°C or lower. However, both GLS-1 and GLS-2 are kept at ambient temperature during the FT synthesis experiments so as to condense as many of the C₆₊ hydrocarbon products as possible, and prepare them for analysis on the offline gas chromatograph coupled with a mass spectrometer or GC-MS (described in section 3.5.3.1).

3.4.1.4 Back Pressure Regulator

After the GLS section, the product stream passes through a back pressure regulator. This regulator is automatically controlled to maintain the desired pressure set-point within the reactor. System pressure is monitored by an isolated pressure gauge/transducer.

3.4.1.5 GC Sampling Valve

After the back pressure regulator, the product stream then enters the GC Sampling Valve (Figure 3.3 and Figure 3.4 above). This valve rotates between two positions: the collect mode and the transfer mode. In the collect mode the product gases pass through the sampling loop and on to the reactant vent. In the transfer mode, the GC carrier gas (helium) pushes the product gas trapped in the sample loop to the transfer line and on to the online GC, as illustrated in Figure 3.7 below.

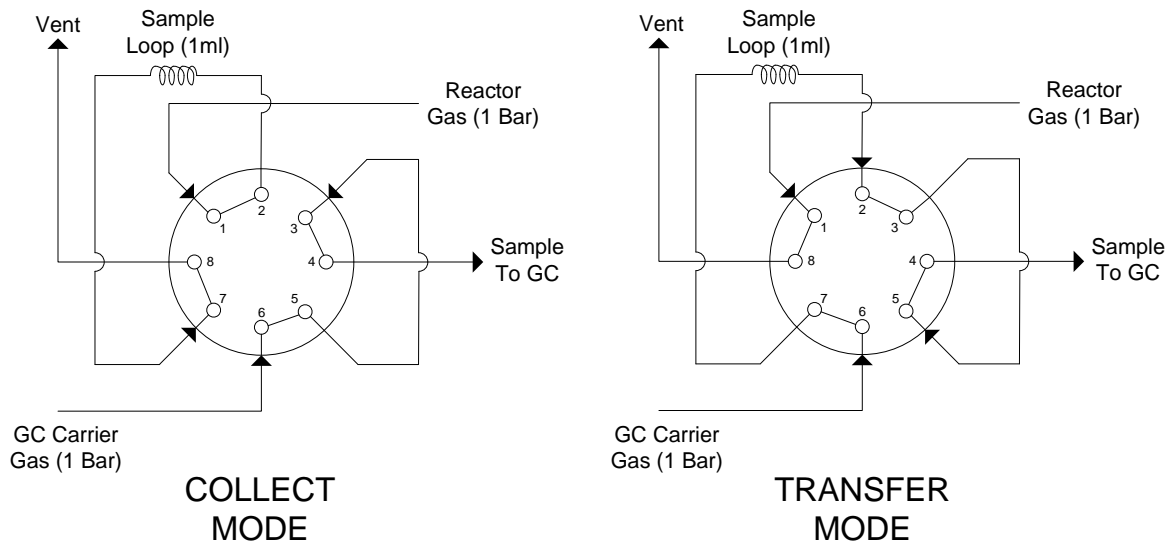


Figure 3.7 – OLD GC Sampling Valve connections

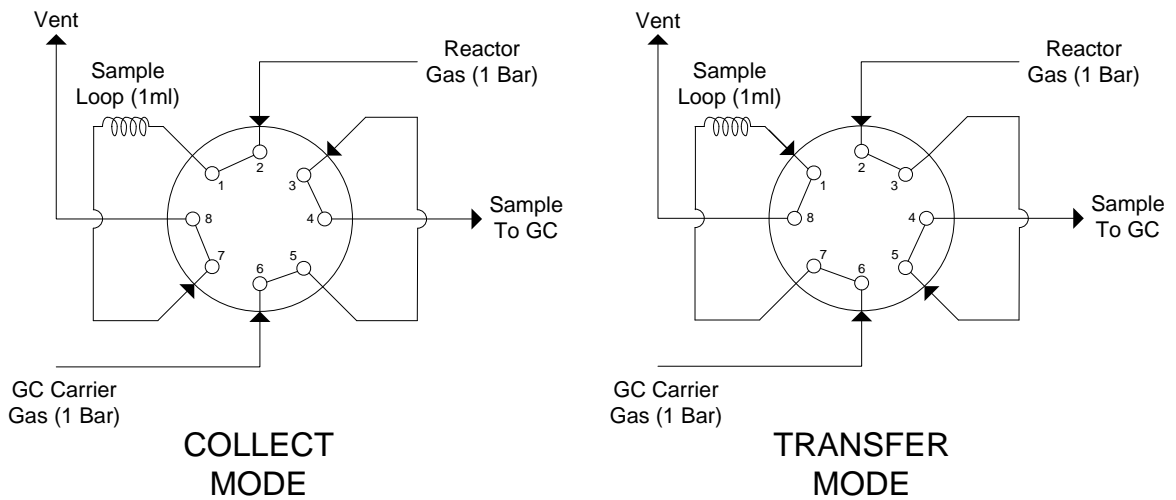


Figure 3.8 – NEW GC Sampling Valve connections

However, two problems were found with this sampling valve. The first problem was that the actuator valve responsible for rotating the sampling valve had been wrongly fitted by the manufacturer and did not rotate the valve correctly. This was later rectified by the manufacturer. The second problem met was that the gas sample trapped in the GC sampling valve 1ml sample loop was not being delivered correctly to the online GC apparatus due to synchronization issues in the delivery of the gas sample between the reactor system and the online GC. This required a modification to the GC sampling valve fittings arrangement. This modification is illustrated in Figure 3.8 above, and involved manually swapping the tube connections in positions 1 and 2. This meant that, essentially, the 1ml sample loop is bypassed when the GC sampling valve is in the transfer mode, and the product gases are directly fed to the online GC.

3.4.1.6 Transfer Line

The GC sampling valve then sends the product gases through to a heated transfer line (maximum T = 180°C). This line is an insulated, stainless steel microbore tube about 3 metres long. The temperature of the transfer line (and, hence, the product gases) is controlled by entering the desired set point on the software display screen (Figure 3.5 above).

3.4.1.7 BTRS Oven

The reactor, mixer tubing, switching valves, and system tubing are all housed in a heated, insulated, stainless steel oven which allows for isothermal operation (maximum temperature of 250°C). The oven temperature is controlled via the oven temperature set-point on the software display screen (Figure 3.5 above).

3.4.2 20cm³ Reactor Commissioning

Significant and unforeseen delays were incurred during the delivery of this reactor system due to issues faced during the tendering process at UK customs. Once it was delivered, however, a commissioning procedure was required for the equipment. This included the following:

- Setting up of a dedicated laboratory in order to house the reactor system which had to be fully equipped with the necessary high-pressure gas lines. As the gases used were both flammable and toxic, these gas lines required the installation of safety alarm trips.
- Initial commissioning of the reactor system and training had to be carried out by the reactor manufacturer for operational, safety and insurance purposes. This commissioning process involved pressurizing the system with nitrogen to check for leaks, as well as checks for overall mechanical and electrical functionality.
- The delivery, set-up, and commissioning of the gas and liquid product analysis equipment (gas chromatographs), as well as the required training by the manufacturer.
- Once all of the above equipment was installed, the joint system (reactor and online gas chromatograph) was re-commissioned using FT synthesis feed gases and typical reaction conditions (section 4.5).

3.4.3 20cm³ Reactor System Limitations

Some equipment limitations were encountered during the work carried out using the 20cm³ reactor system at Aston. These relate to the minimum attainable delivery rate of nitrogen, the availability of pneumatic air supply necessary for automated valve operation, and the absence of a water cooling mechanism. These limitations are discussed in sections 3.4.3.1 to 3.4.3.3 below.

3.4.3.1 Nitrogen Flow Rate

The flow rate of nitrogen into the reactor system is automatically controlled by a mass flow controller, as previously discussed in section 3.4.1.1. The flow rate calibrations that were carried out revealed that the minimum attainable flow of nitrogen into the reactor system was ~13ml/min. The presence of a small amount of nitrogen in the feed syngas is required as an internal standard for GC analysis for the purposes of calculating reactant conversions (section 4.5.2). A compromise had to be made, therefore, between having the lowest possible nitrogen content in the syngas and the lowest possible space velocity. Hence, for the nitrogen content in the syngas mixture to remain low ($\leq 10\text{mol}\%$), a restriction is placed on the minimum flow rate of syngas ($\text{CO} + \text{H}_2$) that could be delivered to the reactor.

Equation 3.1 below, is the re-arranged rate expression for the design of heterogeneous catalytic fixed bed reactors [150]. It states that the reactant conversion, X_A , is proportional to the catalyst weight, W , and inversely proportional to the reactant flow rate, F_{A0} .

$$X_A = \frac{-r_A W}{F_{A0}} \quad (\text{EQ 3.1})$$

According to Equation 3.1, therefore, the limitation on the feed syngas delivery rate, discussed above (in combination with the availability of only a small amount of catalyst previously discussed in section 3.1.1) means that a further constraint is placed on the maximum reactant conversions that could be achieved. In other words, the reactant conversion can not be further increased by lowering the syngas (containing nitrogen) flow rate or increasing the catalyst mass used in the reactor. In addition, the higher (than originally intended) dilution of the syngas with nitrogen as the internal standard ($\leq 10\text{mol}\%$ instead of $\leq 5\text{mol}\%$) also contributes to lowering the potential reactant conversion, as this reduces the concentration of CO and H_2 in the syngas and, therefore, on the catalyst surface during the FT reaction.

3.4.3.2 Pneumatic Air Supply

All the automated valves in this reactor system are operated by pressurized air (at 6 bar). This means that a constant supply of air is required during each experiment run. This constant air supply is not available in the laboratory facilities and, therefore, the air is delivered in standard pressurized cylinders. The air supply needs careful monitoring as the air cylinders require manual replacement once depleted, even while the experiment runs are in progress. The above limitation in combination with the department building access schedule (closed during weekends), meant that the experiments could only be conducted on week days. Hence, the length of an FT synthesis runs is limited to a total period of 48 hours. The reasons for this selected duration can be clarified by consideration of the length of time required for each stage in the complete FT synthesis experiment

procedure that is outlined in section 3.7, in relation to the number of accessible days available per week.

3.4.3.3 Reactor Temperature Control

An additional limitation on this reactor system is the absence of an efficient temperature control mechanism surrounding the reactor, i.e. cooling water. The temperature of the reactor is controlled by adjusting the temperature of the ceramic heating jacket that surrounds it. Any temperature runaways are controlled by turning the heating jacket off. This means that the reactor temperature can not be so easily controlled and needs careful monitoring (and sometimes adjustment).

3.5 Product Analysis Equipment

Two types of analysis equipment are employed for the identification and quantification of products; online GC analyzers for product gases and an offline GC/MS analyzer for liquid and wax products. The specifications of the analysis equipment used in conjunction with each reactor are discussed in sections 3.5.1 to 3.5.3 below.

3.5.1 2cm³ Reactor Product Analysis at UFRJ

Complete online analyses of the products from the 2cm³ reactor are carried out on a GC-17A Shimadzu gas chromatograph equipped with a thermal conductivity detector (TCD) and a flame ionisation detector (FID). The TCD detector aids in the identification and quantification of permanent gases (CO and He), whereas the FID detector is used for identifying a wide range of hydrocarbon products (C₁-C₉₀₊) and other volatiles. However, separate gas injections are necessary in order to use either detector (TCD or FID), as these detectors are not connected in series. For a TCD injection, the volatile products are first passed through a cold trap at 16°C (cooled using ethylene glycol), thus allowing only permanent gases and low molecular weight hydrocarbons to pass through to the GC-TCD for analysis. The specifications of the columns used for each of these detectors are given in Table 3.1 below.

Table 3.1 – 2cm³ reactor: GC column specifications

Detector	Column Type	Column Dimensions
TCD	CP-Porabond Q	50m x 0.32mm
FID	CP-Sil 5CB	50m x 0.32mm

For a FID injection, the volatiles are set to bypass the cold trap and are transferred directly to the GC. The GC oven chamber has been modified to use cryogenic cooling in order to analyze a very wide spectrum of hydrocarbon products (C₁-C₉₀₊) in the following way; the GC oven chamber is first cryogenically cooled by injecting CO₂ (at 60 bar and -25°C) for the first 5 minutes, thus

bringing the column temperature down to -25°C . After 5 minutes, the CO_2 flow is switched off, and the temperature ramp is set to $5^{\circ}\text{C}/\text{min}$. As the temperature is slowly raised in the column this achieves individual compound separation and detection by the FID detector. Some examples of chromatograms obtained from the GC-FID analysis of the products from the 2cm^3 reactor are provided in section 4.4.2.

3.5.2 20cm^3 Reactor Online Gas Product Analysis at Aston

The GC connected online to the 20cm^3 reactor is equipped with a TCD and a FID connected in series, and therefore only one gas injection is necessary for analysis using both detectors. The FID in this GC, however, is only capable of detecting $\text{C}_1\text{-C}_5$ hydrocarbon products. Hence, the GLS chambers or ‘cold traps’ in the 20cm^3 reactor system (Figure 3.4 above) are kept at ambient temperature in order to condense as many C_{6+} products as possible. Online product analysis is performed on a Varian 450-GC gas chromatograph equipped with five columns (Table 3.2 below), which have specific functions within a two ‘channel’ system, that include a permanent gas analyzer ‘channel’ (connected to the TCD detector) and a light hydrocarbon analyzer ‘channel’ (connected to the FID detector). The specifications of the GC columns used are provided in Table 3.2 below.

Table 3.2 – 20cm^3 reactor: online GC column specifications

Detector	Column Type	Specifications	Dimensions
TCD	Hayesep T (CP81072)	80-100 Mesh, Ultimet	0.5m x 1/8" x 2.0mm
	Molecular Sieve 13X (CP81071)	80-100 Mesh	1.5m x 1/8" x 2.0mm
	Hayesep Q (CP81073)	80-100 Mesh	0.5m x 1/8" x 2.0mm
FID	Varian Capillary Column (CP81522)	CP-Sil 5 CB	12.5m x 0.32mm x 1.2 μm
	Varian Capillary Column (CP7568)	CP- $\text{Al}_2\text{O}_3/\text{Na}_2\text{SO}_4$	50m x 0.53mm x 10 μm

3.5.2.1 Permanent Gas Analyzer Channel

This “channel” is an analytical tool developed by Varian principally for the simultaneous determination of non-condensable gases (nitrogen, carbon monoxide, carbon dioxide, methane, and C_2 isomers) in various gas samples. The channel is set for the determination of the mentioned components down to 0.01%. The 1mL sample is injected by means of a gas-sampling valve onto a series of Hayesep columns. The fraction containing nitrogen, carbon monoxide and methane is flushed onto a Molecular Sieve column and ‘parked’. In the meantime, carbon dioxide and the C_2 isomers are eluted to the TCD detector, bypassing the Molecular Sieve column. After the elution of H_2 , the Molecular Sieve column is set to flow again giving the separation of nitrogen, carbon monoxide and methane.

3.5.2.2 Light Hydrocarbon Analyzer Channel

This “channel” is designed to measure the range of low boiling hydrocarbons (C₁-C₅). The system consists of a CP-Sil 5 CB pre-column and the Al₂O₃/Na₂SO₄ column. The highly selective Al₂O₃/Na₂SO₄ column separates all individual isomers from the light hydrocarbon fraction. The channel is set for determination of the hydrocarbon isomers down to 0.01%.

3.5.2.3 Gas Calibration

For compound identification and quantification, both analyzer channels are calibrated by injecting standard mixtures of C₂-C₅ hydrocarbon and permanent gases, including carbon monoxide, hydrogen, carbon dioxide, nitrogen and methane (using gas cylinders containing certified component concentrations). The gas mixtures and concentrations used for GC calibration are provided in APPENDIX A. Based on account of their relative abundance in typical FT gas product mixtures as found in the literature, the hydrocarbon gases that the GC equipment is calibrated for include methane, ethane, ethene, propene, propane, iso-butane, 1-butene, n-butane, neo-pentane, 1-pentene and n-pentane. The GC method used for identification and quantification of the permanent gases and C₁-C₅ hydrocarbon gases is outlined in Table 3.3 below.

Table 3.3 – GC method used for permanent gases and C₁-C₅ hydrocarbon analysis

Parameter	Settings
Carrier	Argon at 1mL/min
Oven	1. 50°C for 10 min 2. 50-180°C at 8°C/min 3. 180°C for 5 min
Injectors	TCD at 150°C, FID at 220°C
Injection Volume	TCD = 1.0 mL, FID = 0.25 mL
Detectors	TCD at 200°C, FID at 200°C
Total Analysis Time	31.25 minutes

Figure 3.9 and Figure 3.10 below, provide two examples of the chromatograms obtained from the permanent gas and C₁-C₅ hydrocarbon gases calibrations in the GC-TCD and GC-FID channels, respectively.

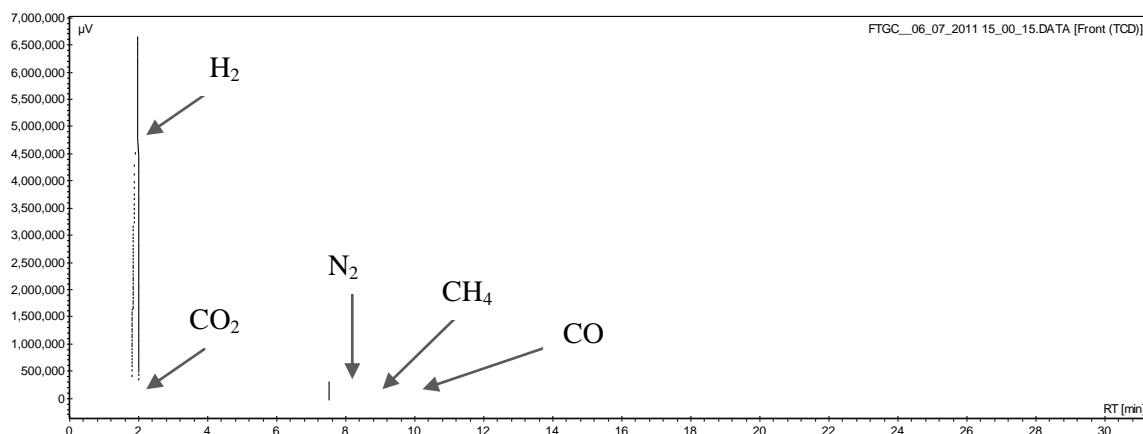


Figure 3.9 – Chromatogram obtained from GC-TCD calibration of permanent gases at Aston

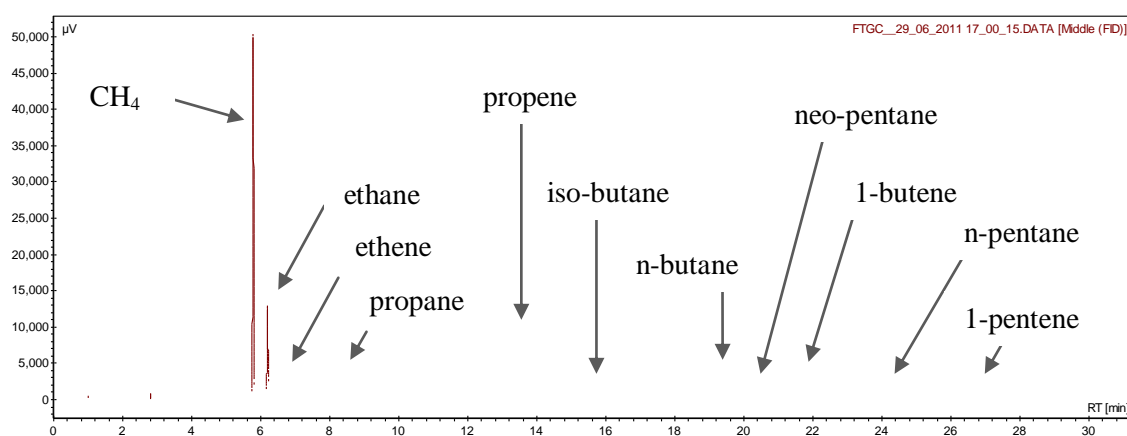


Figure 3.10 – Chromatogram obtained from GC-FID calibration of C₁-C₅ hydrocarbon gases at Aston

3.5.2.4 Reactant Conversion and Product Distribution

The reactant conversion is measured by the conversion of carbon monoxide, as it is the reactant taking part in smaller amounts according to stoichiometry (Equation 2.2 in section 2.2) and therefore plays a limiting role on the FT reaction [151]. As discussed previously in section 2.3, the distribution of the resulting carbon containing products in FT synthesis is commonly referred to as the product selectivity [43] and represents the molar composition of the products formed. Product selectivities are calculated for main reaction products that include carbon dioxide, methane, C₂-C₅ and C₆₊ hydrocarbon products. Their distribution or selectivities can be determined on the basis of carbon monoxide conversion in the synthesis reaction using Equations 3.2 to 3.6 below, according to the methods that have been used by Xu *et al.* [83], Mirzaei *et al.* [86], Feyzi *et al.* [103], Rafiq *et al.* [116], Mohanty *et al.* [91], and Dry [43]. These equations are important as they are used for calculating both the reactant conversion and product selectivities for the FT synthesis experiments that will be conducted in chapter 5. As an example, a C₆₊ selectivity of 70% indicates that 70% of the carbon atoms in the carbon monoxide that react to become hydrocarbons end up in the C₆₊ product fraction.

$$\text{CO conversion (\%)} = \frac{\text{moles of inlet CO} - \text{moles of outlet CO}}{\text{moles of inlet CO}} \times 100 \quad (\text{EQ 3.2})$$

$$\text{CO}_2 \text{ Selectivity (\%)} = \frac{\text{moles of CO}_2 \text{ produced}}{\text{moles of inlet CO} - \text{moles of outlet CO}} \times 100 \quad (\text{EQ 3.3})$$

$$\text{CH}_4 \text{ Selectivity (\%)} = \frac{\text{moles of CH}_4 \text{ produced}}{\text{moles of inlet CO} - \text{moles of outlet CO}} \times 100 \quad (\text{EQ 3.4})$$

$$\text{C}_2\text{-C}_5 \text{ Selectivity (\%)} = \frac{\text{moles of C}_2\text{-C}_5 \text{ produced}}{\text{moles of inlet CO} - \text{moles of outlet CO}} \times 100 \quad (\text{EQ 3.5})$$

$$\text{C}_{6+} \text{ Selectivity (\%)} = 100 - S_{\text{CO}_2} - S_{\text{CH}_4} - S_{\text{C}_2\text{-C}_5} \quad (\text{EQ 3.6})$$

3.5.3 20cm³ Reactor Offline Liquid Product Analysis

At the beginning of each FT synthesis experiment, the GLS chambers (Figure 3.4) are dismantled from the reactor system, weighed and then re-assembled on to the reactor system. At the end of each experiment the liquids (and waxes) are drained and collected from the GLS chambers. The GLS chambers are then dismantled and weighed in order to account for the accumulation of any waxes and liquids in the vessels. The liquid products include an oil phase (liquid hydrocarbons and waxes) and a water phase (water plus oxygenated compounds). The equipment and methods used to analyze these liquids are described in sections 3.5.3.1 to 3.5.3.3 below.

3.5.3.1 Liquid Hydrocarbon Product Analysis

Typical analyses of FT liquid/wax hydrocarbon products are usually performed in gas chromatographs and produce chromatograph spectra that include carbon number products from C₆ up to C₄₀ or higher. Liquid product analysis is performed on a Varian 450-GC chromatograph coupled with a Varian MS-220 mass spectrometer. According to the manufacturer, the experimental error due to the syringe sample injection in these analyses was $\pm 1\%$. The specifications of the column used for analysis are given in Table 3.4 below.

Table 3.4 – GC-MS liquid hydrocarbon analyzer column specifications

Detector	Column	Dimensions
Mass Spectrometer (MS)	Varian FactorFOUR® Capillary Column	VF-5ms, 30m, 0.25mm ID, 0.25µm DF

Using this column, a GC method capable of detecting and identifying this wide range of hydrocarbon compounds was developed in this project. The method development procedure that led to the final preferred method that is used is discussed below. Full details of this method

development procedure are provided in APPENDIX D. Table 3.5 below, summarizes the final GC method that was arrived at.

Table 3.5 – GC method used for C₇-C₄₀ liquid hydrocarbon analysis

Parameter	Settings	
Carrier Gas	Helium at 1mL/min	
Oven Temperature, hold time and heating rate	1. 40°C for 5 min 2. 40-180°C at 2°C/min 3. 180°C for 5 min	4. 180-260°C at 2°C/min 5. 260°C for 5 min 6. 260-330°C for 10 min
Injector	250°C	
Injection Volume	1.0 µL	
Detector Temperature	TCD at 200°C, FID at 200°C	
MS molecular weight scanning range	30-650 (m/z)	

As discussed previously in section 2.2, a typical FT hydrocarbon product mixture consists mainly of paraffins (alkanes) and olefins (alkenes) [43]. Hence, a saturated alkane standard mixture could be used in the procedure for developing an appropriate method for GC analysis. According to GC principles, the saturated alkanes in the standard mixture would elute from the column at distinct retention times and in order of ascending molecular weight [152]. The retention time of each alkane compound could then be compared to the spectra obtained from the product oil analyses to identify alkanes (and their isomers) in the liquid hydrocarbon product collected. In addition, this would aid in categorizing other products (such as alkenes and alcohols) eluting at relatively close retention times and, hence, belonging to the same carbon number product group. The product peaks could then be categorized into distinct carbon number groups, i.e. C₇, C₈, C₉, etc., and then, in turn, into product groups, i.e. naphtha (C₇-C₁₀), diesel (C₁₁-C₁₈) and waxes (C₁₉₊) [35]. The product peak areas could then be used in calculating the relative percentage composition of the product groups in the liquid hydrocarbon sample.

A standard C₇-C₄₀ saturated alkane mixture in a 1mL hexane solution was provided by Supelco[®] Analytical. The individual concentrations of the alkanes in this hexane solution were 1000 µg/mL (+/- 0.5%). Hence, each liquid hydrocarbon (plus waxes) sample collected from the FT synthesis experiments were also diluted in pure hexane before analysis. After a number of hexane solutions containing different concentrations of dissolved liquid hydrocarbons (and waxes) were prepared and analyzed, the optimum hydrocarbon concentration that was determined was approximately 3.0 wt.% (± 5%). This concentration, in combination with the GC method outlined in Table 3.5 above, allowed for complete separation of C₇-C₄₀ compounds within the FT liquid samples. Figure 3.11 below, shows the chromatogram obtained from the analysis of the standard saturated alkane mixture.

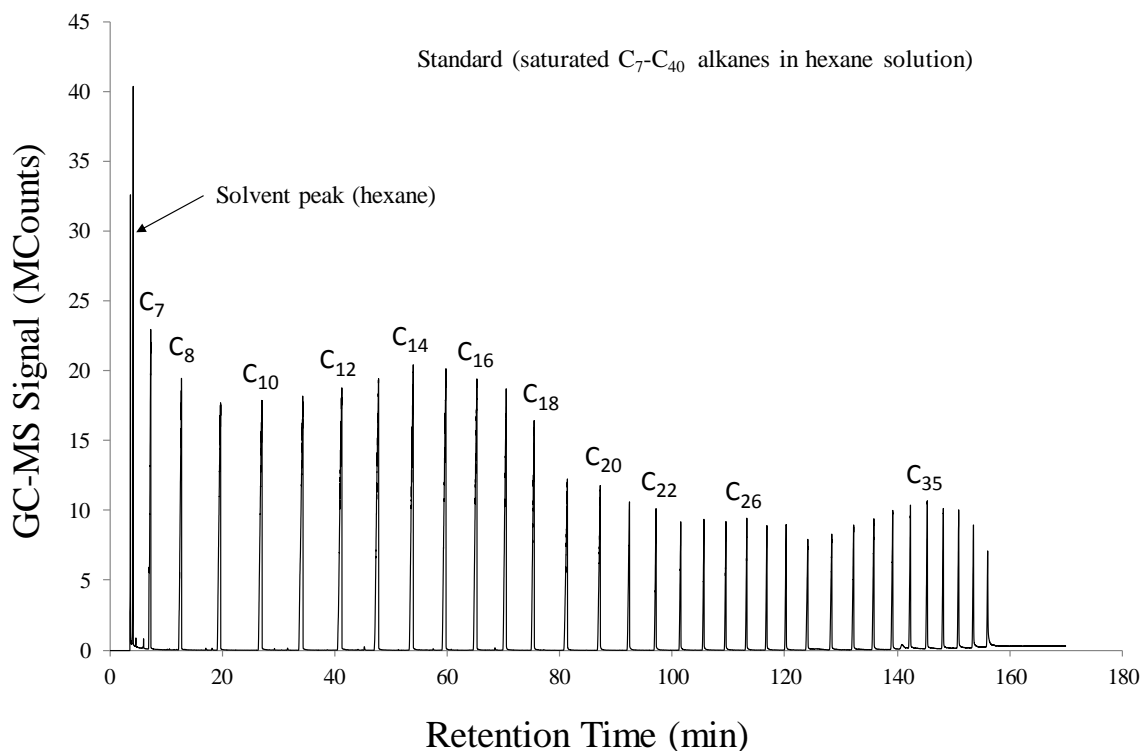


Figure 3.11 – GC-MS chromatogram of standard saturated C₇-C₄₀ alkane solution

Figure 3.12 below, shows the chromatogram obtained from the analysis of a liquid hydrocarbon (plus waxes) product sample collected from an FT synthesis run (test FT4 in Table 4.4, in section 4.5) superimposed on to the chromatogram from the standard solution (Figure 3.11). This is done in order to verify that the product peaks and their retention times coincide with the retention times determined from the analysis of the standard alkane solution. For added certainty, the chromatograms obtained from the analyses of all the liquid hydrocarbon samples collected during the FT synthesis runs were also superimposed onto the standard saturated alkane chromatogram. Further examples of these superimposed chromatograms are provided in APPENDIX F. In all cases, the compound peaks and retention times were well matched.

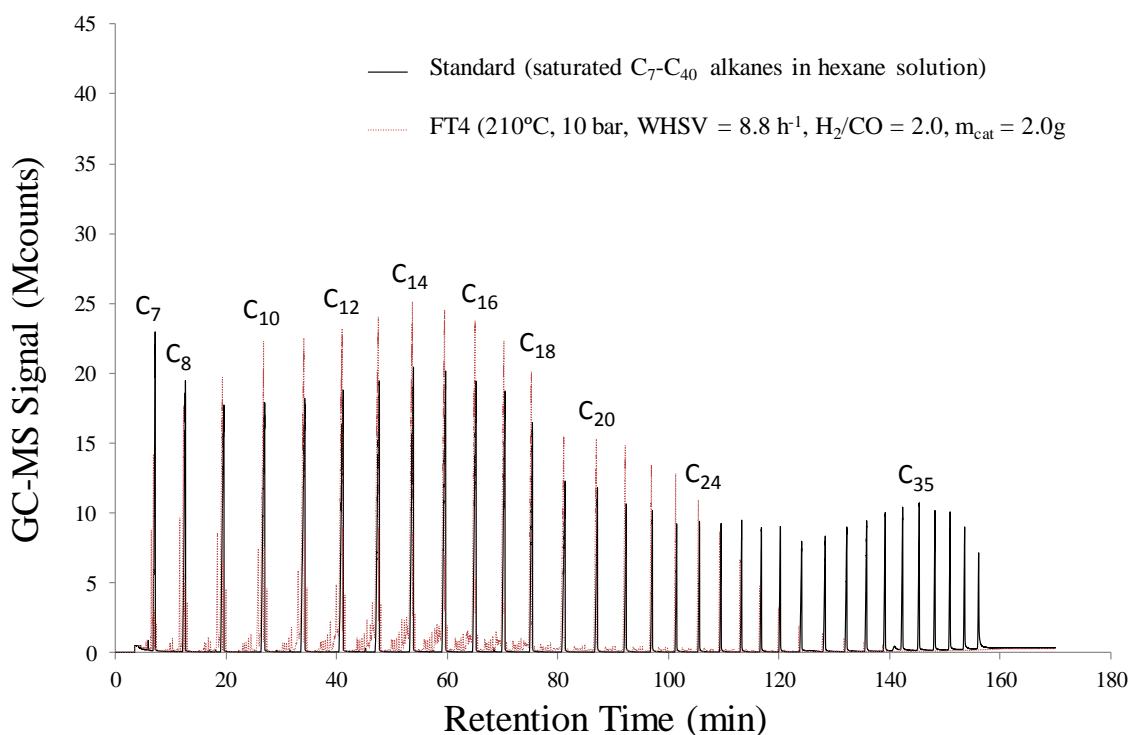


Figure 3.12 – GC-MS chromatogram: comparison of standard versus liquid hydrocarbon product from FT synthesis test FT4 (at 210°C)

3.5.3.2 Aqueous Product Analysis

Water content analysis of the aqueous phase is performed using a Karl-Fischer titration method performed on a Mettler Toledo V20 Volumetric KF Titrator, using ‘Hydranal® 34849 – water standard 10.0’ as the standard solution, ‘Hydranal® 34816 – Composite 5k’ as the titrant and ‘Hydranal® 34817’ as the working medium. Prior to each sample analysis, the titrant is standardized against the water standard solution in triplicate. The sample is then added to deduce the concentration of water (and, hence, soluble oxygenated compounds by difference) within the sample in triplicate. A similar Karl-Fischer titration method for the determination of the water present in the FT aqueous phase was also used by Bukur, Patel and Lang [104].

3.5.3.3 Liquid Hydrocarbon Calorific Value Determination

Ultimate (CHN) analyses of the liquid hydrocarbon samples that are collected after each FT synthesis experiment in the parameter study (chapter 5) are carried out by Medac Ltd (elemental oxygen content is determined by difference). Their energy content (HHV) is determined by the unified correlation for estimating HHV from ultimate analysis put forward by Channiwala and Parikh [153] (Equation 3.7 below). This correlation is used as it is the basis for all HHV calculations at Aston and thus provides a consistent database for comparison.

$$\text{HHV}_{\text{dry}} \text{ (MJ/kg): } 0.3491 \cdot \text{C} + 1.1783 \cdot \text{H} + 0.1005 \cdot \text{S} - 0.1034 \cdot \text{O} - 0.0151 \cdot \text{N} - 0.0211 \cdot \text{ash} \text{ (EQ 3.7)}$$

3.6 Catalyst Characterization Techniques

Catalyst characterization studies are carried at various institutions in the UK, both at Aston University and Catal International Ltd, as well as in cooperation with the Federal University of Rio de Janeiro (UFRJ), in Brazil. The specific techniques that are used are commonly used in FT catalyst research [86, 103] and include morphological studies, powder X-ray diffraction (XRD), temperature programmed reduction (TPR), thermo-gravimetric analysis (TGA) and scanning electron microscopy (SEM). These techniques, the reasons for their implementation and the equipment used for each one are discussed in sections 3.6.1 to 3.6.4 below.

3.6.1 Morphological Studies

These studies aim to investigate some of the textural and physical properties of the available catalysts, which include BET and SEM analyses that are outlined in sections 3.6.1.1 and 3.6.1.2 below.

3.6.1.1 Specific Surface Area, Porosity, Particle Size and Bulk Density

These studies aim to determine the specific surface area, pore volume and pore size of the catalysts. These properties, in combination with the catalyst formulation and composition, help to characterize or define the catalyst. Brunauer-Emmet-Teller (BET) surface area measurements for the cobalt/alumina catalyst were carried out at UFRJ, Brazil at a temperature of -196°C using a Micrometrics ASAP2010 gas adsorption instrument according to the method reported by Sing and Everett [154]. The sample is degassed at 300°C overnight prior to the adsorption experiments. The specific BET surface area is determined from the linear part of the BET (Brunauer curve in 0.05-0.35 partial pressure range) and the pore size distribution is determined by the Barrett-Joyner-Halenda (BJH) method from the desorption branch of the isotherm. BET surface area measurements for the cobalt/titania and iron/alumina catalysts were carried out by Catal International Ltd.

The bulk densities of the catalysts are found by determining the exact mass of each catalyst that occupied 1cm^3 in volume of a volumetric cylinder. Knowledge of the bulk density of each catalyst is required in order to plan the reactor packing method which, in combination with the reactor dimensions and volume (provided in APPENDIX E), enables the determination of the catalyst bed height. Information on the average particle diameters for both the cobalt/titania and iron/alumina catalysts were provided by their manufacturer, Catal International Ltd, whereas for the cobalt/alumina catalyst formulated in the laboratory at UFRJ, this was determined using standard fine mesh sieve plates.

3.6.1.2 Scanning Electron Microscopy (SEM)

This analysis technique is performed on all three available catalysts so as to take a magnified look at the morphology of the catalyst surface prior to and after reaction. Potentially, it also enables the observation of the effects of reaction conditions on catalyst deactivation due to the mechanisms of carbon deposition and/or wax deposition, discussed previously in section 2.4.3. The catalyst samples are scanned using a Cambridge Instruments Stereoscan S90 scanning electron microscope. Each sample is dried in an oven at 105°C for 24 hours and then placed on a double-sided conductive carbon tape and scanned at a wide range of magnification strengths. SEM images of the available catalysts prior to reaction are provided in section 4.2.1. Images of the cobalt/alumina catalyst before reaction as well as after all the FT synthesis parameter study experiments (detailed in chapter 5) are provided in APPENDIX B.

3.6.2 X-Ray Diffraction (XRD)

Powder XRD is an analysis technique that can be used to identify the active phase(s) in the catalyst, as well as the promoters and supports that are incorporated into the catalyst structure, thus verifying the presence of the catalyst components. XRD measurements are performed using a Rigaku Miniflex X-Ray Diffractometer Ultimate+ 2200, operated at 30 kV and 15 mA, using copper radiation ($\lambda_{\text{CuK}\alpha} = 1.5406 \text{ \AA}$). The values of θ ranged from 2-100° with a step size of 0.05° and 2 θ /min. The basic theory behind this technique can be explained as follows [155, 156]. When an X-ray beam strikes a plane of atoms in a crystalline solid, a portion is diffracted (reflected) and one crosses the plane going to reach a subsequent plane. If two or more planes are considered, the conditions for the diffraction phase will depend on the path followed by the X-ray beam. The condition for diffraction in the phase is given by Bragg's Law (Equation 3.8 below):

$$n\lambda = 2d\sin\theta \quad (\text{EQ 3.8})$$

where n is the order of diffraction, λ is the wavelength of the incident wave, d is the spacing between the planes in the atomic lattice, and θ is the angle between the incident ray and the scattering planes. The basic idea behind XRD analysis is to vary the θ until Bragg's Law is satisfied. This can be done by turning the crystal or by using a large number of randomly oriented crystals (powder method). Thus, for a given plane characterized by d , there exist a significant number of crystals in which this plane will be guided through the beam at an appropriate angle, θ [157].

3.6.3 Temperature Programmed Reduction

This characterization technique is used in order to identify the temperature range at which the catalyst undergoes reduction (section 4.2.3). This enables the right temperatures to be selected for the thermal pre-treatment of the catalyst prior to FT reaction and ensure that the catalyst has indeed

been reduced and activated before the start of the reaction. The samples (50 mg) are placed in a quartz micro-reactor coupled to a GC-TCD detector. The pretreatment consists of dehydrating the powder at 300 °C for one hour in a flow of pure Ar at 30 ml/min prior to the reduction. After cooling to room temperature the gas mixture is switched to 10% H₂/Ar at 30 ml/min and the sample is heated to 1000 °C at 10°C/min. After the reaction, the reactor is cooled to 25°C. Calibration with CuO powder is used to quantify the extent of reduction of the samples.

3.6.4 Thermo-Gravimetric Analysis (TGA)

TGA measurements are carried out using a PerkinElmer Pyris 1TG apparatus with an auto-sampler. The TGA records the change in mass of a sample as temperature varies (heated, cooled or held at a constant temperature). The weight loss profile that the TGA analysis provides makes it possible to determine the moisture retained in the catalyst sample and to estimate the amount of coke and/or wax deposited on the catalyst surface after reaction, as this would be burned off at high temperatures. The relative weight loss is attributed to the amounts of carbon and/or wax present on the catalyst surface and therefore the extent of deposition during the FT reaction. The same method for determination of coke deposition on the catalyst surface using TGA analysis was also used by Mohanty *et al.* [91]. Approximately 20mg samples of the catalyst are taken after each FT synthesis reaction and analyzed using a constant heating rate of 5°C/min from room temperature to 800°C using a steady flow rate of air at 30ml/min and at atmospheric pressure.

3.7 FT Synthesis Experiment Procedure

The experimental procedure that is followed for the FT synthesis experiments, both in the catalyst selection procedure (stage 3A) and the parameter study (stage 3B), can be broken down into four stages. These stages are depicted in Figure 3.13 below, and a detailed description of what each stage entails is provided in sections 3.7.1 to 3.7.4 that follow. During each experiment, the data collected during these stages is recorded on a laboratory record sheet, an example of which is provided in APPENDIX H.

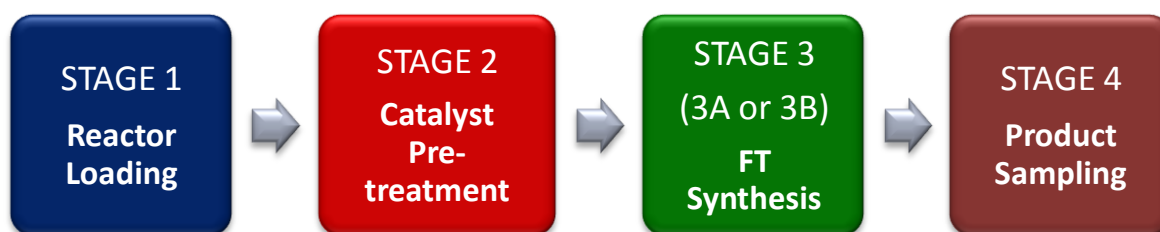


Figure 3.13 – Stages in FT experiment procedure

3.7.1 Stage 1 – Reactor Loading

This first procedural step involves the packing of the reactors. The catalyst loading procedures for each fixed-bed reactor are provided in sections 3.7.1.1 and 3.7.1.2 below. Both methods employ the

ideal loading ratio of **bed height: reactor diameter** being greater than **20:1**, according to advice from an industrial contact with fixed bed FT synthesis catalysis expertise [158]. Whereas the quartz wool layers (used in both methods) secure in place and support the catalyst bed, the glass bead layers aid in primarily enhancing the gas distribution and flow patterns inside the reactor by minimizing the voidage along the reactor length. This also contributes to maintaining isothermal conditions along the entire length of both reactors.

3.7.1.1 2cm^3 Reactor Loading

In the 2cm^3 reactor, the thermocouple is attached on the outside wall of the reactor shaft, hence, the shaft is easily disassembled, packed and reassembled back onto its supporting metal framework. The particular packing method used is illustrated in Figure 3.14 below.

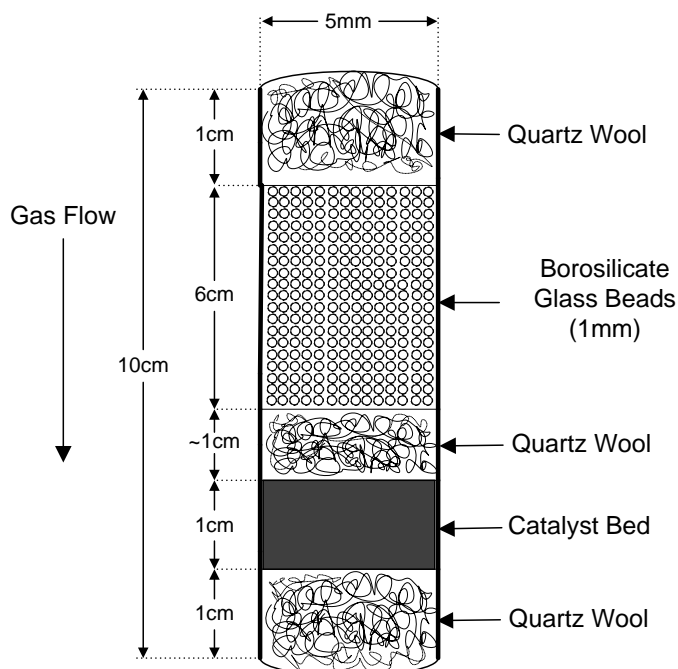


Figure 3.14 – 2cm^3 reactor loading method

3.7.1.2 20cm^3 Reactor Loading

In order to pack the 20cm^3 reactor, the shaft is removed from the automated reactor system and then disassembled, in order to isolate it from the heating jacket (the catalyst bed thermocouple is left attached to the reactor tube). The stainless steel tube is first turned upside down, and then the following loading sequence is performed:

First a layer of quartz wool is pushed down the reactor shaft using a $\frac{1}{4}$ inch, thin-walled tube. Next, 1mm borosilicate glass beads are dropped onto the quartz wool. This is followed by the catalyst, and then another layer of quartz wool. The remaining reactor volume is occupied with borosilicate glass beads, which are supported on a final layer of quartz wool. The catalyst-laden reactor is then

re-assembled and re-connected to the automated reactor system, and is ready for the next stage of the experimental procedure. This devised packing method is illustrated in Figure 3.15 below.

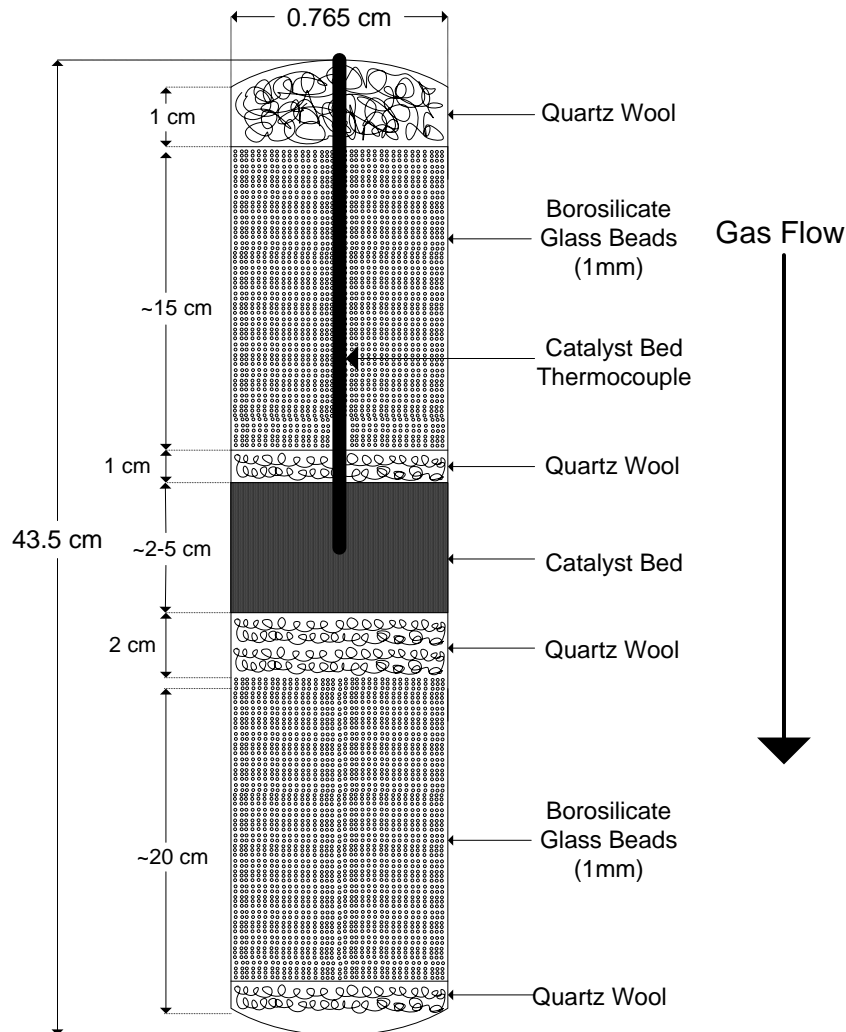


Figure 3.15 – 20cm³ reactor loading method

3.7.2 Stage 2 – Catalyst Pre-Treatment

The second stage of the FT synthesis experimental procedure involves subjecting the catalysts to thermal treatment and reduction or activation, which are necessary prior to taking part in the FT reaction for the following reasons:

- Firstly, moisture accumulates on the catalyst surface and pores during storage which has to be evaporated before the FT synthesis reaction. This is because the presence of water has been found to hinder the reduction of the metal oxide to the metallic active phase, by deactivating the catalyst [159].
- Secondly, the metal oxide phase needs to be reduced in hydrogen to the metallic phase which possesses the necessary activity for the FT reaction.

The catalysts that were provided by Catal International Ltd (namely the cobalt/titania and iron/alumina catalysts) each came with their own manufacturer recommended pre-treatment/activation procedures [160]. The activation procedure recommended for the cobalt/titania catalyst is comparable to that published for a similar catalyst formulation by Li *et al.* [161]. The activation procedure followed for the cobalt/alumina catalyst was recommended by UFRJ (where the catalyst was formulated [157]), and is analogous to those commonly found in the literature for cobalt supported on alumina (10%Co/Al₂O₃) [159]. The determining factors for the appropriate pre-treatment conditions for each catalyst are discussed in more detail in section 4.2.3. The activation procedures followed in each reactor are discussed in sections 3.7.2.1 and 3.7.2.2 below. The time needed for the pre-treatment of each catalyst varied from 9 to 19 hours depending on the catalyst.

3.7.2.1 2cm³ Reactor Catalyst Activation Procedure (UFRJ)

The pre-treatment procedure followed for the FT synthesis experiments on the 2cm³ reactor is the same for both catalysts used and only differs in detail from the 20cm³ reactor catalyst activation procedures described in section 3.7.2.2. This is the standard catalyst activation procedure carried out at UFRJ [157] and includes first drying in a flow of pure helium (133ml/min) for one hour at 105°C, followed by reduction in pure hydrogen (133ml/min) at 350°C (1°C/min) for 10 hours, and subsequent cooling to 180°C.

3.7.2.2 20cm³ Reactor Catalyst Activation Procedures (Aston)

The catalyst pre-treatment procedures followed on the 20cm³ fixed bed reactor are different for each catalyst and are summarized in Table 3.6 below. These procedures are similar to those used in the available literature [83, 114, 156, 162]. Despite the differences, the overall procedure involves the following:

1. Drying in a nitrogen atmosphere (for 1 or 2 hours at 105°C), followed by
2. Reduction in a flow of hydrogen, partial flow of hydrogen in nitrogen, or in syngas in the case of the iron/alumina catalyst, for a defined period of time as the temperature is raised, at the appropriate heating rate, up to the corresponding reduction temperature.
3. Once this temperature is reached, the catalysts are reduced at these conditions for a specific amount of time.
4. In the case of the cobalt-based catalysts, once the reduction in hydrogen is complete, the reactor is cooled down to 180°C, prior to reaction, so as to avoid any temperature runaways once the FT synthesis reaction is initiated.

Table 3.6 – Summary of catalyst pre-treatment procedures followed for catalyst screening test runs on 20cm³ reactor

Catalyst	Procedure	Stage	Temperature (°C)	Heating Rate (°C/min)	Duration (h)	Gas Composition	Gas Flow Rate (ml/min)	WHSV (h ⁻¹)
Co/Al ₂ O ₃	DRYING	1	25-105	5	0.25	100% N ₂	133	10
		2	105	-	1.00	100% N ₂	133	10
	REDUCTION	3	105-350	1	4.08	100% H ₂	133	0.7
		4	350	-	11.00	100% H ₂	133	0.7
	COOLING	5	350-180	-	1.00	-	0	0
Co/TiO ₂	DRYING	1	25-150	1	2.08	100% N ₂	133	10
		2	150	-	1.00	100% N ₂	133	10
	REDUCTION	3	150	1	0.50	25% H ₂ + 75% N ₂	133	7.7
		4	150-350	1.33	2.51	25% H ₂ + 75% N ₂	133	7.7
		5	350	-	12.00	25% H ₂ + 75% N ₂	133	7.7
	COOLING	6	350-180	-	1.00	100% N ₂	133	7.7
Fe/Al ₂ O ₃	DRYING	1	25-125	5	0.33	100% N ₂	75	5.6
		2	125	-	3.00	100% N ₂	75	5.6
	REDUCTION	3	125	-	1.00	50% N ₂ + 50% Syngas	75	4.1
		4	125-175	5	1.20	50% N ₂ + 50% Syngas	75	4.1
		5	175-225	5	1.20	50% N ₂ + 50% Syngas	75	4.1
		6	225-275	5	1.20	30% N ₂ + 70% Syngas	75	3.4
		7	275-290	5	1.05	30% N ₂ + 70% Syngas	75	3.4

3.7.3 Stage 3 – FT Synthesis

Stage three of the overall experimental procedure involves the actual FT synthesis tests. This entails either the catalyst screening (or selection) tests or the parameter study tests. The experiments conducted during the catalyst selection procedure, the conditions that are employed and the results that are obtained are presented and discussed in detail in chapter 4. Conversely, those conducted during the FT synthesis parameter study, the conditions that are employed and the results that are obtained are presented and discussed in detail in chapter 5.

3.7.4 Stage 4 – Product Sampling

The equipment used for gas and liquid product analysis was described in detail in section 3.5. The product analysis procedures that are followed for the products obtained from both fixed-bed micro-reactors are outlined in sections 3.7.4.1 and 3.7.4.2 below.

3.7.4.1 2cm³ Reactor Product Sampling (UFRJ)

All product analyses during the FT synthesis reactions carried out using this reactor are performed online. Samples, containing permanent gases (e.g. CO, H₂ and He) and product vapours (C₁-C₄₀), leaving the reactor are injected at regular intervals into the gas chromatograph. Separate injections are made for permanent gas detection and quantification into the GC-TCD channel, and conversely, for hydrocarbon product detection and quantification into the GC-FID channel as previously described in section 3.5.1. TCD injections are performed every 2-4 hours during the day, whereas only 3 FID injections are carried out at the beginning (2 hours), middle (24 hours) and end (48 hours) of each experiment.

3.7.4.2 20cm³ Reactor Product Sampling (Aston)

As previously discussed in sections 3.5.2 and 3.5.3, the gaseous and liquid products from this reactor are analyzed separately. A sample of the gases leaving the reactor (permanent gases, including CO, H₂, N₂, CO₂ and methane, as well as C₁-C₅ hydrocarbon gases) during each FT synthesis experiment is automatically injected every one hour via a heated transfer line (at 180°C) into the online GC equipped with a TCD and an FID detector. The values obtained for the molar composition of the product gases at the time of the injections, therefore, are assumed to be constant for each hour in between sample injections. The CO conversion and product selectivity values (calculated using Equations 3.2 to 3.6 in section 3.5.2.4) are used to determine the gas product yields, as well as the yield of unreacted syngas. The liquid (and wax) products are also drained, collected and weighed at the end of each experiment. These values are then used to perform a mass balance over the reactor for each run, from which an energy balance over the reactor can also be carried out. The liquid products are usually comprised of an oil phase (liquid hydrocarbons) and a water phase (water plus soluble oxygenated compounds). Samples from each phase are extracted for analysis. The liquid hydrocarbons are analyzed for their fuel composition on the offline GC-MS (section 3.5.3.1), and also for their calorific values using ultimate analysis (section 3.5.3.3). The water product samples are analyzed for water content in the volumetric titrator (section 3.5.3.2) and the soluble oxygenated product content is calculated by difference.

4 Catalyst Selection

This chapter describes the procedure that is followed in order to compare the three catalysts that are available for this work and enable the selection of the most suitable catalyst for further FT synthesis parameter studies. The catalysts are subjected to characterization studies, as well as catalytic activity tests during FT synthesis, for which the two different fixed-bed micro-reactors described in sections 3.3 and 3.4 are used. The results of both the catalyst characterization studies and the FT synthesis catalyst screening tests are presented and discussed within this chapter.

4.1 Introduction

As previously discussed in section 3.1.1, there are three catalysts available for this work. The composition of these catalysts and a summary of the methods used to prepare them are presented in Table 4.1 below. For convenience, the shorthand description for each catalyst presented in the first column in Table 4.1 (giving the metal and the support material) will be used in the remainder of this thesis when reference to any of these catalysts is made. The techniques used to prepare each of these catalysts are provided in APPENDIX C.

Table 4.1 – Available catalysts: composition and preparation methods

Catalyst (Metal/Support)	Composition (wt.%)	Preparation Method
1) Co/Al ₂ O ₃	Co: 10% Al ₂ O ₃ : 90%	Incipient wetness impregnation on alumina support (prepared in collaboration with and at the Federal University of Rio de Janeiro, Brazil).
2) Co/TiO ₂	Co: 9.80% Ru: 0.22% TiO ₂ : 89.98%	Pore volume impregnation on titania support (recommended by BP [84] and externally prepared by CATAL International Ltd, UK, according to the method used by Li <i>et al.</i> [161]).
3) Fe/Al ₂ O ₃	Fe ₂ O ₃ phase: 60% Al ₂ O ₃ : 40%. (Fe₂O₃ phase: Fe ₂ O ₃ : 91.9% La: 2.6%, Re: 3.2%, Ru: 1.5%, Cr: 0.8%)	Precipitation – successive impregnations on alumina support (externally prepared by CATAL International Ltd, UK).

These three catalysts are compared in a screening procedure to determine their suitability for the main project aims outlined in section 1.3, which included obtaining an intermediate liquid hydrocarbon product for further integration into existing refineries. The factors influencing the catalyst selection are centred on the products that are obtained and their composition. Hence, the catalyst candidate that gives the best yields of liquid hydrocarbons with an optimum composition of

diesel range products is opted for. The activities and product distribution of the catalysts listed in Table 4.1, therefore, are compared during FT synthesis. These FT synthesis catalyst screening tests are outlined and discussed in section 4.3. In preparation for these FT synthesis catalyst screening tests, however, some basic catalyst characterization studies are first performed. The results of these characterization studies are presented and discussed in section 4.2 below.

4.2 Catalyst Characterization

The catalyst characterization techniques were described in section 3.6, and the results of these studies provide morphological details (such as surface area and porosity), other physical properties (like the average particle size and bulk density), verification of the catalyst components present (i.e. active phase and support material), as well as the reducibility of each catalyst. The results obtained from these characterization studies are presented and discussed in sections 4.2.1 to 4.2.3 below.

4.2.1 Catalyst Morphological Studies – Results

Table 4.2 below, presents the specific surface areas, pore volume and size, and bulk density of each catalyst using the techniques previously outlined in section 3.6.1.1.

Table 4.2 – Results of catalyst morphological studies

Catalyst	Specific Surface Area (m ² /g)	Pore Volume (cm ³ /g)	Pore Diameter (Å)	Particle Diameter (µm)	Bulk Density (g/cm ³)
Co/Al ₂ O ₃	216	0.85	146	≤ 50	0.28
Co/TiO ₂	28	0.31	2250	≤ 25	0.67
Fe/Al ₂ O ₃	162	0.35	494	≤ 355	0.75

The specific surface area and porosity study results demonstrate some of the structural differences between the three catalysts. The determined values are representative of similar catalyst formulations found in the literature [161, 163-165]. The differences in the specific surface areas of the cobalt-based catalysts is considerable due to the different support materials that are used, where γ -alumina supports typically display much larger surface areas than titania. When the support material has a high surface area like alumina, it has been reported that the cobalt particle size tends to be quite small, forming clusters, whereas the opposite is true in support materials with low surface area like titania, where the particles are more evenly dispersed [156, 159]. A study carried out by Bezemer *et al.* [166], however, concluded that the cobalt particle size (>6nm) does not influence the catalyst activity, hence the differences in specific surface areas of these catalysts are not a major concern. The average particle size of each catalyst, given in Table 4.2 above, is important in the determination of the pressure drop across the catalyst bed. Examples of these calculations using the Co/Al₂O₃ catalyst in the 20cm³ reactor are provided in APPENDIX E.

The differences in the particle sizes, shapes and the texture of the catalysts can be seen in Figure 4.1 below, which displays SEM photographs of the three catalysts, at similar magnification strengths. As shown in the images below, the Fe/Al₂O₃ catalyst has coarse particles of varied sizes (representative of the crushed nature of this catalyst, as described in APPENDIX C) which are, on the whole, much larger than those of the other two catalysts. In contrast, much smaller particle sizes and relatively more uniform particle shapes can be seen in the images representing the cobalt-based catalysts. In both cobalt-based catalysts, agglomeration of the fine particles (probably due to moisture retention) contributes to the formation of clusters. Hence, although seemingly larger particles can be seen in the image representing the Co/TiO₂ catalyst in comparison to that of the Co/Al₂O₃ catalyst, this is due to the much finer powder nature of the Co/TiO₂ catalyst.

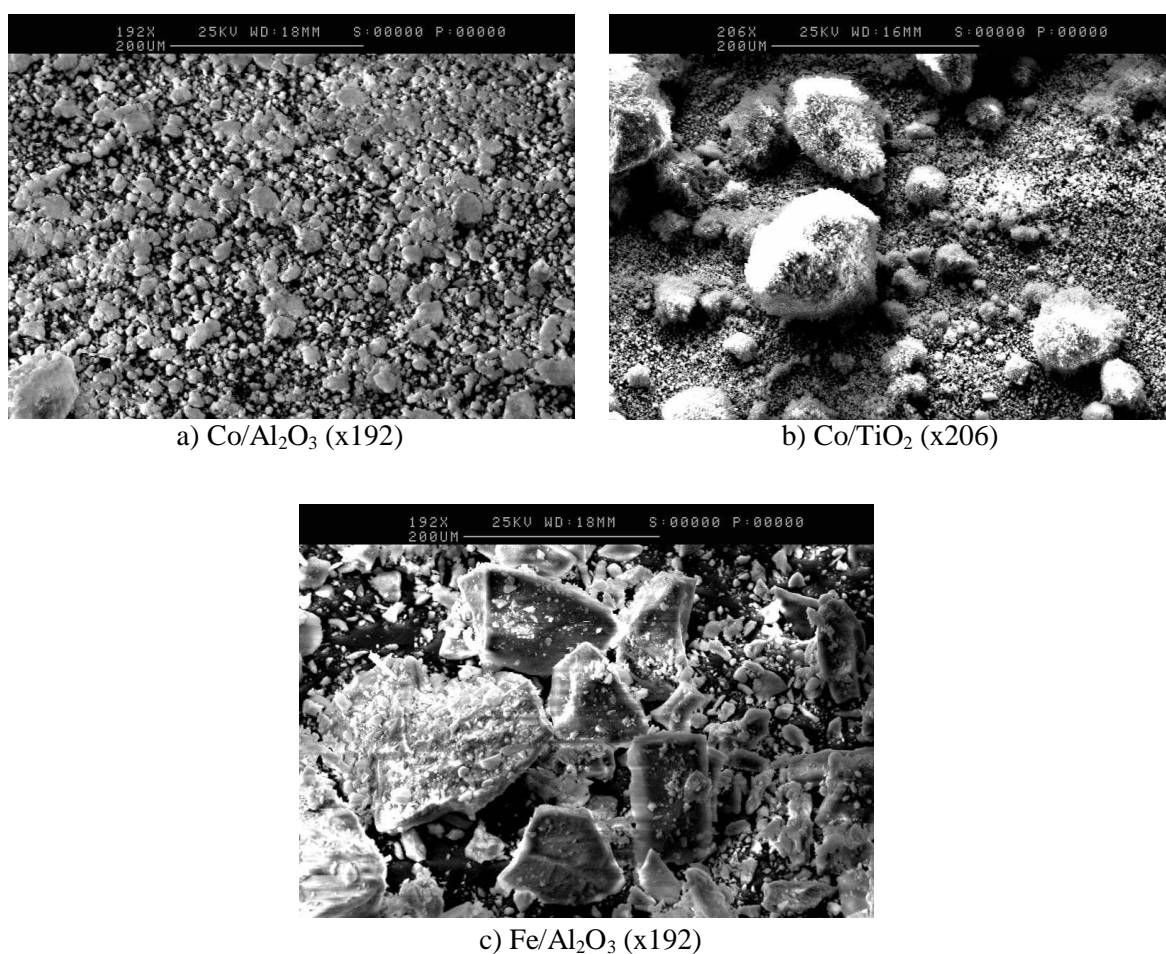


Figure 4.1 – SEM micrographs of the three catalysts prior to FT synthesis reaction

4.2.2 X-Ray Diffraction Results

The presence of the active metallic phases and supporting materials in the overall catalyst structure are verified using X-ray diffraction (XRD), as previously described in section 3.6.2. The results obtained from the XRD analyses of the three catalysts used in the present study are purely for identification of the active metallic phases and support materials in the catalyst, and are discussed in sections 4.2.2.1 to 4.2.2.3 below.

4.2.2.1 XRD of Co/Al₂O₃ Catalyst

It has been reported that different metallic cobalt phases (Co₃O₄ or Co₂AlO₄) can exist in the catalyst framework as the cobalt can penetrate deep into the alumina structure during calcination at high temperatures [67, 156]. These two phases cannot be easily differentiated in the XRD diffractogram, but the presence of Co₂AlO₄ can be verified by an analysis technique known as temperature programmed reduction (TPR), the results of which are discussed in section 4.2.3.1. Figure 4.2 below, shows the XRD diffractogram obtained for the Co/Al₂O₃ catalyst. The peaks that correspond to the metallic phase (Co₃O₄ or Co₂AlO₄), according to the mass spectrometer (MS) library, are indicated with a red circle, whereas those corresponding to the alumina support are indicated by a blue square. Peaks at similar angles were also reported by de la Osa *et al.* [89] using catalysts of similar composition, thus indicating that both metallic cobalt phases (Co₃O₄ or Co₂AlO₄), supported on γ -alumina, are present in the overall catalyst structure.

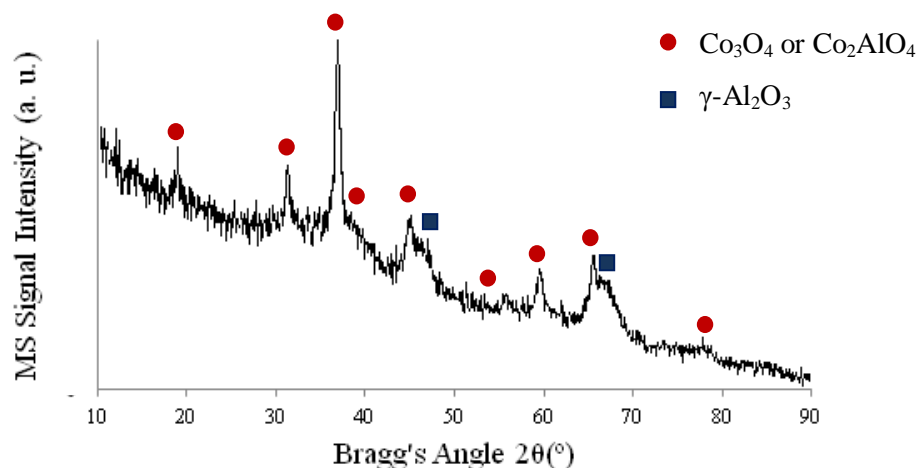


Figure 4.2 – XRD diffractogram of Co/Al₂O₃ catalyst

4.2.2.2 XRD of Co/TiO₂ Catalyst

Figure 4.3 below, shows the XRD diffractogram obtained for the Co/TiO₂ catalyst.

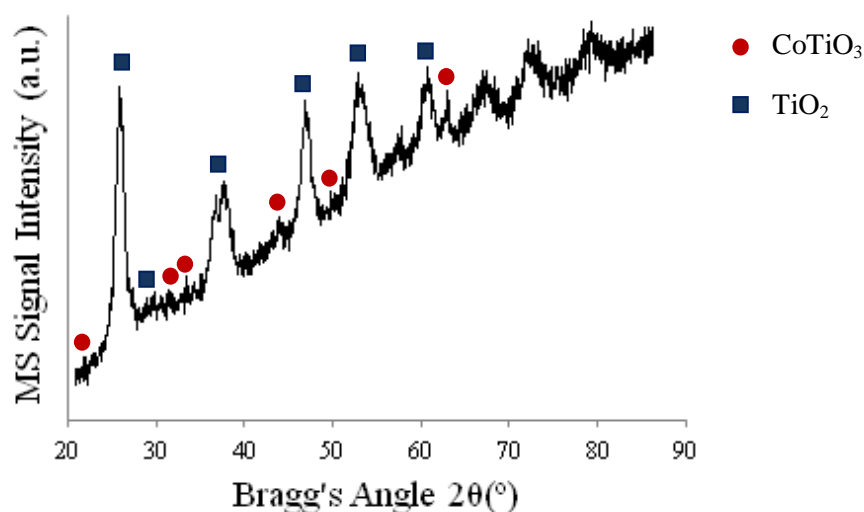


Figure 4.3 - XRD diffractogram of Co/TiO₂ catalyst

The peaks that correspond to the CoO metallic oxide phase, according to the mass spectrometer (MS) library [157], are indicated with a red circle, whereas those corresponding to the titania support are indicated by a blue square. Peaks at similar angles were also reported by Zennaro, Tagliabue and Bartholomew [167] using a catalyst of similar composition, thus indicating that the metallic cobalt phase (CoTiO₃), supported on titania, is present in the overall catalyst structure.

4.2.2.3 XRD of Fe/Al₂O₃ Catalyst

Figure 4.4 below, shows the XRD diffractogram of the Fe/Al₂O₃ catalyst and compares it with MS library patterns of alumina and haematite [157], thus indicating that the metallic iron phase (Fe₂O₃), supported on γ -alumina, is present in the overall catalyst structure.

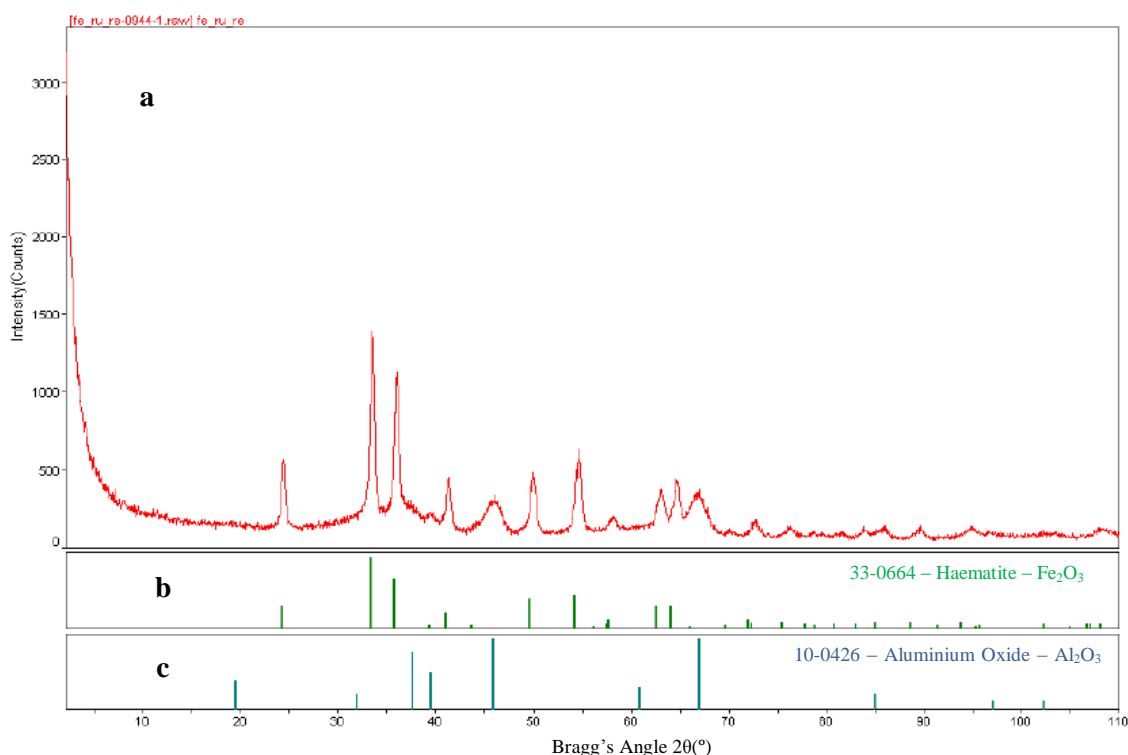


Figure 4.4 – XRD diffractogram of Fe/Al₂O₃ catalyst (a) compared to MS library identity patterns for haematite (b) and aluminium oxide (c)

4.2.3 Catalyst Reducibility – TPR Results

The catalyst activation procedures, which were discussed previously in section 3.7.2, include a drying stage where undesirable moisture retained on the catalyst surface is driven off. According to Jalama *et al.* [159], when cobalt is used on alumina support strong interactions exist between the metal and the support making it harder to reduce. These strong interactions are reported to be enhanced further by the presence of water vapour [159]. For this reason, any surface moisture must be driven off prior to reaction. The presence of surface moisture on each catalyst is verified by means of thermo-gravimetric analyses (TGA), as described previously in section 3.6.4. The results of these analyses show that the surface moisture content of the catalysts varies from 2.5 to 3.8 wt.% (results are the average of three repetitions).

Prior to taking part in the FT synthesis reaction, the appropriate reduction temperature for each catalyst must also be determined. The most common characterization technique for doing this is temperature programmed reduction (TPR), which was discussed previously in section 3.6.3. This technique monitors the reduction behaviour of the catalyst as the temperature is increased, and the results obtained for each catalyst are discussed in sections 4.2.3.1 to 4.2.3.3 below. The temperature profile obtained is then incorporated into the activation procedure, which was discussed previously in section 3.7.2. In the case of the Co/TiO₂ and Fe/Al₂O₃ catalysts activation procedures with appropriate reduction temperatures were recommended by their manufacturer, Catal International Ltd, as discussed previously in section 3.7.2.

4.2.3.1 TPR of Co/Al₂O₃ Catalyst

The reduction profile for the Co/Al₂O₃ catalyst obtained using the TPR technique discussed previously in section 3.6.3, is presented in Figure 4.5 below.

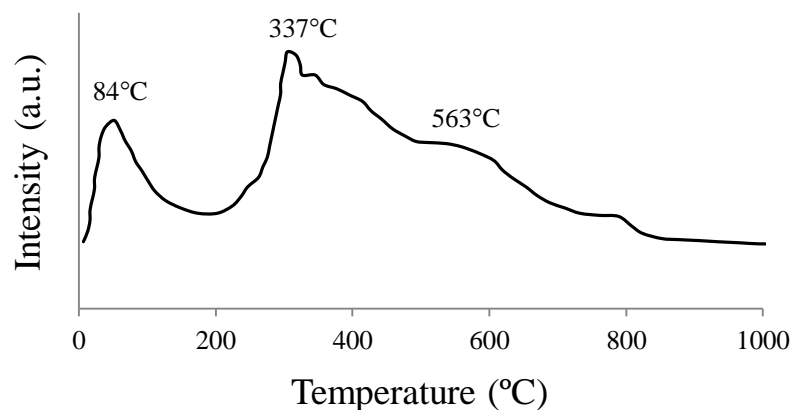


Figure 4.5 – TPR spectrum of Co/Al₂O₃ catalyst used in present study

The two main peaks, at 84°C and 337°C, are commonly reported to represent the reduction of the metal oxide phase, Co₃O₄ to CoO, and then CoO to metallic cobalt, respectively [159]. Similar peaks have been reported by Jalama *et al.* [159], and the much wider peak, at higher temperatures, has been attributed to the much stronger interactions that exist between Co and the alumina support (e.g. Co₂AlO₄) that are harder to reduce [159]. Hence, from this TPR profile, a reduction temperature of 350°C is selected for the Co/Al₂O₃ catalyst activation procedure, so as to ensure that the metal oxide phase is adequately reduced to the catalytically active metallic phase.

4.2.3.2 TPR of Co/TiO₂ Catalyst

The preparation method for the Co/TiO₂ catalyst follows that published by Li *et al.* [161, 163], where TPR is also used to determine its reducibility profile. Initially, it was not possible to perform TPR analysis on the Co/TiO₂ catalyst used in the present study and, therefore, the TPR spectrum obtained by Li *et al.* [161, 163] was used as a guide for its reduction profile. This TPR spectrum is shown in Figure 4.6 below.

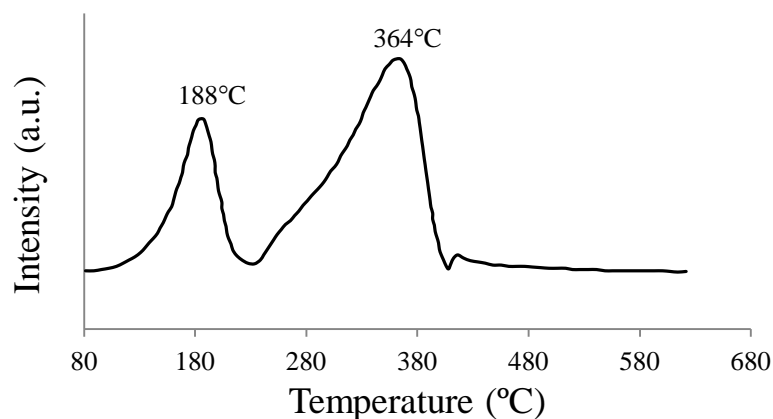


Figure 4.6 – TPR spectrum of a Co/TiO₂ catalyst reported by Li *et al.* [163]
(adapted from [163])

The first peak at 188°C represents the reduction of Co₃O₄ to CoO, whereas the second peak at 364°C represents CoO reducing to metallic cobalt [161, 163]. The appropriate value for the reduction temperature, therefore, would need to be above 364°C. This was in agreement with the manufacturer recommendation of 375°C and, consequently, the proposed activation procedure previously outlined in section 3.7.2 seemed appropriate. However, as will be discussed in section 4.2.3.2 where the performance of the catalyst (CO conversion versus time on stream) is examined, the reduction temperature selected from the study by Li *et al.* [161, 163] was not sufficient to reduce the Co/TiO₂ catalyst. TPR analysis of the Co/TiO₂ catalyst in the present study was performed at a later date (after the catalyst selection procedure and parameter study discussed in chapters 4 and 5, respectively, were carried out) and the reduction profile that was obtained using the TPR technique (discussed previously in section 3.6.3) is presented in Figure 4.7 below.

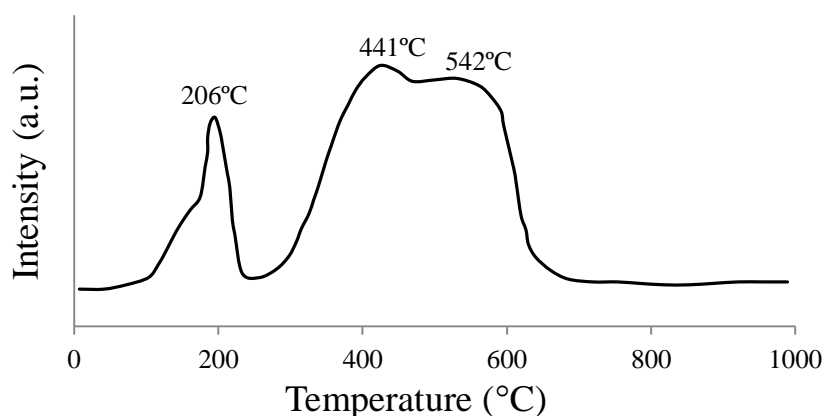


Figure 4.7 – TPR spectrum of Co/TiO₂ catalyst used in present study

The results in Figure 4.7 above, clearly show that a much higher reduction temperature than the 375°C value that was used in the catalyst reduction procedure (previously outlined in section 3.7.2.2) is required to adequately reduce the Co/TiO₂ catalyst used in this work. The first peak at 206°C (representing the reduction of Co₃O₄ to CoO) occurs at a higher temperature than that given in Figure 4.6 above. The same is true for the second peak (representing CoO reducing to metallic

cobalt) which occurs at 441°C. In addition, this second peak is much wider indicating a stronger interaction between the cobalt and the titania support, making the catalyst more difficult to reduce. Hence, a recommendation for future work would be to implement a higher reduction temperature for the Co/TiO₂ catalyst used in the present study.

4.2.3.3 TPR of Fe/Al₂O₃ Catalyst

The reduction profile for the Fe/Al₂O₃ catalyst obtained using the TPR technique discussed previously in section 3.6.3, is presented in Figure 4.8 below. According to Feyzi, Irandoust and Mirzaei [103], the first peak at 153°C can be ascribed to the transformation of Fe₂O₃ to Fe₃O₄, whereas the second peak at 279°C represents the transformation of Fe₃O₄ to Fe. Hence, the reduction temperature of 290°C recommended by the Fe/Al₂O₃ catalyst manufacturer (section 3.7.2.2) appears sufficient in order to ensure that the metal oxide phase is adequately reduced to the catalytically active metallic phase.

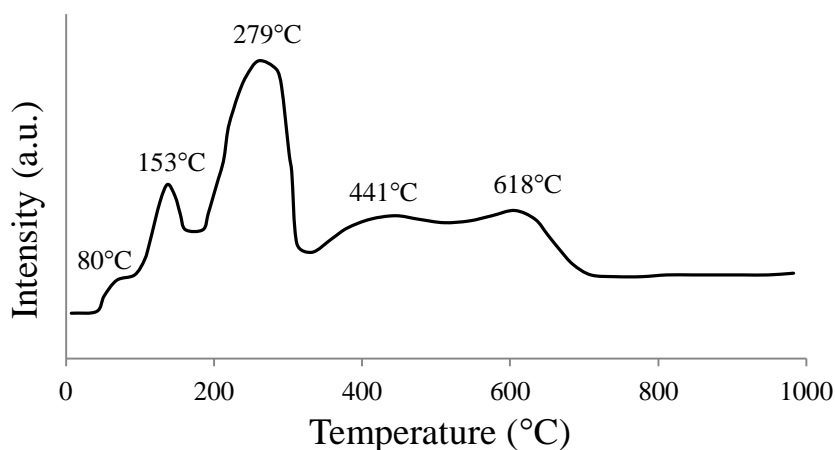


Figure 4.8 – TPR spectrum of Fe/Al₂O₃ catalyst used in present study

4.3 Catalyst Screening – FT Synthesis Tests

After characterization of the available catalysts, their activities and product distribution during the FT synthesis reaction are compared. The screening tests are performed in the two fixed-bed micro-reactors that were described previously in sections 3.3 and 3.4. The 2cm³ reactor (at UFRJ, Brazil) is used to compare the Co/Al₂O₃ and Fe/Al₂O₃ catalysts, whereas the 20cm³ reactor (at Aston) is used for comparing all three available catalysts. The reason for this is that the Co/TiO₂ catalyst had not yet been acquired at the time of this laboratory visit to UFRJ, in Brazil.

The three catalysts are compared at low CO conversion rates and at similar values (maximum CO conversion ~10%), in line with recommendations put forward by Dautzenberg [168] on isothermal catalytic reaction testing. This is necessary as the selectivity or product distribution in FT synthesis depends on the reactant conversion, and the catalysts must, therefore, be compared at a constant CO conversion [114]. The same reasoning was applied in catalyst comparison studies by Tristantini *et al.* [114] and de la Osa *et al.* [67, 68]. These low CO conversions are achieved by using high

space velocities or high reactant flow rates (giving low residence times [116]), lower reactor temperatures and pressures, and small amounts of catalyst mass ($\geq 0.1\text{g}$).

The first reason for employing these conditions is in order to maintain isothermal reactor conditions, as high flow rates help in keeping a more uniform heat distribution along the length of the reactor shaft. The second reason is that at low reactant conversions the three catalysts, which have different compositions of metal, support materials, etc. can be compared on a level ‘playing field’. The catalysts are far from equilibrium; hence the catalysts exhibiting a better overall performance are identified. At these low reactant conversions ($\leq 15\text{ mol\%}$) the relationship between the reaction rate, $-r_A$ (which is a function of the reactant concentration, C_A) and the reactant conversion, X_A , is almost linear, irrespective of the order of the reaction [157]. Therefore, the term for the reaction rate in Equation 4.1 below, can be assumed constant.

$$X_A = \frac{-r_A W}{F_{A0}} \quad (\text{EQ 4.1})$$

The experiment conditions that were used and the results that were obtained using the 2cm^3 and 20cm^3 reactor systems are presented and discussed in sections 4.4 and 4.5, respectively.

4.4 Catalyst Screening – 2cm^3 Reactor Tests (at UFRJ)

Four FT synthesis experiments are carried out using this reactor, each with a total reaction duration of 48 hours (which is the standard duration for FT synthesis catalyst screening runs at UFRJ, Brazil in collaboration with PetroBras [157]). The experiment procedure was previously outlined in section 3.7. The reaction conditions that are selected for these experiments also follow the standard catalyst screening procedure implemented at UFRJ, Brazil, in collaboration with PetroBras [157].

The reactor temperatures used represent values in the optimum activity range for the corresponding catalysts, as previously discussed in section 2.4. The reactor pressure is kept at 10 bar for the reasons previously outlined in section 4.3 above. In addition, this value is in line with the aims of the project for operation at lower pressures than those used for conventional FT processing. The H_2/CO molar ratio in the feed syngas is kept constant in these experiments as the syngas used was provided in pre-mixed gas cylinders at a fixed, and certified molar composition of $\text{H}_2/\text{CO}/\text{He}$ of 63.8/32.1/4.0%. Helium is used as an internal standard in order to calculate the CO conversion. A summary of the reaction conditions implemented in these experiments (tests B1-B4) are provided in Table 4.3 below. Two values for space velocity are implemented for each catalyst in order to examine the influence of space velocity on CO conversion and the product composition, as shown in Table 4.3.

Table 4.3 – 2cm³ reactor FT synthesis catalyst screening tests: Reaction conditions

Exp. No.	Catalyst	Cat. Mass (g)	Reactor Temp. (°C)	Reactor Press. (bar)	WHSV (h ⁻¹)	H ₂ /CO Ratio	CO Conversion (mol %)
B1	Co/Al ₂ O ₃	0.10	210	10	18.0	2.0	3.8
B2	Co/Al ₂ O ₃	0.10	210	10	7.5	2.0	6.4
B3	Fe/Al ₂ O ₃	0.10	300	10	15.0	2.0	9.6
B4	Fe/Al ₂ O ₃	0.10	300	10	24.0	2.0	5.7

4.4.1 Product Analysis: GC-TCD Results

The GC-TCD results from tests B1-B4 aid in determining the CO conversion. This is calculated using Equations 4.2 and 4.3 below, according to Xu *et al.* [83] and the method used at UFRJ [157], where the helium in the syngas mixture is used as an internal standard in the GC:

$$\text{CO conversion (\%)} = \frac{\text{moles of inlet CO} - \text{moles of outlet CO}}{\text{moles of inlet CO}} \times 100 \quad (\text{EQ 4.2})$$

$$\text{CO conversion (mol \%)} = 1 - \frac{\left(\frac{\text{CO}}{\text{He}}\right)_{\text{out}}}{\left(\frac{\text{CO}}{\text{He}}\right)_{\text{in}}} \times 100 \quad (\text{EQ 4.3})$$

For the Co/Al₂O₃ catalyst, a space velocity (WHSV) of 18.0 h⁻¹ is used in Test B1 giving a CO conversion of 3.8 mol%. When the space velocity is reduced to 7.5 h⁻¹ in test B2, CO conversion rises to 6.4 mol%. In the case of the Fe/Al₂O₃ catalyst, a similar trend is observed, where space velocities of 24.0 and 15.0 h⁻¹ give CO conversions of 5.7 and 9.6 mol%, respectively. These trends are in agreement with the findings of Ngwenya *et al.* [162] who observed that feed syngas flow rates are inversely proportional to CO conversion. This is expected as at higher space velocities (or high flow rates) the concentration of the reactants on the catalyst surface is higher, corresponding to lower residence times in the catalyst bed and therefore lower reaction rates.

4.4.2 Product Analysis: GC-FID Results

Figure 4.9 and Figure 4.10 below, show two examples of the chromatograms (retention time versus GC-FID signal response) obtained from the analysis of the products from the 2cm³ reactor catalyst screening tests. The peaks on the chromatograms in Figure 4.9 and Figure 4.10 (from left to right) each represent compounds in ascending order of molecular weight, and hence, ascending order of carbon number group, for the same reasons explained in section 3.5.3.1. For example, C₃ products include propane, propene, propanol, etc, and their isomers. Qualitatively, the intensity (height) of the peaks is proportional to the amount of each compound present in the product mix.

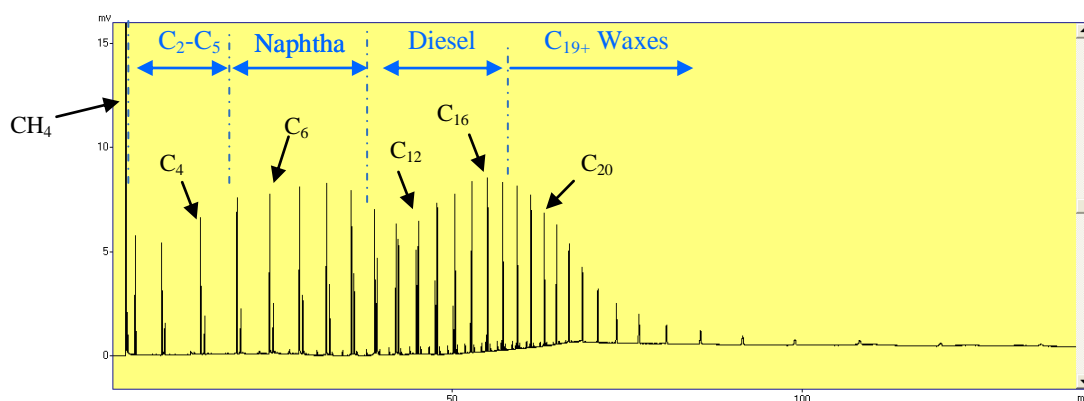


Figure 4.9 –GC-FID chromatogram from 2cm³ reactor catalyst screening test B2 (using Co/Al₂O₃ at 210°C, 10 bar, WHSV = 7.5 h⁻¹, H₂/CO = 2.0, and m_{cat} = 0.1g) (provided courtesy of [157])

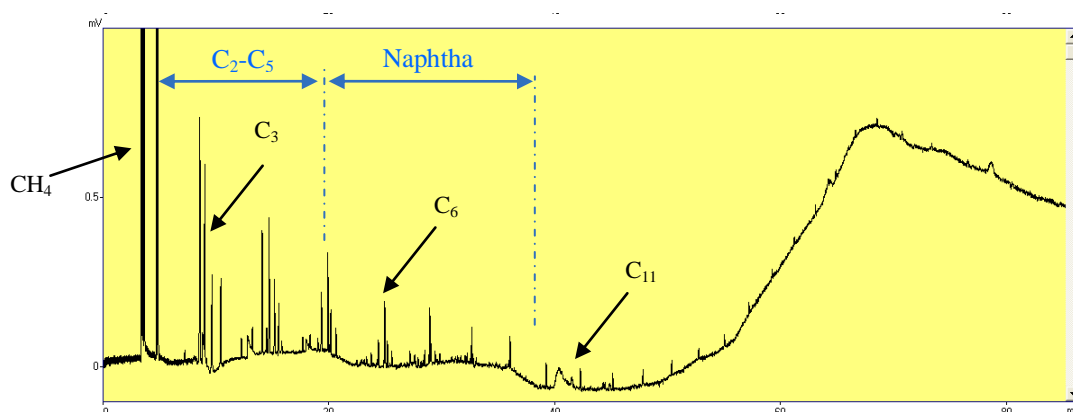


Figure 4.10 – GC-FID chromatogram from 2cm³ reactor catalyst screening test B3 (using Fe/Al₂O₃ at 300°C, 10 bar, WHSV = 15 h⁻¹, H₂/CO = 2.0, and m_{cat} = 0.1g) (provided courtesy of [157])

The chromatograms provided in Figure 4.9 and Figure 4.10 above, show a marked difference in the composition of the products obtained from each catalyst. The product distribution for the Co/Al₂O₃ catalyst covers a very wide range, from C₁ to C₂₀₊ hydrocarbons, displaying a product distribution composed mainly of C₅₊ hydrocarbon products, and more interestingly, C₁₁₊ hydrocarbon products. The Fe/Al₂O₃ catalyst, on the other hand, exhibits a product distribution containing mainly light hydrocarbon gases (C₁-C₅). These results are in agreement with typical product selectivities for LTFT and HTFT processing as shown previously in Figure 2.3 in section 2.2.2 [35].

4.4.2.1 Hydrocarbon Product Composition

The relative composition of the hydrocarbon products from each test (B1-B4) is worked out using the peak areas in the chromatograms obtained. The peak areas in each carbon number group are added together to represent their corresponding group, and then calculated as a percentage of the total of the peak areas. These groups are then put under five main product categories which include CH₄, light hydrocarbons (C₂-C₅), naphtha (C₆-C₁₀), diesel (C₁₁-C₁₈) and waxes (C₁₉₊). The calculated hydrocarbon product compositions for tests B1-B4 are presented in Figure 4.11 below, where the difference in product distribution for each catalyst can be seen more clearly.

Figure 4.11 shows that the Co/Al₂O₃ catalyst yields products mainly in the diesel and wax product range, which account for 58% and 68% of the total product in both tests B1 and B2, respectively. Lower proportions of the total product (24% and 20% in B1 and B2, respectively) are in the naphtha range. The composition of CH₄ and C₂-C₅ products is low in both cases (12-18% of the total product). The product composition obtained from the Fe/Al₂O₃ catalyst, on the other hand, is heavily weighted towards CH₄ and light hydrocarbons (C₂-C₅) which account for more than 80% of the total product in both test B3 and B4. These product compositions are similar to typical product compositions for cobalt and iron-based catalysts at LTFT and HTFT process conditions, as reported by Leckel [35].

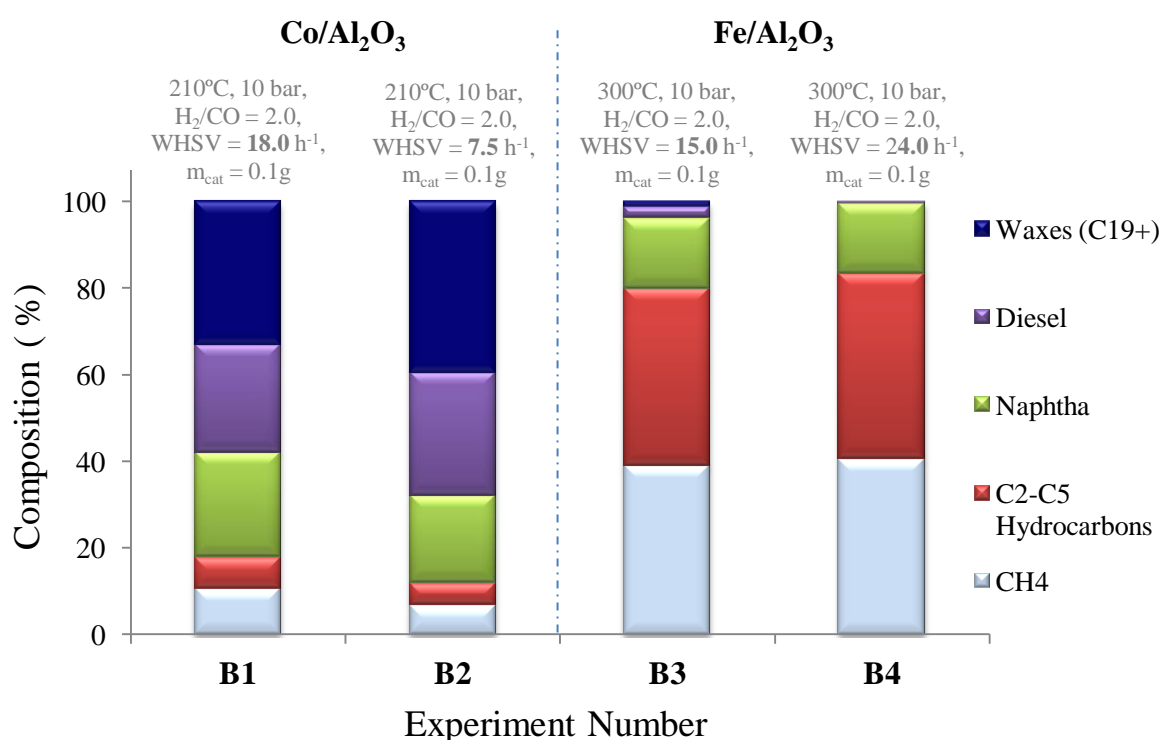


Figure 4.11 – 2cm³ reactor catalyst screening tests (B1-B4) performed at UFRJ: composition of hydrocarbon products

From Figure 4.11 it can also be deduced that a change in space velocity has a more marked effect on the final product composition obtained from the Co/Al₂O₃ catalyst, in comparison to that obtained from the Fe/Al₂O₃ catalyst. A decrease in space velocity from 18.0 h⁻¹ (test B1) to 7.5 h⁻¹ (test B2) using Co/Al₂O₃ favours diesel and C₁₉₊ wax formation, where the products in the diesel and wax ranges increase from 25 to 28% and 33 to 40%, respectively. In the case of the Fe/Al₂O₃ catalyst the product composition is not significantly affected by the increase in space velocity.

4.5 Catalyst Screening – 20cm³ Reactor Tests (at Aston)

The experiment procedure that is followed for the FT synthesis tests on the 20cm³ fixed-bed reactor at Aston was previously outlined in section 3.7. Three FT synthesis catalyst screening tests are performed (tests FT4-FT6 in Table 4.4 below) firstly, so as to determine the repeatability of the

results obtained from the 2cm³ reactor tests when ‘up-scaling’ to this 20cm³ reactor, and secondly, in order to examine the activity and selectivity of the Co/TiO₂ catalyst. There are two reasons why the numbering of the tests performed on this 20cm³ reactor begins at FT4, rather than FT1:

1. Tests FT1 and FT2 were unsuccessful runs due to a problem with the gas sample delivery to the online GC. This problem and its rectification were explained in section 3.4.1.5.
2. Test FT3 was the commissioning run for the 20cm³ reactor. FT feed gases were used, but no catalyst was used (i.e. a blank run), under the following reaction conditions: (210°C, 10 bar, syngas delivery rate = 145ml/min, and H₂/CO = 2.0). The reactor was packed with the quartz wool and borosilicate glass beads, which were the materials used for catalyst support, gas flow enhancement, etc. as previously explained in section 3.7.1.2. This was done in order to verify that these materials were not in any way catalytically active during FT synthesis, and would, therefore have no influence on the reaction. The exit gases from the reactor were monitored for 48 hours and the results indicated that no reactant conversion was achieved throughout this commissioning run.

A summary of the three FT synthesis catalyst screening experiment (FT4-FT6) conditions implemented using this reactor are provided in Table 4.4 below. The criteria for the selection of these specific reaction conditions are discussed in section 4.5.1 below.

Table 4.4 – 20cm³ reactor FT synthesis catalyst screening tests: Reaction conditions

Exp. No.	Catalyst	Cat. Mass (g)	Reactor T (°C)	Reactor P (bar)	WHSV (h ⁻¹)	H ₂ /CO Ratio
FT4	Co/Al ₂ O ₃	0.50	210	10	8.8	2.0
FT5	Co/TiO ₂	0.50	210	10	8.8	2.0
FT6	Fe/Al ₂ O ₃	0.50	300	10	10.8	1.5

Overall, the performance of all three catalysts is assessed in terms of two main criteria which include the catalyst activity and stability (CO conversion versus time on stream), as well as the product profile of the catalyst (including product selectivity, product yields and the composition of the liquid hydrocarbon products obtained). The performance results of the three catalysts are presented and discussed in sections 4.5.2 and 4.5.3 below.

4.5.1 Criteria for Selection of Specific Reaction Conditions

The activities and product distribution of the Co/Al₂O₃ and the Fe/Al₂O₃ catalysts (which were investigated using the 2cm³ reactor at UFRJ in section 4.4) are re-examined in the 20cm³ reactor (at Aston) for comparison. In addition, the performance of the Co/TiO₂ catalyst during FT synthesis is investigated. The catalyst loading used in the experiments depends on the total amounts of each catalyst that are available for the project. Only a small amount of Co/Al₂O₃ (~10g) is available, hence, only 0.5g is used in order to allow for further experimentation. For more accurate

comparison, therefore, only 0.5g of Co/TiO₂ and Fe/Al₂O₃ are also used. Due to the higher capacity of this 20cm³ reactor and the higher space velocities used, larger amounts of catalyst are used, in relation to the 2cm³ tests, so as to increase the reactant conversion (section 3.4.3).

To reproduce the other reaction conditions of the screening tests carried out in the 2cm³ reactor as closely as possible, the same reactor temperatures and pressures are used. These represent values in the optimum activity range for the corresponding catalysts, as previously discussed in section 2.3. The reactor pressure is also kept constant at 10 bar for all three catalysts for the reasons previously outlined in section 4.3. The syngas space velocity is measured in terms of the weight hourly space velocity (WHSV = syngas mass flow rate / catalyst mass) and depends on the individual gas flow rates and therefore, the syngas H₂/CO molar ratio. The values of 8.8 h⁻¹ and 10.8 h⁻¹, for both cobalt catalysts and the Fe/Al₂O₃ catalyst, respectively, correspond to a total syngas flow rate of approximately 145ml/min. Once again, this flow rate is selected due to the equipment limitations relating to the minimum possible nitrogen flow rate explained previously in section 3.4.3.

As opposed to the 2cm³ reactor at UFRJ, in this 20cm³ reactor at Aston the syngas is mixed inside the reactor system before entering the reactor as explained in section 3.4.1.1. This means that the H₂/CO molar ratio in the feed syngas could be varied by altering the individual gas delivery rates, in order to tailor it to the optimum operational range required by each type of catalyst (discussed previously in section 2.5.1). A ratio of 2.0 is used for the cobalt-based catalysts, and a lower one, of 1.5, for the iron catalyst which is expected to display a higher WGS activity. Nitrogen is used as an internal standard for the purposes of CO conversion calculations. Its composition in the syngas is kept at approximately 10 mol% (the same N₂ composition is used by Jalama *et al.* [159] and Yao *et al.* [169]). Prior to each FT synthesis run the syngas mixture (mixed in the reactor system mixer shown in Figure 3.4 in section 3.4) is set to by-pass the reactor. A sample of this mixture is then injected into the online GC (as outlined in section 3.5.2) in order to verify its molar composition and adjust the H₂/CO/N₂ ratios accordingly. These injections are carried out in triplicate.

4.5.2 Catalyst Activity and Stability

A sample of the gases leaving the reactor is analyzed at hourly intervals during the FT synthesis runs (as detailed previously in section 3.7.4.2). The values for the CO conversions at the time of the injections, therefore, are assumed to be constant for each hour in between the injections. The percentage CO conversion is calculated using Equation 4.2 (section 4.4.1) and Equation 4.4 below, according to Xu *et al.* [83], where nitrogen is used as an internal standard in the GC. The total proportions of the CO converted for each catalyst during each complete run are calculated using Equation 4.5 below, and the results are presented in Figure 4.12 below. The experimental error for these CO conversion calculations is approximately ± 5% of the absolute values.

$$\text{CO conversion (mol \%)} = 1 - \frac{\left(\frac{\text{CO}}{\text{N}_2}\right)_{\text{out}}}{\left(\frac{\text{CO}}{\text{N}_2}\right)_{\text{in}}} \times 100 \quad (\text{EQ 4.4})$$

$$\text{Total CO Converted (mol\%)} = \frac{\text{Total moles of inlet CO} - \text{Total moles of outlet CO}}{\text{Total moles of inlet CO}} \times 100 \quad (\text{EQ 4.5})$$

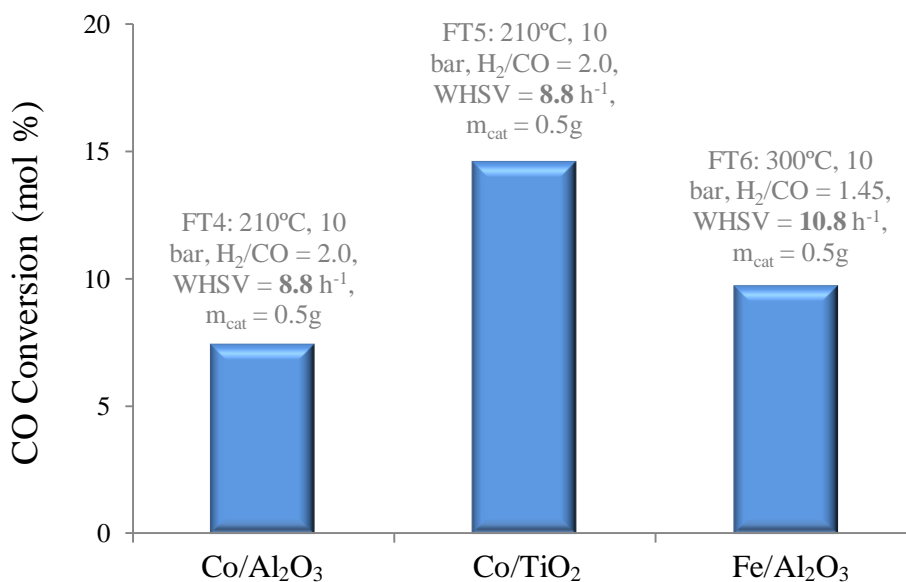


Figure 4.12 – 20cm³ reactor catalyst screening tests (FT4-FT6): Total CO conversion

From Figure 4.12 it is evident that under the reaction conditions that are implemented the highest CO conversion is achieved by the Co/TiO₂ catalyst, followed by Fe/Al₂O₃ and then Co/Al₂O₃. The performance of each catalyst (CO conversion versus time on stream) is compared in Figure 4.13 below, giving a clearer picture of the activity and behaviour of each catalyst with time on stream.

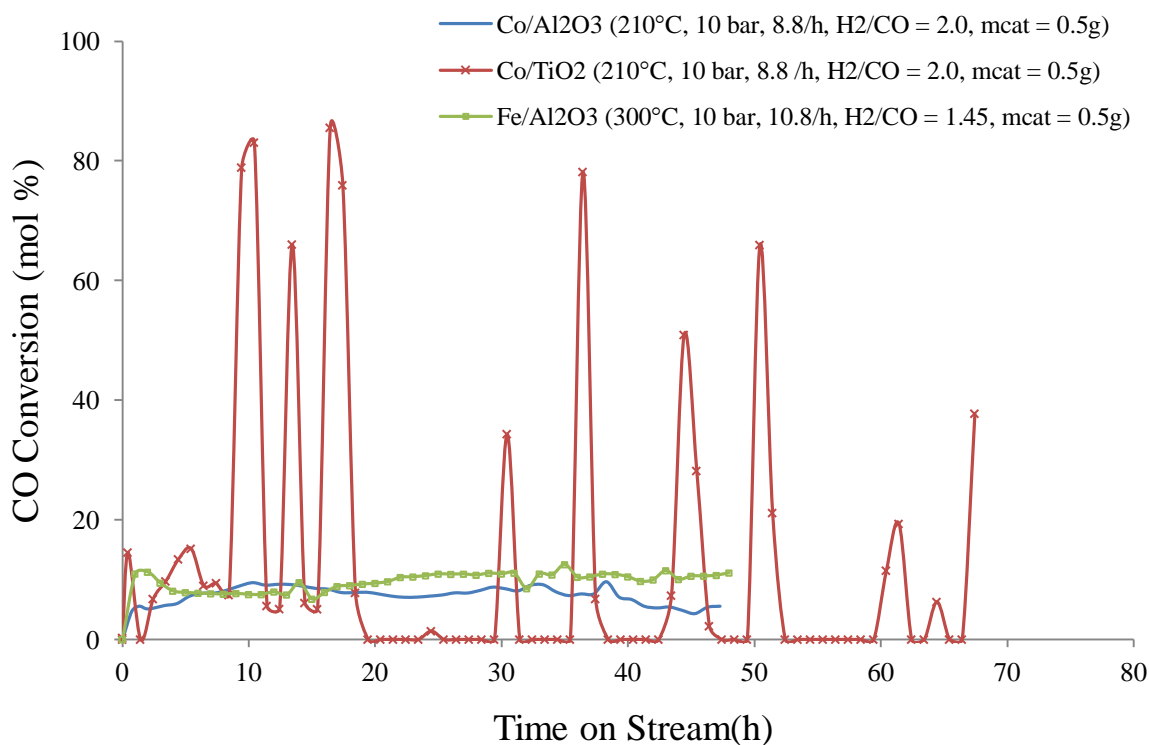


Figure 4.13 – 20cm³ reactor catalyst screening tests (FT4-FT6): Catalyst performance (CO conversion versus time on stream)

Figure 4.13 plainly illustrates the difference in catalyst activities; the Co/Al₂O₃ and Fe/Al₂O₃ catalysts exhibit a relative stability in performance, reaching a steady-state within 5-10 hours of reaction time that is maintained until the end. The average CO conversions that were recorded for the Co/Al₂O₃ and Fe/Al₂O₃ catalysts, once steady-state operation is reached for both, are approximately 8 and 10 mol%, respectively. The difference between the performances of each of these catalysts, as illustrated in Figure 4.13, is that the activity of the Co/Al₂O₃ catalyst slowly declines towards the end of the run, whereas the opposite is observed for the Fe/Al₂O₃ catalyst.

In stark contrast, the Co/TiO₂ catalyst demonstrates sporadic bursts of activity, going through maxima and minima that range from 0-80 mol% CO conversion throughout the test run. The test run for the Co/TiO₂ catalyst was continued for a further 20 hours more than the other catalyst runs in order to investigate if the catalyst would stabilize, given the additional time. As can be seen from Figure 4.13, the Co/TiO₂ catalyst does not achieve steady-state operation even during this added reaction run time and the same intermittent activity is observed. Despite its irregularity, however, this activity appears to be declining over time, as noted by the gradual decreasing intensity of the peaks observed in Figure 4.13 after 48 hours of operation.

These results, displaying a declining trend in CO conversion for the Co/TiO₂ catalyst are in partial agreement with the findings published by Li *et al.* [161], who used a catalyst of similar composition and found that at steady space velocities, CO conversion gradually declined with time on stream. The irregular CO conversion behaviour observed, however, was not reported by the

same authors. As explained previously in section 4.2.3.2, this may have been due to the differences in the activation procedure recommended by the catalyst manufacturer in this project and that followed by Li *et al.* [161], suggesting that the catalyst did not undergo sufficient reduction. The TPR analysis performed on the Co/TiO₂ used in the present study (section 4.2.3.2) showed that a higher reduction temperature than the one used in the activation procedure (outlined in Table 3.6 in section 3.7.2.2) was actually required, and is therefore recommended for future investigation.

The total reactant conversion and catalyst stability during the reaction, however, cannot be used alone in the selection of the optimal catalyst, as the products that are formed need to be investigated as well. The products obtained from each catalyst run are examined in section 4.5.3 below.

4.5.3 Catalyst Product Profile

4.5.3.1 Product Yields

A mass balance was performed over each run (tests FT4-FT6) and the product yield results are presented in Table 4.5 below. The CO₂, CH₄ and C₂-C₅ (light hydrocarbons) yields are calculated using the results obtained from the GC analyses (described previously in section 3.5.2). The mass of the liquid products is obtained by weighing the collected liquids on laboratory scales (error according to manufacturer = ± 0.1 µg), as discussed previously in section 3.5.3. The percentage of unreacted syngas is calculated by difference. One of the assumptions that were made for these calculations was that there are no product losses due to volatilisation, and therefore all C₆₊ products are condensed in the collection chamber (GLS, Figure 3.4 in section 3.4) at ambient temperature and collected at the end of each run.

Table 4.5 – 20cm³ reactor catalyst screening tests (FT4-FT6): Mass balance

Test	Catalyst	Product Yields (wt.%)					Unreacted Syngas (wt.%)
		CO ₂	CH ₄	C ₂ -C ₅	Liquid H/C's & Waxes	Water + Oxygenates	
FT4	Co/Al ₂ O ₃	7.02	0.17	0.14	0.21	1.28	91.18
FT5	Co/TiO ₂	7.33	0.24	0.26	1.07	2.29	88.81
FT6	Fe/Al ₂ O ₃	5.08	1.90	0.89	0	1.55	90.58

The results given in Table 4.5 indicate that the cobalt-based catalysts produced relatively high, but similar amounts of CO₂ (on a mass basis). The amount produced by the Fe/Al₂O₃ catalyst is lower, which can be attributed to the higher extent of WGS equilibrium reaction (Equation 2.5 section 2.1) commonly exhibited by iron-based catalysts [20], where an excess of CO₂ would shift the balance towards the formation of CO and water. This also explains the formation of water in all the catalyst runs. The liquid products from the cobalt-based catalyst runs (tests FT4 and FT5) are composed of two phases; an aqueous phase (containing soluble oxygenated compounds) and an immiscible oil phase (liquid hydrocarbons plus waxes). The liquid product obtained from the Fe/Al₂O₃ run (test

FT6) only contains an aqueous phase. This was confirmed by analyzing its water content (using the volumetric titration method outlined in section 3.5.3.2) which showed that the concentration of water is approximately 97.8 wt.%.

4.5.3.2 Product Selectivity

To get a clearer picture of the product profile obtained from each catalyst, the product selectivities calculated (using Equations 3.2 to 3.6 in section 3.5.2.4) are provided in Table 4.6 below.

Table 4.6 – 20cm³ reactor catalyst screening tests (FT4-FT6): Product selectivities

Test	Catalyst	Product Selectivities (mol %)			
		CO ₂	CH ₄	C ₂ -C ₅	C ₆₊
FT4	Co/Al ₂ O ₃	88.6	6.1	1.2	4.1
FT5	Co/TiO ₂	47.3	4.2	1.6	46.9
FT6	Fe/Al ₂ O ₃	44.5	45.5	10.0	0.00

Under the reaction conditions previously summarized in Table 4.4, the product selectivity results clearly advocate the Co/TiO₂ catalyst for possessing the highest selectivity towards the formation of C₆₊ products (liquid hydrocarbons and waxes) in relation to the other two catalysts. The selectivity of the Fe/Al₂O₃ catalyst towards the formation of mainly methane and light hydrocarbons (C₂-C₅) serve in re-confirming the results obtained from the 2cm³ reactor screening tests (section 4.4.2).

4.5.3.3 Product Physical Characteristics

From a C₆₊ hydrocarbon product selectivity standpoint, therefore, the Co/TiO₂ catalyst seems to emerge as superior over the other two catalysts. These C₆₊ hydrocarbon products, however, require further inspection so as to determine their nature, composition and suitability for the aims of this project. The physical characteristics of the C₆₊ products (liquid hydrocarbons and waxes) obtained from the Co/Al₂O₃ and Co/TiO₂ test runs are summarized in Table 4.7.

Table 4.7 – 20cm³ reactor catalyst screening tests: Physical characteristics of liquid and wax products collected

Test	Catalyst	Product Physical Characteristics
FT4	Co/Al ₂ O ₃	1) Oil phase – immiscible liquid with a yellow tint 2) Wax phase – tiny white solids settled at base of oil phase 3) Water phase – clear liquid
FT5	Co/TiO ₂	1) Oil phase – tiny amount of clear yellow coloured liquid 2) Wax phase – white waxy solids 3) Water phase – clear liquid
FT6	Fe/Al ₂ O ₃	1) Water phase – clear white liquid 2) No oil or waxes produced

The high C_{6+} product selectivity that the Co/TiO_2 catalyst displays translated into a hydrocarbon product that consisted mainly of white solid waxes (solid at ambient temperature). Incidentally, these waxes condensed at several points (or ‘cold spots’) causing blockages along the pipes and fittings both inside the reactor oven (kept at the maximum attainable temperature of $250^\circ C$) and along the GLS pipes and fittings (Figure 3.4 in section 3.4). The pipelines and fittings were disassembled and the waxes were physically removed by pumping pressurized nitrogen through the pipelines and fittings. The waxes that were removed were weighed in order to aid in mass balance calculations. Industrially, wax formation would not pose such problems as uniform temperatures above the boiling point of high molecular waxes ($250^\circ C+$) could be maintained in the system, thus preventing their condensation. In contrast, the hydrocarbon products formed using the Co/Al_2O_3 catalyst do not cause any blockages as both liquid and wax hydrocarbons are contained in the oil phase which is easily drained out.

4.5.3.4 Liquid Hydrocarbon Product Composition

A sample of the oil phases collected from both cobalt-based catalyst runs were dissolved in hexane and analyzed using the GC-MS method previously outlined in section 3.7.4.2. The resulting chromatograms from test FT4 (using the Co/Al_2O_3 catalyst) and test FT5 (using the Co/TiO_2 catalyst) are presented in Figure 4.14 and Figure 4.15 below, respectively.

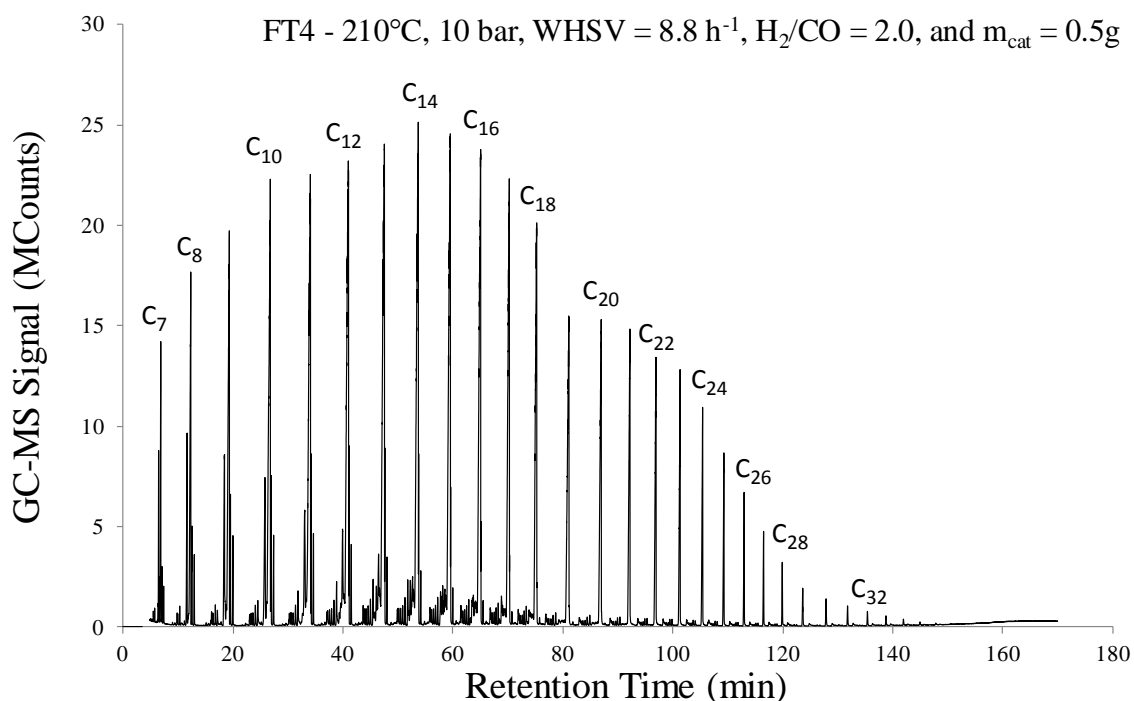


Figure 4.14 – Chromatogram of liquid hydrocarbon products (Test FT4 using Co/Al_2O_3 at $210^\circ C$, 10 bar, $H_2/CO = 2.0$, $WHSV = 8.8 \text{ h}^{-1}$, and $m_{cat} = 0.5g$)

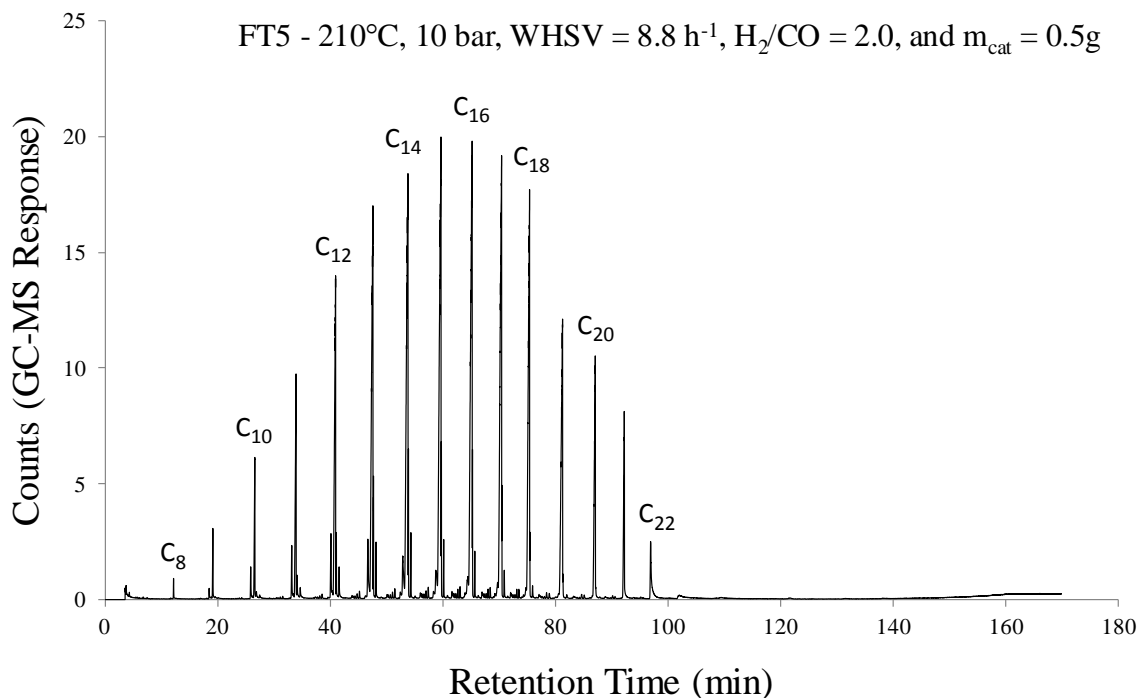


Figure 4.15 – Chromatogram of liquid hydrocarbon products (Test FT5 using Co/TiO₂ at 230°C, 10 bar, H₂/CO = 2.0, WHSV = 8.8 h⁻¹, m_{cat} = 0.5g)

The higher molecular waxes (C₂₀₊ which are solid at ambient temperature) obtained from the Co/TiO₂ run (FT5) did not fully dissolve in hexane, as required by this GC-MS method and therefore only the liquids obtained were analyzed. This is apparent from the chromatograms above, where the product ranges observed for the Co/Al₂O₃ and Co/TiO₂ catalyst were C₇-C₃₅ and C₈-C₂₂, respectively. The relative composition of the hydrocarbon products determined from the chromatogram peak areas are compared in Figure 4.16.

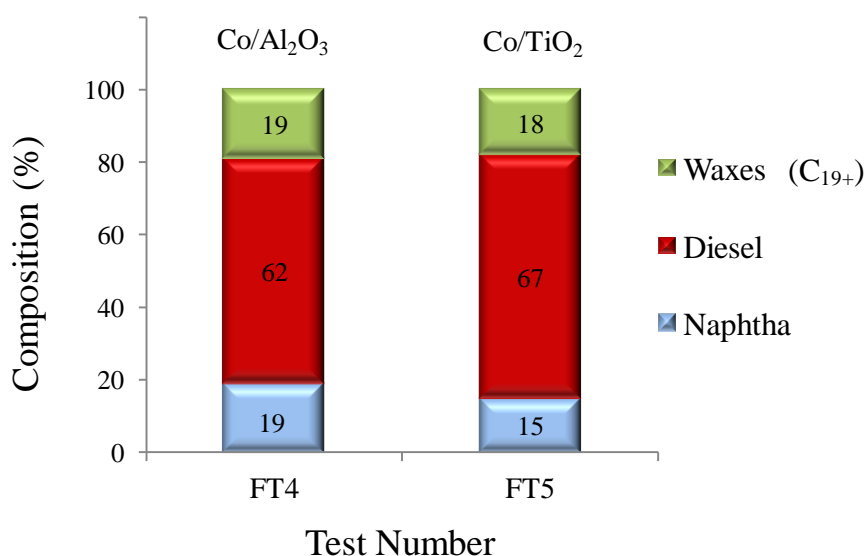


Figure 4.16 – Test FT4 and FT5: Relative composition of liquid hydrocarbon products (at 210°C, 10 bar, H₂/CO = 2.0, WHSV = 8.8 h⁻¹, and m_{cat} = 0.5g)

As the waxes obtained from the Co/TiO₂ catalyst were not analyzed, this figure only contrasts the liquids obtained, and therefore, the Co/TiO₂ composition shown in Figure 4.16 above, cannot be entirely representative of the final product. Hence, despite the fact that from these analyses both cobalt-based catalysts demonstrate selectivities mainly towards diesel grade products, this result is more representative for the Co/Al₂O₃ catalyst.

4.6 Results Summary and Chapter Conclusions

The three catalysts that were available for this project, Co/Al₂O₃, Co/TiO₂ and Fe/Al₂O₃ were compared in the catalyst screening procedure outlined in this chapter. The primary objective of this procedure was the selection of the most suitable catalyst for further investigation on the influence of important process parameters on its activity and performance during the FT synthesis reaction, as well as its product yields and composition. The main criteria that influenced the catalyst selection included the yield of liquid hydrocarbons produced and the fuel composition of these liquids, as high proportions of diesel range products were desired. Another aspect that was considered included the stability of the catalyst during the FT synthesis reaction, i.e. CO conversion (or activity) versus time on stream.

The results from the catalyst screening tests performed on the 2cm³ reactor at UFRJ (which was described in section 3.3), involving the Co/Al₂O₃ and Fe/Al₂O₃ catalysts, showed that the Fe/Al₂O₃ catalyst favours the formation of methane and light hydrocarbons (C₂-C₅), whereas, the Co/Al₂O₃ catalyst exhibited a very high selectivity towards C₆₊ hydrocarbons (naphtha, diesel and C₁₉₊ wax products). As one of the main project aims was to investigate the potential for obtaining a synthetic crude FT liquid fuel mixture, these tests showed that Co/Al₂O₃ is a much more suitable catalyst.

The results from the catalyst screening tests carried out on the 20cm³ reactor (described in section 4.5) also showed that the Fe/Al₂O₃ catalyst is not selective towards the formation of C₆₊ hydrocarbon products and produced mainly carbon dioxide, methane and light hydrocarbons (and water), but no C₆₊ hydrocarbons (liquid fuels). This implied that the Fe/Al₂O₃ catalyst should be ruled out from the selection process as liquid fuels are desired, and the final decision was between the two cobalt-based catalyst candidates.

The results from the same set of screening tests (section 4.5) showed that the Co/TiO₂ catalyst displayed the highest C₆₊ hydrocarbon product selectivity. The hydrocarbon products formed, however, were mainly solid waxes which are not favourable for the operation of this 20cm³ reactor system as they caused blockages at several points in the pipelines and fittings, as previously discussed in section 4.5.3.3. Moreover, the Co/TiO₂ catalyst displayed a very irregular performance (CO conversion) over the course of the synthesis run, as opposed to the other two catalysts which exhibited a relatively steady CO conversion throughout the experiment runs. The erratic performance in activity displayed by the Co/TiO₂ catalyst was initially thought to be due to either the activation procedure (outlined in section 3.7.2.2) not being adequate for reducing the catalyst or

differences in the catalyst preparation method used by the manufacturer, Catal International Ltd (section 4.1), in comparison to the preparation method used by Li *et al.* [161] for a catalyst of similar composition. However, TPR analysis (described in section 3.6.3) was performed on this catalyst at a later date and showed that a significantly higher reduction temperature than the 375°C value that was used in the catalyst reduction procedure (outlined previously in section 3.7.2.2) was required to adequately reduce the Co/TiO₂ catalyst used in the present study. Hence, future work using this particular catalyst would be recommended using the appropriate reduction temperature as determined from its TPR reduction profile.

The Co/Al₂O₃ catalyst, on the other hand, demonstrated stability in performance, in terms of steady CO conversion, during the FT synthesis reaction and did not give wax products that blocked the pipelines and fittings in the 20cm³ reactor system. Furthermore, the results from the GC-MS analyses of these liquid hydrocarbons revealed a product with a high diesel composition that has the potential for fulfilling the aims of this project. Hence, the catalyst selected from the screening procedure is the Co/Al₂O₃ catalyst for the following reasons:

1. A good stability in activity and performance, in terms of CO conversion, was displayed over the duration of the experiment run. This showed that the catalyst was sufficiently reduced by the conditions used in the activation method outlined in section 3.7.2.2 and that it could adequately perform during the FT synthesis reaction for sustained periods of time without deactivating quickly.
2. The product distribution was primarily weighted towards C₆₊ hydrocarbon products, containing mainly diesel and C₁₉₊ waxes. This showed that this catalyst is inclined to forming liquid and wax hydrocarbon fuels that could potentially comprise a synthetic crude liquid fuel mixture that can be integrated into decentralized refineries.
3. GC-MS analysis of the liquid hydrocarbon product collected (even though in small yields) showed that it is composed of mainly diesel grade hydrocarbon products. This is favourable from a refining perspective as potentially no further upgrading to this fuel fraction is required if diesel is targeted as one of the final products.

It must be noted, however, that despite the suitability of the Co/Al₂O₃ catalyst for operation on the 20cm³ fixed-bed reactor at Aston and for the requirements of this project, this catalyst may not be suitable for operation in a commercial scale BTL-FT application.

5 FT Synthesis Parameter Study

This chapter describes the FT synthesis parameter study that incorporated the use of the catalyst selected in chapter 4. The experiments are carried out on the 20cm³ fixed-bed reactor at Aston that was described in section 3.4. The influence of reaction conditions on the catalyst activity, product selectivity, product composition and product yields are investigated, and the results obtained are presented and discussed. The impact of the results found on process investment costs is also discussed.

5.1 Introduction

The parameters that influence the FT synthesis reaction and the resulting product distribution include the reactor temperature, pressure, space velocity, the H₂/CO molar ratio in the feed syngas and the catalyst. These variables were discussed previously in section 2.5. A parameter study is carried out in this chapter that aims to investigate the influence of the above reaction parameters on several performance criteria, which include the catalyst activity (CO conversion), product distribution and product yields, as well as the stability (in terms of activity versus time on stream) of the selected Co/Al₂O₃ catalyst during the runs on the 20cm³ reactor at Aston (which was described in section 3.4). This is done in order to explore the potential for cost reduction in the FT process, as well as the prospect of obtaining a synthetic crude liquid fuel product that can be integrated into existing refineries, in line with the main aims and objectives of the project that were outlined in section 1.3. The parameter study included twelve FT synthesis experiments (including one repeated run) which were divided into five test sets that are listed below and discussed in sections 5.1.1 to 5.1.5.

1. Temperature profile
2. Pressure profile
3. Space velocity profile
4. Syngas composition profile, and
5. Catalyst loading (mass) profile.

5.1.1 *Temperature Profile*

As discussed previously in section 2.5.1, temperature is one of the most important variables in FT processing due to the highly exothermic nature of the FT reaction, and has a profound influence on the product distribution and product yields (section 2.2.2). The reactor temperature, therefore, needs to be carefully controlled and maintained within a constant range in order to avoid temperature runaways that have been reported to lead to the predominant formation of CH₄ and rapid catalyst deactivation [43]. In addition, the selection of an appropriate reactor temperature is necessary for determining the conditions that target high CO conversion and liquid hydrocarbon

product yields (as well as desirable product distributions or selectivities). Therefore, the appropriate reactor temperature (or temperature range) must be experimentally determined. Hence, the first set of tests includes three experiments and is designed to study the influence of the reactor temperature. In the 20cm³ reactor system at Aston, the reactor temperature is measured as the catalyst bed temperature (using the catalyst bed thermocouple which was illustrated in Figure 3.4 in section 3.4). Cobalt catalysts are commonly used in low temperature FT (LTFT) processes in the range of 200-250°C (section 2.4.2). Temperatures above this range have been documented to significantly decrease the yield of C₅₊ hydrocarbons and maximize the formation of CH₄ and C₂-C₄ hydrocarbon gases [60]. As the selected catalyst is cobalt-based the above operating range is suitable for its operation and has, therefore, been selected for this set of tests.

Three values for reactor temperature are arbitrarily selected covering the range of 200-250°C in order to examine the relationships for the influence of this parameter on CO conversion, product distribution, product yields, liquid product composition and the catalyst stability during the FT synthesis runs. The three reactor temperatures studied are 210, 230 and 250°C. From these three reactor temperatures, the preferred value is identified and selected for use in the remaining parameter profiling test sets. The criteria for determining the preferred conditions for operation on the 20cm³ fixed-bed reactor at Aston are discussed in section 5.2. The other reaction conditions in this test set are kept constant at the following values: (10 bar, H₂/CO = 2.0, WHSV = 8.8 h⁻¹, and m_{cat} = 0.5g).

5.1.2 Pressure Profile

The reactor pressure can have a significant influence on the process costs and can also have a considerable effect on the product distribution and product yields (as previously discussed in section 2.5.2). Therefore, the reactor pressure can be used to direct FT synthesis towards obtaining a narrower distribution of products or maximizing liquid hydrocarbon yields. The second set of tests, therefore, includes four experiments which examine the influence of low reactor pressures in the range of 2-10 bar; pressures that are much lower than the 20-40 bar typically implemented in conventional FT processing (section 2.5.2). As discussed previously in the review of studies that have investigated the influence of reaction conditions on FT product distribution in section 2.6, work performed at these lower pressures is not as common. However, the influence of these milder conditions on the FT synthesis process is of interest as, industrially, both capital and operating costs increase as the operating pressure is increased (section 2.5.2).

Four values for reactor pressure are arbitrarily selected covering the range of 2-10 bar in order to examine the relationships for the influence of this parameter on CO conversion, product distribution, product yields, liquid product composition and the catalyst stability during the FT synthesis runs. The four selected values for reactor pressure investigated are 2, 5, 8 and 10 bar. From these four values the preferred value is identified and selected for use in the remaining

parameter profiling test sets. The criteria for determining the preferred conditions for operation on the 20cm³ fixed-bed reactor at Aston are discussed in section 5.2. The other reaction conditions in this test set are kept constant at the following values: (230°C, H₂/CO = 2.0, WHSV = 8.8 h⁻¹, and m_{cat} = 0.5g).

5.1.3 Space Velocity Profile

The concept of space velocity was defined and discussed previously in section 2.5.3. As it is the ratio of the feed gas flow rate to the reactor volume or size, it can be used for rating the size of the reactor. The implications of varying the syngas space velocity in a commercial FT application is of interest, as the relationship of space velocity to the size of the FT reactor vessel is inversely proportional, i.e. the higher the space velocity, the smaller the reactor vessel required and the lower the capital cost of the FT processing plant. As low FT reactor operating pressures are also investigated in this work, this would mean that larger FT reactor vessels are necessary to handle the larger gas volumes. Potentially, therefore, an economic balance, in terms of reactor size, could be achieved between having higher space velocities and lower reactor operating pressures.

The third set of tests includes three experiments which investigate the effect of syngas space velocity on CO conversion, product distribution, product yields, liquid product composition and the catalyst stability during the FT synthesis run. Three values for weight hourly space velocity (WHSV) are selected covering the range of 8.8-11.5 h⁻¹, including 8.8, 10.5 and 11.5 h⁻¹. The reason for selecting 8.8 h⁻¹ as the lowest value is due to the equipment limitation related to the minimum possible flow rate of nitrogen that was explained in section 3.4.3. Ideally, however, lower space velocities would have been preferred in order to maximize CO conversion. The other two higher values are arbitrarily selected. From these three values for space velocity, the preferred value is identified and selected for use in the remaining parameter profiling test sets. The criteria for determining the preferred conditions for operation on the 20cm³ fixed-bed reactor at Aston are discussed in section 5.2. The other reaction conditions in this test set are kept constant at the following values: (230°C, 10 bar, H₂/CO = 2.0, and m_{cat} = 0.5g).

5.1.4 H₂/CO Molar Ratio Profile

The fourth set of tests includes three experiments that investigate the effect of the H₂/CO molar ratio in the feed syngas (section 2.5.4). As discussed previously in section 2.4.2, H₂/CO molar ratios in the feed syngas of 2.0 are most commonly used with cobalt-based catalysts in commercial FT applications. However, the H₂/CO molar ratios in syngas produced from the gasification of biomass are significantly lower than 2.0 (typically in the range of 0.5-1.8 [47]), and therefore require conditioning in a shift reactor to increase this ratio (section 2.7.3.2). As discussed previously in section 2.5.4, if lower H₂/CO molar ratios than 2.0 could be used in the FT reactor using cobalt-based catalysts, then the conditioning requirements could be reduced leading to potential savings in the process.

Three values for the H₂/CO molar ratio in the feed syngas are arbitrarily selected covering the range of 1.6-2.0 in order to examine the relationships for the influence of this parameter on CO conversion, product distribution, product yields, liquid product composition and the catalyst stability during the FT synthesis run. The three H₂/CO molar ratios studied are 1.6, 1.8, and 2.0. From these three values for H₂/CO molar ratios, the preferred value is identified and selected for use in the next parameter profiling test set. The criteria for determining the preferred conditions for operation on the 20cm³ fixed-bed reactor at Aston are discussed in section 5.2. The other reaction conditions in this test set are kept constant at the following values: (230°C, 10 bar, WHSV = 8.8h⁻¹, and m_{cat} = 0.5g).

5.1.5 Catalyst Loading Profile

The fifth and final test set includes two experiments that examine the influence of catalyst loading (or mass). The two catalyst loading values studied are 0.5 and 2.0g. The reason for the selection of 0.5g as the lower value is related to the amount of catalyst that is available (discussed previously in section 3.1.1). A higher catalyst loading of 2.0g is used in this test set as a ‘proof of principles’ in order to ensure that the Co/Al₂O₃ catalyst is capable of achieving higher CO conversions and producing higher liquid hydrocarbon yields. The results from this test set are also used in calculating the mass and energy balances over the FT reactor. The preferred value is identified and selected to complete the total picture of a set of reaction conditions giving the preferred Co/Al₂O₃ catalyst performance on the 20cm³ reactor, in line with the main project aims that were outlined in section 1.3. The criteria for determining the preferred conditions for operation on the 20cm³ fixed-bed reactor at Aston are discussed in section 5.2. The other reaction conditions in this test set are kept constant at the following values: (230°C, 10 bar, WHSV = 8.8 h⁻¹, and H₂/CO = 2.0).

5.1.6 Experiment Outline and Summary

The experiment procedure (including the reactor packing method, catalyst activation, FT synthesis test runs, and product sampling and analysis) was previously outlined in section 3.7. In summary, the catalyst is activated prior to the FT synthesis reaction under the following conditions: drying for one hour in N₂ at atmospheric pressure, followed by 11 hours reduction at atmospheric pressure in pure hydrogen at 350°C, with a heating rate of 1°C/min. The reactor is then cooled to 180°C and the FT reaction is then initiated using the conditions for each of the 12 experiments making up the five test sets, summarized in Table 5.1 below. The results obtained are presented and discussed in section 5.3. The total reaction duration for each FT synthesis experiment is 48 hours due to the limitations relating to the pneumatic air supply and department access schedule discussed previously in section 3.4.3.2. The effluent gas compositions are analyzed online before the beginning of the reaction, and at hourly intervals after the initiation of the FT synthesis reaction as previously described in section 3.7.4, where the offline analysis of the liquid products was also detailed. The nitrogen molar composition in the syngas (internal standard for GC analysis) used in all the experiments is 10 mol% due to the equipment limitations related to the minimum possible

delivery rate of nitrogen that were explained in section 3.4.3.1. The mass of the Co/Al₂O₃ catalyst used is kept constant (0.5g) in the first four parameter profile tests for the reasons relating to catalyst availability that were explained previously in section 3.1.1. This amount is increased to 2.0g in the last parameter profile test set for the reasons explained previously in section 5.1.5.

Table 5.1 – Parameter study tests: Summary of reaction conditions used in the 20cm³ reactor

Parameter Study Test Set	Exp. No.	Catalyst Loading (g)	Reactor Temp. (°C)	Reactor Pressure (bar)	WHSV (h ⁻¹)	H ₂ /CO Ratio
1. Temperature Profile	FT4	0.5	210	10	8.8	2.0
	FT7	0.5	230	10	8.8	2.0
	FT8	0.5	250	10	8.8	2.0
2. Pressure Profile	FT9	0.5	230	2	8.8	2.0
	FT10	0.5	230	5	8.8	2.0
	FT11	0.5	230	8	8.8	2.0
	FT11 (REP.)	0.5	230	8	8.8	2.0
	FT7	0.5	230	10	8.8	2.0
3. Space Velocity Profile	FT7	0.5	230	10	8.8	2.0
	FT12	0.5	230	10	10.5	2.0
	FT13	0.5	230	10	11.5	2.0
4. H ₂ /CO Molar Ratio Profile	FT14	0.5	230	10	8.8	1.6
	FT15	0.5	230	10	8.8	1.8
	FT7	0.5	230	10	8.8	2.0
5. Catalyst Loading Profile	FT7	0.5	230	10	8.8	2.0
	FT16	2.0	230	10	8.8	2.0

5.2 Performance Criteria for Selection of Preferred Conditions

The preferred set of conditions on the 20cm³ reactor at Aston would ideally represent a compromise between the results of the selected performance criteria. This would include a balance between high reactant (CO) conversions and stability in catalyst activity (CO conversion) with time on stream, low selectivities and yields of CO₂, CH₄ and C₂-C₅ hydrocarbon products, high C₆₊ product selectivity, high yields of liquid hydrocarbons, and finally, a liquid hydrocarbon composition weighted towards diesel grade products. Hence, the performance of the selected Co/Al₂O₃ catalyst is assessed in terms of five main criteria which include CO conversion, product selectivity, product yields, liquid hydrocarbon product composition and the stability of the catalyst. These criteria are discussed in sections 5.2.1 to 5.2.4 below.

5.2.1 CO Conversion and Product Selectivity Criteria

High reactant or CO conversions are desired in FT synthesis, as in most chemical processes. However, the desired products are liquid hydrocarbon fuels and therefore high C₆₊ hydrocarbon product selectivities are desired, as opposed to high selectivities of CO₂, CH₄ and light hydrocarbon gases (C₂-C₅). This is because a high C₆₊ hydrocarbon product selectivity usually corresponds to a final product containing a high proportion of C₆₊ liquid hydrocarbon products. This normally implies maximum liquid hydrocarbon fuel production and therefore minimizes the commercial requirement for FT reactor off-gas steam reforming and recycling (discussed previously in section 2.7.5.1), which would bring added processing costs. The resulting product distribution from each experiment run in the present study is represented by the individual (or group) selectivities (as described previously in section 3.5.2). The CO conversion is calculated using Equations 4.4 and 4.5 in section 4.5.2. The product selectivities are calculated using Equations 3.3 to 3.6 that were presented in section 3.5.2.4. The results obtained from each parameter test set for the CO conversion and the product selectivities are compared to the results of similar studies using cobalt-based catalysts in the available literature, which were reviewed in section 2.6.2.

5.2.2 Product Yields Criterion

As discussed previously in section 2.6, product yields are very rarely reported in FT synthesis research publications. No research studies investigating the influence of reaction conditions on the product distribution using cobalt-based catalysts have been found that provide data on FT product yields. Instead, product selectivities are usually presented. As previously discussed in section 2.3, product selectivity provides information on the distribution of products from a molar composition perspective and gives an overall picture of the type of products the catalyst is inclined to form. This does not represent the actual amounts of products obtained, the knowledge of which is industrially important. High liquid hydrocarbon yields maximize the viability of the process if liquid fuels are being targeted, whereas gas products are usually undesirable. Once again, this is because of the lower requirements for FT reactor off-gas steam reforming and recycling that would be implied, as discussed previously in section 2.7.5.1. The ratio of the yields of these FT products (liquid/gas) can therefore be useful in differentiating between the various processing conditions examined to reveal the preferred set of values; the higher this ratio, the higher the relative proportion of liquids to gases in the product and, therefore, the lower the requirement for FT reactor off-gas reforming and recycling. These ratios are also reported in the present study. The methods used for calculating the product yields were outlined in section 3.7.4.2.

5.2.3 Liquid Hydrocarbon Product Composition Criterion

In addition to the yield of liquid hydrocarbon products, knowledge of their composition is required. Synthetic FT diesel is a very high quality fuel (section 2.7.5) in terms of its combustion properties and from an environmental perspective, as it has been reported to produce less emissions [42]. Naphtha grade products in the mixture are reported to lower the quality of the diesel, and would

normally require significant upgrading to gasoline-grade products if they are to be used in gasoline engines [42]. This would imply additional process stages which are accompanied by extra process complexity and costs. Targeted product control, such as maximizing diesel yields, can be more easily achieved by hydro-cracking the wax products (C_{19+}) into diesel grade products, and therefore a higher wax content would be preferred over that of naphtha grade products in the fuel mixture (as carried out by Shell [135, 137]). However, in a decentralized FT process scheme, maximum yields of straight-run diesel and minimum yields of wax products would potentially be more desirable from a logistical perspective. Therefore, a final synthetic crude liquid product with a high diesel fuel (C_{11} - C_{18}) composition, containing minimum amounts of naphtha and wax (C_{19+}) grade products, is preferred.

5.2.4 Catalyst Stability Criterion

The catalyst stability (measured in terms of CO conversion versus time on stream) reflects on its activity and provides information on its effectiveness in the synthesis process, as well as how quickly or slowly it deactivates. Industrially, FT catalysts require periodical regeneration or replacement which results in the loss of production and profits, as well as added maintenance and other costs. Hence, a high and steady catalyst activity over sustained periods of time is also desirable.

5.3 Results and Discussion

The results obtained from the FT synthesis parameter study summarized in Table 5.1 above, are presented and discussed in sections 5.3.1 to 5.3.5 below. Each section contains the results from each parameter profile test set described previously in section 5.1. Each parameter is discussed in relation to its effect on the performance criteria discussed in sections 5.2.1 to 5.2.4 above and the reactant conversion and product selectivity results are compared to similar studies in the available literature. The reaction conditions implemented in these literature studies were previously summarized in Table 2.4 in section 2.6.2. The influence of the parameters studied on the above performance criteria are then compared in section 5.3.6.

5.3.1 Influence of Reactor Temperature

5.3.1.1 CO Conversion

The results obtained in the present study for the effect of reactor temperature on CO conversion (at 10 bar, $H_2/CO = 2.0$, $WHSV = 8.8 \text{ h}^{-1}$, and $m_{\text{cat}} = 0.5\text{g}$) are compared to the results of similar studies using cobalt-based catalysts (reviewed previously in section 2.6.2 and summarized in Table 2.4) that have investigated the influence of temperature on CO conversion in Figure 5.1 below. These include studies by de la Osa *et al.* [89] and Woo *et al.* [115] (both working with $\text{Co}/\text{Al}_2\text{O}_3$ catalysts at higher pressures ≥ 20 bar), as well as Mohanty *et al.* [91] (working above 28 bar, but with a $\text{CuO-CoO}/\text{Cr}_2\text{O}_3$ catalyst combined with MFI Zeolite), and Xu *et al.* [83] (who used a

pressure of 10 bar and a Pt/ZrO₂ modified Co/Al₂O₃ catalyst, but at a significantly lower space velocity than the one used in the present study). As discussed previously in section 2.6, studies using cobalt-based catalysts that have specifically addressed the influence of low operating pressures (< 20 bar) on FT product distribution, and catalyst activity are very limited. Therefore, although different reaction conditions were implemented in these other studies, including higher reactor pressures (by de la Osa *et al.*, Woo *et al.* and Mohanty *et al.*) than the reactor pressure used in the present study, and lower space velocities (by all), these are the only studies that have been found for comparison of results.

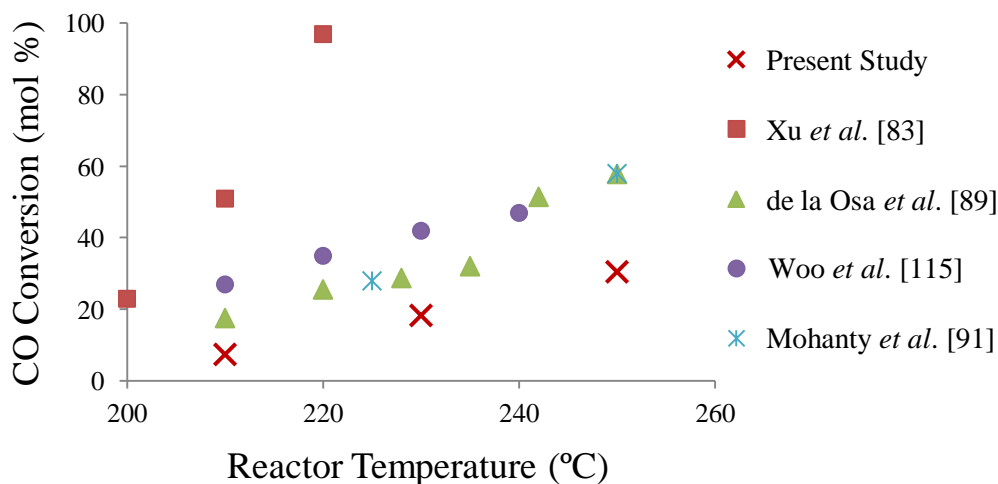


Figure 5.1 – Influence of reactor temperature on CO conversion in the present study (at 10 bar, H₂/CO = 2.0, WHSV = 8.8 h⁻¹, and m_{cat} = 0.5g) in comparison to similar studies by Xu *et al.* [83], de la Osa *et al.* [89], Woo *et al.* [115], and Mohanty *et al.* [91]

In all work reported CO conversion increases with increasing reactor temperature in an almost linear fashion. The trend observed in the present study is comparable to the other trends shown in Figure 5.1 above (apart from Xu *et al.*), but the absolute figures are not. The lower CO conversions achieved in the present study may be due to the limitations of the 20cm³ reactor system at Aston relating to the minimum possible space velocity, the amount of catalyst available and reactor temperature control that were explained previously in section 3.4.3. Hence, in order to carry out all the planned tests, each experiment was limited to using 0.5g of the Co/Al₂O₃ catalyst and high space velocities (~17 Lg_{cat}⁻¹h⁻¹). In contrast, larger amounts of catalyst (ranging from 1.0-5.0g), and much lower space velocities (as low as 0.5 Lg_{cat}⁻¹h⁻¹ by Xu *et al.*) were used in the studies compared in Figure 5.1 above. The low value for space velocity used by Xu *et al.* may justify the much higher CO conversion figures they report with increasing reactor temperature, as lower space velocities imply longer residence times (section 2.5.3). Higher conversions could not be achieved in the present study by increasing the catalyst loading used in the reactor, or by decreasing the space velocity (Equation 3.1 in section 3.4.3.1). The higher range of space velocities used in the present study in comparison to other studies that have investigated the influence of space velocity on FT product distribution and CO conversion are discussed in section 5.3.3.

5.3.1.2 CO₂ Selectivity

CO₂ formation is attributed to the WGS reaction (Equation 2.2 section 2.2), an equilibrium reaction, the extent of which depends on CO conversion, which in turn, increases with rising reactor temperature. The results obtained for the effect of reactor temperature on CO₂ selectivity (at 10 bar, H₂/CO = 2.0, WHSV = 8.8 h⁻¹, and m_{cat} = 0.5g) are presented in Figure 5.2 below. From the studies investigating the influence of reaction conditions on FT product distribution that were reviewed in section 2.6.2 and summarized in Table 2.4, only a few report on the effect of reactor temperature on CO₂ selectivity. The results of these studies are also presented in Figure 5.2 below, for comparison.

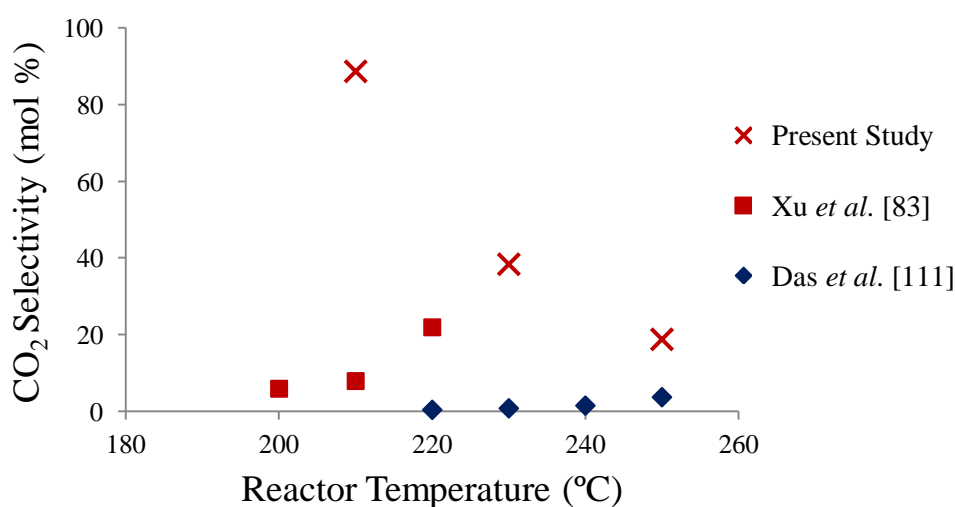


Figure 5.2 – Influence of reactor temperature on CO₂ selectivity in the present study (at 10 bar, H₂/CO = 2.0, WHSV = 8.8 h⁻¹, and m_{cat} = 0.5g) in comparison to similar studies by Xu *et al.* [83] and Das *et al.* [111]

The results from the present study show that CO₂ selectivity is greatly dependent on reactor temperature and decreases sharply as the reactor temperature is increased. The opposite trend, however, is reported by both Xu *et al.* [83] and Das *et al.* [111], as shown in Figure 5.2 above. The different reaction conditions and catalyst formulations implemented in these studies, including a higher reactor pressure (20 bar) by Das *et al.*, a different catalyst by Xu *et al.* (Pt/ZrO₂ modified Co/Al₂O₃ catalyst), as well as significantly lower space velocities by both studies (0.5 and 2 L_{gcat}⁻¹h⁻¹ by Xu *et al.* and Das *et al.*, respectively) may be contributing factors to these opposing trends. Above 220°C, the results from the present study are in more general agreement with those reported by Xu *et al.* and Das *et al.*, however, below 220°C the results disagree considerably. As previously discussed in section 3.5.2.4, product selectivity represents the molar composition of the products formed. In particular, the CO₂ selectivity represents the proportion of the carbon atoms in the CO ending up as CO₂ in the final product. CO₂ is always produced during FT synthesis (EQ 2.2 in section 2.2), hence, at the low CO conversions observed at 210°C (as previously discussed in section 5.3.1.1) the high CO₂ selectivity shown in Figure 5.2 above, does not necessarily represent a high yield of CO₂ but, rather, reflects on the poor hydrocarbon product formation achieved at the

specific reaction conditions implemented for experiment FT4 (Table 5.1 in section 5.1.6) at 210°C. This is also later verified in section 5.3.1.5 where the CO₂ yields obtained at all temperatures investigated were found to be similar. This potentially justifies the differences in results shown in Figure 5.2 above, as at the reaction conditions implemented in the studies by Xu *et al.* and Das *et al.* significantly higher CO conversions were reported below 220°C (Figure 5.1). Further investigation into the influence of reactor temperature on CO₂ selectivity, including repetition of the FT synthesis run at 210°C, however would be recommended for future work for clarification of results. What can be drawn from the results of the present study, however, is that under the reaction conditions implemented in the 20cm³ reactor, operation at higher reactor temperatures (in the range of 200-250°C) is preferred as the CO₂ selectivity is lower. As CO₂ is an inert gas, a lower concentration of CO₂ in the product would require less FT reactor off-gas conditioning (i.e. CO₂ removal discussed in section 2.7.3.2) and, in addition, imply higher yields of once-through liquid hydrocarbon products.

5.3.1.3 CH₄ and C₂-C₅ Selectivity

The results obtained for the effect of reactor temperature on CH₄ and C₂-C₅ hydrocarbon selectivities (at 10 bar, H₂/CO = 2.0, WHSV = 8.8 h⁻¹, and m_{cat} = 0.5g) are presented in Figure 5.3, and Figure 5.4 below, respectively. The results from similar studies using cobalt-based catalysts (reviewed previously in section 2.6.2 and summarized in Table 2.4) that have investigated the influence of reactor temperature on CH₄ and C₂-C₅ selectivities are also presented in these figures for comparison. In all the studies reported, both CH₄ and light hydrocarbon (C₂-C₅) selectivities are found to increase with increasing reactor temperature. The reasons for this relate to the increased rate of chain termination reactions (section 2.2.1) as the temperature rises, where the -CH₂-monomers are hydrogenated to CH₄ as discussed previously in section 2.5.1. A much less marked effect is observed with light hydrocarbon (C₂-C₅) selectivity.

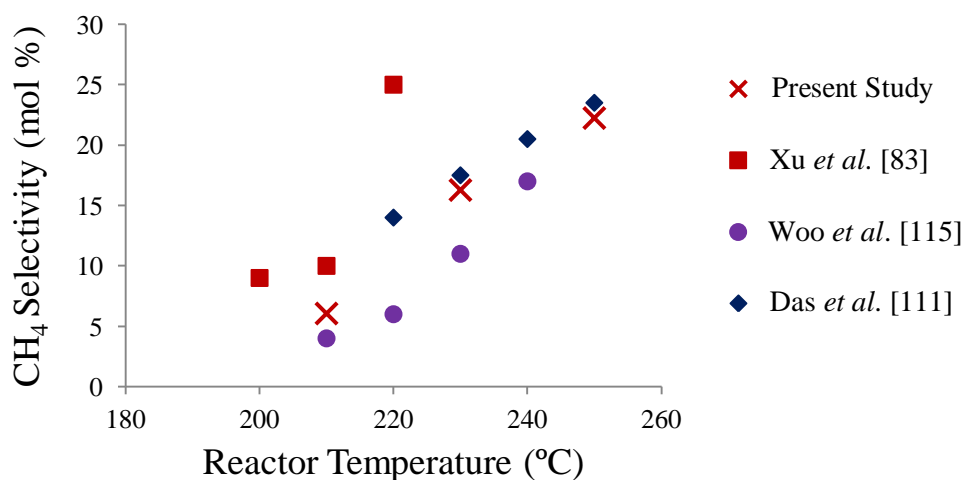


Figure 5.3 – Influence of reactor temperature on CH₄ selectivity in the present study (at 10 bar, H₂/CO = 2.0, WHSV = 8.8 h⁻¹, and m_{cat} = 0.5g) in comparison to similar studies by Xu *et al.* [83], Woo *et al.* [115], and Das *et al.* [111]

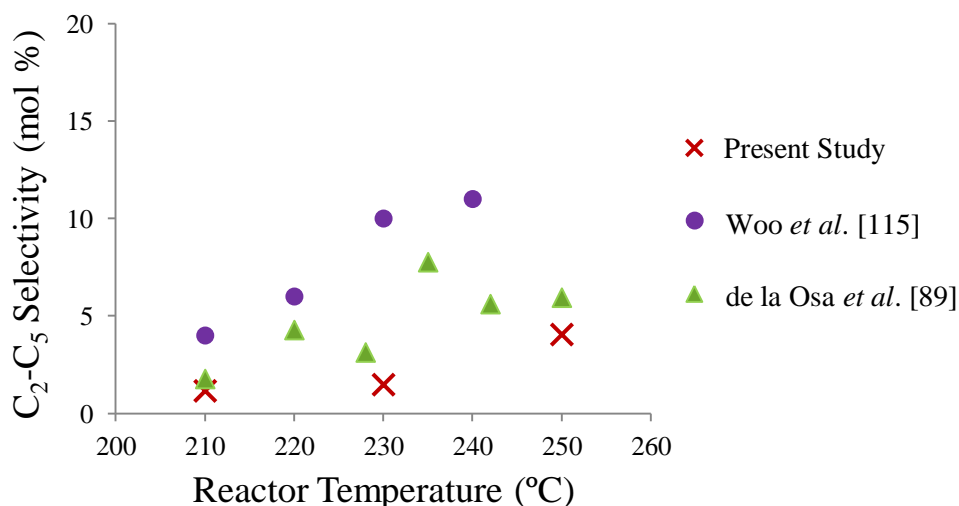


Figure 5.4 – Influence of reactor temperature on C₂-C₅ selectivity in the present study (at 10 bar, H₂/CO = 2.0, WHSV = 8.8 h⁻¹, and m_{cat} = 0.5g) in comparison to similar studies by Woo et al. [115], de la Osa et al. [89]

The trend observed for CH₄ selectivity in the present study is comparable to the trends by Woo *et al* and Das *et al.*, as shown in Figure 5.3 above, but not with Xu *et al.*, who reported higher figures for CH₄ selectivity with increasing reactor temperature. The difference in these results may also be due to the lower space velocities employed by Xu *et al.* than those used in the present study, as discussed in section 5.3.1.1 above. The trend for C₂-C₅ hydrocarbon selectivity observed in the present study is most comparable to that reported by de la Osa *et al.* [89], although absolute figures are not, whereas higher figures were reported by Woo *et al.* [115], as shown in Figure 5.4 above (the influence of reactor temperature on the selectivity of C₂-C₅ hydrocarbons was not reported by Xu *et al.*). This may indicate that under the reaction conditions implemented in the 20cm³ reactor in the present study, the selectivity of the Co/Al₂O₃ catalyst towards the formation of light hydrocarbon gases is low and not significantly affected by reactor temperature.

5.3.1.4 C₆₊ Selectivity

The results obtained for the effect of reactor temperature on C₆₊ hydrocarbon selectivity (at 10 bar, H₂/CO = 2.0, WHSV = 8.8 h⁻¹, and m_{cat} = 0.5g) are presented in Figure 5.5 below. The results from similar studies using cobalt-based catalysts (reviewed previously in section 2.6.2 and summarized in Table 2.4) that have investigated the influence of reactor temperature on the selectivity of C₆₊ hydrocarbons are also presented in Figure 5.5 for comparison.

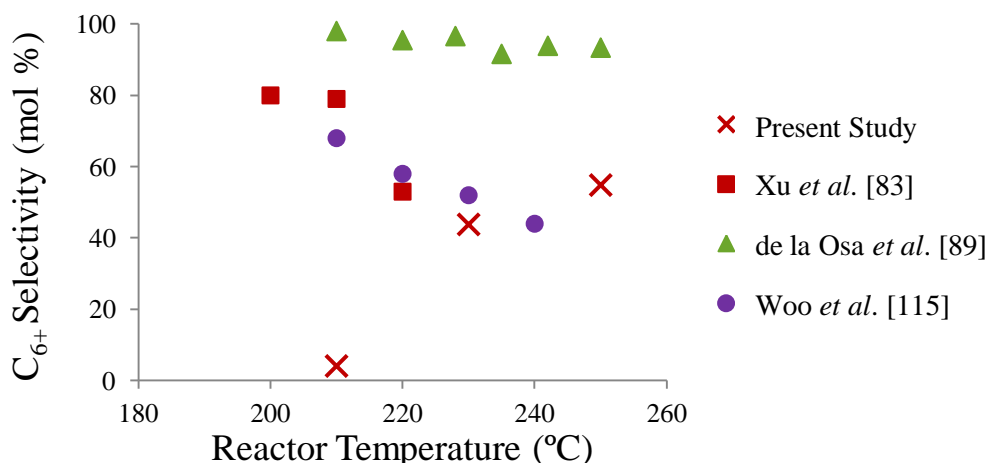


Figure 5.5 – Influence of reactor temperature on C_{6+} selectivity in the present study (at 10 bar, $H_2/CO = 2.0$, $WHSV = 8.8 h^{-1}$, and $m_{cat} = 0.5g$) in comparison to similar studies by Xu *et al.* [83], de la Osa *et al.* [89] and Woo *et al.* [115]

In the present study, C_{6+} hydrocarbon selectivity increases significantly with increasing reactor temperature. As shown in Figure 5.5 above, the opposite trends (and higher figures) are reported by Woo *et al.* [115] and Xu *et al.* [83]. Higher figures are also reported by de la Osa *et al.* who, in contrast to the other two studies, report that C_{6+} selectivity is not significantly affected by variation in reactor temperature in the range of 210-250°C. The different reaction conditions and catalyst formulations implemented in these three studies (as discussed previously in section 5.3.1.1) may be contributing factors to these opposing trends.

Similar to the discussion made previously in section 5.3.1.2, the results from the present study above 220°C are in more general agreement with those reported by Xu *et al.* and de la Osa *et al.*, and Woo *et al.*, whereas below 220°C there is considerable disagreement. The C_{6+} selectivity represents the proportion of the carbon atoms in the CO ending up as C_{6+} or liquid hydrocarbons in the final product. Hence, at the low CO conversions observed at 210°C (as previously discussed in section 5.3.1.1), the low C_{6+} hydrocarbon product selectivity shown in Figure 5.5 above, does not necessarily represent a low yield of C_{6+} hydrocarbon products but, rather, reflects on the poor hydrocarbon product formation achieved at the specific reaction conditions implemented for experiment FT4 (Table 5.1 in section 5.1.6). This potentially justifies the differences in results shown in Figure 5.5 above, as at the reaction conditions implemented in the studies by Xu *et al.* de la Osa *et al.* and Woo *et al.* higher CO conversions were reported below 220°C (Figure 5.1). Once again, further investigation into the influence of reactor temperature on C_{6+} hydrocarbon selectivity, including repetition of the FT synthesis run at 210°C, however would be recommended for future work for clarification of results. What can be drawn from the results of the present study, however, is that under the reaction conditions implemented in the 20cm³ reactor using the Co/Al₂O₃ catalyst, operation at higher reactor temperatures (>220°C) is preferred as C_{6+} hydrocarbon selectivity is higher, which usually implies higher yields of once-through liquid hydrocarbon products.

5.3.1.5 Product Yields

The product yields are calculated as described previously in section 3.7.4.2. The unreacted syngas is calculated by difference. The product yields obtained in this parameter test set (Table 5.1 in section 5.1.6) reflect the trends observed in sections 5.3.1.2 to 5.3.1.4 above, for product selectivity with increasing reactor temperature. These results are presented in Table 5.2 below. As discussed previously in section 5.2.2, product yields are very rarely reported in FT synthesis research publications, and no research studies (investigating the influence of reaction conditions on the product distribution using cobalt-based catalysts) that provide data on FT product yields have been found for comparison to the yields found in the present study.

Table 5.2 – Influence of reactor temperature on FT gas and liquid product yields (at 10 bar, H₂/CO = 2.0, WHSV = 8.8 h⁻¹, and m_{cat} = 0.5g)

Test	Temp. (°C)	Product Yields (wt.%)					Oxyg. In water (wt.%)	Unreacted Syngas (wt.%)
		CO ₂	CH ₄	C ₂ -C ₅	Liquid H/C's + Waxes	Water + Oxyg.		
FT4	210	7.0	0.2	0.1	0.2	1.3	3.8	91.2
FT7	230	7.5	1.2	0.3	2.2	3.6	3.7	85.2
FT8	250	6.1	2.6	1.6	2.3	7.8	2.5	79.6

The yields of CH₄ and light hydrocarbons (C₂-C₅) increase with reactor temperature as expected (section 2.2.1). The yield of CO₂ peaks at 230°C, and then drops again as the reactor temperature is raised to 250°C. The yield of water (containing soluble oxygenated compounds) more than doubles for every 20°C increase in reactor temperature, indicating that the WGS reaction (Equation 2.2 section 2.2), through which water is produced, is significantly influenced by variation in reactor temperature. The variation of the soluble oxygenate concentration in the aqueous phase with increasing reactor temperature is minimal, indicating that the formation of oxygenated compounds is not significantly influenced by reactor temperature. The yield of liquid hydrocarbons and waxes (C₆₊ products) is negligible at 210°C, whereas similar yields are obtained at 230 and 250°C. This shows that under the reaction conditions used with the Co/Al₂O₃ catalyst in the 20cm³ reactor in the present study, increasing the reactor temperature above 230°C does not have a significant influence on liquid hydrocarbon formation. In contrast, the formation of water is significantly influenced by increasing the reactor temperature, indicating that increasing temperature in the range of 210-250°C favours the reverse WGS reaction (CO₂ hydrogenation producing water) which was discussed in section 2.2.

Figure 5.6 below, illustrates the influence of reactor temperature on the ratio of liquid products to gas products (excluding unreacted syngas). As shown in this figure, the highest total liquid products to gas products ratio (~1.0) is obtained at 250°C. Similar ratios are obtained, however, for the liquid hydrocarbon to gas products at both 230 and 250°C. Hence, although higher C₆₊

selectivities are obtained at 250°C (as discussed previously in section 5.3.1.4), which could imply higher yields of liquid hydrocarbon products, this is not the case as shown in Figure 5.6 below.

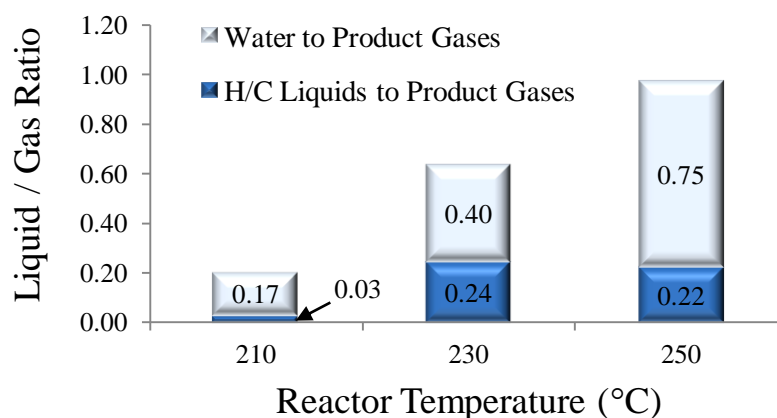


Figure 5.6 – Influence of reactor temperature on the ratio of liquid products to product gases (at 10 bar, $H_2/CO = 2.0$, $WHSV = 8.8 h^{-1}$, and $m_{cat} = 0.5g$)

5.3.1.6 Energy Content and Composition of Liquid Hydrocarbon Products

Figure 5.7 below, shows a photograph of the liquid products collected from the GLS chamber(s) in the 20cm³ reactor system (Figure 3.4 in section 3.4) at the end of the FT synthesis experiment run FT7 at 230°C (Table 5.1 in section 5.1.6). This photograph is representative of most of the liquid products collected from all the parameter study experiments (tests FT4-FT16, listed in Table 5.1 in section 5.1.6). These liquid products consisted of a clear aqueous phase (water plus soluble oxygenates) and an immiscible oil phase (liquid hydrocarbons) which sometimes contained small amounts of visible solid waxes. After collection, these phases were analyzed according to the methods previously discussed in sections 3.5.3.1 and 3.7.4.2.

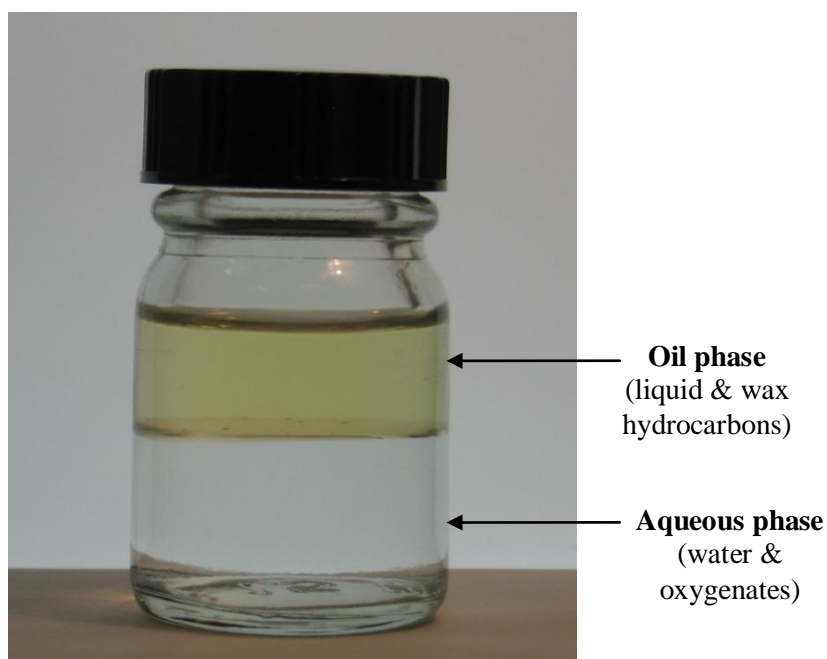


Figure 5.7 – FT liquid products collected at the end of experiment FT7 (at 230°C, 10 bar, $WHSV = 8.8 h^{-1}$, $H_2/CO = 2.0$, and $m_{cat} = 0.5g$)

The calorific values of the liquid hydrocarbon samples collected from experiment runs FT4, FT7 and FT8 (Table 5.1 in section 5.1.6) are calculated using the method outlined in section 3.5.3.3, and are given in Table 5.3 below. Although very slight increases in calorific value are observed with increasing reactor temperature, these results show that the energy content of the liquid hydrocarbons is not significantly influenced by variation in reactor temperature.

Table 5.3 – Influence of reactor temperature on the energy content of liquid hydrocarbon products (at 10 bar, $H_2/CO = 2.0$, $WHSV = 8.8 h^{-1}$, and $m_{cat} = 0.5g$)

Test	T (°C)	Content (%)				HHV (MJ/kg)
		C	H	N	O	
FT4	210	84.09	15.12	0.10	0.69	47.10
FT7	230	84.21	15.20	0.10	0.49	47.26
FT8	250	84.35	15.24	0.10	0.31	47.36

The GC-MS chromatograms obtained from the analysis of the liquid hydrocarbons obtained at the three reactor temperatures investigated (210, 230, and 250°C) in tests FT4, FT7 and FT8 are shown in Figure 5.8, Figure 5.9, and Figure 5.10 below, respectively.

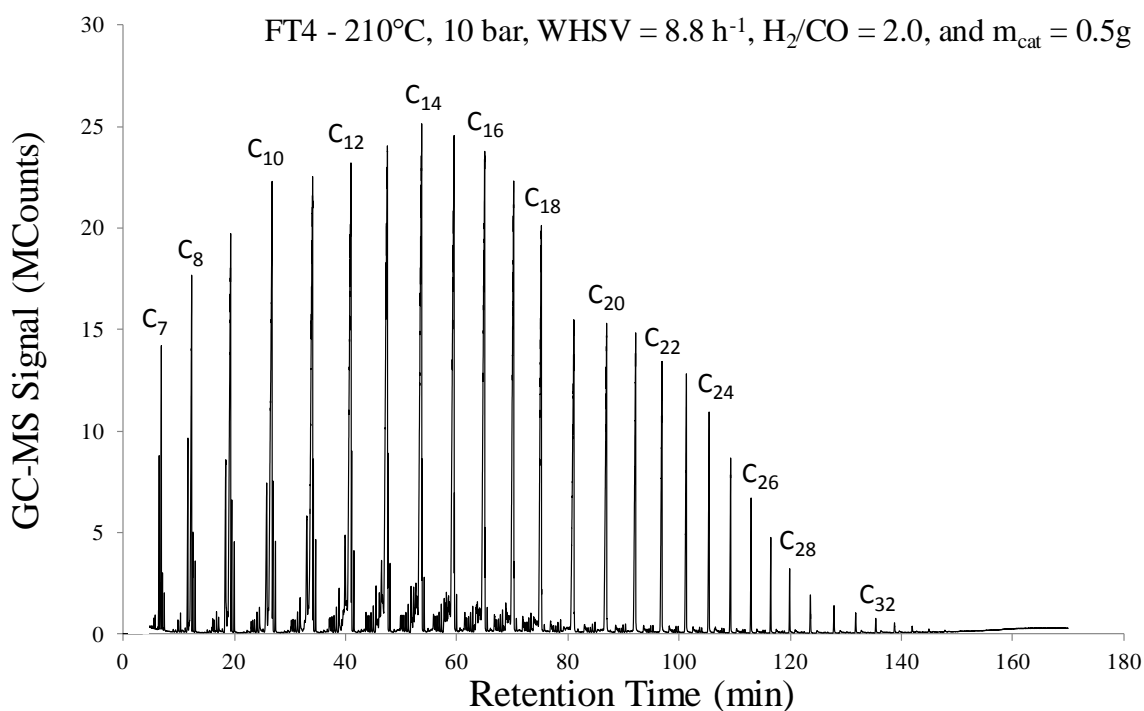


Figure 5.8 – GC-MS chromatogram of liquid hydrocarbons collected from temperature profile test FT4 at 210°C

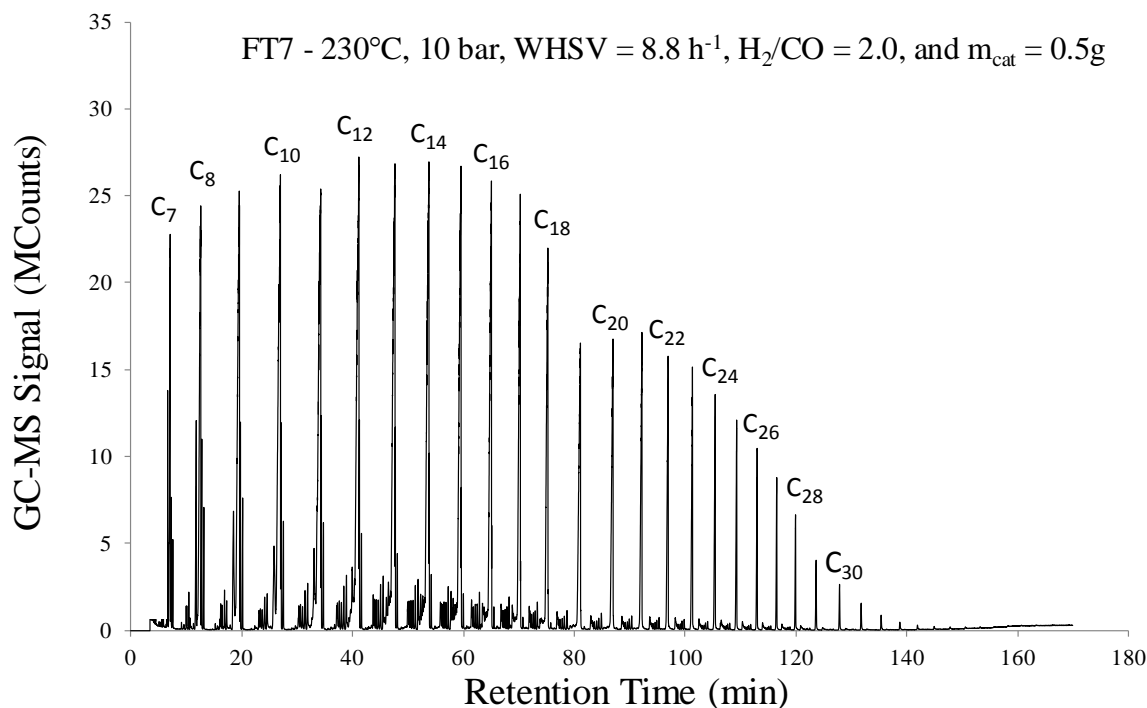


Figure 5.9 – GC-MS chromatogram of liquid hydrocarbons collected from temperature profile test FT7 at 230°C

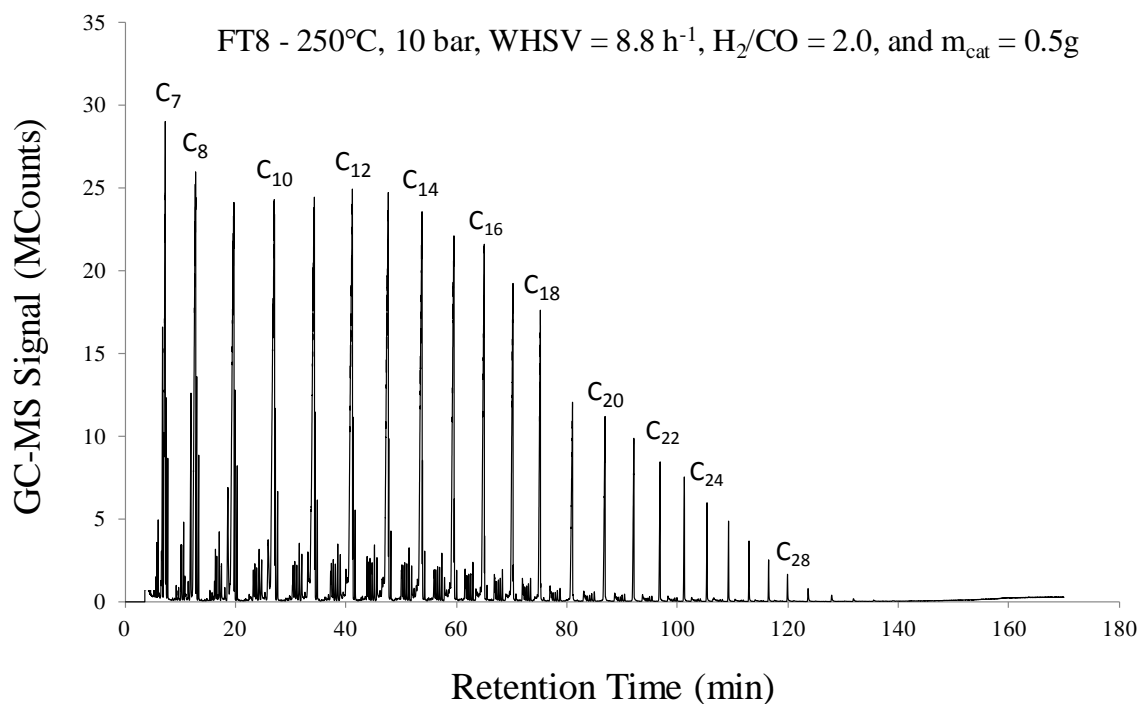


Figure 5.10 – GC-MS chromatogram of liquid hydrocarbons collected from temperature profile test FT8 at 250°C

The relative fuel compositions of the liquid hydrocarbons collected are calculated from the chromatograms in the figures above, using the method outlined previously in section 3.5.3. The results are illustrated in Figure 5.11 below.

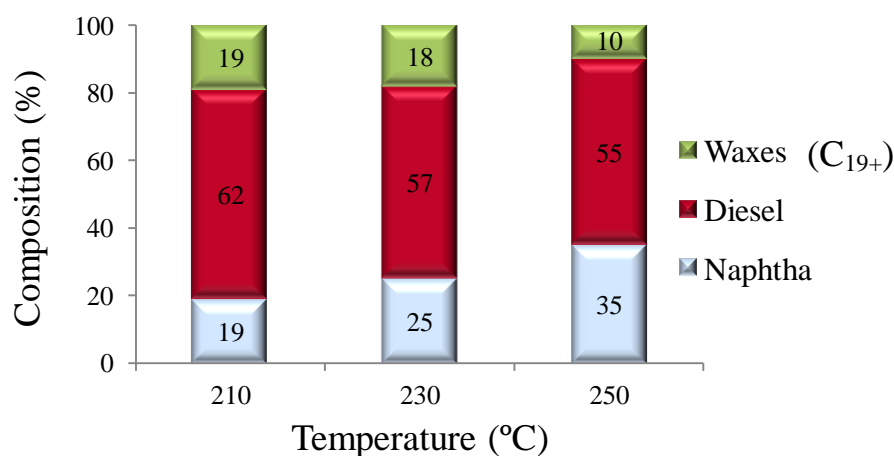


Figure 5.11 – Influence of reactor temperature on liquid hydrocarbon product composition (at 10 bar, $H_2/CO = 2.0$, $WHSV = 8.8 h^{-1}$, and $m_{cat} = 0.5g$)

These results show that the liquid hydrocarbon product composition is significantly influenced by the reactor temperature. As discussed previously in section 2.5.1, higher temperatures have been shown to favour the formation of shorter-chain carbon products [20]. This is mainly reflected in the naphtha (C_7-C_{10}) composition that noticeably increases as the reactor temperature rises, as well as the wax (C_{19+}) composition which varies slightly from 210 to 230°C but then sharply decreases by almost half at 250°C. This difference is also visibly evident in the liquids obtained, as the immiscible oil phases collected at 210 and 230°C have a yellow tint due to the suspension of small amounts of tiny wax particles (Figure 5.7 above), whereas the oil phase collected at 250°C does not appear to have suspended solid waxes and, as a result, has a more transparent appearance.

From the point of view that maximum diesel contents are desired in the liquid hydrocarbon fuel (as discussed previously in section 5.2.3), it would appear that 210°C is the most favourable reactor temperature giving the highest diesel composition of 62%. However, the results discussed in the previous sections show the lowest CO conversion, C_{6+} hydrocarbon product selectivity and liquid hydrocarbon product yields at this reactor temperature. Hence, under the reaction conditions implemented in the 20cm³ reactor in the present study, using the Co/Al_2O_3 catalyst, the preferred diesel composition is observed at 230°C. This is because at 250°C the naphtha content is significantly higher, and conversely, the wax content is much lower than at 230°C.

5.3.1.7 Catalyst Stability

The influence of reactor temperature on the stability of the Co/Al_2O_3 catalyst (CO conversion versus time on stream) during the synthesis experiments (FT4, FT7 and FT8 in Table 5.1 in section 5.1.6) is compared in Figure 5.12 below.

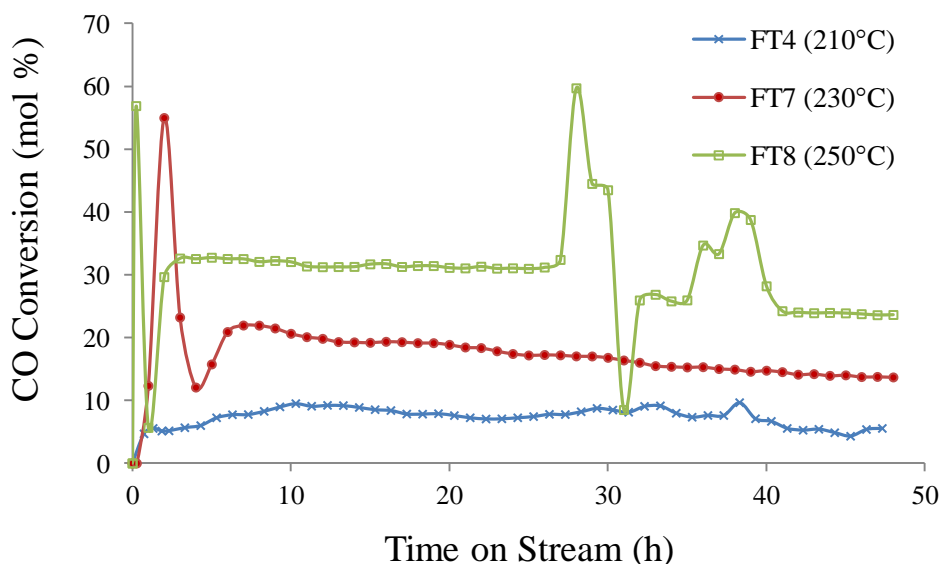


Figure 5.12 – Influence of reactor temperature on catalyst stability: CO conversion versus time on stream (at 10 bar, $H_2/CO = 2.0$, $WHSV = 8.8 h^{-1}$, and $m_{cat} = 0.5g$)

As shown in Figure 5.12 above, a relative stability in activity is demonstrated by the Co/Al_2O_3 catalyst over the 48 hour period within the reactor temperature range studied. The initial ‘spikes’ observed at the beginning of the reactions at 230 and 250°C are due to the extreme exothermicity of the FT synthesis reaction [156]. This firstly results in high initial activity because of the increased reaction rate at higher temperatures, and then a sudden drop in activity due to catalyst surface carburisation and/or wax deposition (deactivation mechanisms discussed previously in section 2.4.3). The activity then stabilizes at a lower conversion rate as the reaction progresses. No such spikes are recorded at 210°C, suggesting that there is a much lower reaction rate at this reactor temperature, and inconsistent activity is displayed by the catalyst as the reaction progresses further. Both of these observations signify that a reactor temperature of 210°C is not adequate for achieving favourable catalyst activity under the conditions implemented (Table 5.1 in section 5.1.6).

The results obtained at 250°C display the most favourable consistency for the first 26 hours of reaction, after which point a temperature runaway occurred in the reactor during the experiment run. As there is no water cooling mechanism surrounding the reactor (an equipment limitation discussed previously in section 3.4.3.3), the temperature setting had to be significantly decreased in order to bring the value back down to the desired reactor temperature of 250°C. Once this value was reached in the reactor, the setting was restored to the original value of 250°C. This adjustment is reflected in the irregular behaviour of the 250°C plot in Figure 5.12, where dramatic fluctuations in CO conversion are recorded with time on stream. These eventually stabilize after 40 hours of operation when the reactor temperature had cooled down to 250°C once again.

Overall, the observed CO conversions at different reactor temperatures in Figure 5.12 suggest a decline in catalyst activity (or deactivation) with time on stream. This gradual deactivation is evident at all the reactor temperatures studied, and can be attributed to mainly coke and/or wax

deposition on the catalyst surface (section 2.4.3). To investigate the extent of these deactivation mechanisms, TGA analyses of the catalyst samples are performed according to the method that was outlined in section 3.6.4. The mass loss results obtained from these analyses are presented in Table 5.4 below. These results show that the extent of carbon and wax deposition is inversely proportional to increasing reactor temperature. The mass loss due to these surface deposition deactivation mechanisms shows a small decline from 210 to 230°C and then a steep decrease at 250°C. However, due to the temperature runaway that occurred during the run at 250°C, as discussed above, these results may not be entirely representative of the catalyst resistance to the deactivation mechanisms at this reactor temperature. SEM micrographs (at x764 magnification) of the Co/Al₂O₃ catalyst before and after reaction in runs FT4, FT7 and FT8 (Table 5.1 in section 5.1.6) are provided in APPENDIX B. Small differences can be seen in these micrographs, however, the magnification strength used was not sufficient in order to allow for definite conclusions to be drawn. Higher magnification strengths are therefore recommended for future investigation.

Table 5.4 – Influence of reactor temperature on the extent of carbon and wax deposition on the catalyst surface (TGA results)

Catalyst Sample Origin	Reactor Temperature (°C)	Total Mass Loss (wt.% dry basis)	Mass Loss Due to Carbon & Wax Deposition (wt.%)
Co/Al ₂ O ₃ before reaction	-	4.7	-
Test FT4	210	45.0	40.3
Test FT7	230	40.3	35.6
Test FT8	250	16.5	11.8

5.3.1.8 Reactor Temperature Selection for Further Experiments

Under the conditions used (Table 5.1 in section 5.1.6) in the 20cm³ reactor with the Co/Al₂O₃ catalyst in the present study, operation at 210°C is not recommended as this results in very low CO conversion and poor C₆₊ hydrocarbon product selectivity, and therefore very low yields of liquid hydrocarbon products (despite their favourable diesel composition). In addition, the catalyst displayed an inconsistent activity (in terms of CO conversion with time on stream) at this reactor temperature. Hence, the choice of the preferred reactor temperature remains between the values of 230 and 250°C.

As discussed previously in section 5.2.1, higher yields of liquid hydrocarbons and lower yields of inert gases (requiring less FT reactor off-gas reforming and recycling) are desirable qualities from a commercial perspective as process profitability is increased. Higher syngas conversions are achieved at 250°C than at 230°C that result in a higher C₆₊ hydrocarbon product selectivity and a higher ratio of total liquids to product gases formed. Also contributing to this higher ratio is the observation that an increase in reactor temperature favours CO₂ hydrogenation (reverse WGS

reaction) resulting in a lower CO₂ selectivity and yield at 250°C than at 230°C. However, at 250°C more than double the yield of CH₄ and light hydrocarbon gases (C₂-C₅) are obtained than at 230°C. The yield of liquid hydrocarbons, however, is similar at both reactor temperatures, indicating that increasing the reactor temperature above 230°C does not influence liquid hydrocarbon formation. Hence, water comprises a greater proportion of the total liquids that are produced at 250°C (in comparison to 230°C) where it is observed that more than double the yield of water is produced at 250°C than at 230°C (but contained less soluble oxygenates). The calorific values of the liquid hydrocarbons collected at 230 and 250°C are similar, indicating that reactor temperature does not have a significant influence on the energy content of the liquid hydrocarbons obtained. The compositions of diesel and waxes in the liquid hydrocarbon product are lower at 250°C, whereas a significantly higher composition of naphtha grade products is observed, making operation at 230°C more favourable.

From the results displayed in Figure 5.12 above, a lower stability is seemingly observed in catalyst activity with time on stream at 250°C. However, this is due to the equipment limitations relating to temperature control (explained previously in section 3.4.3.3), which is an important consideration in the selection of the appropriate operating temperature. Industrially, operation at 250°C would not pose the same temperature control problems that were encountered on the 20cm³ reactor in the present study, as appropriate heat exchange systems (e.g. water cooling) would be employed. At a research level, future work carried out on the 20cm³ reactor at Aston, using the same or other catalysts, could incorporate the use of inert diluents in the catalyst bed (e.g. silica carbide) to aid in achieving better isothermal control. From this test set and under the reaction conditions used with the Co/Al₂O₃ catalyst in the present study, therefore, the preferred reactor temperature that is selected for operation on the 20cm³ fixed-bed reactor at Aston, and as the value to be used in the remaining parameter profiling test sets, is 230°C.

5.3.2 Influence of Reactor Pressure

Section 5.3.1 resulted in identification of the preferred reactor temperature for subsequent tests.

5.3.2.1 CO Conversion

The results obtained in the present study for the effect of reactor pressure on CO conversion (at 230°C, H₂/CO = 2.0, WHSV = 8.8 h⁻¹, and m_{cat} = 0.5g) are presented in Figure 5.13 below. The results from similar studies using cobalt-based catalysts (reviewed previously in section 2.6.2 and summarized in Table 2.4) that have investigated the influence of reactor pressure on CO conversion are also presented in Figure 5.13 for comparison. These include studies by Xu *et al.* [83] (using a Pt/ZrO₂ modified Co/Al₂O₃ catalyst in the pressure range of 5-35 bar), Das *et al.* [89] (using a Co/Al₂O₃ catalyst in the pressure range of 1-35 bar), Woo *et al.* [115] (also using a Co/Al₂O₃ catalyst, but in the pressure range of 10-30 bar), Zheng *et al.* [110] (using a Co/SiO₂ catalyst in the pressure range of 2-20 bar), and Mohanty *et al.* [91] (using a cobalt-based catalyst in combination

with a MFI zeolite in the higher pressure range of 28-38 bar). As discussed previously in section 2.6, studies using cobalt-based catalysts that have specifically addressed the influence of low operating pressures (< 20 bar) on FT product distribution, and catalyst activity are very limited. Therefore, although different reaction conditions were implemented in these other studies, including lower space velocities and different catalyst compositions than those used in the present study, these are the only studies that have been found for comparison of results.

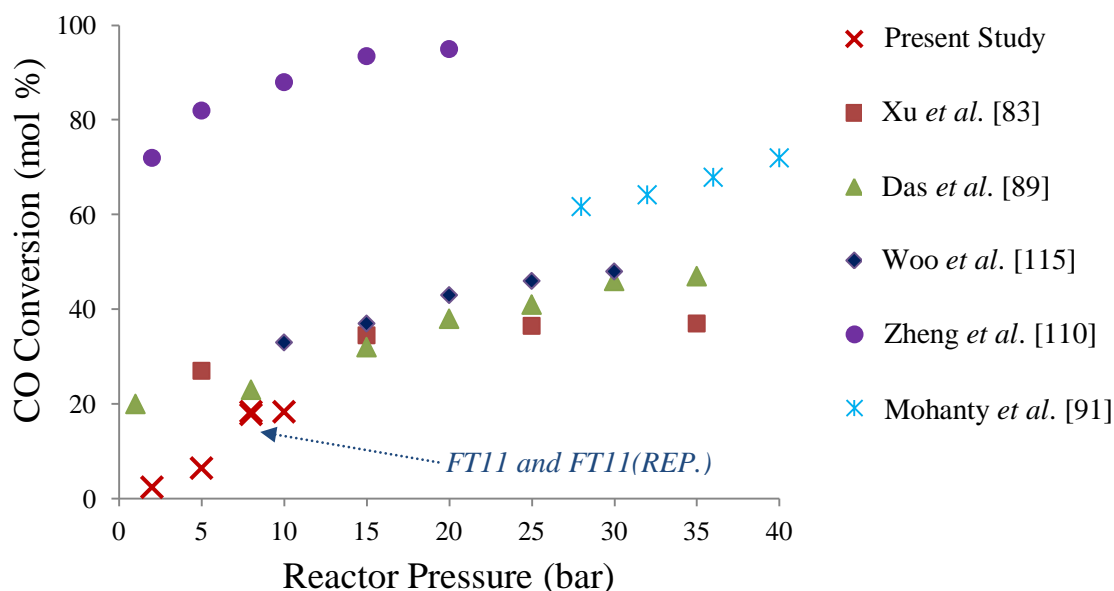


Figure 5.13 – Influence of reactor pressure on CO conversion in the present study (at 230°C, H₂/CO = 2.0, WHSV = 8.8 h⁻¹, and m_{cat} = 0.5g) in comparison to similar studies by Xu et al. [83], Das et al. [89], Woo et al. [115], Zheng et al. [110], and Mohanty et al. [91]. (Arrow represents results of experiments repeated at 8 bar)

In all the studies reported CO conversion increases with increasing reactor pressure. This is expected due to the contraction in volume that takes place as pressure rises, which has been reported to increase the concentration and dissociation of CO molecules on the catalyst surface and promote chain growth [43, 97]. The trend observed in the present study is comparable to the other trends shown in Figure 5.13 above (apart from Zheng *et al.* and Mohanty *et al.*), but the absolute figures are not. The lower conversions achieved in the present study may be due to the limitations of the 20cm³ reactor system at Aston relating to the minimum possible space velocity and the amount of catalyst available that were explained previously in section 3.4.3. As discussed in section 5.3.1.1 above, each experiment in this parameter test set (Table 5.1 in section 5.1.6) was limited to using 0.5g of the Co/Al₂O₃ catalyst and high space velocities (~17 Lg_{cat}⁻¹h⁻¹), whereas larger amounts of catalyst (ranging from 1.0-20.0g), and much lower space velocities (as low as 0.46 Lg_{cat}⁻¹h⁻¹ by Mohanty *et al.*) were used in the studies compared in Figure 5.13 above. These factors would contribute to the higher CO conversions reported in the other studies shown in Figure 5.13. In addition, the catalyst composition (including the type of support used) can significantly influence the CO conversion and the product distribution, as previously discussed in section 2.4.2.

These differences may explain the much higher CO conversion figures reported by Zheng *et al.* and Mohanty *et al.*, as shown in Figure 5.13 above. The results reported by Zheng *et al.*, in particular, suggest that relatively high CO conversions can be achieved at low reactor pressures (2-20 bar), and could potentially, therefore, be feasible for application in BTL-FT operations. As shown in Figure 5.13 above, however, much lower CO conversions than those reported by Zheng *et al.* are reported by Xu *et al.*, Das *et al.*, and Woo *et al.*, as well as the present study, which can imply much lower product yields, and more specifically, lower liquid hydrocarbon yields. In contrast to Zheng *et al.*, therefore, the results of these four other studies indicate that operation at low reactor pressures may not be industrially viable as the trade off in lower CO conversions and liquid hydrocarbon product yields has to be carefully weighed against the potential cost savings resulting from process operation at lower pressures (which is discussed later in section 5.4).

Similar results for CO conversion are obtained at 8 bar and 10 bar in the present study, as shown in Figure 5.13 above. As lower CO conversions are expected with decreasing reactor pressure (section 2.5.1), the run at 8 bar was repeated in order to verify this outcome. This repeated run confirmed the initial findings at 8 bar, as similar values for CO conversion were obtained. Furthermore, the results of the repeated run suggest that the run at 10 bar also requires repetition, but this is not possible due to the limitation related to the availability of the Co/Al₂O₃ catalyst in this project (discussed previously in section 3.1.1). However, repetition of the run at 10 bar is a recommendation for future work in order to clarify the influence of reactor pressure on CO conversion at reactor pressures above 8 bar. Without repetition of the run at 10 bar, however, the results of the present study (Figure 5.13 above) signify that reactor pressure does not have a significant effect on CO conversion above 8 bar in the range studied. These results also show that significantly lower CO conversions are achieved below 8 bar, with very poor CO conversions observed at the lowest reactor pressure studied of 2 bar. This indicates that under the reaction conditions implemented in the 20cm³ reactor in the present study using the Co/Al₂O₃ catalyst, operation at higher reactor pressures in the range investigated of 2-10 bar is preferred as higher CO conversions are achieved, whereas operation at the lowest reactor pressure implemented of 2 bar is not recommended.

5.3.2.2 CO₂ Selectivity

The results obtained for the effect of reactor pressure on CO₂ selectivity (at 230°C, H₂/CO = 2.0, WHSV = 8.8 h⁻¹, and m_{cat} = 0.5g) are presented in Figure 5.14 below. From the studies investigating the influence of reaction conditions on FT product distribution (reviewed previously in section 2.6.2 and summarized in Table 2.4), only a few report on the effect of reactor pressure on CO₂ selectivity. The results of these studies are also presented in Figure 5.14 below, for comparison.

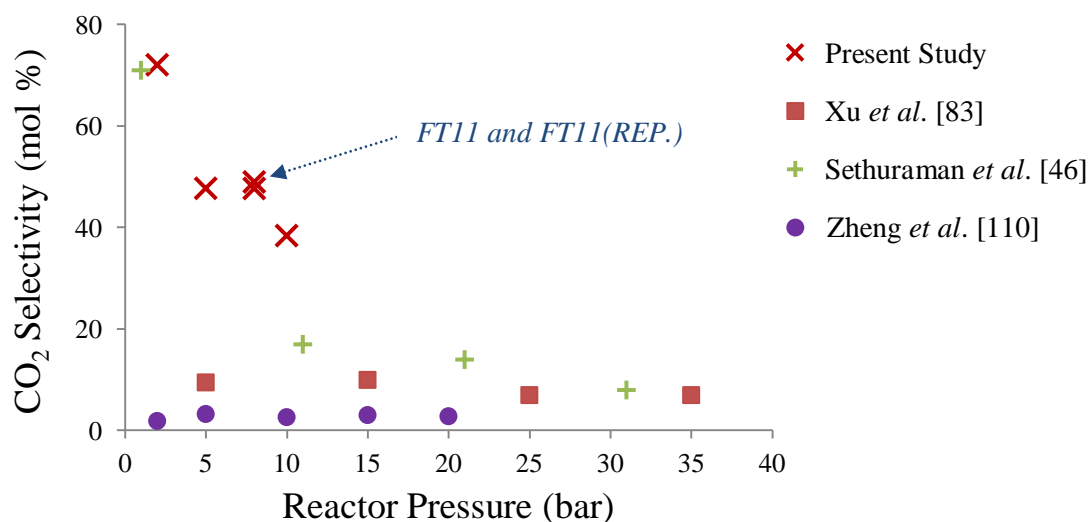


Figure 5.14 – Influence of reactor pressure on CO₂ selectivity in the present study (at 230°C, H₂/CO = 2.0, WHSV = 8.8 h⁻¹, and m_{cat} = 0.5g) in comparison to similar studies by Xu *et al.* [83], Sethuraman *et al.* [46], and Zheng *et al.* [110]. (Arrow represents results of experiments repeated at 8 bar)

The results from the present study show that CO₂ selectivity decreases with increasing reactor pressure. This trend is comparable to that reported by Sethuraman *et al.* [46] who used a different catalyst (Co-Ni/ZrO₂) and a higher space velocity (WHSV = 15 h⁻¹) than the one used in the present study (WHSV = 8.8 h⁻¹), suggesting that at higher values the space velocity has a much more significant influence on CO₂ selectivity. As shown in Figure 5.14 above, different trends were obtained by Xu *et al.* [83] and Zheng *et al.* [110], who reported that CO₂ selectivity is not significantly influenced by variation in reactor pressure. Considerably lower space velocities were implemented in these two studies, however, in comparison to the study by Sethuraman *et al.* and the present study. These lower space velocities used imply higher reactor residence times, and therefore, higher CO conversions, as well as lower CO₂ selectivities as hydrocarbon production is more favoured (section 2.5.3). The higher range of space velocities used in the present study in comparison to other studies that have investigated the influence of reaction conditions and, more specifically, the influence of space velocity on FT product distribution and CO conversion are discussed in section 5.3.3. The results of Sethuraman *et al.* and the present study suggest that reactor pressure has a significant effect on CO₂ selectivity only at lower reactor pressures (≤ 11 bar). Hence, under the reaction conditions used with the Co/Al₂O₃ catalyst in the 20cm³ reactor in the present study, operation at 10 bar is preferred as low CO₂ selectivities are desirable. As discussed previously in section 5.2.1, lower CO₂ selectivities imply lower inert gas dilution in the products and, therefore, a lower requirement for FT reactor off-gas conditioning and recycling, as well as higher yields of once-through liquid hydrocarbon products.

5.3.2.3 CH₄ and C₂-C₅ Selectivity

The results obtained for the effect of reactor pressure on CH₄ and C₂-C₅ hydrocarbon selectivities (at 230°C, H₂/CO = 2.0, WHSV = 8.8 h⁻¹, and m_{cat} = 0.5g) are presented in Figure 5.15 and Figure

5.16 below, respectively. The results from similar studies using cobalt-based catalysts (reviewed previously in section 2.6.2 and summarized in Table 2.4) that have investigated the influence of reactor pressure on CH₄ and C₂-C₅ selectivities are also presented in these figures for comparison. These include studies by Xu *et al.* [83] (using a Pt/ZrO₂ modified Co/Al₂O₃ catalyst), Woo *et al.* [115] (using a 20%Co/Al₂O₃ catalyst, as opposed to the 10%Co/Al₂O₃ catalyst used in the present study) and Zheng *et al.* [110] (using a Co/SiO₂ catalyst), all working at much lower space velocities than the one implemented in the present study.

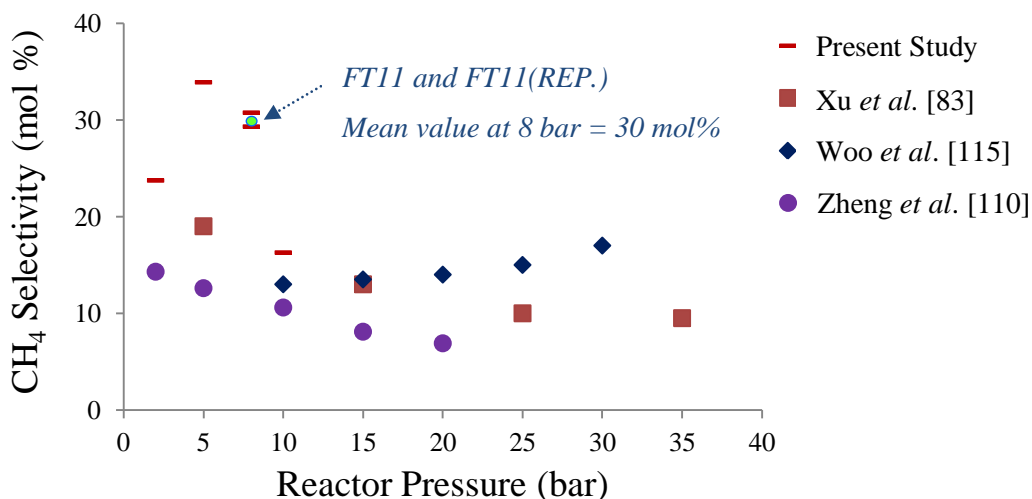


Figure 5.15 – Influence of reactor pressure on CH₄ selectivity in the present study (at 230°C, H₂/CO = 2.0, WHSV = 8.8 h⁻¹, and mcat = 0.5g) in comparison to similar studies by Xu *et al.* [83], Woo *et al.* [115], and Zheng *et al.* [110]. (Arrow represents results of experiments repeated at 8 bar)

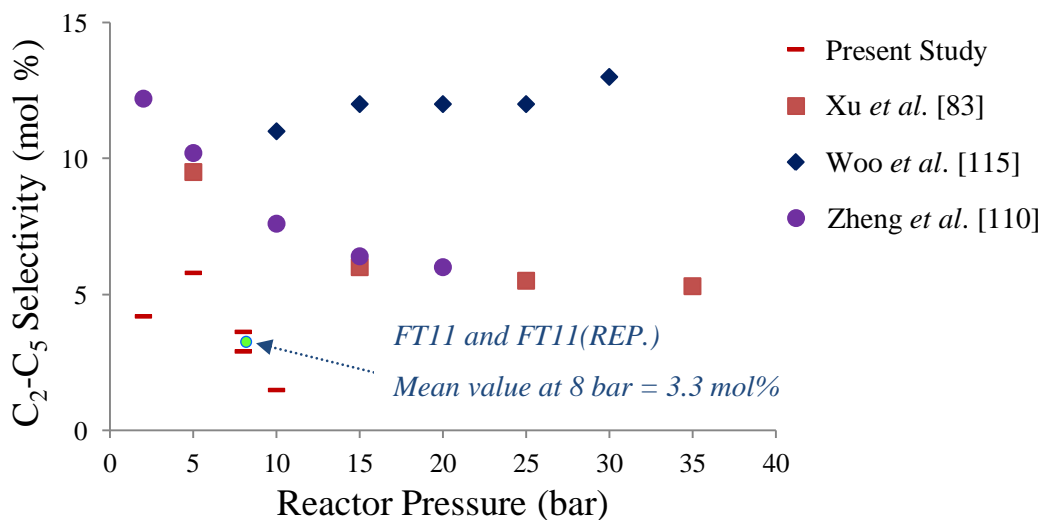


Figure 5.16 – Influence of reactor pressure on C₂-C₅ selectivity in the present study (at 230°C, H₂/CO = 2.0, WHSV = 8.8 h⁻¹, and mcat = 0.5g) in comparison to similar studies by Xu *et al.* [83], Woo *et al.* [115], and Zheng *et al.* [110]. (Arrow represents results of experiments repeated at 8 bar)

As shown in Figure 5.15 and Figure 5.16 above, the trends for CH₄ and C₂-C₅ hydrocarbon selectivities found in the present study are very different to those reported by Xu *et al.*, Woo *et al.*,

and Zheng *et al.* The trends reported by Woo *et al.* (at reactor pressures above 10 bar) contradict the other trends presented in Figure 5.15 and Figure 5.16 above, showing that both CH₄ and C₂-C₅ hydrocarbon selectivities increase with increasing reactor pressure. A possible explanation for this difference between the studies may be because of the higher cobalt metal loading in the catalyst used by Woo *et al.* This corresponds to an increased number of active sites on the catalyst surface, which has been found to favour the formation of low molecular weight hydrocarbon products and, equally, decrease the production of heavier hydrocarbon molecules [170].

Although both Xu *et al.* and Zheng *et al.* also report that CH₄ and C₂-C₅ hydrocarbon selectivities decrease with increasing reactor pressure, much sharper declines in both product selectivities are observed in the present study as the reactor pressure is increased above 5 bar. In addition, higher figures for CH₄ selectivity and lower figures for C₂-C₅ hydrocarbons selectivity are observed in the present study in comparison to the other studies shown in Figure 5.15 and Figure 5.16 above, respectively. These differences may be due to the much higher space velocity that is implemented in the present study in comparison to the other studies. These higher values for space velocity would contribute to shorter residence times and lower reactant conversions, as well as lower chain growth probability and, therefore, increased formation of low molecular weight hydrocarbon products. In the present study, this can be seen in the higher CH₄ selectivities reported. In contrast, the lower C₂-C₅ hydrocarbon product selectivities suggest, once again, that under the reaction conditions implemented in the 20cm³ reactor in the present study, the Co/Al₂O₃ catalyst used is not particularly selective towards the formation of these light hydrocarbon products.

The declining trends in both product selectivities reported by Xu *et al.*, Zheng *et al.* and in the present study are expected due to the contraction in volume that occurs with increasing pressure, which has been found to increase the concentration and dissociation of CO molecules on the catalyst surface and promote chain growth [43, 97]. Hence, as the reactor pressure decreases, both CH₄ and C₂-C₅ selectivities are expected to increase. However, the opposite trends are observed below 5 bar in the present study. These may be explained by the very low catalyst activity that was observed at the low reactor pressure of 2 bar (as discussed in section 5.3.2.1 above), resulting in the limited formation of CH₄ and other hydrocarbon products. Figure 5.15 and Figure 5.16 also show the mean values for CH₄ selectivity and C₂-C₅ selectivity, respectively, for the experiment that was repeated at 8 bar (experiments FT11 and FT11 REP. in Table 5.1 in section 5.1.6). Despite the fact that no other experiments were repeated, these results serve in demonstrating the repeatability of the FT synthesis runs as very small deviation is observed. Overall, the results of the present study indicate that under the reaction conditions implemented in the 20cm³ reactor using the Co/Al₂O₃ catalyst, operation at 10 bar is preferred. This is because lower CH₄ and C₂-C₅ selectivities generally imply higher liquid hydrocarbon yields, and therefore, a lower requirement for FT reactor off-gas reforming and recycling (as discussed previously in section 5.2.1).

5.3.2.4 C₆₊ Selectivity

The results obtained for the effect of reactor pressure on C₆₊ hydrocarbon selectivity (at 230°C, H₂/CO = 2.0, WHSV = 8.8 h⁻¹, and m_{cat} = 0.5g) are presented in Figure 5.17 below. The results from similar studies using cobalt-based catalysts (reviewed previously in section 2.6.2 and summarized in Table 2.4) that have investigated the influence of reactor pressure on the selectivity of C₆₊ hydrocarbons are also presented in Figure 5.17 for comparison.

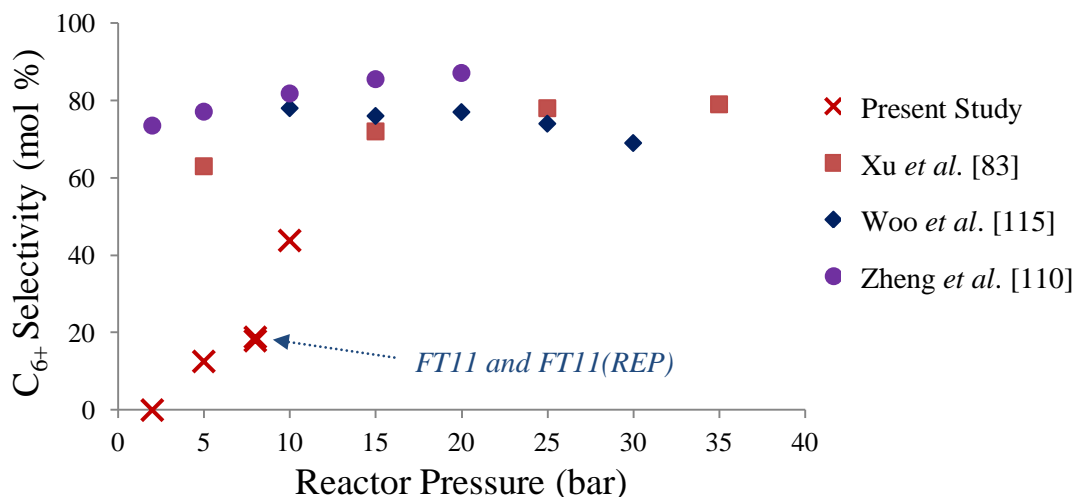


Figure 5.17 – Influence of reactor pressure on C₆₊ selectivity in the present study (at 230°C, H₂/CO = 2.0, WHSV = 8.8 h⁻¹, and m_{cat} = 0.5g) in comparison to similar studies by Xu et al. [83], Woo et al. [115], and Zheng et al. [110]. (Arrow represents results of experiments repeated at 8 bar)

As shown in Figure 5.17 above, an increase in reactor pressure from 2 to 10 bar in the present study results in higher C₆₊ hydrocarbon product selectivities. A negligible C₆₊ hydrocarbon selectivity is observed at 2 bar, but as previously discussed in section 5.3.2.1, under the reaction conditions implemented in the 20cm³ reactor in the present study, the Co/Al₂O₃ catalyst displayed a very low activity at this reactor pressure, making operation at 2 bar unsuitable in this reactor system. Increasing C₆₊ hydrocarbon selectivities with increasing reactor pressure are also reported by Xu *et al.* [83] and Zheng *et al.* [110], although significantly higher figures were reported in both studies. However, considerably lower space velocities were implemented in these studies in comparison to the present study, contributing to longer residence times, higher reactant conversions, as well as higher chain growth probabilities leading to the increased formation of higher molecular weight hydrocarbon products (section 2.5.3). Once again, the higher range of space velocities used in the present study in comparison to other studies that have investigated the influence reaction conditions and, more specifically, the influence of space velocity on FT product distribution and CO conversion are discussed in section 5.3.3.

Higher figures for C₆₊ hydrocarbon selectivity than those found in the present study were also reported by Woo *et al.* However, the trend reported by Woo *et al.* contradicts the other trends presented in Figure 5.17 above, showing that C₆₊ hydrocarbon selectivity decreases with increasing

reactor pressure. As discussed in section 5.3.2.3 above, a possible reason for this difference may be because of the higher cobalt metal loading in the catalyst used by Woo *et al.* This corresponds to an increased number of active sites on the catalyst surface resulting in the increased formation of low molecular weight hydrocarbon products, as opposed to an increase in the formation of higher molecular weight hydrocarbon products.

Despite the differences in the trends reported by Xu *et al.*, Zheng *et al.* and Woo *et al.*, their results suggest that the reactor pressure does not have a significant influence on the C₆₊ hydrocarbon product selectivity above 10 bar. As the present study only investigated the influence of reactor pressure up to 10 bar, further investigation is necessary in order to determine the influence of higher reactor pressures (10-20 bar) on product distribution, and is therefore recommended for future work. The significantly higher figures for C₆₊ hydrocarbon selectivity reported by Xu *et al.*, Zheng *et al.*, and Woo *et al.* appear to advocate operation at low FT reactor pressures, as high C₆₊ hydrocarbon selectivities can also imply high liquid hydrocarbon product yields and could potentially, therefore, be feasible for application in BTL-FT operations. However, as discussed previously in section 2.3, product selectivity represents the molar composition of the products formed rather than their actual yield. Thus product yield results would be more useful, however, these three studies fail to report on the yields of liquid hydrocarbons obtained. The liquid hydrocarbon product yields obtained in the present study, though, are discussed in section 5.3.2.5 below.

5.3.2.5 Product Yields

The product yields are calculated as described previously in section 3.7.4.2. The unreacted syngas is calculated by difference. The product yields obtained in this parameter test set (Table 5.1 in section 5.1.6) reflect the trends observed in sections 5.3.2.2 to 5.3.2.4 above, for product selectivity with increasing reactor pressure. These results are presented in Table 5.5 below. As discussed previously in section 5.2.2, product yields are very rarely reported in FT synthesis research publications, and no research studies (investigating the influence of reaction conditions on the product distribution using cobalt-based catalysts) that provide data on FT product yields have been found for comparison to the yields found in the present study.

**Table 5.5 – Influence of reactor pressure on FT gas and liquid product yields
(at 230°C, H₂/CO = 2.0, WHSV = 8.8 h⁻¹, and m_{cat} = 0.5g)**

Test	P (bar)	Product Yields (wt.%)					Oxyg. In Water (wt.%)	Unreacted Syngas (wt.%)
		CO ₂	CH ₄	C ₂ -C ₅	Liquid H/C's + Waxes	Water + Oxyg.		
FT9	2	16.5	0.2	0.1	0.0	0.0	0.0	83.2
FT10	5	9.3	0.8	0.5	1.1	2.9	9.4	85.2
FT11	8	9.3	2.2	0.8	2.2	3.9	7.4	81.6
FT11 (REP.)	8	8.9	2.9	2.0	2.6	4.3	8.1	79.3
FT7	10	7.5	1.2	0.3	2.2	3.6	3.7	85.3

As shown in Table 5.5 above, at a reactor pressure of 2 bar no liquid products are obtained and mainly CO₂ is formed. Once again, this indicates that under the particular reaction conditions used with the Co/Al₂O₃ catalyst a reactor pressure of 2 bar is not recommended for operation on the 20cm³ reactor in the present study. Further evidence supporting this assumption can be gathered from the catalyst stability at this reactor pressure, which is discussed later in section 5.3.2.7.

The yield of CO₂ decreases with increasing reactor pressure, although the yields are similar at 5 and 8 bar. This indicates that operation above 8 bar is more favourable as a reduction in the inert gas content of the product is achieved. The yields of both CH₄ and C₂-C₅ hydrocarbon products increase as the reactor pressure is increased, reaching a maximum at 8 bar and thereafter decreasing as the reactor pressure is raised further to 10 bar. As discussed previously in section 2.5.2, the formation of lower molecular weight hydrocarbon products, such as CH₄ and C₂-C₅ hydrocarbons, is expected to decrease as the reactor pressure is increased. The opposite trend, however, is observed below 8 bar in the results presented in Table 5.5 above, suggesting that at lower values the reactor pressure has a significant influence on these specific product yields.

A similar trend to those of CH₄ and C₂-C₅ hydrocarbons is observed for the yield of water, indicating that the WGS reaction (Equation 2.2 section 2.2), through which water is produced, is significantly influenced by variation in reactor pressure in the range of 2-10 bar. The soluble oxygenate concentration in the aqueous product decreases as the reactor pressure increases. This is expected as chain growth probability increases with increasing reactor pressure, therefore reducing the formation of soluble oxygenated compounds, which tend to have short carbon chains (as discussed previously in section 2.2). The liquid hydrocarbon (C₆₊) yield also increases as the reactor pressure is increased up to 8 bar, however, similar yields are obtained at 8 and 10 bar. This suggests that under the reaction conditions used in the 20cm³ reactor in the present study with the Co/Al₂O₃ catalyst, reactor pressure does not have a significant effect on liquid hydrocarbon yields above 8 bar in the range studied. Further investigation is required in order to determine the reasons for all the observations made above, including repetition of the run at 10 bar (FT7 in Table 5.1 in

section 5.1.6), as well as additional FT runs at higher reactor pressures (10-20 bar) as previously discussed in section 5.3.2.4 above, and are therefore recommended for future work.

Figure 5.18 below, illustrates the influence of reactor pressure on the ratio of liquid products to gas products (excluding unreacted syngas). As shown in this figure, the highest ratios of total liquid products to gas products (0.64) and liquid hydrocarbons to gas products (0.24) are obtained at 10 bar, making operation at this pressure more favourable than lower values in the range of 2-10 bar. This is because these higher ratios imply a higher proportion of liquids in the product and, conversely, a lower requirement for FT reactor off-gas reforming and recycling, as discussed previously in section 5.2.2.

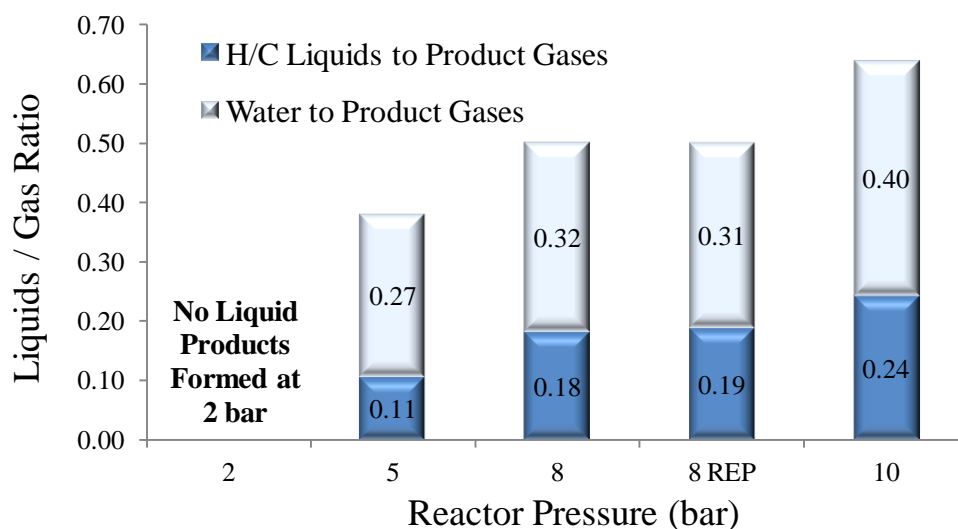


Figure 5.18 – Influence of reactor pressure on the ratio of liquid products to product gases (at 230°C, H₂/CO = 2.0, WHSV = 8.8 h⁻¹, and m_{cat} = 0.5g)

5.3.2.6 Energy Content and Composition of Liquid Hydrocarbon Products

A representative photograph of the liquid products, consisting of a liquid hydrocarbon phase (plus waxes) and a water phase (containing soluble oxygenated compounds), collected from the pressure profile tests (tests FT7-FT11 listed in Table 5.1 in section 5.1.6) was provided in Figure 5.7 in section 5.3.1.6. The product analysis methods were described in sections 3.5.3.1 and 3.7.4.2. The calorific values of the liquid hydrocarbon samples collected from these experiment runs are calculated using the method outlined previously in section 3.5.3.3, and are given in Table 5.6 below. Although very slight differences in calorific value are observed with increasing reactor pressure, these results show that the energy content of the liquid hydrocarbons is not significantly influenced by variation in reactor pressure.

Table 5.6 – Influence of reactor pressure on the energy content of liquid hydrocarbon products (at 230°C, H₂/CO = 2.0, WHSV = 8.8 h⁻¹, and m_{cat} = 0.5g)

Test	P (bar)	Content (%)				HHV (MJ/kg)
		C	H	N	O	
FT9	2	-	-	-	-	-
FT10	5	84.31	15.15	0.10	0.44	47.23
FT11	8	84.22	15.41	0.10	0.27	47.52
FT11 (REP.)	8	84.23	15.39	0.10	0.28	47.51
FT7	10	84.21	15.20	0.10	0.49	47.26

Figure 5.19, Figure 5.20 and Figure 5.21 below, show the GC-MS chromatograms obtained from the analysis of the liquid hydrocarbons obtained from the three different reactor pressures investigated (5, 8 and 10 bar) in tests FT10, FT11 and FT7, respectively. No chromatograms are shown for operation at 2 bar, as no liquid hydrocarbons were produced at this reactor pressure.

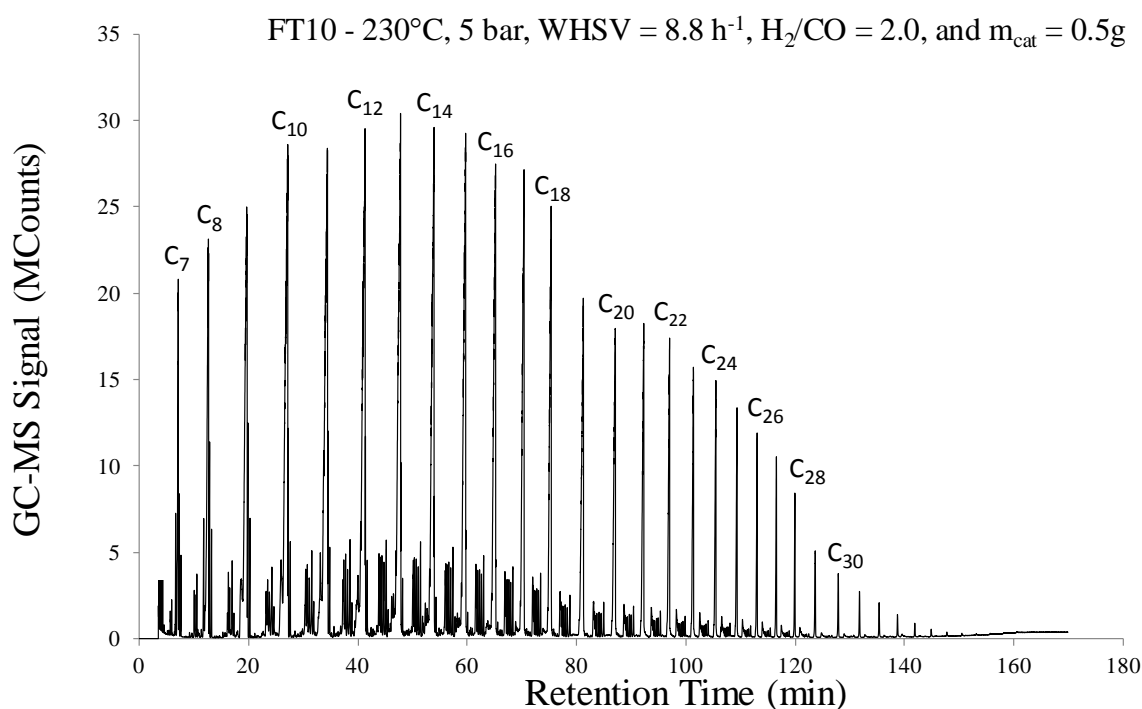


Figure 5.19 – GC-MS chromatogram of liquid hydrocarbons collected from pressure profile test FT10 at 5 bar

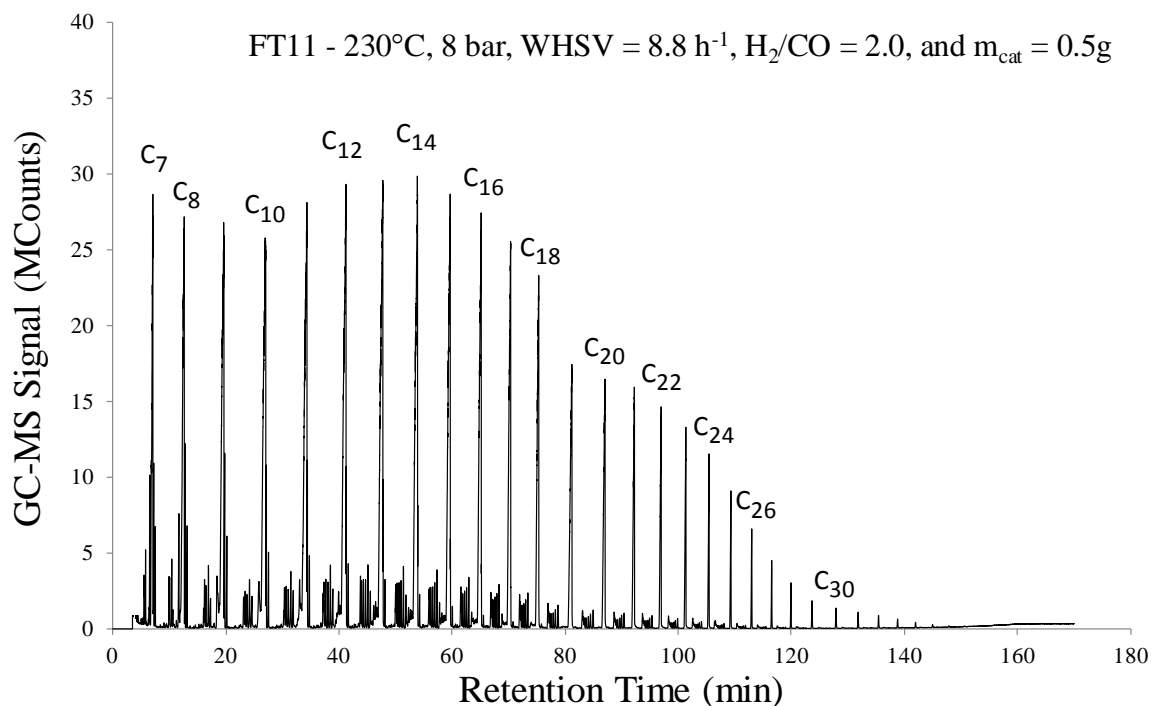


Figure 5.20 – GC-MS chromatogram of liquid hydrocarbons collected from pressure profile test FT11 at 8 bar

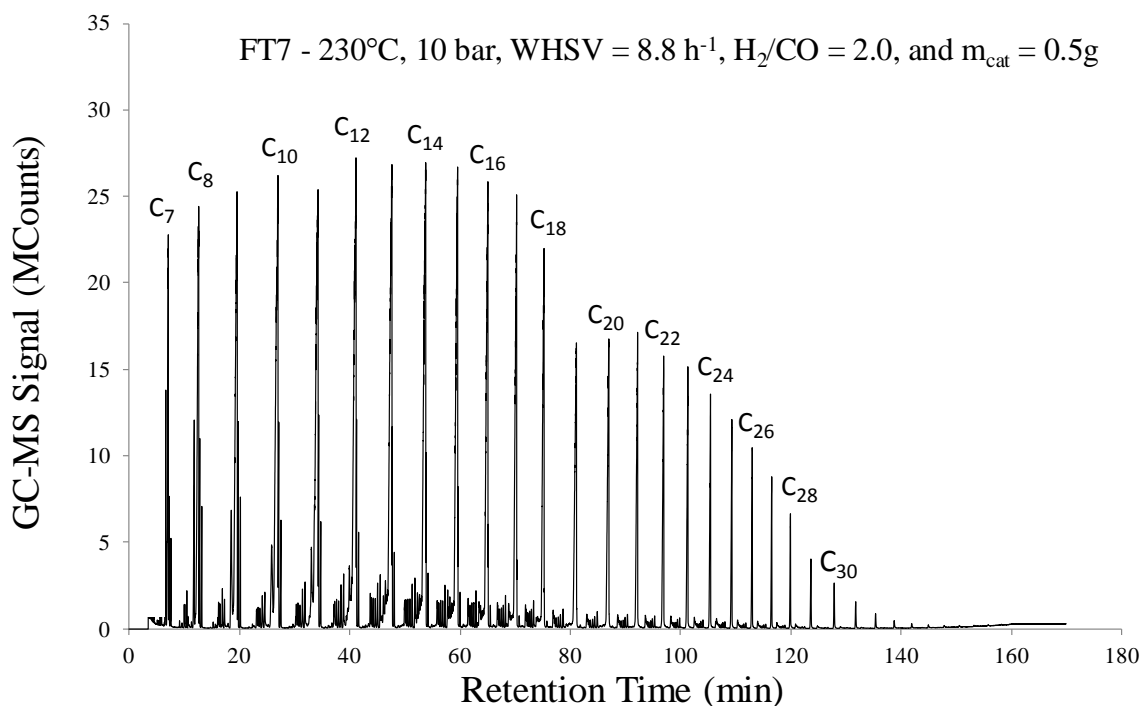


Figure 5.21 – GC-MS chromatogram of liquid hydrocarbons collected from pressure profile test FT7 at 10 bar

The relative fuel compositions of the liquid hydrocarbons collected are calculated from the chromatograms above, using the method outlined in section 3.5.3. The results are illustrated in Figure 5.22 below.

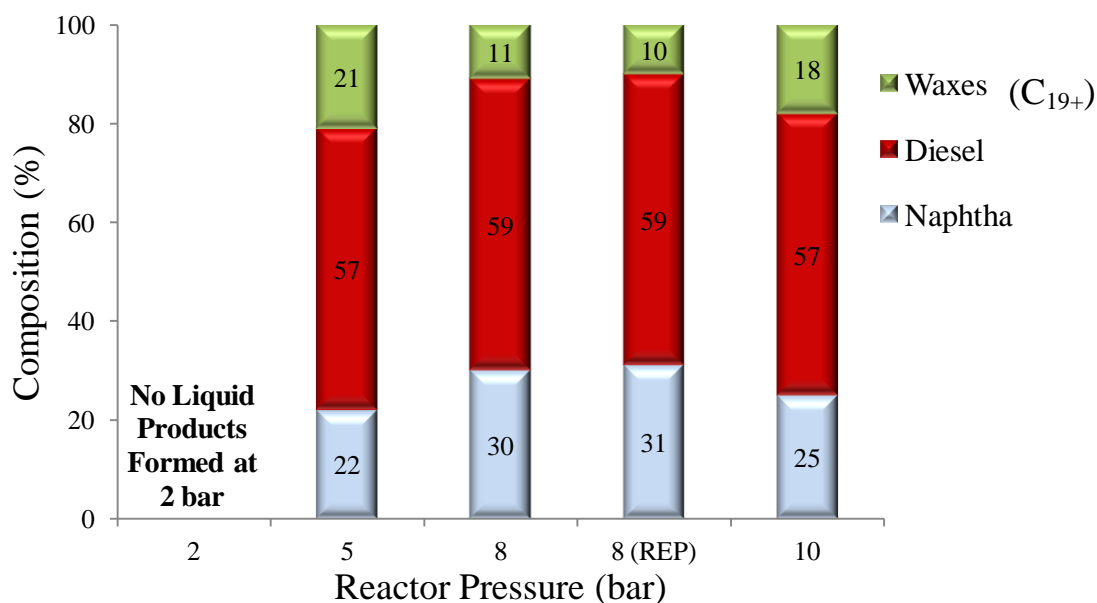


Figure 5.22 – Influence of reactor pressure on liquid hydrocarbon product composition (at 230°C, H₂/CO = 2.0, WHSV = 8.8 h⁻¹, and m_{cat} = 0.5g)

These results show that the most favourable diesel composition is obtained at 8 bar; however, this is at the expense of an increased naphtha and reduced wax content. This difference is also visibly evident in the immiscible oil phases collected at the end of the runs at 8 bar; those at 5 and 10 bar have a yellow tint due to the suspension of small amounts of tiny wax particles (Figure 5.7 in section 5.3.1.6), whereas the oil phases collected at 8 bar are more transparent as they do not appear to contain suspended solid waxes. As discussed previously in section 5.2.3, higher wax contents are preferred to higher naphtha contents in the liquid product, as waxes can be hydro-processed to maximize diesel yields, whereas the naphtha fraction (low-grade gasoline) requires significant processing in order to be upgraded to gasoline, which adds process costs and complexity [138]. From this perspective, therefore, the hydrocarbon liquids obtained at 5 bar have the most favourable diesel composition. However, as previously shown in Table 5.5, the yield of liquid hydrocarbons obtained at 5 bar is significantly lower than the yields obtained at higher reactor pressures. Hence, it can be determined that the liquid hydrocarbons obtained at 10 bar have the preferred fuel composition.

5.3.2.7 Catalyst Stability

The stability of the catalyst, in terms of CO conversion versus time on stream, over the duration of the synthesis experiments (FT9, FT10, FT11, FT11 REP and FT7 in Table 5.1 in section 5.1.6) using different reactor pressures is compared in Figure 5.23 below. As illustrated in this figure, the activity of the catalyst is similar at reactor pressures of 8 and 10 bar. As discussed earlier in section 5.3.2.1, experiment FT11 (Table 5.1 in section 5.1.6) was repeated for verification of the catalyst activity at 8 bar and the results, displayed in Figure 5.23 below, do show a very similar trend in activity. Once again, this demonstrates the reproducibility of the FT synthesis runs as previously discussed in section 5.3.2.3.

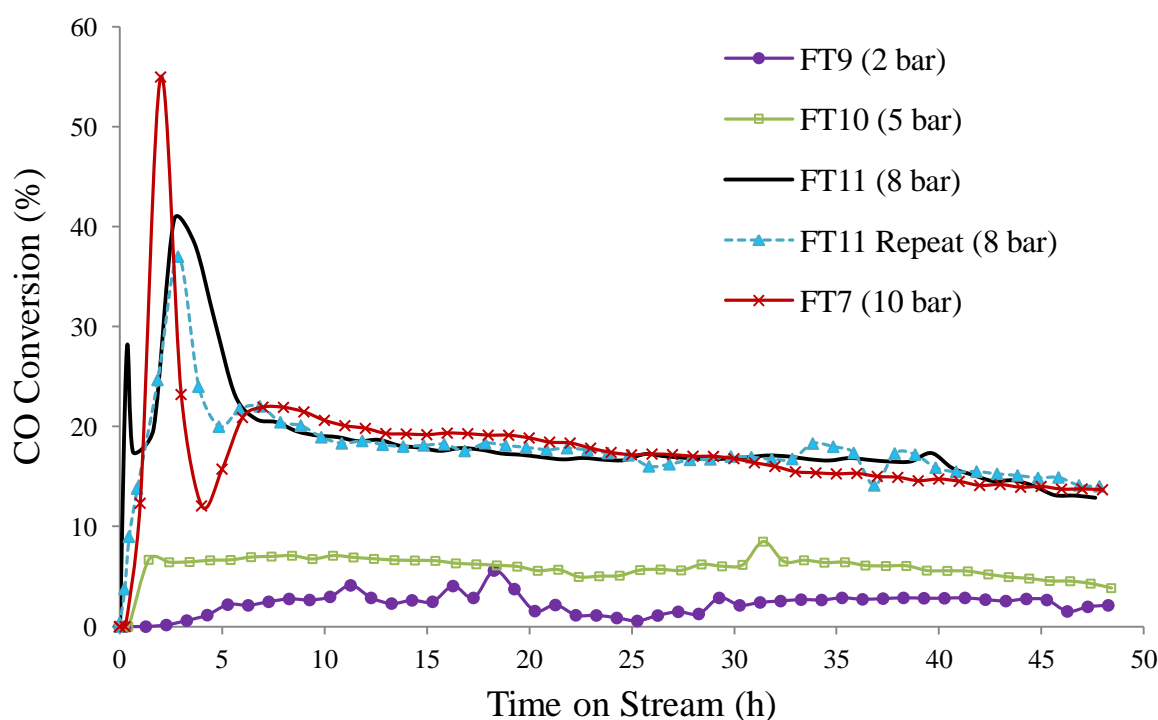


Figure 5.23 – Influence of reactor pressure on catalyst stability: CO conversion versus time on stream (at 230°C, H₂/CO = 2.0, WHSV = 8.8 h⁻¹, and m_{cat} = 0.5g)

The initial ‘spikes’ in CO conversion observed at 8 and 10 bar are due to the very exothermic nature of the FT reaction as previously explained in section 5.3.1.7. These are not observed during operation at the lower reactor pressures of 2 and 5 bar, suggesting that the reaction rates are much lower at these reduced reactor pressures. This is particularly true for operation at 2 bar, as at this reactor pressure the catalyst displays a much slower initiation of activity, followed by low and inconsistent CO conversion with time on stream. Again, this shows that under the conditions used (Table 5.1 in section 5.1.6), 2 bar is an inadequate reactor pressure for achieving favourable activity using the Co/Al₂O₃ catalyst in the 20cm³ reactor in the present study. At 5 bar, the catalyst activity is higher and more consistent (though gradually declining with time on stream) than at 2 bar, signifying that steady-state is reached and that this higher reactor pressure is slightly more favourable for the synthesis reaction. As shown in the figure above, similar catalytic activities are achieved for operation at both 8 and 10 bar, where the initial ‘spikes’ in CO conversion, are followed by steady activity as the reactions progress. Overall, this implies that under the reaction conditions used (Figure 5.23 above), and in the pressure range of 2-10 bar, the activity of the Co/Al₂O₃ catalyst is not significantly influenced above 8 bar.

The visible decline in catalyst activity that is observed with time on stream in the experiment runs is due to gradual deactivation caused by the carbon and/or wax deposition mechanisms that were discussed previously in section 5.3.1.7. The influence of reactor pressure on the extent of these deactivation mechanisms is examined by TGA analysis, as previously outlined in section 3.6.4. The mass loss results obtained from these analyses are presented in Table 5.7 below.

Table 5.7 – Influence of reactor pressure on the extent of carbon and wax deposition on the catalyst surface (TGA results)

Catalyst Sample Origin	Reactor Pressure (bar)	Total Mass Loss (wt.% dry basis)	Mass Loss Due to Carbon & Wax Deposition (wt.%)
Co/Al ₂ O ₃ before Reaction	-	4.7	-
Test FT9	2	5.1	0.4
Test FT10	5	16.6	11.9
Test FT11	8	45.9	41.2
Test FT7	10	40.3	35.6

These results show that the extent of carbon and wax deposition is proportional to increasing reactor pressure up to 8 bar. As the reactor pressure is further increased to 10 bar, less carbon and wax are deposited on the catalyst surface by the end of the run. This suggests that operation at pressures above 8 bar, in the range of 2-10 bar, inhibits carbon and wax deposition to a greater extent in comparison to operation at lower pressures. Despite the similar catalytic activities observed at 8 and 10 bar, the higher deactivation rate observed at 8 bar is supported by the evidence from the TGA results given in Table 5.7 above. Hence, operation at 10 bar is preferred as slower catalyst deactivation is observed. SEM micrographs (at x764 magnification) of the Co/Al₂O₃ catalyst before and after reaction in runs FT7, FT9, FT10, and FT11 (Table 5.1 in section 5.1.6) are provided in APPENDIX B. Small differences can be seen in these micrographs, however, the magnification strength used was not sufficient in order to allow for definite conclusions to be drawn. Higher magnification strengths are therefore recommended for future investigation.

5.3.2.8 Reactor Pressure Selection for Further Experiments

Under the reaction conditions used (Table 5.1 in section 5.1.6) in the 20cm³ reactor using the Co/Al₂O₃ catalyst in the present study, operation at 2 bar results in very low CO conversion, producing mainly CO₂ and no liquid hydrocarbons. Hence, only the higher reactor pressures of 5, 8 and 10 bar are considered for final selection of the preferred operating value. The results show that CO conversion increases with increasing reactor pressure up to 8 bar. A further increase in reactor pressure, however, does not appear to influence CO conversion but has a significant effect on C₆₊ hydrocarbon product selectivity, where a maximum value for C₆₊ selectivity is observed at 10 bar. Minimum values for the selectivities of CO₂, CH₄ and light hydrocarbons (C₂-C₅) are also obtained at 10 bar. The catalyst displays similar activity with time on stream at both 8 and 10 bar, however, catalyst deactivation is more evident at 8 bar, and this is verified by TGA analysis, where the recorded mass loss due to carbon and wax deposition on the catalyst surface is higher than at 10 bar.

The calorific values of the liquid hydrocarbons collected at 5, 8 and 10 bar are comparable, indicating that reactor pressure does not have a significant influence on the energy content of the liquid hydrocarbons obtained. Similar yields of liquid hydrocarbons and water are collected at both 8 and 10 bar, indicating that increasing the reactor pressure above 8 bar does not influence liquid hydrocarbon formation. However, higher ratios of both total liquids to product gases and hydrocarbon liquids to product gases are obtained at 10 bar. GC-MS analyses of the liquid hydrocarbons showed that the most favourable fuel composition, containing the highest proportion of diesel (and, conversely, the lowest naphtha content) is obtained at 5 bar, followed by that at 10 bar. Since higher liquid hydrocarbon yields are obtained at 10 bar, however, this value is selected as the preferred reactor pressure to be used for operation on the 20cm³ fixed-bed reactor in the present study, and in the remaining parameter profiling test sets.

5.3.3 Influence of Space Velocity

Sections 5.3.1 and 5.3.2 resulted in identification of the preferred reactor temperature and reactor pressure for subsequent tests.

5.3.3.1 CO Conversion

The results obtained in the present study for the effect of space velocity on CO conversion (at 230°C, 10 bar, H₂/CO = 2.0, and m_{cat} = 0.5g) are compared to the results of similar studies using cobalt-based catalysts (reviewed previously in section 2.6.2 and summarized in Table 2.4) that have investigated the influence of space velocity on CO conversion in Figure 5.24 below. These include studies by Rafiq *et al.* [116], de la Osa *et al.* [89], and Woo *et al.* [115] (all working with Co/Al₂O₃ catalysts at higher reactor pressures than in the present study ≥ 20 bar), as well as Mohanty *et al.* [91] (also working at higher reactor pressures but with a CuO-CoO/Cr₂O₃ catalyst combined with MFI Zeolite). These studies report on space velocity in terms of GHSV (usually expressed in Lg_{cat}⁻¹h⁻¹) whereas in the present study, the space velocity is calculated in terms of WHSV (as discussed previously in section 2.5.3). Hence, the WHSV values calculated in the present study are converted into GHSV for ease of comparison. As discussed previously in section 2.6, studies using cobalt-based catalysts that have specifically addressed the influence of low reactor pressures (< 20 bar) on FT product distribution and catalyst activity are very limited. However, no studies have been found that investigate the influence of space velocity at these lower reactor pressures. Therefore, although different reaction conditions were implemented in these other studies, including higher reactor pressures than those used in the present study, as well as catalysts of different composition, these are the only studies that have been found for comparison of results.

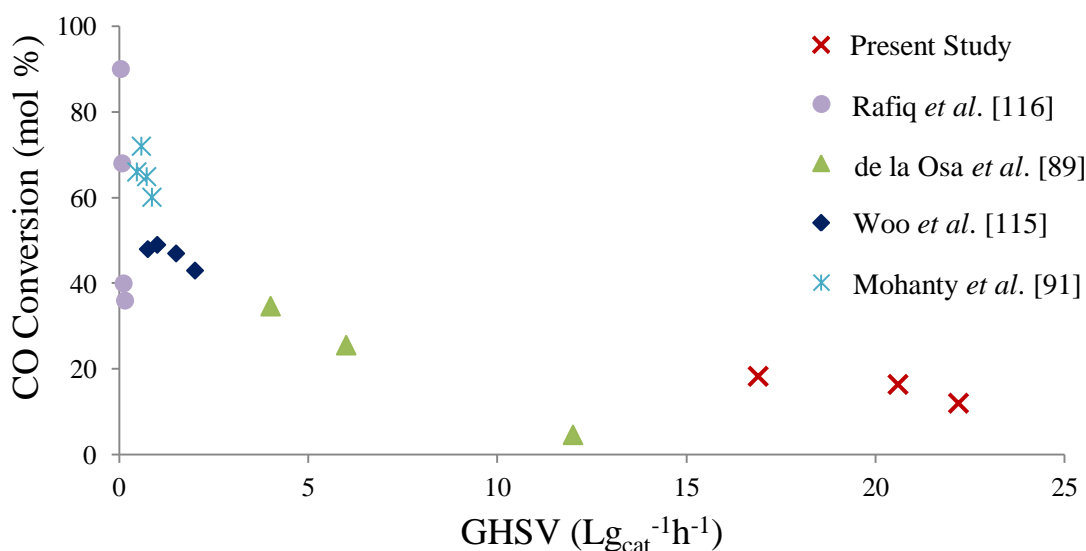


Figure 5.24 – Influence of space velocity on CO conversion in the present study (at 230°C, 10 bar, H₂/CO = 2.0, and m_{cat} = 0.5g) in comparison to similar studies by Rafiq *et al.* [116], de la Osa *et al.* [89], Woo *et al.* [115], and Mohanty *et al.* [91]

In all the studies reported above CO conversion decreases with increasing space velocity. This is expected as higher space velocities correspond to shorter reactor residence times, implying reduced reactant adsorption on the catalyst surface and, therefore, lower reactant conversions. As shown in Figure 5.24 above, the space velocities that are investigated in the present study are significantly higher than those investigated by Rafiq *et al.*, de la Osa *et al.*, Woo *et al.* and Mohanty *et al.*, (as well as other studies using cobalt-based catalysts that were reviewed previously in section 2.6.2). This is due to the limitations of the 20cm³ reactor system at Aston relating to the minimum possible space velocity (explained previously in section 3.4.3), resulting in the lower CO conversions that are reported in the present study in comparison to the other studies presented in Figure 5.24 above. These observations further support the argument that higher CO conversions could have been achieved if this equipment limitation did not exist. Interestingly, at the lower range of space velocities investigated by Woo *et al.* and Mohanty *et al.*, they report that CO conversion reaches a maximum and thereafter declines as the space velocity increases, suggesting that there is a threshold value of space velocity for optimum CO conversion. Based on achieving maximum CO conversion, the results from the present study indicate that under the reaction conditions implemented, operation on the 20cm³ reactor with the Co/Al₂O₃ catalyst at a GHSV of 16.9 h⁻¹ (or WHSV of 8.8 h⁻¹) is preferred.

5.3.3.2 CO₂ Selectivity

The results obtained for the effect of space velocity on CO₂ selectivity (at 230°C, 10 bar, H₂/CO = 2.0, and m_{cat} = 0.5g) are presented in Figure 5.25 below. From the studies investigating the influence of reaction conditions on FT product distribution using cobalt-based catalysts that were reviewed in section 2.6.2 (and summarized in Table 2.4), only a few report on the effect of space velocity on CO₂ selectivity. Studies by Rafiq *et al.* [116] and de la Osa *et al.* [89], both working at

much a lower range of space velocities than the range used in the present study (but at a higher reactor pressure of 20 bar), found that CO₂ selectivity is negligible. However, in a study by Sethuraman *et al.* [46], working at a wider and higher range of space velocities than that in the present study (but using a Co-Ni/ZrO₂ catalyst at a lower reactor pressure of one bar), CO₂ selectivity is reported to increase as the space velocity is increased. The results from this study by Sethuraman *et al.* are also presented in Figure 5.25 below.

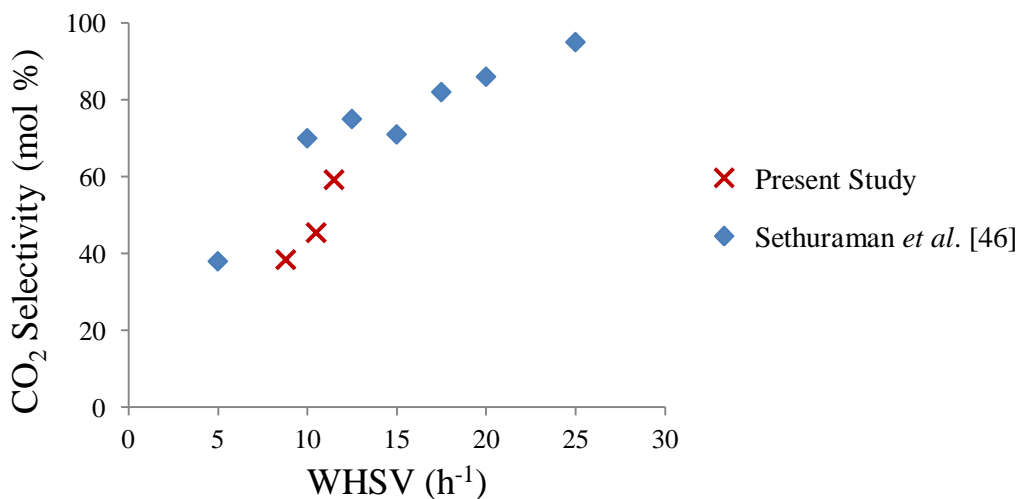


Figure 5.25 – Influence of space velocity on CO₂ selectivity in the present study (at 230°C, 10 bar, H₂/CO = 2.0, and m_{cat} = 0.5g) in comparison to a similar study by Sethuraman *et al.* [46]

The results from the present study show that CO₂ selectivity increases with increasing space velocity. This trend is comparable to the trend reported by Sethuraman *et al.*, who also show that further increases to the space velocity lead to the predominant formation of CO₂ at atmospheric pressure. This may also be true for the higher reactor pressure of 10 bar implemented in the present study, however, further investigation using higher space velocities at this or higher reactor pressures would be required in order to verify this assumption, and can therefore be recommended for future work. From the results of the present study, it can be deduced that under the reaction conditions used with the Co/Al₂O₃ catalyst in the 20cm³ reactor, operation at a WHSV of 8.8 h⁻¹ is preferred as low CO₂ selectivities are desirable. This is because low CO₂ selectivities imply lower inert gas dilution in the products and, therefore, a lower requirement for FT reactor off-gas conditioning and recycling, as well as higher yields of once-through liquid hydrocarbon products (as discussed previously in section 5.2.1).

5.3.3.3 CH₄ and C₂-C₅ Selectivity

The results obtained for the effect of space velocity on CH₄ and C₂-C₅ hydrocarbon selectivities (at 230°C, 10 bar, H₂/CO = 2.0, and m_{cat} = 0.5g) are presented in Figure 5.26 and Figure 5.27 below, respectively. The results from similar studies using cobalt-based catalysts (reviewed previously in section 2.6.2 and summarized in Table 2.4) that have investigated the influence of space velocity on CH₄ and C₂-C₅ hydrocarbon selectivities are also presented in these figures for comparison.

These include studies that have all used Co/Al₂O₃ catalysts at 20 bar by Rafiq *et al.* [116] and Woo *et al.* [115], as well as de la Osa *et al.* (who only reports on the influence of space velocity on the C₂-C₅ hydrocarbon selectivity). No studies have been found that investigate the influence of space velocity on CH₄ and C₂-C₅ hydrocarbon selectivities at lower reactor pressures (≤ 20 bar). Therefore, although higher reactor pressures were implemented in these other studies, these are the only studies that have been found for comparison of results.

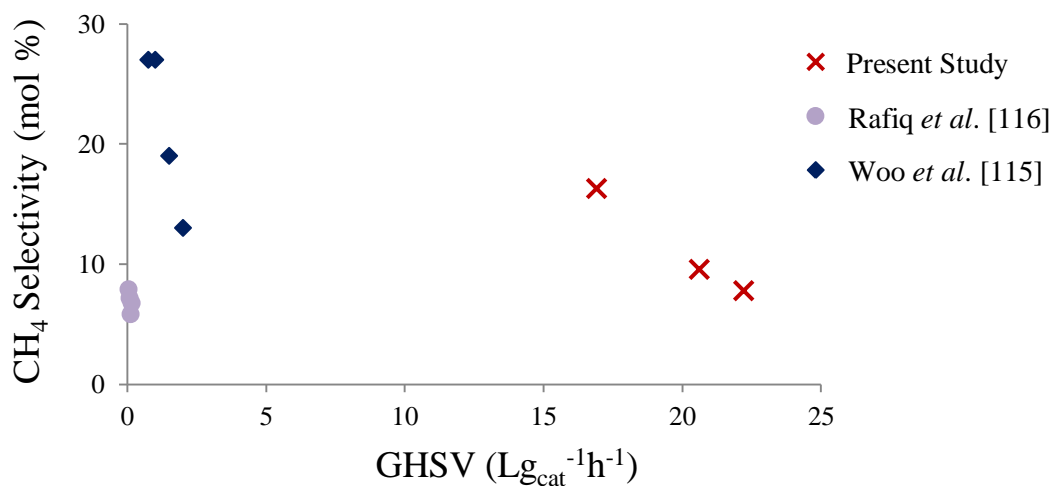


Figure 5.26 – Influence of space velocity on CH₄ selectivity in the present study (at 230°C, 10 bar, H₂/CO = 2.0, and m_{cat} = 0.5g) in comparison to similar studies by Rafiq *et al.* [116], and Woo *et al.* [115]

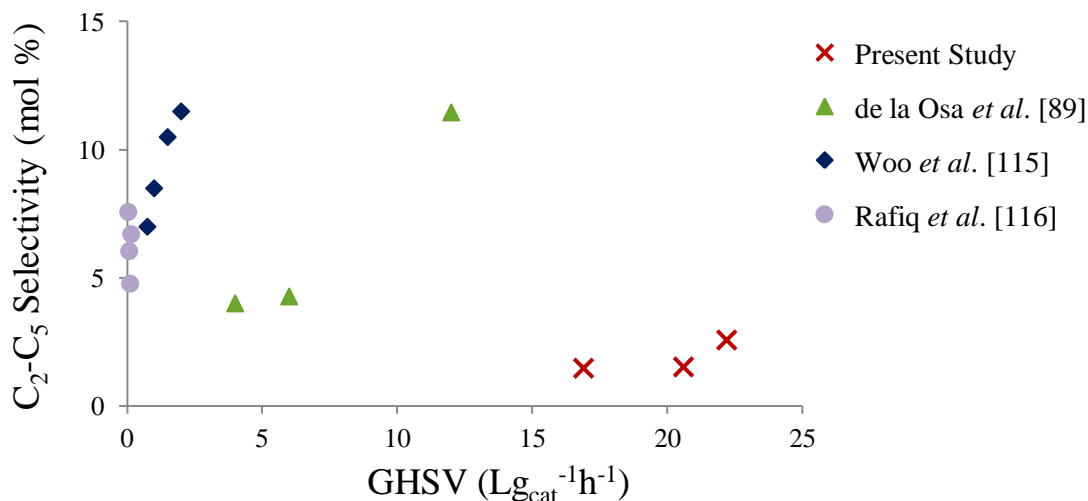


Figure 5.27 – Influence of space velocity on C₂-C₅ selectivity in the present study (at 230°C, 10 bar, H₂/CO = 2.0, and m_{cat} = 0.5g) in comparison to similar studies by de la Osa *et al.* [89], Woo *et al.* [115], and Rafiq *et al.* [116]

As discussed previously in section 2.5.3, higher space velocities correspond to shorter reactor residence times. Therefore, lower CO conversions (section 5.3.3.1) and an increased formation of CH₄ and low molecular weight hydrocarbons are expected as the space velocity is increased. Conversely, the production of heavier hydrocarbon products (C₆₊) is expected to decrease with increasing space velocity (section 5.3.3.4 below). In all the studies reported above, CH₄ selectivity

decreases with increasing space velocity, whereas light hydrocarbon (C₂-C₅) selectivity increases with increasing space velocity. As higher space velocities are implemented in the present study in comparison to these other studies, lower values for these product selectivities are generally observed than those reported in the other studies, as shown in Figure 5.26 and Figure 5.27 above. In addition, the higher reactor pressure of 20 bar implemented in these other studies (in comparison to that of 10 bar used in the present study) would enhance chain growth and, therefore, the formation of higher molecular weight products, resulting in lower CH₄ selectivities and higher C₂-C₅ hydrocarbon selectivities (section 2.5.2). However, higher figures for CH₄ selectivity are reported by Woo *et al.* potentially due to the higher cobalt metal loading in the catalyst they used (as discussed previously in section 5.3.2.3), which has been found to favour the formation of CH₄ and low molecular weight hydrocarbon products and, equally, decrease the production of heavier hydrocarbon molecules (C₆₊) [170]. Moreover, the results reported by Rafiq *et al.* (Figure 5.26), suggest that at the higher reactor pressure of 20 bar implemented in their study, CH₄ selectivity is significantly reduced at very low space velocities (0.037-0.180 h⁻¹).

Overall, the results from the present study suggest that under the reaction conditions implemented in the 20cm³ reactor using the Co/Al₂O₃ catalyst, operation at higher space velocities appears to be more favourable. This is because lower CH₄ selectivities generally imply higher hydrocarbon liquid yields, and therefore, a lower requirement for FT reactor off-gas reforming and recycling. However, higher C₂-C₅ hydrocarbon selectivities may also imply lower hydrocarbon liquid yields, and therefore, the results obtained for C₆₊ hydrocarbon selectivity (section 5.3.3.4 below) must be examined in order to identify the preferred space velocity for operation on the 20cm³ reactor using the Co/Al₂O₃ catalyst in the present study.

5.3.3.4 C₆₊ Selectivity

The results obtained for the effect of space velocity on C₆₊ hydrocarbon selectivity (at 230°C, 10 bar, H₂/CO = 2.0, and m_{cat} = 0.5g) are presented in Figure 5.28 below. The results from similar studies using cobalt-based catalysts (reviewed previously in section 2.6.2 and summarized in Table 2.4) that have investigated the influence of space velocity on the selectivity of C₆₊ hydrocarbons are also presented in Figure 5.28 for comparison.

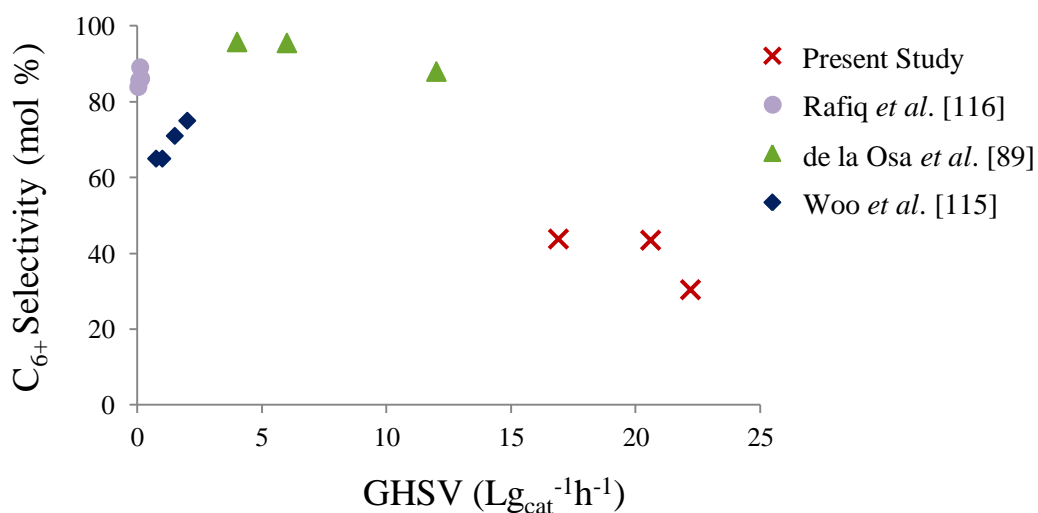


Figure 5.28 – Influence of space velocity on C₆₊ selectivity in the present study (at 230°C, 10 bar, H₂/CO = 2.0, and m_{cat} = 0.5g) in comparison to similar studies by Rafiq *et al.* [116], de la Osa *et al.* [89], and Woo *et al.* [115]

In the present study, C₆₊ hydrocarbon product selectivity decreases as the space velocity is increased. This is expected as higher space velocities correspond to shorter reactor residence times and, therefore, lower reactant conversions (section 5.3.3.1), and a decrease in the formation of heavier molecular weight products. A similar trend is reported by de la Osa *et al.* [89] at lower space velocities, although higher figures for C₆₊ selectivity were reported in their study. However, at even lower space velocities, the opposite trend is reported by both Rafiq *et al.* and Woo *et al.* suggesting that there is a threshold value of space velocity for optimum C₆₊ hydrocarbon selectivity. From the results obtained in the present study it can be deduced that under the reaction conditions implemented in the 20cm³ reactor using the Co/Al₂O₃ catalyst, operation at lower space velocities in the range of 16.9-22.2 Lg_{cat}⁻¹h⁻¹ (or WHSV = 8.8-11.5 h⁻¹) is preferred as the C₆₊ hydrocarbon selectivity is higher, implying higher yields of once-through liquid hydrocarbon products.

5.3.3.5 Product Yields

The product yields are calculated as described previously in section 3.7.4.2. The unreacted syngas is calculated by difference. The product yields obtained in this parameter test set (Table 5.1 in section 5.1.6) reflect the trends observed in sections 5.3.3.1 to 5.3.3.4 for product selectivity with increasing space velocity. These results are presented in Table 5.8 below. As discussed previously in section 5.2.2, product yields are very rarely reported in FT synthesis research publications, and no research studies (investigating the influence of reaction conditions on the product distribution using cobalt-based catalysts) that provide data on FT product yields have been found for comparison to the yields found in the present study.

**Table 5.8 – Influence of space velocity on FT gas and liquid product yields
(at 230°C, 10 bar, H₂/CO = 2.0, and m_{cat} = 0.5g)**

Test	WHSV (h ⁻¹)	Product Yields (wt.%)					Oxyg. In Water (wt.%)	Unreacted Syngas (wt.%)
		CO ₂	CH ₄	C ₂ -C ₅	Liquid H/C's + Waxes	Water + Oxyg.		
FT7	8.8	7.5	1.2	0.3	2.2	3.6	3.7	85.2
FT12	10.5	8.0	0.8	0.4	1.7	2.7	2.7	86.4
FT13	11.5	8.4	0.6	0.5	1.3	2.4	1.7	86.8

As discussed previously in section 5.3.3.3, when the space velocity is increased the reactor residence time becomes shorter leading to lower reactant conversion, as well as lower production of liquid hydrocarbons due to reduced chain growth probability (section 2.2.1). This is reflected in the results presented in Table 5.8 above, which show that higher yields of CO₂ and C₂-C₅ hydrocarbon gases are produced as the space velocity increases, whereas the opposite trend is observed for CH₄ yields. The yield of liquid hydrocarbons also decreases with increasing space velocity, in harmony with the results reported for C₆₊ selectivity in the present study, discussed previously in section 5.3.3.4. The yield of water (containing soluble oxygenated compounds) decreases as the space velocity is increased, indicating that the WGS equilibrium reaction (Equation 2.2 section 2.2), through which water and/or CO₂ are produced, shifts towards the formation of CO₂ as lower CO conversions are achieved. Lower CO conversion and reduced chain growth probabilities are also possible explanations for the reduction in the concentration of soluble oxygenated compounds in the water product with increasing space velocity.

CO₂, CH₄ and C₂-C₅ hydrocarbon gases are generally undesired products in a FT synthesis process that aims to maximize liquid hydrocarbon liquids. Hence, the results presented in Table 5.8 above indicate that under the reaction conditions implemented in the 20cm³ reactor using the Co/Al₂O₃ catalyst in the present study, operation at the lower WHSV of 8.8 h⁻¹ is preferred because higher yields of once-through liquid hydrocarbon products are obtained. This is further demonstrated in Figure 5.29 below, which illustrates the influence of space velocity on the ratio of liquid products to gas products (excluding unreacted syngas), showing that the highest ratios of total liquid products to gas products (0.64) and liquid hydrocarbons to gas products (0.24) are obtained at a WHSV of 8.8 h⁻¹.

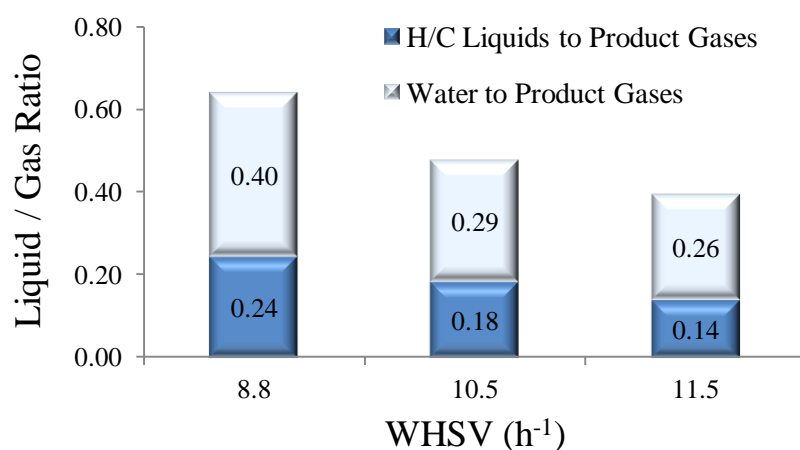


Figure 5.29 – Influence of space velocity on the ratio of liquid products to product gases (at 230°C, 10 bar, H₂/CO = 2.0, and m_{cat} = 0.5g)

5.3.3.6 Energy Content and Composition of Liquid Hydrocarbon Products

A representative photograph of the liquid products, consisting of a liquid hydrocarbon phase (plus waxes) and a water phase (containing soluble oxygenated compounds), collected from the space velocity profile tests (tests FT7, FT12 and FT13 listed in Table 5.1 in section 5.1.6) was provided in Figure 5.7 in section 5.3.1.6. The product analysis methods were described in sections 3.5.3.1 and 3.7.4.2. The calorific values of the liquid hydrocarbon samples collected from these experiment runs are calculated using the method outlined previously in section 3.5.3.3, and are given in Table 5.9 below. Although slight differences in calorific value are observed with increasing space velocity, these results show that the energy content of the liquid hydrocarbons is not significantly influenced by variation in space velocity.

Table 5.9 – Influence of space velocity on the energy content of liquid hydrocarbon products (at 230°C, 10 bar, H₂/CO = 2.0, and m_{cat} = 0.5g)

Test	WHSV (h ⁻¹)	Content (%)				HHV (MJ/kg)
		C	H	N	O	
FT7	8.8	84.21	15.20	0.10	0.49	47.26
FT12	10.5	84.40	15.39	0.10	0.11	47.59
FT13	11.5	84.62	15.24	0.10	0.04	47.49

Figure 5.30, Figure 5.31 and Figure 5.32 below, show the GC-MS chromatograms from the analysis of the liquid hydrocarbons obtained at the three different space velocities investigated in tests FT7, FT12 and FT13, respectively.

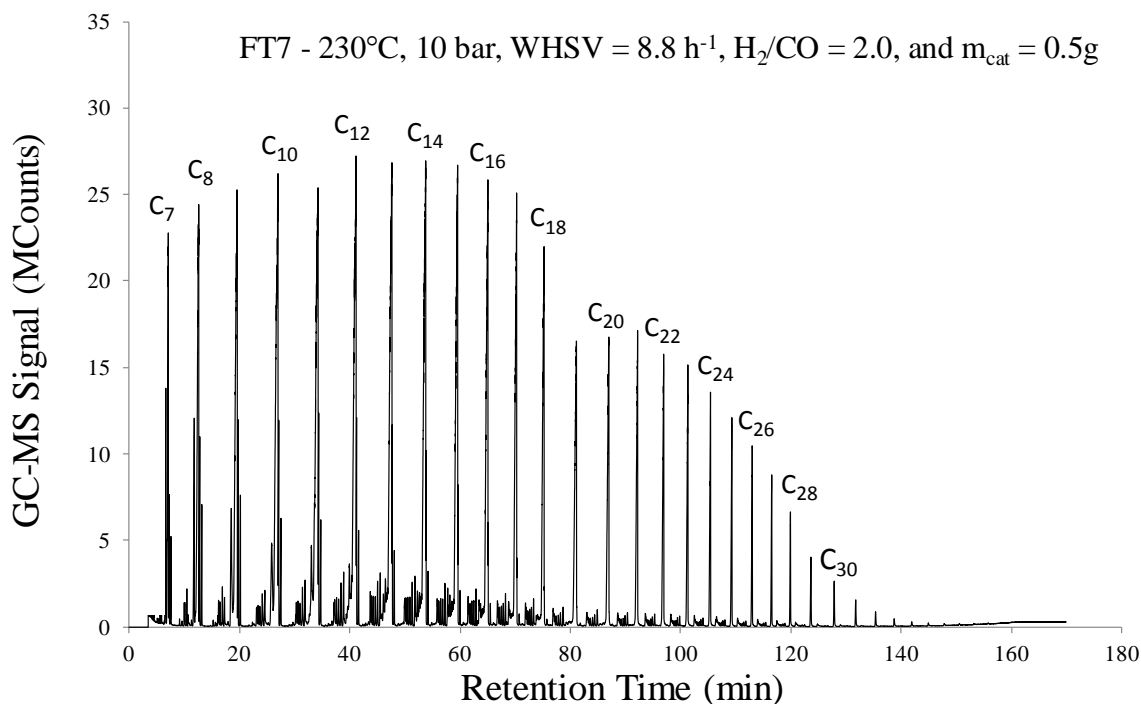


Figure 5.30 – GC-MS chromatogram of liquid hydrocarbons collected from space velocity profile test FT7 at WHSV = 8.8 h⁻¹

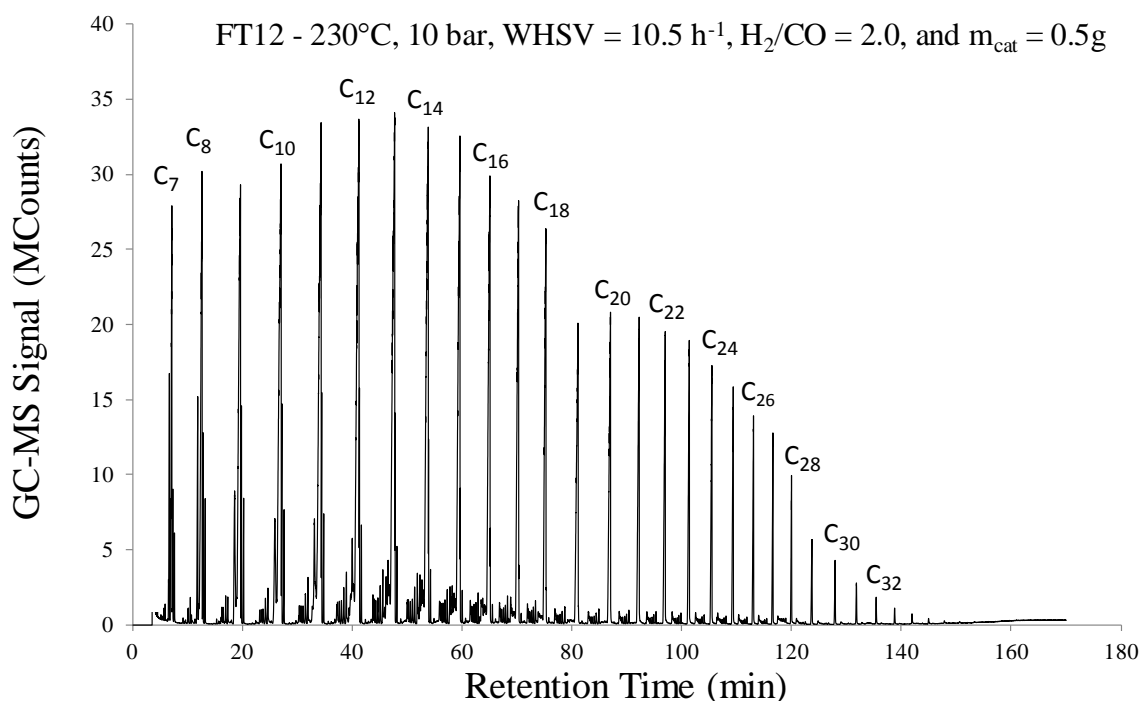


Figure 5.31 – GC-MS chromatogram of liquid hydrocarbons collected from space velocity profile test FT12 at WHSV = 10.5 h⁻¹

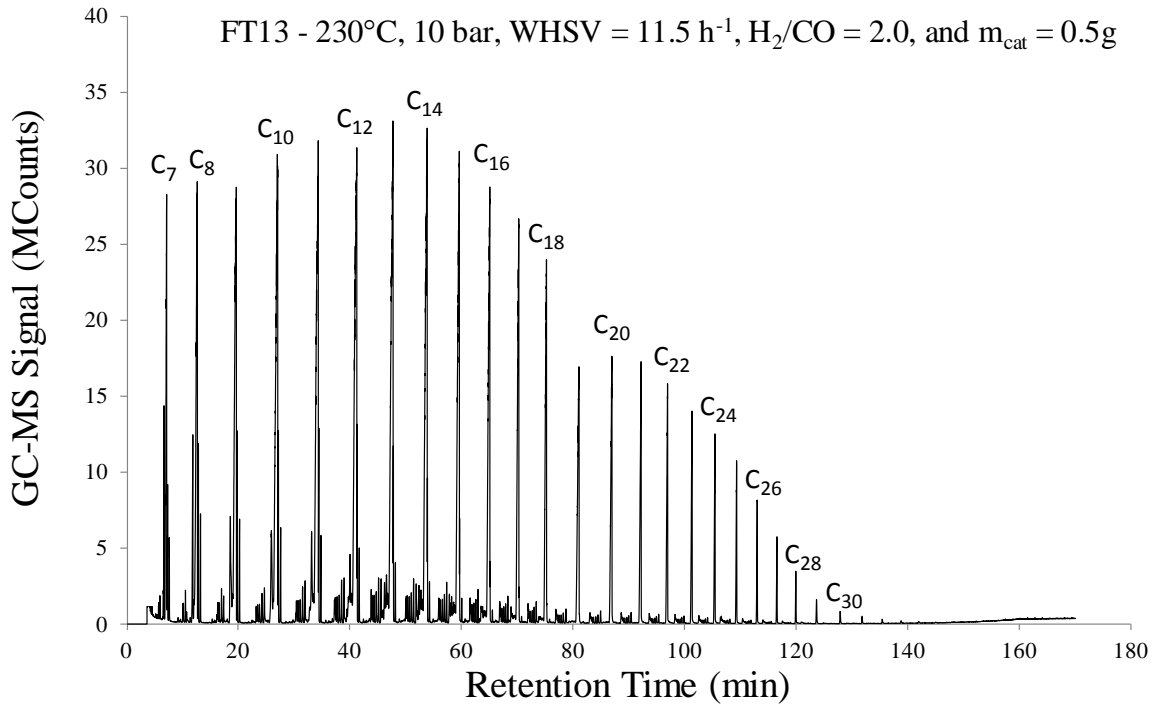


Figure 5.32 – GC-MS chromatogram of liquid hydrocarbons collected from space velocity profile test FT13 at WHSV = 11.5 h⁻¹

The relative fuel compositions of the liquid hydrocarbons collected are calculated from the chromatograms in the figures above, using the method outlined in section 3.5.3. The results are illustrated in Figure 5.33 below.

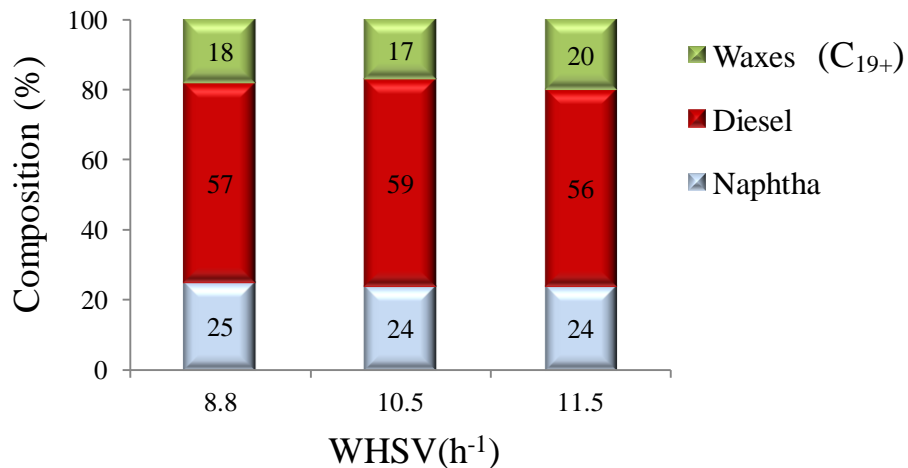


Figure 5.33 – Influence of space velocity on liquid hydrocarbon product composition (at 230°C, 10 bar, H₂/CO = 2.0, and m_{cat} = 0.5g)

These results show that the composition of naphtha is not significantly affected by changes in the space velocity. Slightly more favourable fuel compositions are obtained at the higher space velocities used, where the highest composition of diesel-grade products is obtained at a WHSV of 10.5 h⁻¹. However, the results presented previously in Table 5.8 and Figure 5.29 showed that both

the yields of liquid hydrocarbons and the ratio of these liquids to the gases produced (excluding unreacted syngas) significantly decrease with increasing space velocity. The highest liquid hydrocarbon yields are obtained at a WHSV of 8.8 h^{-1} . In this respect, therefore, it is this value for space velocity that is preferred for operation in the present study.

5.3.3.7 Catalyst Stability

The stability of the catalyst, in terms of CO conversion versus time on stream, over the duration of the synthesis experiments (FT7, FT12 and FT13 in Table 5.1 in section 5.1.6) using different space velocities is compared in Figure 5.34 below.

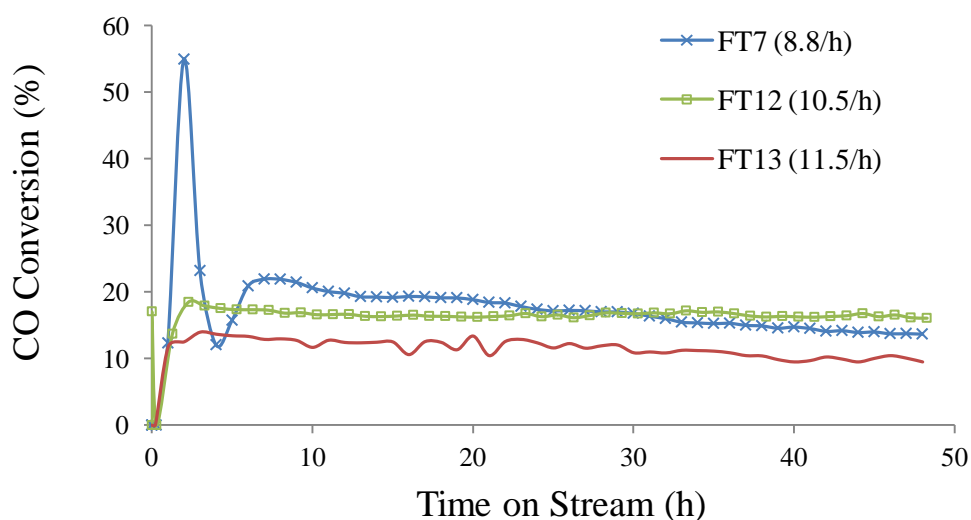


Figure 5.34 – Influence of space velocity on catalyst stability: CO conversion versus time on stream (at 230°C , 10 bar, $\text{H}_2/\text{CO} = 2.0$, and $m_{\text{cat}} = 0.5\text{g}$)

The initial ‘spike’ in CO conversion observed at a WHSV of 8.8 h^{-1} is due to the exothermicity of the reaction explained previously in section 5.3.1.7. The same behaviour is not observed during operation at the higher space velocities of 10.5 and 11.5 h^{-1} , because, theoretically, the increased mass flow of reactants (associated with higher space velocities) aids in carrying away the excess heat given off by the reaction. As illustrated in Figure 5.34 above, the $\text{Co}/\text{Al}_2\text{O}_3$ catalyst displays the most favourable stability at a WHSV of 10.5 h^{-1} , where CO conversion is almost constant during the entire experiment run. This suggests that at this space velocity, the catalyst surface is continuously and sufficiently ‘cleaned’ of carbon and wax deposits by the increased mass flow of reactants, thus allowing for more enhanced CO dissociation and chain propagation (section 2.2.1) [156]. A further increase in space velocity results in lower CO conversion and a more unstable activity by the catalyst, indicating that space velocities above 10.5 h^{-1} are not recommended for operation on the 20cm^3 reactor with the $\text{Co}/\text{Al}_2\text{O}_3$ catalyst.

A gradual decline in catalytic activity is observed during experiment runs FT7 and FT13, and to a much lesser extent in run FT12 (Figure 5.34 above), due to deactivation by the carbon and wax deposition mechanisms discussed previously in section 5.3.1.7. The influence of space velocity on

the extent of these deactivation mechanisms is examined by TGA analysis as previously outlined in section 3.6.4. The mass loss results obtained from these analyses are presented in Table 5.10 below. These results show that the extent of carbon and wax deposition is proportional to increasing space velocity, indicating that catalyst deactivation caused by these mechanisms is reduced at lower space velocities. SEM micrographs (at x764 magnification) of the Co/Al₂O₃ catalyst, before and after reaction in runs FT7, FT12 and FT13 (Table 5.1 in section 5.1.6), are provided in APPENDIX B. Small differences can be seen in these micrographs, however, the magnification strength used was not sufficient in order to allow for definite conclusions to be drawn. Higher magnification strengths are therefore recommended for future investigation.

Table 5.10 – Influence of space velocity on the extent of carbon and wax deposition on the catalyst surface (TGA results)

Catalyst Sample Origin	WHSV (h ⁻¹)	Total Mass Loss (wt.% dry basis)	Mass Loss Due to Carbon & Wax Deposition (wt.%)
Co/Al ₂ O ₃ before Reaction	-	4.7	-
FT7	8.8	40.3	35.6
FT12	10.5	44.8	40.1
FT12	11.5	47.7	43.0

5.3.3.8 Space Velocity Selection for Further Experiments

Under the reaction conditions used (Table 5.1 in section 5.1.6) in the 20cm³ reactor using the Co/Al₂O₃ catalyst in the present study, an increase in space velocity results in lower CO conversions. CO₂ selectivity increases with increasing space velocity, whereas the opposite is observed for CH₄ selectivity. Similar C₆₊ hydrocarbon selectivities are observed at a WHSV of 8.8 and 10.5 h⁻¹, whereas a lower value is obtained at a higher WHSV of 11.5 h⁻¹. The product yields follow similar trends to these product selectivities, where increasing space velocity results in lower yields of liquid products (both liquid hydrocarbons and water) and, conversely, higher yields of product gases (CO₂, CH₄ and C₂-C₅ hydrocarbons). The catalyst displays the most favourable activity with time on stream at a WHSV of 10.5 h⁻¹. However, TGA analysis shows that the recorded mass loss due to carbon and wax deposition on the catalyst surface is significantly higher than at a lower WHSV of 8.8 h⁻¹. GC-MS analyses of the liquid hydrocarbons showed that the most favourable fuel composition, containing the highest proportion of diesel, is obtained at a WHSV of 10.5 h⁻¹. The difference in diesel composition of the liquid hydrocarbons obtained at a lower WHSV of 8.8 h⁻¹ is small, however, higher liquid hydrocarbon yields are obtained at this lower space velocity. Therefore, a WHSV of 8.8 h⁻¹ is selected as the preferred value for space velocity to be used for operation on the 20cm³ fixed-bed reactor in the present study, and in the remaining parameter profiling test sets.

5.3.4 Influence of H₂/CO Molar Ratio in Syngas

Sections 5.3.1 to 5.3.3 resulted in identification of the preferred reactor temperature, reactor pressure and space velocity for subsequent tests.

5.3.4.1 CO Conversion

The results obtained in the present study for the effect of the H₂/CO molar ratio in the feed syngas on CO conversion (at 230°C, 10 bar, WHSV = 8.8 h⁻¹, and m_{cat} = 0.5g) are compared to the results of similar studies using cobalt-based catalysts (reviewed previously in section 2.6.2 and summarized in Table 2.4) that have investigated the influence of the H₂/CO molar ratio in the feed syngas on CO conversion in Figure 5.35 below. These include studies by Tristantini *et al.* [114] and de la Osa *et al.* [89] (both working with Co/Al₂O₃ catalysts at a higher reactor pressure of 20 bar), as well as Sharifnia *et al.* [113] (working at a similar reactor pressure to the present study of 9 bar, but with a Co/SiO₂ catalyst). As discussed previously in section 2.6, studies using cobalt-based catalysts that have specifically addressed the influence of low operating pressures (< 20 bar) on FT product distribution and catalyst activity are very limited. Therefore, although different reaction conditions were implemented in these other studies, including higher reactor pressures than those used in the present study and different catalyst compositions, these are the only studies that have been found for comparison of results.

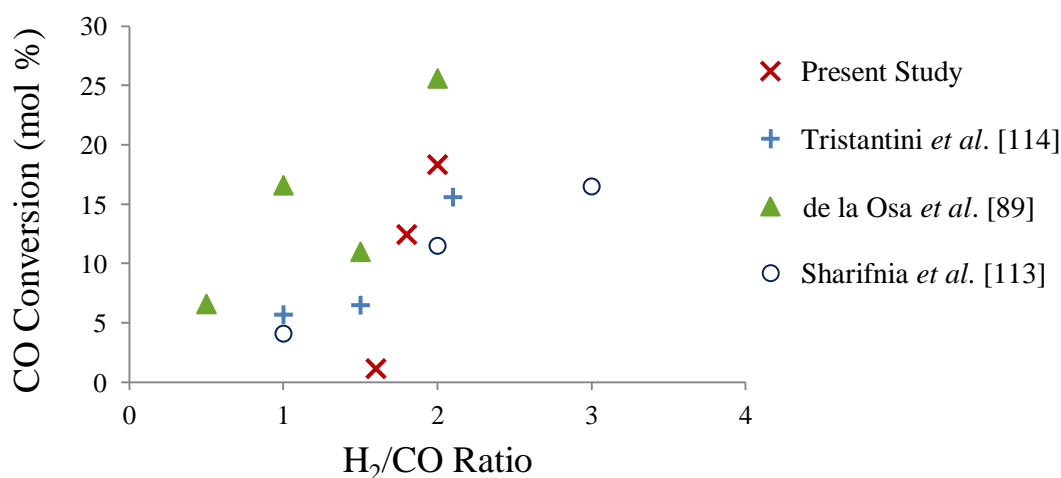


Figure 5.35 – Influence of the H₂/CO molar ratio on CO conversion in the present study (at 230°C, 10 bar, WHSV = 8.8 h⁻¹, and m_{cat} = 0.5g) in comparison to similar studies by Tristantini *et al.* [114], de la Osa *et al.* [89], and Sharifnia *et al.* [113]

In all the studies reported above CO conversion increases as the H₂/CO molar ratio in the feed syngas increases. This is expected as higher H₂/CO molar ratios imply a higher concentration of H₂ species on the catalyst surface, which have been reported to promote chain termination reactions (section 2.2.1) and increase CO conversion, but result in the increased formation of lower molecular weight hydrocarbons [89, 91]. The figures for CO conversion found using H₂/CO molar ratios of 1.8 and 2.0 in the present study are comparable to those found by Tristantini *et al.*, de la Osa *et al.* and Sharifnia *et al.* for H₂/CO molar ratios in the same region, as shown in Figure 5.35

above. At the lower H_2/CO molar ratio of 1.6 investigated, a very poor CO conversion was observed. This suggests that under the reaction conditions implemented on the 20cm^3 reactor with the Co/Al_2O_3 catalyst, operation at this lower H_2/CO molar ratio is not recommended, and therefore higher H_2/CO molar ratios are required. Further evidence supporting this assumption can be gathered from the catalyst stability at a H_2/CO molar ratio of 1.6, which is discussed later in section 5.3.4.7. Based on achieving maximum CO conversion, therefore, the results from the present study indicate that operation at a H_2/CO molar ratio in the feed syngas of 2.0 is preferred.

5.3.4.2 CO_2 Selectivity

The results obtained for the effect of the H_2/CO molar ratio in the feed syngas on CO_2 selectivity (at 230°C , 10 bar, $WHSV = 8.8\text{ h}^{-1}$, and $m_{\text{cat}} = 0.5\text{g}$) are presented in Figure 5.36 below. From the studies investigating the influence of reaction conditions on FT product distribution that were reviewed previously in section 2.6.2 (and summarized in Table 2.4), only a few report on the effect of the H_2/CO molar ratio in the feed syngas on CO_2 selectivity. These include studies by de la Osa *et al.* [89] and Tristantini *et al.* [114], both working with a Co/Al_2O_3 catalyst at a reactor pressure of 20 bar, and space velocities (GHSV) of 6 and 12 h^{-1} , respectively. The results of these studies are also presented in Figure 5.36 below, for comparison. Although higher reactor pressures and lower space velocities were implemented in these studies than those used in the present study, these are the only studies that have been found for comparison of results.

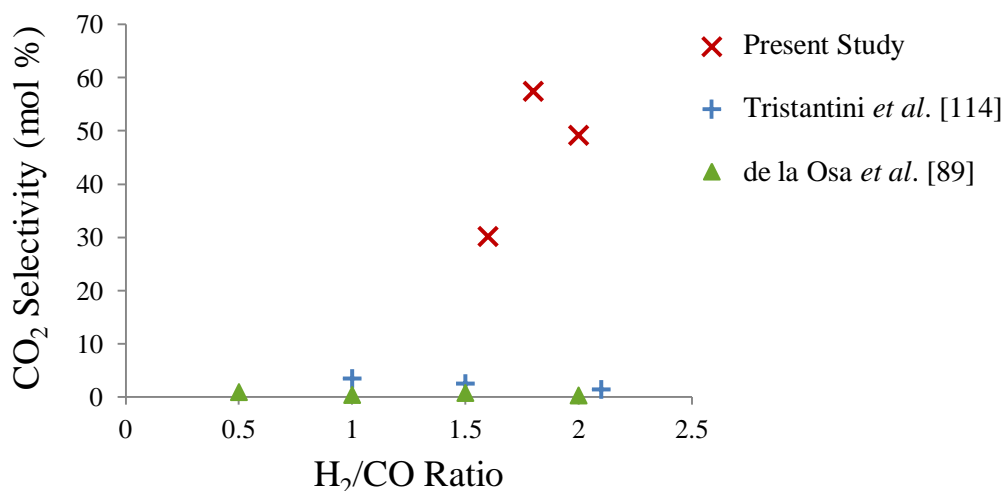


Figure 5.36 – Influence of the H_2/CO molar ratio on CO_2 selectivity in the present study (at 230°C , 10 bar, $WHSV = 8.8\text{ h}^{-1}$, and $m_{\text{cat}} = 0.5\text{g}$) in comparison to similar studies by Tristantini *et al.* [114], and de la Osa *et al.* [89]

As shown in Figure 5.36 above, a potentially more complex relationship for the influence of the H_2/CO molar ratio in the feed syngas on CO_2 selectivity is observed in the results from the present study in comparison to the other trends reported in Figure 5.36 above. CO_2 selectivity increases as the H_2/CO molar ratio is increased in the range of 1.6-2.0 in the present study, reaching a maximum at a H_2/CO molar ratio of 1.8 and thereafter declining as this ratio is further increased to 2.0. In

contrast, Tristantini *et al.* report much lower figures for CO₂ selectivity showing a trend that slowly decreases as the H₂/CO molar ratio is increased. In addition, de la Osa *et al.* report negligible CO₂ selectivities, suggesting that CO₂ selectivity is not affected by variation in the H₂/CO molar ratio in the range of 0.5-2.0.

The different reaction conditions implemented in these three studies (as discussed above) may be contributing factors to these contrasting results, but the exact reasons for these differences are not known. Further investigation is required in order to determine the relationship between the H₂/CO molar ratio in the feed syngas and CO₂ selectivity and is, therefore, recommended for future work. This includes repetition of the FT synthesis run performed at a H₂/CO molar ratio of 2.0 (FT7 in Table 5.1 in section 5.1.6), as well as additional experimental runs covering a wider range of H₂/CO molar ratios (e.g. H₂/CO = 1.0-3.0). Still, what can be drawn from the results of the present study is that under the reaction conditions implemented in the 20cm³ reactor, operation at lower H₂/CO molar ratios in the range of 1.6-2.0 is apparently more favourable as a low CO₂ selectivity is desirable. This is because low CO₂ selectivities imply lower inert gas dilution in the products and, therefore, a lower requirement for FT reactor off-gas conditioning and recycling, as well as higher yields of once-through liquid hydrocarbon products (as discussed previously in section 5.2.1). However, as discussed earlier in section 5.3.4.1, operation at a H₂/CO molar ratio of 1.6 resulted in very low CO conversion. Hence, operation at a H₂/CO molar ratio in the feed syngas of 2.0 is preferred as it results in the next lowest CO₂ selectivity, as well as a higher CO conversion.

5.3.4.3 CH₄ and C₂-C₅ Selectivity

The results obtained for the effect of the H₂/CO molar ratio in the feed syngas on CH₄ and C₂-C₅ hydrocarbon selectivities (at 230°C, 10 bar, WHSV = 8.8 h⁻¹, and m_{cat} = 0.5g) are presented in Figure 5.37 and Figure 5.38 below, respectively. From the studies investigating the influence of reaction conditions on FT product distribution that were reviewed previously in section 2.6.2 (and summarized in Table 2.4), the effect of the H₂/CO molar ratio in the feed syngas on CH₄ selectivity is only reported by Sharifnia *et al.* [113] (working with a Co/SiO₂ catalyst at a similar reactor pressure of 9 bar), whereas both Sharifnia *et al.* and de la Osa *et al.* [89] (the latter working with a Co/Al₂O₃ catalyst but at a higher reactor pressure of 20 bar) report on the effect of the H₂/CO molar ratio in the feed syngas on C₂-C₅ selectivity. Their results are also presented in Figure 5.37 and Figure 5.38 below. Hence, although different reaction conditions were implemented in these studies than those used in the present study, these are the only studies that have been found for comparison of results.

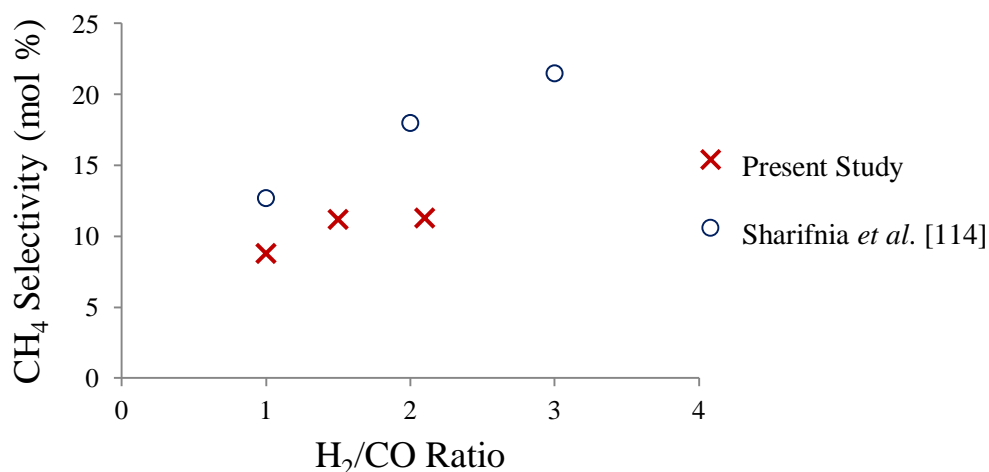


Figure 5.37 – Influence of the H₂/CO molar ratio on CH₄ selectivity in the present study (at 230°C, 10 bar, WHSV = 8.8 h⁻¹, and m_{cat} = 0.5g) in comparison to a similar study by Sharifnia *et al.* [113]

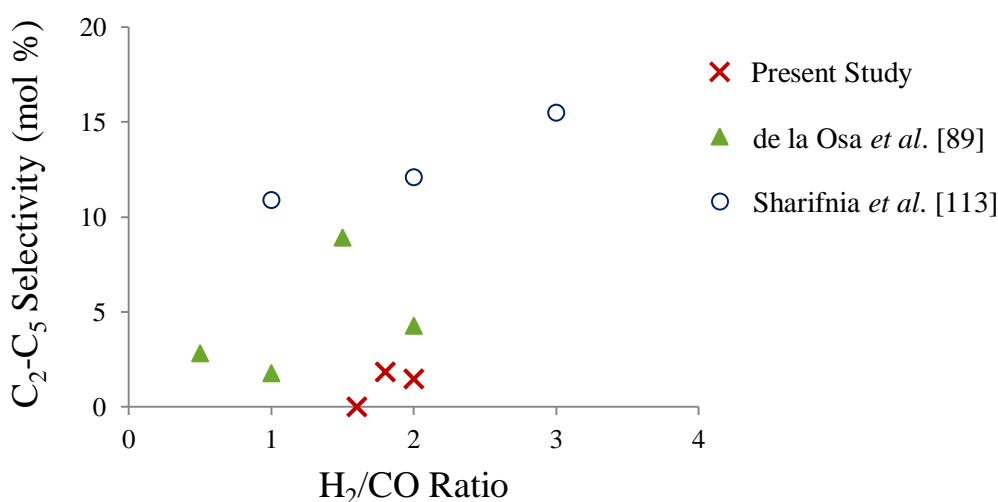


Figure 5.38 – Influence of the H₂/CO molar ratio on C₂-C₅ selectivity in the present study (at 230°C, 10 bar, WHSV = 8.8 h⁻¹, and m_{cat} = 0.5g) in comparison to similar studies by de la Osa *et al.* [89] and Sharifnia *et al.* [113]

In all the studies – reported above both CH₄ and C₂-C₅ product selectivities increase as the H₂/CO molar ratio in the feed syngas increases. As discussed previously in section 5.3.4.1 above, this is expected as higher H₂/CO molar ratios imply a higher concentration of H₂ species on the catalyst surface. These higher H₂ concentrations have been reported to promote chain termination reactions (section 2.2.1) and increase CO conversion, but result in the increased formation of lower molecular weight hydrocarbons [89, 91]. The higher figures reported for CH₄ and C₂-C₅ product selectivities by Sharifnia *et al.* and de la Osa *et al.* in comparison to the present study may be due to the different reaction conditions implemented in these studies. Although a similar reactor pressure to the present study was implemented by Sharifnia *et al.*, a cobalt catalyst with a different support material was used in their study which, under the conditions implemented (space velocity not reported in their study), may be more selective towards the formation of lighter hydrocarbons. The lower space velocity used by de la Osa *et al.* (6 Lg_{cat}⁻¹h⁻¹ in comparison to 17 Lg_{cat}⁻¹h⁻¹ used in the

present study), and higher reactor pressure used possibly account for the higher C₂-C₅ product selectivities reported. As discussed previously in section 5.3.3.3, this is because higher reactor pressures and lower space velocities would result in increased reactant concentration on the catalyst surface and shorter residence times, respectively, therefore increasing CO conversion and enhancing chain growth probability.

What can be deduced from the results of the present study is that under the reaction conditions implemented in the 20cm³ reactor using the Co/Al₂O₃ catalyst, despite the fact that the lowest CH₄ and C₂-C₅ hydrocarbon products selectivities were observed at a H₂/CO molar ratio of 1.6, operation at this lower ratio is not recommended as this results in poor CO conversion (as discussed earlier in section 5.3.4.1). Thus, operation at a H₂/CO molar ratio in the feed syngas of 2.0 is preferred as this not only results in the highest CO conversion (section 5.3.4.1) but in low CH₄ and C₂-C₅ hydrocarbon product selectivities, which imply a lower requirement for FT reactor off-gas reforming and recycling, and potentially higher liquid hydrocarbon yields (as discussed previously in section 5.2.1).

5.3.4.4 C₆₊ Selectivity

The results obtained for the effect of the H₂/CO molar ratio in the feed syngas on C₆₊ hydrocarbon selectivity (at 230°C, 10 bar, WHSV = 8.8 h⁻¹, and m_{cat} = 0.5g) are presented in Figure 5.39 below. The results from similar studies using cobalt-based catalysts (reviewed previously in section 2.6.2 and summarized in Table 2.4) that have investigated the influence of the H₂/CO molar ratio in the feed syngas on the selectivity of C₆₊ hydrocarbons are also presented in Figure 5.39 for comparison.

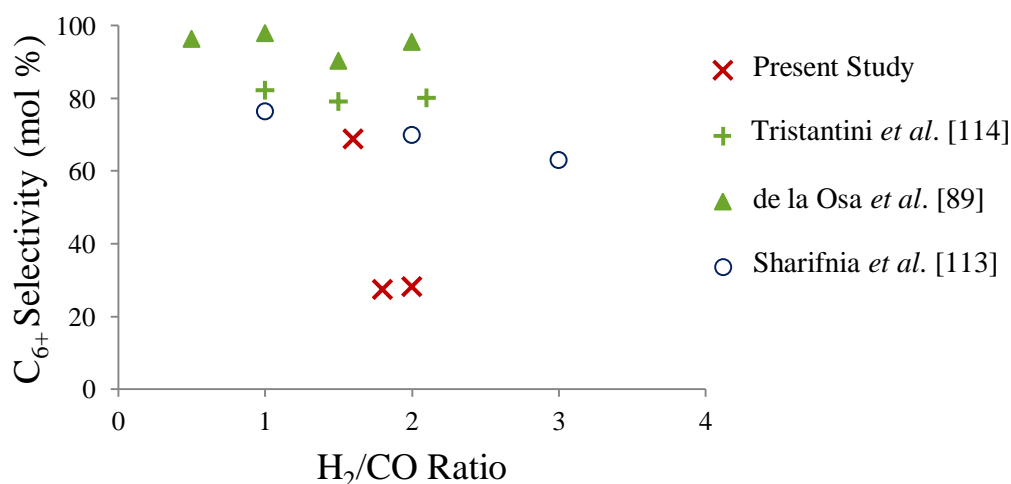


Figure 5.39 – Influence of the H₂/CO molar ratio on C₆₊ selectivity in the present study (at 230°C, 10 bar, WHSV = 8.8 h⁻¹, and m_{cat} = 0.5g) in comparison to similar studies by Tristantini *et al.* [114], de la Osa *et al.* [89] and Sharifnia *et al.* [113]

In all the studies reported above C₆₊ selectivity decreases as the H₂/CO molar ratio in the feed syngas increases. As discussed in section 5.3.4.3 above, this is expected as higher H₂/CO molar

ratios imply a higher concentration of H₂ species on the catalyst surface, which have been reported to increase CO conversion and promote chain termination reactions (section 2.2.1) which, in turn, result in the decreased production of higher molecular weight hydrocarbons [89, 91]. However, a much sharper decline in C₆₊ hydrocarbon selectivity with increasing H₂/CO molar ratio is observed in the present study in comparison to the gradually declining trends reported by Tristantini *et al.*, de la Osa *et al.*, and Sharifnia *et al.*, as shown in Figure 5.39 above. The reasons for the sharper decline in the present study are not known, but could potentially be due to the different reaction conditions implemented in these three studies, including a higher reactor pressure and lower space velocity by both Tristantini *et al.* and de la Osa *et al.*, as well as the use of a different catalyst support by Sharifnia *et al.* Hence, further investigation is required in order to determine the relationship between the H₂/CO molar ratio in the feed syngas and C₆₊ hydrocarbon selectivity and is, therefore, recommended for future work. This includes repetition of the FT synthesis runs performed at H₂/CO molar ratios in the range of 1.6-2.0 (FT7, FT14 and FT15 in Table 5.1 in section 5.1.6), as well as additional experimental runs covering a wider range of H₂/CO molar ratios (e.g. H₂/CO = 1.0-3.0).

What can be drawn from the results of the present study, however, is that under the reaction conditions implemented in the 20cm³ reactor using the Co/Al₂O₃ catalyst, operation at lower H₂/CO molar ratios in the range of 1.6-2.0 is apparently more favourable as high C₆₊ hydrocarbon selectivity is desirable. This is because high C₆₊ selectivities imply higher yields of once-through liquid hydrocarbon products (as discussed previously in section 5.2.1). However, as discussed earlier in section 5.3.4.1, operation at a H₂/CO molar ratio of 1.6 resulted in very low CO conversion. Hence, operation at a H₂/CO molar ratio in the feed syngas of 2.0 is preferred as this resulted in the highest CO conversion (section 5.3.4.1), as well as a favourable C₆₊ hydrocarbon selectivity.

5.3.4.5 Product Yields

The product yields are calculated as described previously in section 3.7.4.2. The unreacted syngas is calculated by difference. The product yields obtained in this parameter test set (Table 5.1 in section 5.1.6) reflect the trends observed in sections 5.3.4.1 to 5.3.4.4 for product selectivity with increasing H₂/CO molar ratio in the feed syngas. These results are presented in Table 5.11 below. As discussed previously in section 5.2.2, product yields are very rarely reported in FT synthesis research publications, and no research studies (investigating the influence of reaction conditions on the product distribution using cobalt-based catalysts) that provide data on FT product yields have been found for comparison to the yields found in the present study.

Table 5.11 – Influence of the H₂/CO molar ratio in the feed syngas on FT gas and liquid product yields (at 230°C, 10 bar, WHSV = 8.8 h⁻¹, and m_{cat} = 0.5g)

Test	H ₂ /CO	Product Yields (wt.%)					Oxyg. In Water (wt.%)	Unreacted Syngas (wt.%)
		CO ₂	CH ₄	C ₂ -C ₅	Liquid H/C's + Waxes	Water + Oxyg.		
FT14	1.6	9.0	0.1	0.1	0.2	0.4	2.1	90.1
FT15	1.8	7.6	0.7	0.3	2.7	3.7	5.1	84.9
FT7	2.0	7.5	1.2	0.2	2.2	3.6	3.7	85.2

When the H₂/CO molar ratio in the feed syngas increases the concentration of H₂ species on the catalyst surface increases (as discussed previously in section 5.3.4.4). This has been reported to increase CO conversion and promote chain termination reactions (section 2.2.1) which, in turn, result in the increased production of lower molecular weight hydrocarbons [89, 91]. Conversely, the formation of heavier molecular weight hydrocarbons (C₆₊) would decrease as the H₂/CO molar ratio is increased, resulting in lower liquid hydrocarbon yields. Equally, as the H₂/CO molar ratio in the feed syngas decreases, the concentration of CO species on the catalyst surface increases. This has been found to propagate chain growth to a greater extent than at higher H₂/CO molar ratios in the feed syngas (section 2.5.4).

The above observations are reflected in the results presented in Table 5.11 above, which show that as the H₂/CO molar ratio in the feed syngas increases both the yields of CH₄ and C₂-C₅ hydrocarbons increase, whereas the yield of liquid hydrocarbons (plus waxes) decreases as the H₂/CO molar ratio is increased from 1.8-2.0. Below a H₂/CO molar ratio of 1.8, however, the yield of liquid hydrocarbons decreases, which is contrary to the expected trend. This can be attributed to the poor CO conversion that was achieved at a H₂/CO ratio of 1.6, as discussed previously in section 5.3.4.1. The poor performance of the Co/Al₂O₃ catalyst at this lower H₂/CO ratio of 1.6 is also discussed later on in section 5.3.4.7. The yield of water (containing soluble oxygenated compounds) increases as the H₂/CO molar ratio in the feed syngas is increased, whereas the yield of CO₂ decreases indicating that the WGS equilibrium reaction (Equation 2.2 section 2.2), through which water and/or CO₂ are produced, shifts towards the formation of water rather than CO₂ as higher CO conversions are achieved. No definite trend is observed for the concentration of soluble oxygenated compounds in the water.

The results presented in Table 5.11 above indicate that under the reaction conditions implemented in the 20cm³ reactor using the Co/Al₂O₃ catalyst in the present study, operation at a H₂/CO molar ratio in the feed syngas of 1.8 would be preferred over operation at a ratio of 2.0 because higher yields of once-through liquid hydrocarbon products are obtained. Operation at this lower H₂/CO molar ratio would also be more favourable from a processing perspective as less conditioning or H₂/CO molar ratio adjustment of the syngas (typically H₂/CO molar ratio for biomass derived

syngas is 0.5-1.5 [69]) would be required for FT synthesis using the Co/Al₂O₃ catalyst. These results are further demonstrated in Figure 5.40 below, which illustrates the influence of the H₂/CO molar ratio in the feed syngas on the ratio of liquid products to gas products (excluding unreacted syngas), showing that the highest ratios of total liquid products to gas products (0.72) and liquid hydrocarbons to gas products (0.30) are obtained at a H₂/CO ratio of 1.8.

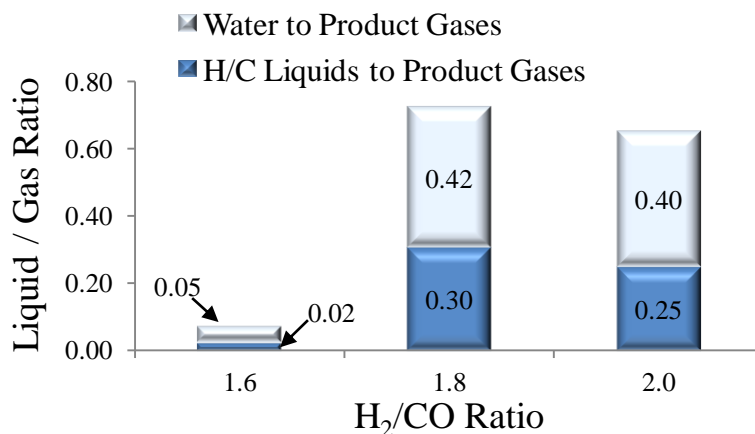


Figure 5.40 – Influence of the H₂/CO molar ratio in the feed syngas on the ratio of liquid products to product gases (at 230°C, 10 bar, WHSV = 8.8 h⁻¹, and m_{cat} = 0.5g)

5.3.4.6 Energy Content and Composition of Liquid Hydrocarbon Products

A representative photograph of the liquid products, consisting of a liquid hydrocarbon phase (plus waxes) and a water phase (containing soluble oxygenated compounds), collected from the H₂/CO molar ratio profile tests (tests FT7, FT14 and FT15 listed in Table 5.1 in section 5.1.6) was provided in Figure 5.7 in section 5.3.1.6. The product analysis methods were described in sections 3.5.3.1 and 3.7.4.2. The calorific values of the liquid hydrocarbon samples collected from these experiment runs are calculated using the method outlined previously in section 3.5.3.3, and are given in Table 5.12 below. Although very slight differences in calorific value are observed with increasing H₂/CO molar ratio in the feed syngas, these results show that the energy content of the liquid hydrocarbons is not significantly influenced by variation in the H₂/CO molar ratio in the feed syngas.

Table 5.12 – Influence of the H₂/CO molar ratio in the feed syngas on the energy content of liquid hydrocarbon products (at 230°C, 10 bar, WHSV = 8.8 h⁻¹, and m_{cat} = 0.5g)

Test	H ₂ /CO	Content (%)				HHV (MJ/kg)
		C	H	N	O	
FT14	1.6	84.40	15.39	0.10	0.11	47.56
FT15	1.8	84.62	15.24	0.10	0.04	47.46
FT7	2.0	84.21	15.20	0.10	0.49	47.26

Figure 5.41, Figure 5.42, and Figure 5.43 below, show the GC-MS chromatograms of the liquid hydrocarbons that were obtained at the three different H₂/CO molar ratios in the feed syngas investigated in tests FT14, FT15 and FT7, respectively.

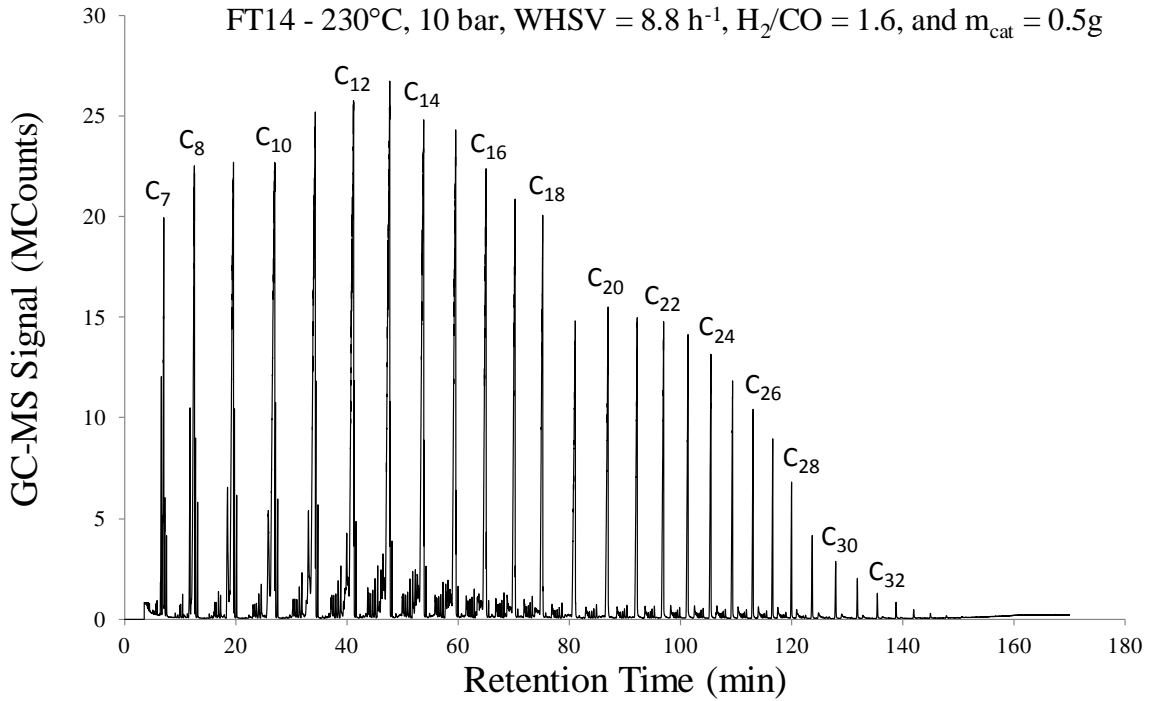


Figure 5.41 – GC-MS chromatogram of liquid hydrocarbons collected from H₂/CO molar ratio in the feed syngas profile test FT14 at H₂/CO = 1.6

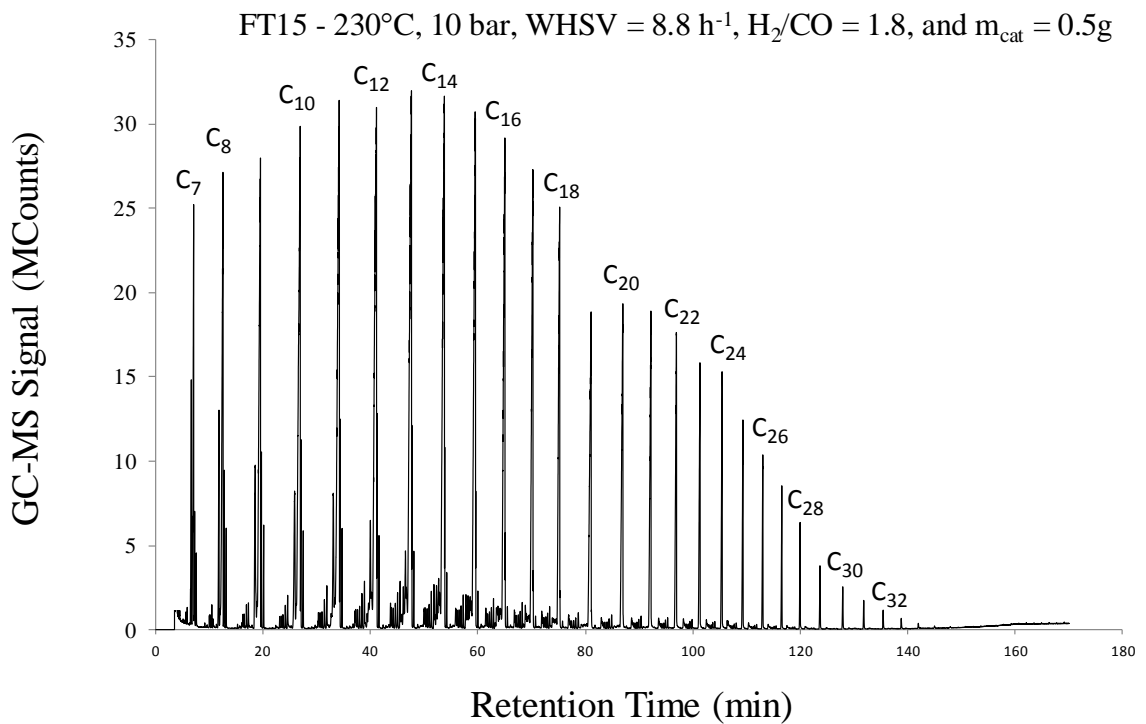


Figure 5.42 – GC-MS chromatogram of liquid hydrocarbons collected from H₂/CO molar ratio in the feed syngas profile test FT15 at H₂/CO = 1.8

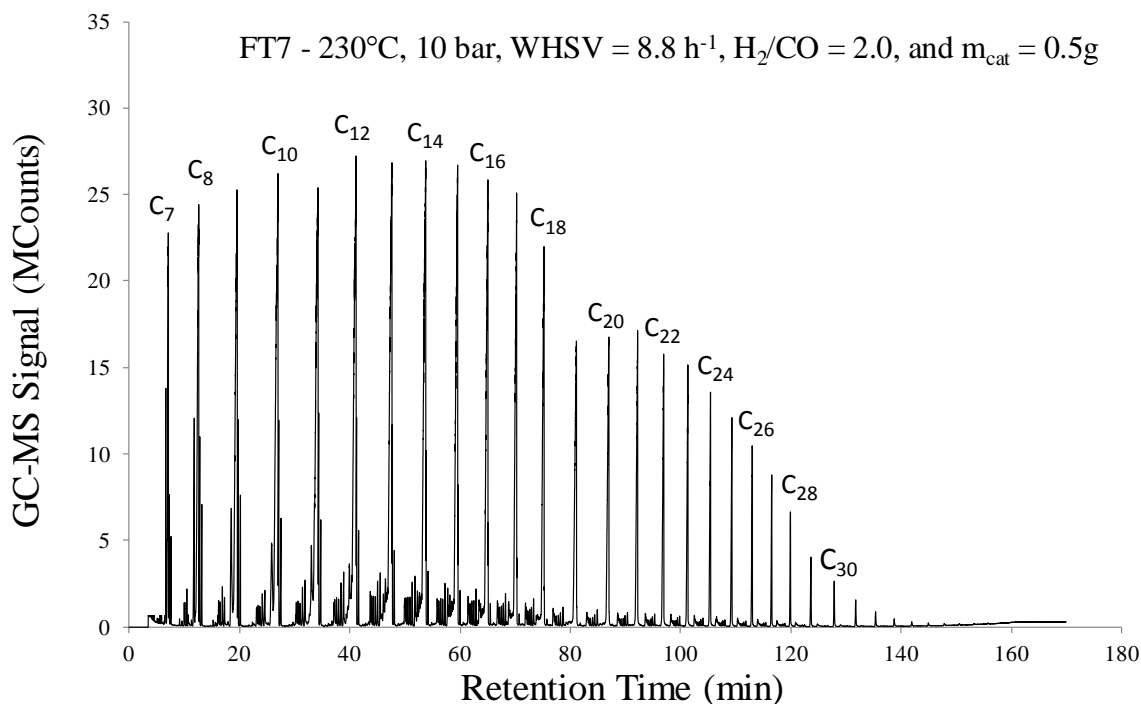


Figure 5.43 – GC-MS chromatogram of liquid hydrocarbons collected from H₂/CO molar ratio in the feed syngas profile test FT7 at H₂/CO = 2.0

The relative fuel compositions of the liquid hydrocarbons collected are calculated from the chromatograms in the figures above, using the method outlined in section 3.5.3. The results are illustrated in Figure 5.44 below.

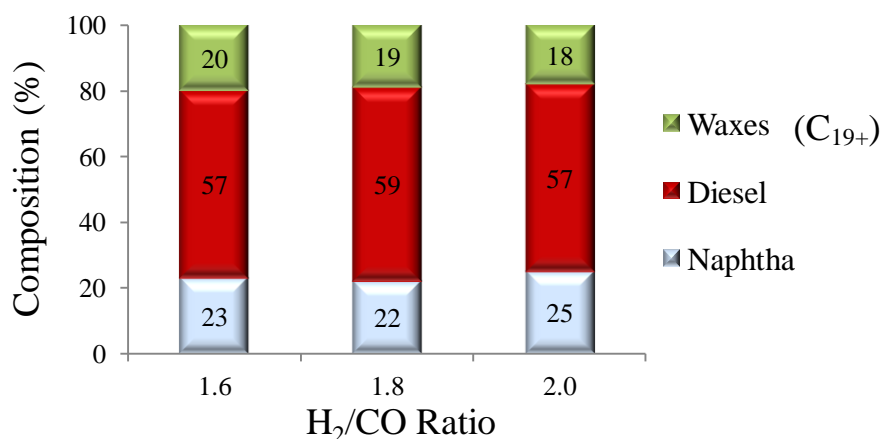


Figure 5.44 – Influence of the H₂/CO molar ratio in the feed syngas on liquid hydrocarbon product composition (at 230°C, 10 bar, WHSV = 8.8 h⁻¹, and m_{cat} = 0.5g)

These results show that the most favourable fuel composition (highest diesel and lowest naphtha content) are obtained at a H₂/CO molar ratio of 1.8. The fuel composition obtained at a H₂/CO molar ratio of 2.0 is in fact less favourable than the one obtained at a molar ratio of 1.6, although the liquid hydrocarbon yield at a H₂/CO molar ratio of 1.6 was very low (as discussed previously in section 5.3.4.5). The highest naphtha content (and, conversely, the lowest C₁₉₊ waxes content) is observed at a H₂/CO molar ratio of 2.0. This result further supports the argument (made previously

in section 5.3.4.1) that higher H_2/CO molar ratios in the feed syngas promote chain termination reactions due to higher H_2 partial pressures in the syngas, producing lower chain length hydrocarbon products. As the highest liquid hydrocarbon yield (discussed previously in section 5.3.4.5) containing the highest proportion of diesel in the fuel mix was obtained at a H_2/CO molar ratio of 1.8, this value appears to be the preferred value for operation in the 20cm^3 reactor using the Co/Al_2O_3 catalyst under the reaction conditions implemented in the present study. However, further investigation into the activity of the catalyst with time on stream is required before selection of the preferred H_2/CO molar ratio in the feed syngas is made (section 5.3.4.7 below).

5.3.4.7 Catalyst Stability

The stability of the catalyst over the duration of the synthesis experiments using different H_2/CO molar ratios in the feed syngas is compared in Figure 5.45 below. The initial ‘spike’ in CO conversion observed at a H_2/CO molar ratio of 2.0 is due to the exothermic nature of the reaction explained previously in section 5.3.1.7. To a lesser extent, a similar effect is observed at a H_2/CO molar ratio of 1.8, where sudden activity is recorded approximately two hours after the reaction is initiated. As opposed to the reaction at a H_2/CO molar ratio of 2.0, however, this is followed by a more initially stable activity.

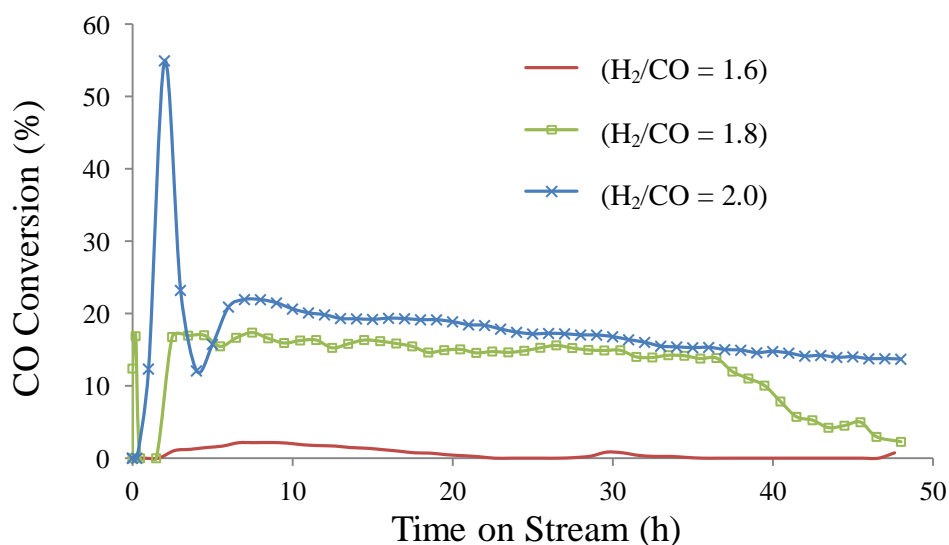


Figure 5.45 – Influence of the H_2/CO molar ratio in the feed syngas on catalyst stability: CO conversion versus time on stream (at 230°C , 10 bar, $WHSV = 8.8\text{ h}^{-1}$, and $m_{\text{cat}} = 0.5\text{g}$)

As illustrated in Figure 5.45, the catalyst displays the most favourable stability at a H_2/CO molar ratio of 2.0, where CO conversion is more consistent, though a gradual but smooth decline is recorded over the duration of the run. As shown in Figure 5.45 above, at a H_2/CO molar ratio of 1.6 intermittent short periods of very low CO conversion are observed in comparison to the runs performed at higher H_2/CO molar ratios. This indicates that under the reaction conditions used in the 20cm^3 reactor with the Co/Al_2O_3 catalyst a H_2/CO molar ratio of 1.6 is not recommended for operation. At a H_2/CO molar ratio of 1.8 the catalyst displays a relatively stable behaviour up to

approximately 36 hours of reaction time, at which point the activity begins to rapidly decline over the last 12 hours of the run. The decline in catalyst activity recorded during the runs at H₂/CO molar ratios of 1.8 and 2.0 can be attributed to deactivation by the carbon and wax deposition mechanisms discussed previously in section 5.3.1.7. However, the reasons for the rapid decline in catalyst activity recorded at a H₂/CO molar ratio of 1.8 are not known. Further investigation is required, therefore, in order to justify this observed behaviour, including repetition of the FT synthesis runs performed at H₂/CO molar ratios in the range of 1.6-2.0 (FT7, FT14 and FT15 in Table 5.1 in section 5.1.6), as well as additional experimental runs covering a wider range of H₂/CO molar ratios (e.g. H₂/CO = 1.0-3.0), as discussed previously in section 5.3.4.4.

The influence of the H₂/CO molar ratio in the feed syngas on the extent of the above deactivation mechanisms was examined by TGA analysis as previously outlined in section 3.6.4. The mass loss results obtained from these analyses are presented in Table 5.13 below. The results show that significantly higher amounts of carbon and wax are deposited on the catalyst surface at a H₂/CO molar ratio of 1.8 in comparison to molar ratios of 1.6 and 2.0. This potentially explains the rapid decline in activity that is observed at this value (Figure 5.45 above), as the excessive deposition of carbon and wax can “block” the catalyst active sites and inhibit the progression of the reaction. SEM micrographs (at x764 magnification) of the Co/Al₂O₃ catalyst before and after reaction in runs FT7, FT14 and FT15 (Table 5.1 in section 5.1.6) are provided in APPENDIX B. Small differences can be seen in these micrographs, however, the magnification strength used was not sufficient in order to allow for definite conclusions to be drawn. Higher magnification strengths are therefore recommended for future investigation.

Table 5.13 – Influence of the H₂/CO molar ratio in the syngas on the extent of carbon and wax deposition on the catalyst surface (TGA results)

Catalyst Sample Origin	H ₂ /CO	Total Mass Loss (wt.% dry basis)	Mass Loss Due to Carbon & Wax Deposition (wt.%)
Co/Al ₂ O ₃ before Reaction	-	4.7	-
FT14	1.6	41.9	37.2
FT15	1.8	55.5	50.8
FT7	2.0	40.3	35.6

5.3.4.8 H₂/CO Molar Ratio Selection for Further Experiments

Under the reaction conditions used (Table 5.1 in section 5.1.6) in the present study, a H₂/CO molar ratio of 1.6 results in poor catalyst performance and is, therefore, not recommended for operation on the 20cm³ reactor. Despite this, the liquid hydrocarbons collected at this lower H₂/CO molar ratio had a more favourable fuel composition (high diesel, low naphtha contents) than those collected at a higher H₂/CO molar ratio of 2.0. Maximum liquid hydrocarbon yields and the most

favourable fuel product composition were obtained at a H₂/CO molar ratio of 1.8, indicating that chain growth reactions are enhanced at H₂/CO molar ratios in the range of 1.8–2.0. The activity of the catalyst at a H₂/CO molar ratio of 1.8, however, was found to rapidly decline towards the end of the run due to excessive carbon and wax deposition, ultimately leading to quicker deactivation than at a H₂/CO molar ratio of 2.0. Hence, despite the advantages of operation at a H₂/CO molar ratio of 1.8 discussed above, a H₂/CO molar ratio in the feed syngas of 2.0 is selected as the preferred value to be used for operation on the 20cm³ fixed-bed reactor in the present study, and in the final parameter profiling test set. This is because at this H₂/CO molar ratio in the feed syngas the catalyst displays more consistent activity with time on stream.

5.3.5 Influence of Catalyst Loading

Sections 5.3.1 to 5.3.4 resulted in identification of the preferred reactor temperature, reactor pressure, space velocity and H₂/CO molar ratio in the feed syngas for subsequent tests.

5.3.5.1 CO Conversion & Product Selectivity

The results obtained in the present study for the effect of catalyst loading on CO conversion and product selectivity (at 230°C, 10 bar, H₂/CO = 2.0, and WHSV = 8.8 h⁻¹) are presented in Table 5.14 below. As discussed previously in section 5.1.5, this parameter profiling test set is carried out as ‘a proof of principles’ in order to ensure that the Co/Al₂O₃ catalyst used in the present study is capable of achieving higher CO conversions and producing higher liquid fuel yields. The results from this test set are also used in calculating the mass and energy balances over the FT reactor (section 5.3.5.3). The calorific values of the liquid hydrocarbon samples collected from experiment runs FT7 and FT16 (Table 5.1 in section 5.1.6) are calculated using the method outlined previously in section 3.5.3.3 and are also provided in Table 5.14.

Table 5.14 – Influence of catalyst loading on CO conversion, product selectivity and energy content of liquid hydrocarbon products (at 230°C, 10 bar, H₂/CO = 2.0, and WHSV = 8.8 h⁻¹)

Test	Catalyst Loading (g)	CO Conversion (mol %)	Product Selectivity (mol %)				HHV (MJ/kg)
			CO ₂	CH ₄	C ₂ -C ₅	C ₆₊	
FT7	0.5	18.3	49.2	20.8	1.9	28.0	47.26
FT16	2.0	39.6	16.5	14.8	4.3	64.4	47.68

These results show that a fourfold increase in catalyst loading results in significantly higher CO conversion, and higher C₂-C₅ and C₆₊ hydrocarbon selectivities, but lower CO₂ and CH₄ selectivities. As the same feed syngas mass flow rate conditions are used in both experiments (FT7 and FT16 in Table 5.1 in section 5.1.6) these results are expected. This is because a higher catalyst loading corresponds to a longer catalyst bed height and, therefore, a lower space velocity and a higher residence time in the catalyst bed. This is also in agreement with the relationship that was expressed previously in Equation 3.1 in section 3.4.3.1, stating that the reactant conversion is

proportional to the catalyst weight. In turn, this results in higher reactant conversion and higher chain growth probability leading to the increased formation of heavier molecular weight hydrocarbons (C_{6+}), and conversely, a decreased production of CH_4 and low molecular weight hydrocarbons. These results indicate that under the reaction conditions implemented on the 20cm^3 reactor with the $\text{Co}/\text{Al}_2\text{O}_3$ catalyst using a higher catalyst loading of 2.0g is preferred. This is because lower CO_2 and CH_4 selectivities imply a lower requirement for FT reactor off-gas reforming, conditioning and recycling, whereas the higher C_{6+} hydrocarbon selectivity can be considered equivalent to higher yields of once-through liquid hydrocarbon products (as discussed previously in section 5.2.1). Once again, although very slight differences in calorific value are observed as the catalyst loading is increased, these results show that the energy content of the liquid hydrocarbons is not significantly influenced by variation in the catalyst loading.

5.3.5.2 Product Yields

The methods used for calculating the product yields were previously outlined in section 3.7.4.2. The unreacted syngas is calculated by difference. The product yields obtained in this parameter test set (Table 5.1 in section 5.1.6) reflect the results for CO conversion and product selectivity for the different catalyst loadings presented previously in Table 5.14 (section 5.3.5.1 above), and are provided in Table 5.15 below.

Table 5.15 – Influence of catalyst loading on FT gas and liquid product yields (at 230°C , 10 bar, $\text{H}_2/\text{CO} = 2.0$, and $\text{WHSV} = 8.8\text{ h}^{-1}$)

Test	Catalyst Loading (g)	Product Yields (wt.%)					Oxyg. In Water (wt.%)	Unreacted Syngas (wt.%)
		CO_2	CH_4	$\text{C}_2\text{-C}_5$	Liquid H/C's + Waxes	Water + Oxyg.		
FT7	0.5	7.5	1.2	0.3	2.2	3.6	3.7	85.2
FT16	2.0	7	2.3	2.2	5.1	14.2	1.6	69.2

As discussed previously in section 5.3.5.1, higher catalyst loading results in higher reactant conversion and higher chain growth probability leading to the increased formation of heavier molecular weight hydrocarbons (C_{6+}), and a decreased production of lower molecular weight hydrocarbons. This is reflected in the results presented in Table 5.15 above, which show that a higher catalyst loading results in higher yields of liquid hydrocarbons (plus waxes). Although higher yields of both CH_4 and $\text{C}_2\text{-C}_5$ hydrocarbons are obtained when a higher catalyst loading is used, these figures are still in relative proportion to those obtained at the lower catalyst loading. The yield of water (containing soluble oxygenated compounds) increases in direct proportion to the catalyst loading, where a fourfold increase in yield is observed. A small decrease in the yield of CO_2 is observed as the catalyst loading is increased, indicating that the WGS equilibrium reaction (Equation 2.2 section 2.2), through which water and/or CO_2 are produced, shifts towards the formation of water rather than CO_2 as higher CO conversions are achieved. The reduction in the

concentration of soluble oxygenated compounds in the water when the catalyst loading is increased may be due to the higher chain growth probability, which would result in heavier molecular weight products (including heavier molecular weight oxygenated compounds which are not soluble in water, as discussed previously in section 2.2). However, this reduction in the concentration of soluble oxygenated compounds may also be simply due to the increased yield of water.

The results presented in Table 5.15 above, indicate that under the reaction conditions implemented in the 20cm³ reactor using the Co/Al₂O₃ catalyst in the present study, a higher catalyst loading of 2.0g is preferred because higher yields of once-through liquid hydrocarbon products are obtained. These results are further demonstrated in Figure 5.46 below, which illustrates the influence of catalyst loading on the ratio of liquid products to gas products (excluding unreacted syngas), showing that significantly higher ratios of total liquid products to gas products (1.69) and liquid hydrocarbons to gas products (0.45) are obtained at a higher catalyst loading of 2.0g.

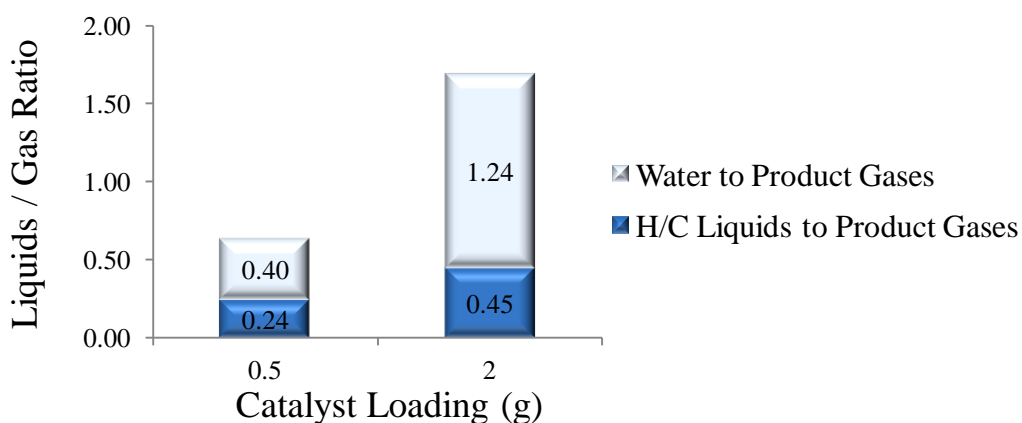


Figure 5.46 – Influence of catalyst loading on the ratio of liquid products to product gases (at 230°C, 10 bar, H₂/CO = 2.0, and WHSV = 8.8 h⁻¹)

5.3.5.3 Mass and Energy Balances

The methods used for calculating the mass balance over the reactor during test run FT16 (Table 5.1 in section 5.1.6) were previously outlined in section 3.7.4.2. The energy balance calculations and the assumptions made are provided in APPENDIX E. The results of these balances are presented in Table 5.16 below.

**Table 5.16 – Mass and energy balances over 20 cm³ reactor at Aston
(test FT16 at 230°C, 10 bar, WHSV = 8.8 h⁻¹, H₂/CO = 2.0, and m_{cat} = 2.0g)**

Component	CO	H ₂	N ₂	CO ₂	CH ₄	C ₂ -C ₅	Liquids H/C's	Water	Total
Total Mass IN (kg)	0.144	0.024	0.045	0	0	0	0	0	0.213
Total Mass OUT (kg)	0.087	0.015	0.045	0.015	0.005	0.005	0.011	0.030	0.213
Mass flow rate IN (x 10⁻⁷ kg/s)	8.27	1.34	2.61	0	0	0	0	0	12.2
Mass flow rate OUT (x 10⁻⁷ kg/s)	4.99	0.86	0.26	0.85	0.28	0.26	0.62	1.73	12.2
C_p @ 215°C (x 10⁻³ MJ/kg/K)	1.06	14.50	1.05	1.01	2.84	2.55	-	1.87	-
HHV(MJ/kg)	10.10	141.80	-	-	55.54	49.96	47.52	-	-
Energy IN (W)	8.51	19.30	0.05	0	0	0	0	0	27.86
Energy OUT (W)	5.16	12.50	0.06	0.02	1.56	1.33	2.95	0.07	23.65

As discussed previously in section 3.7.4.2, a sample of the gases leaving the reactor was automatically injected at hourly intervals into the online GC for analysis. Hence, the values obtained from these analyses for the molar composition of the product gases at the time of each injection are assumed to be constant for each hour in between the sample injections. This introduced an error in the mass balance calculations as the reactant conversion calculations were based on this hourly molar composition which may not have been constant, especially at the beginning of the reaction as the catalyst activity is not yet stable. In addition, it is assumed that all the water (containing soluble oxygenated compounds), liquid hydrocarbons and wax produced during the reaction were condensed in the GLSs (Figure 3.4 in section 3.4) and collected. However, this is not accurate as there would be losses of these products as volatiles in the vapours leaving the reactor system. To account for these losses, therefore, the unreacted syngas during the reaction was calculated by difference, giving a 100% closure on the mass balance as shown in Table 5.16 above. The mass loss associated with these products, however, has an influence on the energy balance calculations, as the energy they contain is unaccounted for, resulting in energy losses as shown in Table 5.16.

5.3.5.4 Energy Content and Composition of Liquid Hydrocarbon Products

A representative photograph of the liquid products, consisting of a liquid hydrocarbon phase (plus waxes) and a water phase (containing soluble oxygenated compounds), collected from the catalyst loading profile tests (tests FT7 and FT16 listed in Table 5.1 in section 5.1.6) was provided in Figure 5.7 in section 5.3.1.6. The product analysis methods were described in sections 3.5.3.1 and 3.7.4.2. Figure 5.47 and Figure 5.48 below, show the GC-MS chromatograms of the liquid hydrocarbons that were obtained at the two different values for catalyst loading investigated in tests FT7 and FT16, respectively.

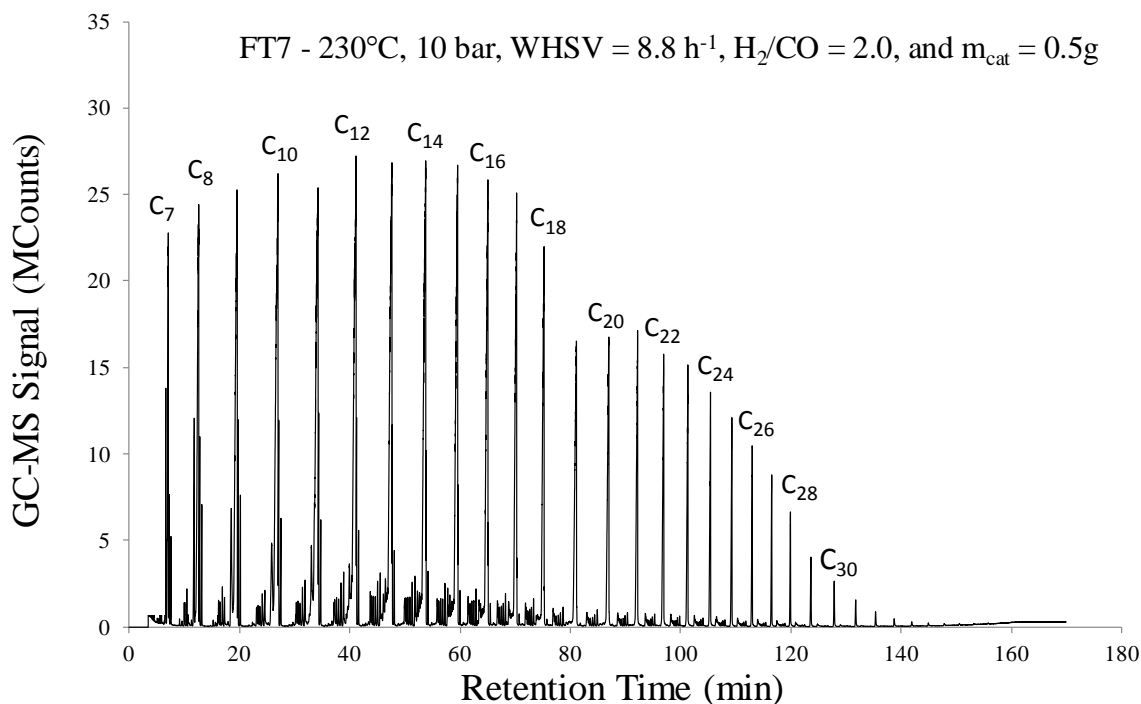


Figure 5.47 – GC-MS chromatogram of liquid hydrocarbons collected from catalyst loading profile test FT7 at 0.5g

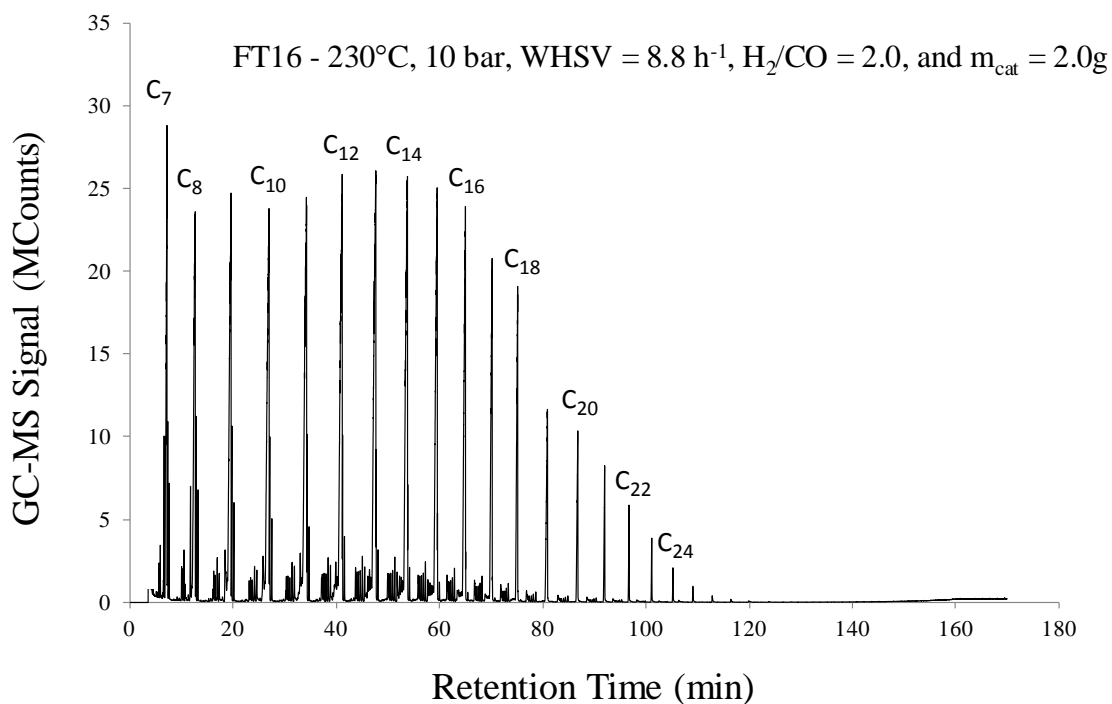


Figure 5.48 – GC-MS chromatogram of liquid hydrocarbons collected from catalyst loading profile test FT16 at 2.0g

The relative fuel compositions of the liquid hydrocarbons collected are calculated from the chromatograms in the figures above, using the method outlined in section 3.5.3. The results are illustrated in Figure 5.49 below.

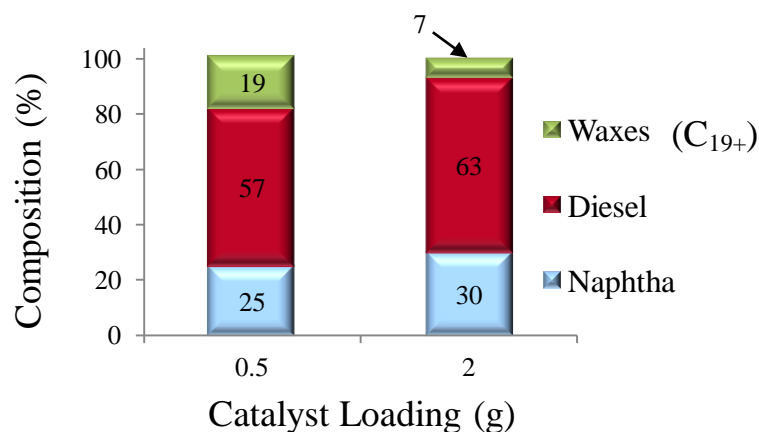


Figure 5.49 – Influence of catalyst loading on liquid hydrocarbon product composition (at 230°C, 10 bar, H₂/CO = 2.0, and WHSV = 8.8 and 2.2 h⁻¹, respectively)

These results show that the higher catalyst loading gives a liquid hydrocarbon fuel with a significantly higher diesel composition, but contains a higher proportion of naphtha grade products at the expense of high molecular weight compounds (C₁₉₊ waxes). Nevertheless, because of the higher liquid hydrocarbon yields (as well as the higher diesel composition) obtained at this higher catalyst loading, a catalyst mass of 2.0g is preferred for operation in the 20cm³ reactor using the Co/Al₂O₃ catalyst under the reaction conditions implemented in the present study.

5.3.5.5 Catalyst Stability

The stability of the catalyst, in terms of CO conversion versus time on stream, over the duration of the synthesis experiments using different catalyst loadings is compared in Figure 5.50 below. The initial ‘spikes’ in CO conversion observed in both runs at different catalyst loadings are due to the exothermic nature of the reaction explained previously in section 5.3.1.7.

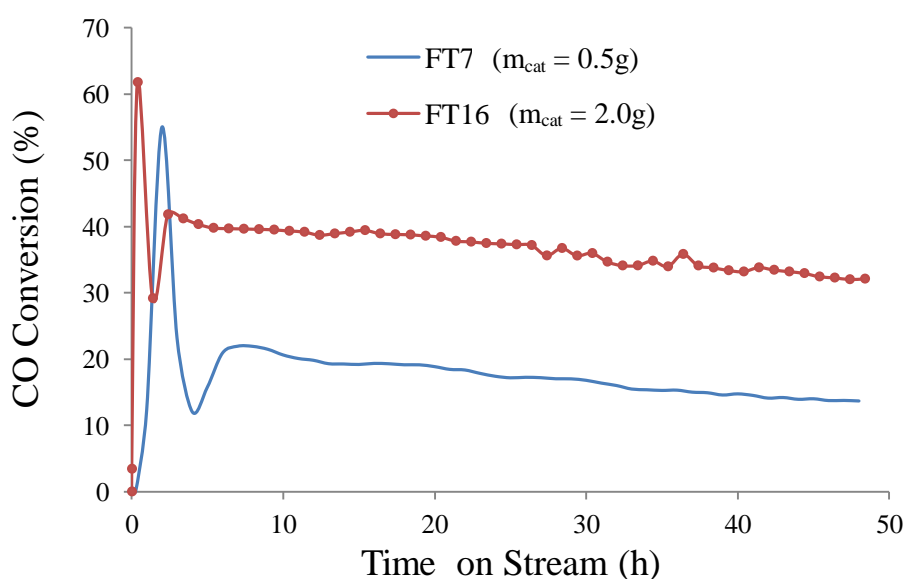


Figure 5.50 – Influence of catalyst loading on catalyst stability: CO conversion versus time on stream (at 230°C, 10 bar, H₂/CO = 2.0 and WHSV = 8.8 and 2.2 h⁻¹, respectively)

As illustrated in Figure 5.50, steady and higher CO conversion is achieved faster when the higher catalyst loading is used. Despite these differences, the activity profiles recorded for the different catalyst loadings are quite comparable, although the absolute values are not. A similar decline in catalyst activity is also recorded over the duration of each experiment which can be attributed to deactivation by the carbon and wax deposition mechanisms discussed previously in section 5.3.1.7. The influence of catalyst loading on the extent of these deactivation mechanisms is examined by TGA analysis as previously outlined in section 3.6.4. The mass loss results obtained from these analyses are presented in Table 5.17 below.

Table 5.17 – Influence of catalyst loading on the extent of carbon and wax deposition on the catalyst surface (TGA results)

Catalyst Sample Origin	Catalyst Loading (g)	Total Mass Loss (wt.% dry basis)	Mass Loss Due to Carbon & Wax Deposition (wt.%)
Co/Al ₂ O ₃ before Reaction	-	4.7	-
FT7	0.5	40.3	35.6
FT16	2.0	43.7	39.0

These results show that slightly higher amounts of carbon and wax are deposited on the catalyst surface when a higher catalyst loading of 2.0g is used. However, this difference is possibly justified by the higher CO conversions, as well as the higher activity that was achieved faster at the higher catalyst loading (Figure 5.50 above), allowing more time for carbon and wax deposition on the catalyst surface than at the lower catalyst loading. In addition, the gradual deactivation observed during the runs using different catalyst loadings, shown in Figure 5.50 above, followed similar (or parallel) declining trends, indicating that catalyst loading does not significantly influence catalyst deactivation.

5.3.5.6 Selection of Preferred Catalyst Loading

Under the reaction conditions used in the present study (Table 5.1 in section 5.1.6), a higher catalyst loading of 2.0g compared to 0.5g, results in more than doubling CO conversion, C₆₊ hydrocarbon product selectivity and liquid hydrocarbon yields. Similar overall trends in catalyst activity and deactivation patterns were also recorded at both catalyst loadings used. The selectivities of both CO₂ and CH₄ were significantly reduced when higher catalyst loading was used. A fivefold increase in the yield of water (containing soluble oxygenated compounds) was also observed, contributing to significantly higher liquid to gas product ratios, which are favourable from a processing perspective. A marked increase in the diesel composition of the liquid hydrocarbons obtained, from 57 to 63%, was also observed at the higher catalyst loading. Hence, under the reaction conditions implemented in the 20cm³ reactor with the Co/Al₂O₃ catalyst in the present study, using a higher catalyst loading of 2.0g is preferred.

5.3.6 Comparison of Effect of Parameters on Performance Criteria

The influence of the parameters studied in section 5.3 on the performance criteria discussed previously in section 5.2, including CO conversion, product selectivity, and the yield and composition of the liquid hydrocarbon products are compared in sections 5.3.6.1 and 5.3.6.3 below.

5.3.6.1 CO Conversion Criterion

Figure 5.51 below summarizes the influence of each parameter investigated in section 5.3 on CO conversion, which increased with increasing reactor temperature and reactor pressure, as well as increasing H₂/CO molar ratio in the feed syngas and catalyst loading. The opposite trend was observed, however, with increasing space velocity. Although all the parameters studied influenced CO conversion in varying degrees, it was found that reactor temperature and catalyst loading had the most significant effect on CO conversion, as shown in Figure 5.51 below.

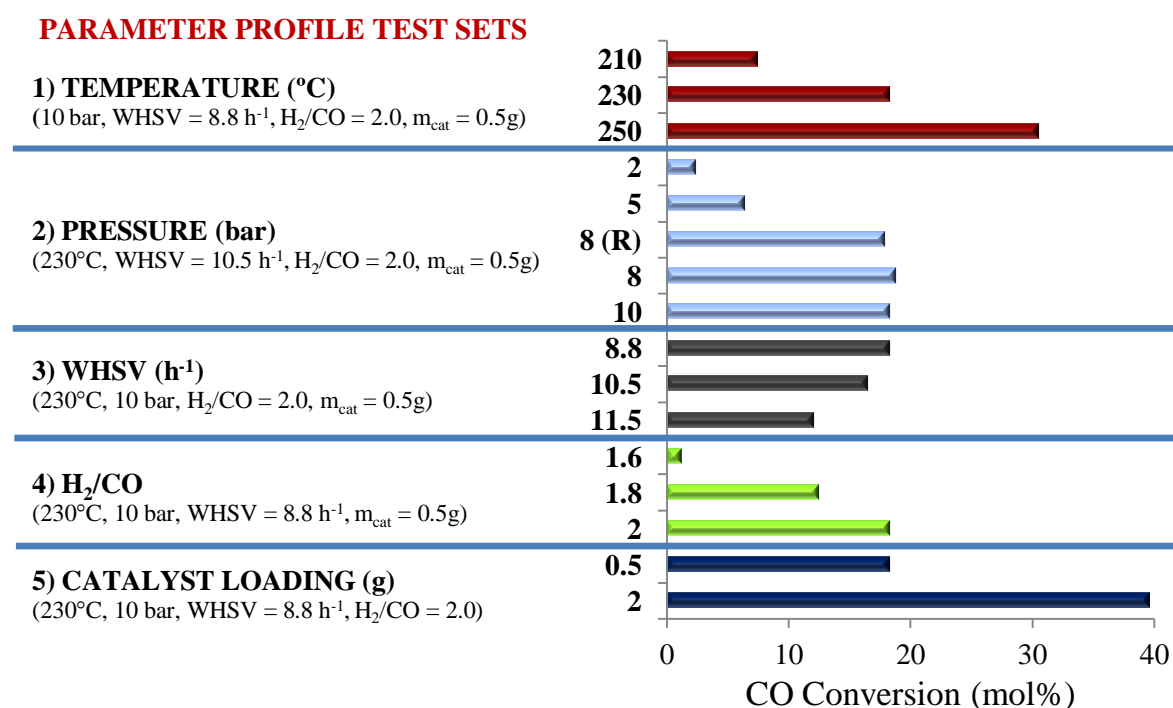


Figure 5.51 – Comparison of influence of parameters investigated on CO conversion

The highest CO conversion was observed at the following set of reaction conditions: (T = 230°C, P = 10 bar, WHSV = 2.2 h⁻¹, H₂/CO = 2.0 and m_{cat} = 2.0g). Higher CO conversions could potentially have been achieved under similar conditions but at the higher temperature of 250°C that was investigated. As discussed previously in section 5.3.1.7, however, operation at 250°C was not recommended using the Co/Al₂O₃ catalyst in the 20cm³ reactor in the present study. This was due to the equipment limitation related to reactor temperature control (outlined in section 3.4.3.3) that led to a temperature runaway during the FT run conducted at 250°C (FT8 in Table 5.1 in section 5.1.6).

5.3.6.2 Product Selectivity Criterion

CO₂ selectivity was found to decrease with increasing reactor temperature, reactor pressure, H₂/CO molar ratio in the feed syngas and catalyst loading, whereas as the opposite trend was observed with increasing space velocity. CH₄ selectivity was found to increase with increasing reactor temperature and H₂/CO molar ratio in the feed syngas, whereas an increase in reactor pressure, space velocity and catalyst loading resulted in lower CH₄ selectivities. Although much lower figures were obtained for C₂-C₅ hydrocarbon selectivity than CH₄ selectivity, the trends observed for C₂-C₅ selectivity with increasing reactor temperature and reactor pressure were similar, whereas the opposite trends to CH₄ selectivity with increasing space velocity, H₂/CO molar ratio in the feed syngas and catalyst loading were observed for C₂-C₅ selectivity.

Figure 5.52 below, summarizes the influence of each parameter investigated on C₆₊ hydrocarbon selectivity, which increased with increasing reactor temperature, reactor pressure and catalyst loading. The opposite trends, however, were observed with increasing space velocity and H₂/CO molar ratio in the feed syngas. The highest C₆₊ hydrocarbon selectivity was observed when a low H₂/CO molar ratio in the feed syngas of 1.6 (test set 4 in Figure 5.52 below) was implemented. However, these conditions resulted in poor CO conversion and low yields of liquid hydrocarbons, as shown in Figure 5.51 above and further down in Figure 5.53, respectively. Therefore, the next highest value for C₆₊ hydrocarbon selectivity was observed at the following set of conditions: (T = 230°C, P = 10 bar, WHSV = 2.2h⁻¹, H₂/CO = 2.0 and m_{cat} = 2.0g).

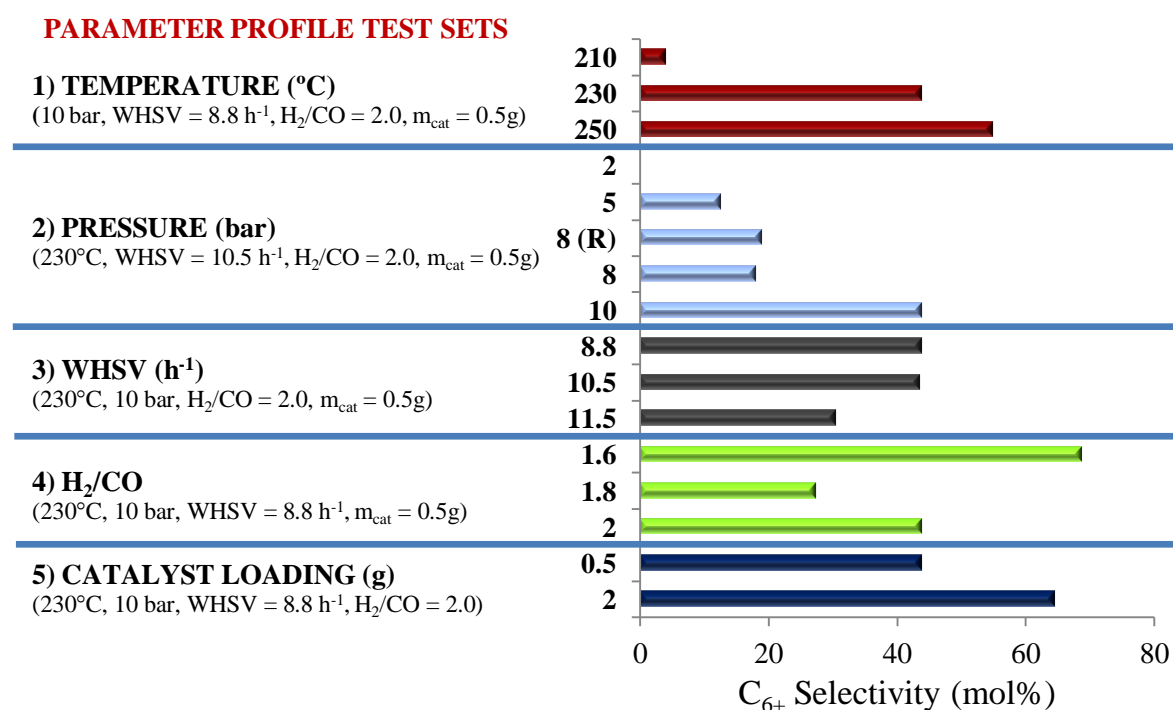


Figure 5.52 – Comparison of influence of parameters investigated on C₆₊ selectivity

5.3.6.3 Liquid Hydrocarbons – Yields and Composition Criteria

Figure 5.53 below, summarizes the influence of each parameter investigated on the yield of liquid hydrocarbons (plus C₁₉₊ waxes) obtained. These yields were found to increase with increasing reactor temperature, reactor pressure, catalyst loading and H₂/CO molar ratio in the feed syngas, whereas the opposite trend was observed with increasing space velocity. Low liquid hydrocarbon yields were obtained at 210°C (test FT4 in Table 5.1 in section 5.1.6) and when a H₂/CO molar ratio of 1.6 was used (test FT14 in Table 5.1 in section 5.1.6), whereas no liquid hydrocarbons were collected at the low reactor pressure of 2 bar investigated (test FT9 in Table 5.1 in section 5.1.6).

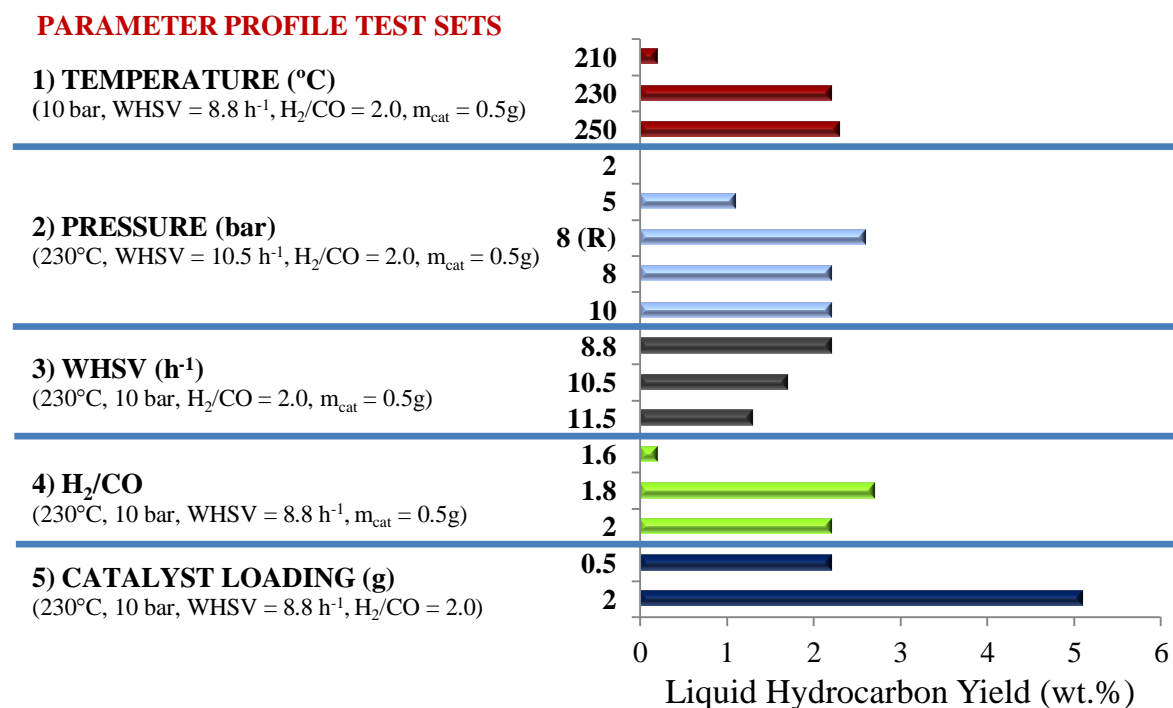


Figure 5.53 – Comparison of influence of parameters on liquid hydrocarbon yields

The composition of the liquid hydrocarbons collected was not significantly influenced by variation in the reaction parameters that were investigated in terms of their fuel content (naphtha, diesel and C₁₉₊ waxes). Small changes in this composition were observed as the reactor pressure, space velocity and H₂/CO molar ratio in the feed syngas were varied, whereas slightly more significant changes in this composition were observed with increasing reactor temperature and catalyst loading. An increase in reactor temperature resulted in gradually increasing naphtha (C₇-C₁₀) contents, and conversely, lower diesel and C₁₉₊ wax contents. An increase in catalyst loading resulted in a considerably higher diesel composition, but this was at the expense of a higher naphtha composition and, equally, a much lower composition of C₁₉₊ waxes.

5.3.7 Summary of Results

The parameter study results discussed in section 5.3 are summarized in Table 5.18 below. The influence of increasing the parameters investigated on CO conversion, C₆₊ selectivity, liquid hydrocarbon yield and liquid hydrocarbon composition are summarized in Table 5.19 below.

Table 5.18 – Parameter study results

Experiment	FT4	FT7	FT8	FT9	FT10	FT11	FT11 (REP)	FT12	FT13	FT14	FT15	FT16
Catalyst Loading (g)	0.5	0.5	0.5	0.5	0.5	0.5	0.5	0.5	0.5	0.5	0.5	2.0
Pressure (bar)	10	10	10	2	5	8	8	10	10	10	10	10
Temperature (°C)	210	230	250	230	230	230	230	230	230	230	230	230
WHSV (h ⁻¹)	8.8	8.8	8.8	8.8	8.8	8.8	8.8	10.5	11.5	8.8	8.8	8.8
H ₂ /CO	2.0	2.0	2.0	2.0	2.0	2.0	2.0	2.0	2.0	1.6	1.8	2.0
CO Conversion (mol%)	7.4	18.3	30.5	2.4	6.4	18.8	17.8	16.5	12.1	1.2	12.5	39.6
CO ₂ Selectivity (mol%)	88.7	38.4	18.9	72.1	47.8	47.7	49.0	45.4	59.2	30.1	57.4	16.5
CH ₄ Selectivity (mol%)	6.1	16.3	22.2	23.7	33.9	30.7	29.3	7.8	9.6	1.1	13.4	14.8
C ₂ -C ₅ Selectivity (mol%)	1.2	1.5	4.1	4.2	5.8	3.6	2.9	1.5	2.6	0.0	1.9	4.3
C ₆₊ Selectivity (mol%)	4.0	43.8	54.8	0	12.6	17.9	18.8	43.5	30.4	68.8	27.4	64.4
CO ₂ Yield (wt.%)	7.0	7.5	6.1	16.5	9.3	9.3	8.9	8.4	8.0	9.0	7.8	7.0
CH ₄ Yield (wt.%)	0.2	1.2	2.6	0.2	0.8	2.2	2.9	0.6	0.8	0.1	0.7	2.3
C ₂ -C ₅ Yield (wt.%)	0.1	0.3	1.6	0.1	0.5	1.1	2.0	0.4	0.5	0.1	0.3	2.2
Liquid h/c Yield (wt.%)	0.2	2.2	2.3	0	1.1	2.2	2.6	1.7	1.3	0.2	2.7	5.1
Water + Oxyg. Yield (wt.%)	1.3	3.6	7.8	0	2.9	3.9	4.3	2.7	2.4	0.4	3.7	14.2
Unreacted Syngas (wt.%)	91.2	85.2	79.6	83.2	85.4	81.3	79.3	86.2	87.1	90.2	84.8	69.2
Oxygenates in Water (wt.%)	3.8	3.7	2.5	0	9.4	7.4	8.1	2.7	1.7	2.1	5.1	1.6
Naphtha in h/c Liquids (%)	19	24	35	0	22	26	25	24	24	23	22	30
Diesel in h/c Liquids (%)	62	57	55	0	57	58	59	59	56	57	59	63
C ₁₉₊ waxes in h/c Liquids (%)	19	19	10	0	21	16	16	17	20	20	19	7

Table 5.19 – Parameter study results summary: Influence of increasing reaction parameters on CO conversion, product selectivity and yield of liquid hydrocarbons

Increasing Parameter	CO Conversion (mol%)	Product Selectivity (mol%)				Liquid Hydrocarbon Yield (wt.%)
		CO ₂	CH ₄	C ₂ -C ₅	C ₆ +	
Temperature	↑	↓	↑	↑	↑	↑
Pressure	↑	↓	↓	↓	↑	↑
WHSV	↓	↑	↓	↑	↓	↓
H ₂ /CO	↑	↑	↑	↑	↓	↓
Catalyst Loading	↑	↓	↓	↑	↑	↑

5.4 Economic Impact

The results of the parameter study showed that reactor temperature and catalyst loading had the most significant effect on liquid hydrocarbon yields. An increase in reactor temperature in the range investigated resulted in higher liquid hydrocarbon yields. Even though only a small increase in yields was observed above 230°C, operation at higher reactor temperatures in the range studied would be preferred in an industrial context. Cost reduction estimates for operation at higher reactor temperatures in the range studied can be drawn from the same step count estimating procedures used in section 2.5.2 for estimating cost reduction for process operation at lower pressures. These calculations show that an increase in operating temperature from one extreme to the other in the range studied would only result in less than a 2% increase in investment. The cost implications of process operation at higher reactor temperatures in the range studied, therefore, are insignificant. An increase in catalyst loading in the reactor led to a considerable increase in liquid hydrocarbon yields; a fourfold increase in catalyst loading resulted in more than 100% increase in yield. The typical cost of standard FT cobalt-based catalysts as reported by Swanson *et al.* [92] are approximately \$33/kg. These costs are trivial in comparison to the total process investment required. In addition, the benefit of a significant increase in liquid hydrocarbon yields favours the use of higher catalyst loading in the FT reactor.

Although the results of the parameter study showed that the influence of reactor pressure on liquid hydrocarbon yields was not as marked as that of reactor temperature and catalyst loading, industrially the operating pressure has a much more significant impact on the process economics. This impact on capital costs was discussed previously in section 2.5.2, where it was seen that a reduction of up to 60% in capital costs could potentially be realised if the working pressure is reduced from 25 bar down to 5 bar. According to a techno-economic assessment on the production of FT transportation fuels from biomass carried out by Hamelinck *et al.* [12], the total investment required for a BTL-FT process (where an oxygen-blown gasifier is operated at 25 bar and a 90% total syngas conversion is achieved by means of FT off-gas recycling) was reported to be approximately €320 million. Based on this indicative figure, as well as the assumption made above

that a 60% cost reduction can potentially be realised if the process is operated at a lower pressure, process operation at 5 bar would require a significantly lower investment of €128 million. For process operation at a pressure of 10 bar, a simple extrapolation shows that the total investment required would be €176 million; an increase of approximately 40% in capital cost in comparison to process operation at 5 bar. The results of the parameter study showed that variation in reactor pressure in the range studied did have a significant influence on the liquid hydrocarbon yields, which increased by 100% when the reactor pressure was increased from 5 to 10 bar. Based on these results, the capital cost figures signify that process operation at 10 bar would be preferred as the liquid hydrocarbon yields are doubled at the expense of only a 40% increase in investment.

Despite the 100% increase in the yield of liquid hydrocarbons observed when the reactor pressure was increased from 5 to 10 bar, however, the results of the parameter study showed that operation at low reactor pressures (2-10 bar) results in low CO conversions and low liquid hydrocarbon yields with the Co/Al₂O₃ catalyst tested. However, the composition and the calorific value (which was higher than that of conventional diesel) of these liquid hydrocarbon products were not significantly influenced by variation in reactor pressure (or variation in any of the other parameters studied for that matter). This implies that one of the aims of this project for obtaining an intermediate FT synthetic crude liquid product that can be integrated into existing refineries is potentially feasible, irrespective of the reactor pressure implemented within the range studied. Potentially higher CO conversions and product yields could have been obtained in the present study if the limitations relating to minimum possible syngas flow rate, catalyst availability, and reactor temperature control (discussed previously in section 3.4.3) did not exist. Relatively low CO conversions and C₆₊ selectivities were also reported in similar studies that also investigated the influence of low FT operating pressures (discussed previously in sections 5.3.3.1 to 5.3.3.4). However, these studies failed to report on the actual yields of liquid hydrocarbons obtained, but the C₆₊ hydrocarbon selectivities they report can serve as an indication for catalyst performance. Hence, the results reported by these studies, as well as those reported in the present study, indicate that operation at low reactor pressures may not be viable for application in BTL-FT processes, as the trade off in lower CO conversions and lower once-through liquid hydrocarbon product yields has to be carefully weighed against the cost savings that can potentially be realised from process operation at lower pressures. Therefore, a techno-economic analysis comparing the capital, operating and production costs of BTL-FT processes at both low and conventional (high) pressure operation (of both gasifier and FT reactor) is recommended for future investigation.

5.5 Chapter Conclusions

The parameter study discussed in this chapter was carried out using the Co/Al₂O₃ catalyst (selected in the catalyst screening procedure described in chapter 4). Sections 5.3.1 to 5.3.5 discussed the effect of the process parameters investigated on catalyst performance criteria, including CO conversion, product selectivity, product yields, liquid hydrocarbon product composition and catalyst stability, whereas section 5.3.6 compared the influence of the process parameters investigated on these performance criteria. The conclusions that were made based on the results found are discussed in the following paragraphs.

The parameters that had the most significant influence on CO conversion, product selectivity and liquid hydrocarbon yields were reactor temperature and catalyst loading. Operation at higher reactor temperatures in the range studied (210-250°C) is more favourable, in terms of process efficiency, as higher yields of once-through liquid hydrocarbon products are produced, whereas the content of CO₂ and light hydrocarbon gases is lower. In addition, operation at higher reactor temperatures results in more steady catalyst activity over longer periods of time, as catalyst deactivation due to carbon and wax deposition is reduced. The magnification strength used for SEM analysis was not sufficient for definite conclusions to be drawn on the influence of the reaction parameters investigated on the extent of carbon and/or wax deposition on the catalyst surface. However, TGA analysis proved to be a helpful technique in examining the extent of these catalyst deactivation mechanisms. Increased catalyst loading was found to increase the composition of diesel-grade products in the liquid hydrocarbon product.

Although space velocity did not have a significant influence on CO conversion, product selectivity and liquid hydrocarbon yields, the range of space velocities implemented in the present study were considerably high (due to system limitations) resulting in lower CO conversions and liquid yields. H₂/CO molar ratios in the feed syngas above 1.8 are recommended for operation with the Co/Al₂O₃ catalyst. The calorific value of the liquid hydrocarbons collected was not significantly influenced by variation in any of the reaction parameters investigated. The average calorific value (HHV) of these hydrocarbon liquids was found to be approximately 47.5 MJ/kg which is considerably higher than that of conventional diesel (~43MJ/kg).

Within the range of reactor pressures investigated (2-10 bar), reactor pressure does not have a significant effect on CO conversion and liquid hydrocarbon yields above 8 bar. Operation at 2 bar is not recommended due to low catalyst activity and no liquid hydrocarbon product formation. Generally, operation at the low range of reactor pressures investigated results in low CO conversions and liquid hydrocarbon yields, but could potentially be higher if the system limitations did not exist. Comparison of the liquid hydrocarbon yields obtained in the present study to results from similar studies in the literature was not possible as yield data is not commonly provided. The

composition and the calorific value of the liquid hydrocarbons are not significantly affected by variation in reactor pressure in the range studied. Hence, there is potential for obtaining an intermediate FT synthetic crude liquid product that can be integrated into existing refineries if the CO conversions and liquid hydrocarbon yields can be increased at the low range of reactor pressures investigated. The low liquid hydrocarbon yields obtained in the range of reactor pressures studied, however, indicate that operation at low pressures may not be industrially viable as the trade off in lower CO conversions and once-through liquid hydrocarbon product yields has to be carefully weighed against the potential cost savings resulting from process operation at lower pressures.

The following set of reaction conditions were identified as the preferred values for operation with the Co/Al₂O₃ catalyst on the 20cm³ reactor: T = 230°C, P = 10 bar, H₂/CO = 2.0, WHSV = 2.2 h⁻¹, and catalyst loading = 2.0g.

6 Conclusions

This chapter summarizes the major conclusions that were drawn from the work that was carried out.

6.1 Evaluation and Comparison of Available Catalysts

The three catalysts that were available for this project, Co/Al₂O₃, Co/TiO₂ and Fe/Al₂O₃, were compared in the catalyst screening procedure outlined in chapter 4, resulting in the following conclusions:

- Temperature programmed reduction (TPR) was one of the most important and useful catalyst characterization techniques used.
- The complete online FT product GC analysis method at UFRJ proved to be a more convenient and accurate approach for determining the hydrocarbon product composition than the GC analysis methods used at Aston. However, complete mass balances were more easily performed at Aston.
- The Fe/Al₂O₃ catalyst produced mainly methane and light hydrocarbon gases (C₁-C₅) in both the 2cm³ and the 20cm³ reactor systems. It was concluded, therefore, that the Fe/Al₂O₃ catalyst was not suitable for further application in this work.
- The Co/TiO₂ catalyst produced mainly solid waxes and was not suitable for operation on the 20cm³ reactor at Aston.
- The Co/Al₂O₃ catalyst produced liquid hydrocarbons (no solid waxes) with a high composition of diesel-grade products and was selected as the most suitable catalyst, from the three that were available, for operation on the 20cm³ fixed-bed reactor at Aston.

6.2 Parameter Study

The influence of a range of process parameters (including reactor temperature, reactor pressure, space velocity, H₂/CO molar ratio in the feed syngas and catalyst loading) on the performance of the selected Co/Al₂O₃ catalyst was assessed in terms of five main criteria (which included CO conversion, catalyst stability, product selectivity, product yields and the composition of the liquid hydrocarbon products obtained), resulting in the following conclusions:

- The results obtained for CO conversion and product selectivities were in general agreement with those reported in similar studies found in the available literature. In the cases where the results for product selectivity are different from reported literature, this is attributed to the difference in reaction conditions and/or catalysts implemented.

- Reactor temperature and catalyst loading had the most significant influence on CO conversion, product selectivity and liquid hydrocarbon yields.
- Higher reactor temperatures are more favourable, in terms of process efficiency, as higher yields of once-through liquid hydrocarbon products are produced, whereas the content of CO₂ and light hydrocarbon gases is lower.
- In addition, catalyst activity with time on stream is higher and more consistent at higher reactor temperatures in the range studied, as catalyst deactivation due to carbon and wax deposition is reduced.
- A clear indication of the extent of carbon and/or wax deposition on the Co/Al₂O₃ catalyst surface after reaction could not be provided by means of the SEM micrographs taken as the magnification strength used for SEM analysis was not sufficient. However, TGA analysis proved to be a helpful technique in examining the extent of these catalyst deactivation mechanisms.
- Increased catalyst loading increases the composition of diesel-grade products in the liquid hydrocarbon product.
- Although space velocity did not have a significant influence on CO conversion, product selectivity and liquid hydrocarbon yields, the range of space velocities implemented in the present study were too high (due to system limitations) resulting in lower CO conversions and liquid yields than potentially possible.
- H₂/CO molar ratios in the feed syngas greater than 1.8 are recommended for operation with the Co/Al₂O₃ catalyst.
- The calorific value of the liquid hydrocarbons collected was not significantly influenced by variation in any of the reaction parameters investigated. The average calorific value (HHV) of these hydrocarbon liquids was found to be approximately 47.5 MJ/kg which is considerably higher than that of conventional diesel (~43 MJ/kg).
- Reactor pressure does not have a significant effect on CO conversion and liquid hydrocarbon yields above 8 bar in the range investigated. Operation at the higher reactor pressures in the range studied is recommended as higher yields of liquid hydrocarbons are obtained. Operation at 2 bar is not recommended due to low catalyst activity and no liquid hydrocarbon product formation.

- The reproducibility of the FT synthesis results was confirmed by the repeated runs at 8 bar using the 20cm³ reactor at Aston University.
- The composition and calorific value of the liquid hydrocarbons is not significantly affected by variation in reactor pressure in the range investigated. Hence, there is potential for obtaining an intermediate FT synthetic crude liquid product that can be integrated into existing refineries if the CO conversions and liquid hydrocarbon yields can be increased within the reactor pressure range studied.
- Operation in the low range of reactor pressures investigated results in low CO conversions and liquid hydrocarbon yields, which could potentially be higher if the system limitations did not exist. This indicates that operation at low reactor pressures may not be viable for application in BTL-FT processes as the trade off in lower CO conversions and once-through liquid hydrocarbon product yields has to be carefully weighed against the cost savings that could potentially be realised from process operation at lower pressures.
- The preferred reaction conditions identified for operation with the Co/Al₂O₃ catalyst on the 20cm³ reactor are: T = 230°C, P = 10 bar, H₂/CO = 2.0, WHSV = 2.2 h⁻¹, and catalyst loading = 2.0g.

7 Recommendations for Future Work

Based on the work carried out in this project the following recommendations for future investigation are proposed:

- Catalyst characterization using temperature programmed reduction (TPR) is strongly recommended for determination of the appropriate reduction temperature to be used during the catalyst activation procedure.
- Implementation of higher magnification strengths for SEM analysis of catalysts before and after FT reaction.
- The Co/TiO₂ catalyst can be used for investigation on the influence of process parameters on catalyst activity, product selectivity and liquid hydrocarbon yields. However, it needs to be reduced at an appropriate temperature as determined by TPR. This would be useful as no such studies using Co/TiO₂ catalysts have been found in the available literature. If this catalyst still forms mainly heavy waxes, a series-bed approach using a bi-functional, hydro-cracking catalyst can be considered for maximizing diesel yields.
- Examination of the influence of varying the activation procedure followed for the unpromoted Co/Al₂O₃ catalyst on catalyst activity, product selectivity and liquid hydrocarbon yields. Variations could include reduction at higher (or lower) temperatures and/or shorter (or longer) durations of catalyst activation at the reduction temperature, than the 350°C and 11 hours used in this work, respectively.
- Investigation of the influence of adding promoters, such as CaO or Au, in the Co/Al₂O₃ catalyst on the TPR profile (or reduction temperature), as well as on the product selectivity and liquid hydrocarbon yields.
- Longer FT synthesis runs are recommended and would be possible if an air compressor unit was added to the set-up thus providing a continuous air supply for pneumatic valve operation on the 20cm³ reactor. This would enable monitoring of the catalyst activity over longer periods of time, providing data on its behaviour that can more accurately relate to its application in longer-term, industrial operation.
- Better temperature control can be achieved in the 20cm³ reactor by either possibly employing a water cooling mechanism or mixing in an inert diluent material (such as silica carbide) with the catalyst in the catalyst bed, which would allow for operation at higher temperatures and therefore result in higher reactant conversions.

- Re-calibration of the nitrogen mass flow controller in the 20cm³ reactor system would be advisable so as to achieve lower gas delivery rates. Alternatively, an external gas regulator can be added to the nitrogen delivery line in order to reduce the flow rate.
- The number of experiments carried out in the parameter study using the Co/Al₂O₃ catalyst was limited by the amount of catalyst that was available for this project, as well as department access restrictions (as discussed above) and project time limitations. However, more experiments covering a wider range of values for each parameter investigated are required in order to determine the relationship for their influence on catalyst activity and stability, CO conversion, product selectivity (CO₂, CH₄, C₂-C₅ hydrocarbons and C₆₊ hydrocarbons), product yields, and liquid hydrocarbon product composition.
- More specifically, repetition of the FT synthesis runs investigating the influence of reactor temperature and H₂/CO molar ratio in the feed syngas, as well as additional runs covering a wider range of values for these parameters is recommended in order to determine the relationships for the influence of these parameters on the selectivities of CO₂ and C₆₊ hydrocarbon products. In addition, the influence of a wider range of reactor pressures (e.g. 2-20 bar) would be of interest. Repetition of the FT synthesis run conducted at 10 bar is also recommended in order to clarify the influence of reactor pressure on CO conversion at reactor pressures above 8 bar.
- Performance of a techno-economic analysis comparing the capital, operating and production costs of BTL-FT processes at both low and conventional (high) pressure operation of both gasifier and FT reactor.
- Investigation of the influence of typical syngas contaminants on the activity, product selectivity and product yields using unpromoted and/or promoted Co/Al₂O₃ catalysts (or the Co/TiO₂ catalyst as described above). To do this, pre-certified syngas mixtures in cylinders can be ordered containing a number of typical contaminants at different levels.
- Development of a GC-MS method for identification and quantification of individual peaks obtained from analysis of liquid hydrocarbons collected at the end of each FT synthesis run. Further characterization of the liquid hydrocarbons collected (e.g. density, viscosity, etc.) would also be beneficial in order to examine the influence of reaction parameters on the fuel characteristics of liquid FT fuels.
- Analysis of the water product (containing soluble oxygenated compounds) collected at the end of each FT synthesis run using a liquid chromatography technique for identification and quantification of oxygenated compounds present.

List of References

1. Fernandes, F.A.N., *Polymerization Kinetics of Fischer-Tropsch Reaction on Iron Based Catalysts and Product Grade Optimization*. Chemical Engineering Technology, 2005. **28**(8): p. 930-938.
2. Steynberg, A.P. and Dry, M.E., eds. *Introduction to Fischer-Tropsch Technology*. Fischer-Tropsch Technology, ed. G. Centi. 2004, Elsevier.
3. Shi, B. and Davis, B.H., *Fischer-Tropsch Synthesis: The Paraffin to Olefin Ratio as a Function of Carbon Number*. Catalysis Today, 2005. **106**(1-4): p. 129-131.
4. Bradshaw, M.J., *Global Energy Dilemmas: A Geographical Perspective*. Geographical Journal, 2010. **176**(4): p. 275-290.
5. Schulz, H., *Short History and Present Trends of Fischer-Tropsch Synthesis*. Applied Catalysis A: General, 1999. **186**(1-2): p. 3-12.
6. Asif, M. and Muneer, T., *Energy Supply, its Demand and Security Issues for Developed and Emerging Economies*. Renewable and Sustainable Energy Reviews, 2007. **11**(7): p. 1388-1413.
7. Huber, G.W., Iborra, S., and Corma, A., *Synthesis of Transportation Fuels from Biomass: Chemistry, Catalysts, and Engineering*. Chemical Reviews, 2006. **106**(9): p. 4044-4098.
8. Bridgwater, A.V. and Maniatis, K., *The Production of Biofuels by the Thermochemical Processing of Biomass*. Molecular to Global Photosynthesis, ed. M.D. Archer and Barber, J. 2004: IC Press.
9. Tijmensen, M.J.A., Faaij, A.P.C., Hamelinck, C.N., and van Hardeveld, M.R.M., *Exploration of the Possibilities for Production of Fischer Tropsch Liquids and Power via Biomass Gasification*. Biomass and Bioenergy, 2002. **23**(2): p. 129-152.
10. Bridgwater, A.V., Meier, D., and Radlein, D., *An Overview of Fast Pyrolysis of Biomass*. Organic Geochemistry, 1999. **30**(12): p. 1479-1493.
11. Bridgwater, A.V., *Renewable Fuels and Chemicals by Thermal Processing of Biomass*. Chemical Engineering Journal, 2003. **91**(2-3): p. 87-102.
12. Hamelinck, C.N., Faaij, A.P.C., den Uil, H., and Boerrigter, H., *Production of FT Transportation Fuels from Biomass; Technical Options, Process Analysis and Optimisation, and Development Potential*. Energy, 2004. **29**(11): p. 1743-1771.
13. Ding, M., Yang, Y., Xu, J., Tao, Z., Wang, H., Wang, H., Xiang, H., and Li, Y., *Effect of Reduction Pressure on Precipitated Potassium Promoted Iron-Manganese Catalyst for Fischer-Tropsch synthesis*. Applied Catalysis A: General, 2008. **345**(2): p. 176-184.
14. Demirbas, A., *Progress and Recent Trends in Biofuels*. Progress in Energy and Combustion Science, 2007. **33**(1): p. 1-18.
15. Larson, E.D. and Jin, H. *Biomass Conversion to Fischer-Tropsch Liquids: Preliminary Energy Balances*. in *Proceeding of the 4th Biomass Conference of the Americas*. 1999: Elsevier Science, Oxford, UK.
16. Takeshita, T. and Yamaji, K., *Important Roles of Fischer-Tropsch Synfuels in the Global Energy Future*. Energy Policy, 2008. **36**(8): p. 2773-2784.

17. Jager, B., Parmaliana, A., Sanfilippo, D., Frusteri, F., Vaccari, A., and Arena, F., *Developments in Fischer-Tropsch Technology*, in *Studies in Surface Science and Catalysis*. 1998, Elsevier. p. 25-34.
18. Boerrigter, H., Uil, H.d., and Calis, H.P. *Green Diesel from Biomass Fischer Tropsch Synthesis: New Insights in Gas Cleaning and Process Design*. in *Pyrolysis and Gasification of Biomass and Waste, Expert Meeting*. 2002. Strasbourg: ECN Biomass.
19. Dry, M.E., *The Fischer-Tropsch Synthesis*. Catalysis-Science and Technology, ed. J.R. Anderson and Boudart, M. Vol. Volume 1. 1981, New york: Springer-Verlag.
20. Steynberg, A.P., Andre, S., and Mark, D., *Introduction to Fischer-Tropsch Technology*, in *Studies in Surface Science and Catalysis*. 2004, Elsevier. p. 1-63.
21. Dry, M.E., *The Fischer-Tropsch Process: 1950-2000*. Catalysis Today, 2002. **71**(3-4): p. 227-241.
22. van Vliet, O.P.R., Faaij, A.P.C., and Turkenburg, W.C., *Fischer-Tropsch Diesel Production in a Well-to-Wheel Perspective: A Carbon, Energy Flow and Cost Analysis*. Energy Conversion and Management, 2009. **50**(4): p. 855-876.
23. Vosloo, A.C., *Fischer-Tropsch: a Futuristic View*. Fuel Processing Technology, 2001. **71**(1-3): p. 149-155.
24. Kreutz, T.G., Larson, E.D., Liu, G., and Williams, R.H., *Fischer-Tropsch Fuels from Coal and Biomass*, in *25th Annual International Pittsburgh Coal Conference*. 2008, Princeton Environmental Institute, Princeton University: Pittsburgh, Pennsylvania, USA.
25. Hofbauer, H., Rauch, R., and Ripfel-Nitsche, K., eds. *Gas Cleaning for Synthesis Applications*. Thermal Biomass Conversion, ed. A.V. Bridgwater, Hofbauer, H., and van Loo, S. 2009, CPL Press. 211-265.
26. Boerrigter, H., Calis, H.P., Slort, D.J., Bodenstaff, H., Kaandorp, A.J., den Uil, H., and Rabou, L.P.L.M., *Gas Cleaning for Integrated Biomass Gasification and Fischer-Tropsch (FT) Systems: Experimental Demonstration of two BG-FT Systems ("Proof-of-Principle")*. ECN-C--04-056 (available on www.ecn.nl). 2004, ECN Biomass, The Netherlands.
27. Valero, A. and Usón, S., *Oxy-co-Gasification of Coal and Biomass in an Integrated Gasification Combined Cycle (IGCC) Power Plant*. Energy, 2006. **31**(10-11): p. 1643-1655.
28. Furimsky, E., *Gasification in Petroleum Refinery of 21st Century*. Oil & Gas Science and Technology, 1999. **54**: p. 597-618.
29. Umeki, K., Yamamoto, K., Namioka, T., and Yoshikawa, K., *High Temperature Steam-Only Gasification of Woody Biomass*. Applied Energy, 2010. **87**(3): p. 791-798.
30. *Second Generation Transport Biofuels: – a Mission to the Netherlands, Germany and Finland*. March 2006, Report of a DTI Global Watch Mission.
31. Casci, J.L., Lok, C.M., and Shannon, M.D., *Fischer-Tropsch Catalysis: The Basis for an Emerging Industry with Origins in the Early 20th Century*. Catalysis Today, 2009. **145**(1-2): p. 38-44.
32. Henrici-Olivé, G. and Olive, S., *The Fischer-Tropsch Synthesis: Molecular Weight Distribution of Primary Products and Reaction Mechanism*. Angewandte Chemie International Edition in English, 1976. **15**(3): p. 136-141.
33. Fischer, F. and Tropsch, H., *DRP484337*. 1925.

34. Fischer, F. and Tropsch, H., *The Synthesis of Petroleum at Atmospheric Pressure from Gasification Products of Coal*. Brennstoff-Chem., 1926(7): p. 276-285.
35. Leckel, D., *Diesel Production from Fischer-Tropsch: The Past, the Present, and New Concepts*. Energy & Fuels, 2009. **23**(5): p. 2342-2358.
36. Guettel, R., Kunz, U., and Turek, T., *Reactors for Fischer-Tropsch Synthesis*. Chemical Engineering & Technology, 2008. **31**(5): p. 746-754.
37. Overett, M.J., Hill, R.O., and Moss, J.R., *Organometallic Chemistry and Surface Science: Mechanistic Models for the Fischer-Tropsch Synthesis*. Coordination Chemistry Reviews, 2000. **206-207**: p. 581-605.
38. Stranges, A. *Fischer-Tropsch Archive*. [cited 2011 01/06/2011]; Available from: www.fischer-tropsch.org.
39. Spath, P.L. and Dayton, D.C., *Preliminary Screening - Technical and Economic Assessment of Synthesis Gas to Fuels and Chemicals with Emphasis on the Potential for Biomass-Derived Syngas*. NREL/TP-510-34929. 2003, National Renewable Energy Laboratory (NREL): Golden, Colorado.
40. Spath, P.L. and Dayton, D.C., *Preliminary Screening - Technical and Economic Assessment of Synthesis Gas to Fuels and Chemicals with Emphasis on the Potential for Biomass-Derived Syngas*. 2003, National Renewable Energy Laboratory (NREL).
41. Tillmetz, K.D., *Chemical Engineering Technology*, 1978(48): p. 1065.
42. Dry, M.E., *High Quality Diesel via the Fischer-Tropsch Process - A Review*. Journal of Chemical Technology and Biotechnology, 2001(77): p. 43-50.
43. Dry, M.E., ed. *Chemical Concepts used for Engineering Purposes*. Studies in Surface Science and Catalysis, ed. G. Centi. Vol. 152. 2004, Elsevier.
44. Liu, Y., Teng, B.-T., Guo, X.-H., Li, Y., Chang, J., Tian, L., Hao, X., Wang, Y., Xiang, H.-W., Xu, Y.-Y., and Li, Y.-W., *Effect of reaction conditions on the catalytic performance of Fe-Mn catalyst for Fischer-Tropsch synthesis*. Journal of Molecular Catalysis A: Chemical, 2007. **272**(1-2): p. 182-190.
45. Dry, M.E., Shingles, T., and Boshoff, L.J., *Rate of the Fischer-Tropsch Reaction Over Iron Catalysts*. Journal of Catalysis, 1972(25): p. 99-104.
46. Sethuraman, R., Bakhshi, N.N., Katikaneni, S.P., and Idem, R.O., *Production of C4 Hydrocarbons from Fischer-Tropsch Synthesis in a Follow Bed Reactor Consisting of CO-Ni-ZrO₂ and Sulfated-ZrO₂ Catalyst Beds*. Fuel Processing Technology, 2001(73): p. 197-222.
47. Rezaian, J. and Cheremisinoff, N.P., *Gasification Technologies - A Primer for Engineers and Scientists*. 2005, London: Taylor & Francis Group, LLC.
48. Dry, M.E., ed. *Catalysis - Science and Technology (Chapter 4)*. ed. J.R. Anderson and Boudart, M. 1980, Springer: New York, NY.
49. Claeys, M. and Van Steen, E., *Chapter 8 Basic Studies*. Studies in Surface Science and Catalysis 152. 2004: Elsevier. 601-680.
50. Davis, B.H., *Fischer-Tropsch Synthesis: Current Mechanism and Futuristic Needs*. Fuel Processing Technology, 2001. **71**(1-3): p. 157-166.

51. Davis, B.H., *Fischer-Tropsch Synthesis: Reaction Mechanisms for Iron Catalysts*. Catalysis Today, 2009. **141**(1-2): p. 25-33.
52. Carter, M.K., *A Molecular Mechanism for Fischer-Tropsch Catalysis*. Journal of Molecular Catalysis A: Chemical, 2001. **172**(1-2): p. 193-206.
53. Adesina, A.A., *Hydrocarbon Synthesis via Fischer-Tropsch Reaction: Travails and Triumphs*. Applied Catalysis A: General, 1996. **138**(2): p. 345-367.
54. Gaube, J. and Klein, H.F., *Studies on the Reaction Mechanism of the Fischer-Tropsch Synthesis on Iron and Cobalt*. Journal of Molecular Catalysis A: Chemical, 2008. **283**(1-2): p. 60-68.
55. Dry, M.E., *Practical and Theoretical Aspects of the Catalytic Fischer-Tropsch Process*. Applied Catalysis A: General, 1996. **138**(2): p. 319-344.
56. Davis, B.H., *Anderson-Schulz-Flory Product Distribution - can it be Avoided for Fischer-Tropsch Synthesis?*, in *Historical Development of the Fischer-Tropsch Synthesis Process - I*. 2003, Center for Applied Energy Research, University of Kentucky: Lexington, KY, USA.
57. Schulz, H., vein Steen, E., Claeys, M., Curry-Hyde, H.E., and Howe, R.F., *Selectivity and Mechanism of Fischer-Tropsch Synthesis with Iron and Cobalt Catalysts*, in *Studies in Surface Science and Catalysis*. 1994, Elsevier. p. 455-460.
58. Puskas, I. and Hurlbut, R.S., *Comments about the Causes of Deviations from the Anderson-Schulz-Flory Distribution of the Fischer-Tropsch Reaction Products*. Catalysis Today, 2003. **84**(1-2): p. 99-109.
59. Steynberg, A.P., Espinoza, R.L., Jager, B., and Vosloo, A.C., *High Temperature Fischer-Tropsch Synthesis in Commercial Practice*. Applied Catalysis A: General, 1999. **186**(1-2): p. 41-54.
60. Dry, M.E., *Fischer-Tropsch Reactions and the Environment*. Applied Catalysis A: General, 1999. **189**(2): p. 185-190.
61. Kroschwitz, I. and Howe-Grant, M., *Kirk-Othmer Encyclopedia of Chemical Technology. 4th Edition*. New York: Wiley & Sons. 1996.
62. Gill, S.S., Tsolakis, A., Dearn, K.D., and Rodríguez-Fernández, J., *Combustion Characteristics and Emissions of Fischer-Tropsch Diesel Fuels in IC Engines*. Progress in Energy and Combustion Science, 2011. **37**(4): p. 503-523.
63. Dancuart, L.P., Haan, R.d., and Klerk, A.d., eds. *Processing of Primary Fischer-Tropsch Products*. Studies in Surface Science and Catalysis, ed. G. Centi. Vol. 152. 2004, Elsevier. 482-532.
64. Golumbic, N., *United States Department of the Interior - Bureau of Mines. Some Chemicals from Synthetic Liquid Fuels Processes. R.I. 4467*. 1949.
65. Soled, S., Iglesia, E., and Fiato, R.A., *Activity and Selectivity Control in Iron Catalyzed Fischer-Tropsch Synthesis*. Catalysis Letters, 1990. **7**(1): p. 271-280.
66. Espinoza, R.L., Steynberg, A.P., Jager, B., and Vosloo, A.C., *Low Temperature Fischer-Tropsch Synthesis from a Sasol Perspective*. Applied Catalysis A: General, 1999. **186**(1-2): p. 13-26.

67. de la Osa, A.R., De Lucas, A., Romero, A., Valverde, J.L., and SÁñchez, P., *Influence of the Catalytic Support on the Industrial Fischer-Tropsch Synthetic Diesel Production*. *Catalysis Today*, 2011. **176**(1): p. 298-302.
68. de la Osa, A.R., De Lucas, A., Valverde, J.L., Romero, A., Monteagudo, I., Coca, P., and Sanchez, P., *Influence of Alkali Promoters on Synthetic Diesel Production over Co Catalyst*. *Catalysis Today*, 2011. **167**(1): p. 96-106.
69. Dry, M.E., *The Fischer-Tropsch Process - Commercial Aspects*. *Catalysis Today*, 1990. **6**(3): p. 183-206.
70. Davis, B.H., *Fischer-Tropsch Synthesis: Relationship between Iron Catalyst Composition and Process Variables*. *Catalysis Today*, 2003. **84**(1-2): p. 83-98.
71. Oukaci, R., Singleton, A.H., and Goodwin, J.G., *Comparison of Patented Co FT Catalysts using Fixed-Bed and Slurry Bubble Column Reactors*. *Applied Catalysis A: General*, 1999. **186**(1-2): p. 129-144.
72. Escalona, N., Medina, C., GarcÁa, R., and Reyes, P., *Fischer Tropsch Reaction from a Mixture Similar to Biosyngas. Influence of Promoters on Surface and Catalytic Properties of Co/SiO₂ Catalysts*. *Catalysis Today*, 2009. **143**(1-2): p. 76-79.
73. van Steen, E. and Claeys, M., *Fischer-Tropsch Catalysts for the Biomass-to-Liquids Process*. *Chemical Engineering Technology*, 2008. **31**(5): p. 655-666.
74. Jun, K.-W., Roh, H.-S., Kim, K.-S., Ryu, J.-S., and Lee, K.-W., *Catalytic Investigation for Fischer-Tropsch Synthesis from Biomass Derived Syngas*. *Applied Catalysis A: General*, 2004. **259**(2): p. 221-226.
75. Borg, Ø., Hammer, N., Enger, B.C., Myrstad, R., Lindvåg, O.A., Eri, S., Skagseth, T.H., and Rytter, E., *Effect of Biomass-Derived Synthesis Gas Impurity Elements on Cobalt Fischer-Tropsch Catalyst Performance including in Situ Sulphur and Nitrogen Addition*. *Journal of Catalysis*, 2011. **279**(1): p. 163-173.
76. Kim, Y.H., Jun, K.-W., Joo, H., Han, C., and Song, I.K., *A Simulation Study on Gas-to-Liquid (Natural Gas to Fischer-Tropsch Synthetic Fuel) Process Optimization*. *Chemical Engineering Journal*, 2009. **155**(1-2): p. 427-432.
77. Iglesia, E., Soled, S.L., Fiato, R.A., and Via, G.H., *Bimetallic Synergy in Cobalt Ruthenium Fischer-Tropsch Synthesis Catalysts*. *Journal of Catalysis*, 1993. **143**(2): p. 345-368.
78. Iglesia, E., Soled, S.L., Fiato, R.A., Via, G.H., Curry-Hyde, H.E., and Howe, R.F., *Dispersion, Support, and Bimetallic Effects in Fischer-Tropsch Synthesis on Cobalt Catalysts*, in *Studies in Surface Science and Catalysis*. 1994, Elsevier. p. 433-442.
79. Bao, A., Liew, K., and Li, J., *Fischer-Tropsch Synthesis on CaO-Promoted Co/Al₂O₃ Catalysts*. *Journal of Molecular Catalysis A: Chemical*, 2009. **304**(1-2): p. 47-51.
80. Khodakov, A.Y., *Fischer-Tropsch Synthesis: Relations between Structure of Cobalt Catalysts and their Catalytic Performance*. *Catalysis Today*, 2009. **144**(3-4): p. 251-257.
81. Yakobson, D.L., *Fischer-Tropsch (FT) Technology*, in *LNG-GTL Conference*. 2001, Rentech, Inc.: Buenos Aires, Argentina.
82. Tsakoumis, N.E., Rønning, M., Borg, Ø., Rytter, E., and Holmen, A., *Deactivation of Cobalt Based Fischer-Tropsch Catalysts: A Review*. *Catalysis Today*, 2010. **154**(3-4): p. 162-182.

83. Xu, D., Duan, H., Li, W., and Xu, H., *Investigation on the Fischer-Tropsch Synthesis with Nitrogen-Containing Syngas over CoPtZrO₂/Al₂O₃ Catalyst*. Energy & Fuels, 2006. **20**(3): p. 955-958.
84. Howard, M.J., *Technology Vice President, Conversion Technology Centre, BP International Ltd, Saltend, Hull, HU12 8DS, UK*. 2010, Personal Communication.
85. Bukur, D.B., Lang, X., Akgerman, A., and Feng, Z., *Effect of Process Conditions on Olefin Selectivity during Conventional and Supercritical Fischer-Tropsch Synthesis*. Industrial & Engineering Chemistry Research, 1997. **36**(7): p. 2580-2587.
86. Mirzaei, A.A., Samaneh, V., and Feyzi, M., *Fischer-Tropsch Synthesis over Iron Manganese Catalysts - Effect of Preparation and Operating Conditions on Catalyst Performance*. Advances in Physical Chemistry, 2009. **2009**: p. 1-12.
87. Gibson, E.J. and Hall, C.C., *The Fischer-Tropsch Synthesis with Cobalt Catalysts: The Effect of Process Conditions on the Composition of the Reaction Products*. Journal of Applied Chemistry, 1954. **4**(2): p. 49-61.
88. Dasgupta, D. and Wiltowski, T., *Enhancing Gas Phase Fischer-Tropsch Synthesis Catalyst Design*. Fuel, 2011. **90**(1): p. 174-181.
89. de la Osa, A.R., De Lucas, A., Romero, A., Valverde, J.L., and Sanchez, P., *Fischer-Tropsch Diesel Production over Calcium-Promoted Co/Alumina Catalyst: Effect of Reaction Conditions*. Fuel, 2011. **90**(5): p. 1935-1945.
90. Hayakawa, H., Tanaka, H., and Fujimoto, K., *Studies on Catalytic Performance of Precipitated Iron/Silica Catalysts for Fischer-Tropsch Synthesis*. Applied Catalysis A: General, 2007. **328**(2): p. 117-123.
91. Mohanty, P., Pant, K.K., Parikh, J., and Sharma, D.K., *Liquid Fuel Production from Syngas using Bifunctional CuO-CoO-Cr₂O₃ Catalyst Mixed with MFI Zeolite*. Fuel Processing Technology, 2011. **92**(3): p. 600-608.
92. Swanson, R.M., Platon, A., Satrio, J.A., and Brown, R.C., *Techno-Economic Analysis of Biomass-to-Liquids Production based on Gasification*. Fuel, 2010. **89**, **Supplement 1**(0): p. S11-S19.
93. Bridgwater, A.V., *The Technical and Economic Feasibility of Biomass Gasification for Power Generation*. Fuel, 1995. **74**(5): p. 631-653.
94. Zevniq, F.C. and Buchanan, R.L., *Generalised Correlation for Process Investment*. Chemical Engineering Progress, 1963. **59**(2): p. 70-77.
95. Wilson, G.T., *Capital Investment for Chemical Plant*. British Chemical Engineering, 1971. **16**(10): p. 931-934.
96. Gerrard, M., *A Guide to Capital Cost Estimating. 4th Edition*. 2001, Rugby, UK: IChemE, ACostE.
97. Caldwell, M., *Selectivity in Fischer Tropsch Synthesis: Review and Recommendations for Further Work*. 1980, Council for Scientific and Industrial Research, Chemical Engineering Group: Pretoria, South Africa.
98. Donnelly, T.J. and Satterfield, C.N., *Product Distributions of the Fischer-Tropsch Synthesis on Precipitated Iron Catalysts*. Journal of Molecular Catalysis A: Chemical, 1989. **221**: p. 51-58.

99. Dictor, R.A. and Bell, A.T., *On-line Analysis of Fischer-Tropsch Synthesis Products*. Industrial & Engineering Chemistry Fundamentals, 1984. **23**(2): p. 252-256.
100. Lu, Y. and Lee, T., *Influence of the Feed Gas Composition on the Fischer-Tropsch Synthesis in Commercial Operations*. Journal of Natural Gas Chemistry, 2007. **16**(4): p. 329-341.
101. Wang, Y.-N., Ma, W.-P., Lu, Y.-J., Yang, J., Xu, Y.-Y., Xiang, H.-W., Li, Y.-W., Zhao, Y.-L., and Zhang, B.-J., *Kinetics Modelling of Fischer-Tropsch Synthesis over an Industrial Fe-Cu-K Catalyst*. Fuel, 2003. **82**(2): p. 195-213.
102. Kumabe, K., Sato, T., Matsumoto, K., Ishida, Y., and Hasegawa, T., *Production of Hydrocarbons in Fischer-Tropsch Synthesis with Fe-Based Catalyst: Investigations of Primary Kerosene Yield and Carbon Mass Balance*. Fuel, 2010. **89**(8): p. 2088-2095.
103. Feyzi, M., Irandoust, M., and Mirzaei, A.A., *Effects of Promoters and Calcination Conditions on the Catalytic Performance of Iron-Manganese Catalysts for Fischer-Tropsch Synthesis*. Fuel Processing Technology, 2011. **92**(5): p. 1136-1143.
104. Bukur, D.B., Patel, S.A., and Lang, X., *Fixed Bed and Slurry Reactor Studies of Fischer-Tropsch Synthesis on Precipitated Iron Catalyst*. Applied Catalysis, 1990. **61**(1): p. 329-349.
105. Farias, F.E.M., Silva, F.R.C., Cartaxo, S.J.M., Fernandes, F.A.N., and Sales, F.G., *Effect of Operating Conditions on Fischer-Tropsch Liquid Products*. Latin American Applied Research, 2007(37): p. 283-287.
106. Jung, H., Yang, J.-I., Yang, J.H., Lee, H.-T., Chun, D.H., and Kim, H.-J., *Investigation of Fischer-Tropsch synthesis performance and its intrinsic reaction behavior in a bench scale slurry bubble column reactor*. Fuel Processing Technology, 2010. **91**(12): p. 1839-1844.
107. Farias, F.E.M., Fernandes, F.A.N., and Sales, F.G., *Effect of Operating Conditions on FT Liquid Products Produced by Unpromoted & Potassium-Promoted Iron Catalyst*. Latin American Applied Research, 2010(40): p. 161-166.
108. Storch, H.H., Golumbic, N., and Anderson, R.B., *The Fischer-Tropsch and Related Syntheses*. 1951, New York: John Wiley and Sons.
109. Yates, I.C. and Satterfield, C.N., *Hydrocarbon Selectivity from Cobalt Fischer-Tropsch Catalysts*. Energy & Fuels, 1992. **6**(3): p. 308-314.
110. Zheng, S., Liu, Y., Li, J., and Shi, B., *Deuterium Tracer Study of Pressure Effect on Product Distribution in the Cobalt-Catalyzed Fischer-Tropsch Synthesis*. Applied Catalysis A: General, 2007. **330**: p. 63-68.
111. Das, T.K., Jacobs, G., Patterson, P.M., Conner, W.A., Li, J., and Davis, B.H., *Fischer-Tropsch Synthesis: Characterization and Catalytic Properties of Rhenium Promoted Cobalt Alumina Catalysts*. Fuel, 2003. **82**(7): p. 805-815.
112. Sharifnia, S., Mortazavi, Y., and Khodadadi, A., *Enhancement of Distillate Selectivity in Fischer-Tropsch Synthesis on a Co/SiO₂ Catalyst by Hydrogen Distribution along a Fixed-Bed Reactor*. Fuel Processing Technology, 2005. **86**(12-13): p. 1253-1264.
113. Sharifnia, S., Khodadadi, A., and Mortazavi, Y., *Improving C₁₁+ Hydrocarbon Product Selectivity by Hydrogen Distribution in Fischer-Tropsch Synthesis*. International Journal of Chemical Reactor Engineering, 2008. **6**: p. A83.

114. Tristantini, D., Logdberg, S., Gevert, B., Borg, O., and Holmen, A., *The Effect of Synthesis Gas Composition on the Fischer-Tropsch Synthesis over Co/Al₂O₃ and Co-Re/Al₂O₃ catalysts*. Fuel Processing Technology, 2007. **88**(7): p. 643-649.
115. Woo, K.-J., Kang, S.-H., Kim, S.-M., Bae, J.-W., and Jun, K.-W., *Performance of a Slurry Bubble Column Reactor for Fischer-Tropsch Synthesis: Determination of Optimum Condition*. Fuel Processing Technology, 2010. **91**(4): p. 434-439.
116. Rafiq, M.H., Jakobsen, H.A., Schmid, R., and Hustad, J.E., *Experimental Studies and Modeling of a Fixed Bed Reactor for Fischer-Tropsch Synthesis using Biosyngas*. Fuel Processing Technology, 2011. **92**(5): p. 893-907.
117. Bechara, R., Balloy, D., and Vanhove, D., *Catalytic Properties of Co/Al₂O₃ System for Hydrocarbon Synthesis*. Applied Catalysis A: General, 2001. **207**(1-2): p. 343-353.
118. Faaij, A., Van Ree, R., and Meuleman, B., *Long Term Perspectives of Biomass Integrated Gasification with Combined Cycle Technology - Costs Efficiency and a Comparison with Combustion*. 1998, Novem. Utrecht, The Netherlands.
119. Boerrigter, H., *Economy of Biomass-to-Liquids (BTL) Plants: An Engineering Assessment*. 2006, Energy Research Centre of the Netherlands (ECN): Petten.
120. Hamelinck, C.N. and Faaij, A. *Future Prospects for Production of Methanol and Hydrogen from Biomass*. in *12th European Biomass Conference*. 2002. Amsterdam, The Netherlands.
121. Laan, G.P.v.d., *Kinetics, Selectivity and Scale-up of the Fischer-Tropsch Synthesis*. 1999, University of Groningen.
122. Knoef, H.A.M., *Handbook: Biomass Gasification*. 2005: Enschede: BTG biomass technology group.
123. Hofbauer, H., ed. *Gasification - Technology Overview*. Thermal Biomass Conversion, ed. A.V. Bridgewater, Hofbauer, H., and van Loo, S. 2009, CPL Press. 11-35.
124. Dutta, A. and Acharya, B., eds. *Production of Bio-syngas and Biohydrogen via Gasification*. Woodhead Publishing Series in Energy - Handbook of Biofuels Production: Processes and Technologies, ed. R. Luque, Campelo, J., and Clark, J. Vol. 15. 2011, Woodhead Publishing: Oxford.
125. Göransson, K., Söderlind, U., He, J., and Zhang, W., *Review of Syngas Production via Biomass DFBGs*. Renewable and Sustainable Energy Reviews, 2011. **15**(1): p. 482-492.
126. Mondal, P., Dang, G.S., and Garg, M.O., *Syngas Production through Gasification and Cleanup for Downstream Applications - Recent Developments*. Fuel Processing Technology, 2011. **92**(8): p. 1395-1410.
127. Higman, C. and van der Burgt, M., *Gasification*. 2003, Burlington, MA, USA.: Gulf Professional Publishing, Elsevier Science.
128. Van Ree, R., Oudhuis, A.B.J., and Faaij, A., *Modelling of a Biomass-Integrated-Gasifier / Combined-Cycle (BIG-CC) System with the Flowsheet Simulation Program Aspen-Plus*. 1995, Netherlands Energy Research Foundation ECN: Petten, The Netherlands.
129. van der Drift, A. and Boerrigter, H., *Synthesis Gas from Biomass for Fuels and Chemicals*. 2006, ECN Biomass, Coal and Environmental Research.
130. Srinivas, S., Malik, R.K., and Mahajani, S.M., *Fischer-Tropsch Synthesis using Bio-Syngas and CO₂*. Energy for Sustainable Development, 2007. **11**(4): p. 66-71.

131. Tijmensen, M.J.A., *The Production of Fischer Tropsch Liquids and Power through Biomass Gasification*, in *Science Technology Society*. 2000, Universiteit Utrecht: Utrecht.
132. Steynberg, A.P., Dry, M.E., Davis, B.H., Breman, B.B., Andre, S., and Mark, D., *Chapter 2 - Fischer-Tropsch Reactors*, in *Studies in Surface Science and Catalysis*. 2004, Elsevier. p. 64-195.
133. Davis, B.H., *Overview of Reactors for Liquid Phase Fischer-Tropsch Synthesis*. *Catalysis Today*, 2002. **71**(3-4): p. 249-300.
134. Sie, S.T. and Krishna, R., *Fundamentals and Selection of Advanced Fischer-Tropsch Reactors*. *Applied Catalysis A: General*, 1999. **186**(1-2): p. 55-70.
135. Jager, B. *Development of Fischer-Tropsch Reactors*. in *AIChE Spring Meeting*. 2003. New Orleans.
136. Lappas, A. and Heracleous, E., eds. *Production of Biofuels via Fischer-Tropsch Synthesis: Biomass-to-Liquids*. Woodhead Publishing Series in Energy - Handbook of Biofuels Production: Processes and Technologies, ed. R. Luque, Campelo, J., and Clark, J. Vol. 15. 2011, Woodhead Publishing: Oxford.
137. Boerrigter, H. and Drift, A.v.d., "*Biosyngas*" *Key Intermediate in Production of Renewable Transportation Fuels, Chemicals, and Electricity: Optimum Scale and Economic Prospects of Fischer-Tropsch Plants.*, in *14th European Biomass Conference & Exhibition*. 2005, ECN Biomass. ECN-RX--05-181: Paris, France.
138. Wender, I., *Reactions of Synthesis Gas*. *Fuel Processing Technology*, 1996. **48**(3): p. 189-297.
139. Manganaro, J., Chen, B., Adeosun, J., Lakhapatri, S., Favetta, D., Lawal, A., Farrauto, R., Dorazio, L., and Rosse, D.J., *Conversion of Residual Biomass into Liquid Transportation Fuel: An Energy Analysis*. *Energy & Fuels*, 2011. **25**(6): p. 2711-2720.
140. Sasol. *Sasol and Qatar Petroleum's Oryx GTL plant wins global award*. 2006 [cited 2011 19/09/2011]; Available from: <http://www.sasol.com>.
141. Shell. *Pearl GTL: Building the the world's largest gas to liquids plant*. 2009 [cited 2011 19/09/2011]; Available from: http://www.shell.com/home/content/media/news_and_media_releases.
142. Opdal, O.A., *Project Report - Production of Synthetic Biodiesel via Fischer-Tropsch Synthesis*, in *Department of Energy & Process Engineering, Faculty of Engineering Science and Technology*. 2006, Norwegian University of Science and Technology. Available from: <http://www.zero.no/transport/biodrivstoff/btl-namdalen.pdf>.
143. Platform, E.B.T. *European Biofuels Technology Platform - Biomass to Liquids (BtL)*. 2011 [cited 2011 29/07/2011]; Available from: <http://www.biofuelstp.eu>.
144. *Choren Webpage*. [cited 2011 03/08/2011]; Available from: www.choren.de.
145. Rudloff, M. *Biomass-to-Liquid Fuels (BtL) - Made by CHOREN. Process, Environmental Impact and Latest Developments*. in *10th European Automotive Engineering Congress*. 2005. Belgrade, Serbia.
146. Uhde, T.G. *Uhde's PRENFLOTM process to be part of joint research and development project BioTfuel in France*. 2010 [cited 2011 29/07/2011]; Available from: <http://www.uhde.eu>.

147. "bioliq" Biomass to Liquid Karlsruhe. *Biomass to Liquid - the bioliq Process*. 2011 [cited 2011 29/07/2011]; Available from: <http://www.bioliq.de>.
148. *Neste Oil - Neste Oil and Stora Enso to join Forces in Biofuel Development*. 2007 [cited 2011 29/07/2011]; Available from: <http://www.nesteoil.com>.
149. Rauch, R., Hofbauer, H., Bosch, K., Siefert, I., Aichernig, C., Tremmel, H., Voigtlaender, K., Koch, R., and Lehner, R. *Steam Gasification of Biomass at CHP Plant Guessing – Status of the Demonstration Plant*. in *Proceedings of the 2nd World Conference on Biomass for Energy, Industry and Climate Protection*. 2004. Rome, Italy.
150. Fogler, S.H., *Elements of Chemical Reaction Engineering. 3rd Edition*. 1999: Prentice Hall.
151. Levenspiel, O., *Chemical Reaction Engineering. 3rd Edition*. 1999, NJ, USA: John Wiley & Sons, Inc.
152. Grob, R.L., *Theory of Gas Chromatography*, in *Modern Practice of Gas Chromatography*. 2004, John Wiley & Sons, Inc. p. 23-63.
153. Channiwala, S.A. and Parikh, P.P., *A Unified Correlation for Estimating HHV of Solid, Liquid and Gaseous Fuels*. *Fuel*, 2002. **81**(8): p. 1051-1063.
154. Sing, K.S.W. and Everett, D.H., *Reporting Physisorption Data for Gas Solid Systems with Special Reference to the Determination of Surface Area and Porosity*. *Pure and Applied Chemistry*, 1985. **57**(4): p. 603-619. Great Britain, IUPAC.
155. Warren, B.E., *X-Ray Diffraction. ISBN: 0-486-66317-5*. 1969: Addison-Wesley Publishing Company.
156. Texeira, V., *Personal Communication - Catalyst characterisation techniques, activation procedures and screening conditions*. 2010: Professor of Chemical Engineering at Federal University of Rio de Janeiro, Brazil.
157. Teixeira, V., *Personal Communication - Catalyst Preparation and Characterization Techniques, Activation Procedures and Screening Conditions*. 2010: Professor of Chemical Engineering at Federal University of Rio de Janeiro, Brazil.
158. Lucy, A., *Analytical Chemist and FT Synthesis Work at BP UK (Personal Communication)*. 2011.
159. Jalama, K., Coville, N.J., Xiong, H., Hildebrandt, D., Glasser, D., Taylor, S., Carley, A., Anderson, J.A., and Hutchings, G.J., *A Comparison of Au/Co/Al₂O₃ and Au/Co/SiO₂ Catalysts in the Fischer-Tropsch Reaction*. *Applied Catalysis A: General*, 2011. **395**(1-2): p. 1-9.
160. Holt, A., *R & D Director at CATAL International Ltd, UK. (Personal Communication)*. 2010-11: Sheffield.
161. Li, J., Jacobs, G., Zhang, Y., Das, T., and Davis, B.H., *Fischer-Tropsch Synthesis: Effect of Small Amounts of Boron, Ruthenium and Rhenium on Co/TiO₂ Catalysts*. *Applied Catalysis A: General*, 2002. **223**(1-2): p. 195-203.
162. Ngwenya, T., Glasser, D., Hildebrandt, D., Coville, N., and Mukoma, P., *Fischer-Tropsch Results and Their Analysis for Reactor Synthesis*. *Industrial & Engineering Chemistry Research*, 2005. **44**(16): p. 5987-5994.

163. Li, J., Jacobs, G., Das, T., and Davis, B.H., *Fischer-Tropsch Synthesis: Effect of Water on the Catalytic Properties of a Ruthenium Promoted Co/TiO₂ Catalyst*. Applied Catalysis A: General, 2002. **233**(1-2): p. 255-262.
164. S.-H. Kang, J. W. Bae, J. -J. Lee, K.-S. Ha, D.-H. Lee, and Kim, B.-W., *Catalytic Performance on Iron-Based Fischer-Tropsch Catalyst in Fixed-Bed & Bubbling Fluidised-Bed Reactor*. doi:10.1016/j.apcatb.2011.01.024. Applied Catalysis B: Environmental, 2010.
165. Borg, O., Eri, S., Blekkan, E.A., Storsaeter, S., Wigum, H., Rytter, E., and Holmen, A., *Fischer-Tropsch Synthesis over γ -Alumina-Supported Cobalt Catalysts: Effect of Support Variables*. Journal of Catalysis, 2007. **248**(1): p. 89-100.
166. Bezemer, G.L., Bitter, J.H., Kuipers, H.P.C.E., Oosterbeek, H., Holewijn, J.E., Xu, X., Kapteijn, F., van Dillen, A.J., and de Jong, K.P., *Cobalt Particle Size Effects in the Fischer-Tropsch Reaction Studied with Carbon Nanofiber Supported Catalysts*. Journal of the American Chemical Society, 2006. **128**(12): p. 3956-3964.
167. Zennaro, R., Tagliabue, M., and Bartholomew, C.H., *Kinetics of Fischer-Tropsch Synthesis on Titania-Supported Cobalt*. Catalysis Today, 2000. **58**(4): p. 309-319.
168. Dautzenberg Frits, M., *Ten Guidelines for Catalyst Testing*, in *Characterization and Catalyst Development*. 1989, American Chemical Society. p. 99-119.
169. Yao, Y., Hildebrandt, D., Glasser, D., and Liu, X., *Fischer-Tropsch Synthesis Using H₂/CO/CO₂ Syngas Mixtures over a Cobalt Catalyst*. Industrial & Engineering Chemistry Research, 2010. **49**(21): p. 11061-11066.
170. Medina, C., García, R., Reyes, P., Fierro, J.L.G., and Escalona, N., *Fischer Tropsch Synthesis from a Simulated Biosyngas Feed over Co(x)/SiO₂ Catalysts: Effect of Co-loading*. Applied Catalysis A: General, 2010. **373**(1-2): p. 71-75.
171. Fernandes, F.A.N. and Sousa, E.M.M., *Fischer-Tropsch Synthesis Product Grade Optimization in a Fluidized Bed Reactor*. AIChE Journal, 2006. **52**(8): p. 2844-2850.

APPENDIX A - Gas Mixtures for Online GC Calibration

Table A1 – GC gas calibration mixtures and compositions

Component	Concentration (mol%)						
	Mix 1	Mix 2	Mix 3	Mix 4	Mix 5	Mix 6	Mix 7
Nitrogen	9.959	0.998	5.020	45.000	100	-	-
CO	1.987	29.920	49.770	50.000	-	100	-
Hydrogen	-	-	-	5.000	-	-	100
CO ₂	4.962	1.000	3.020	-	-	-	-
Helium	16.165	26.966	10.991	-	-	-	-
Methane	24.779	5.030	15.020	-	-	-	-
Ethene	15.000	10.000	2.000	-	-	-	-
Ethane	20.461	10.010	5.040	-	-	-	-
Propene	1.996	6.100	4.060	-	-	-	-
Propane	1.505	4.800	2.960	-	-	-	-
Iso-Butane	1.196	0.695	0.301	-	-	-	-
1-Butane	0.791	0.485	0.102	-	-	-	-
N-Butane	0.595	1.000	0.102	-	-	-	-
Neo-Pentane	0.303	0.996	0.602	-	-	-	-
1-Pentene	0.199	1.000	0.508	-	-	-	-
n-Pentane	0.100	1.000	0.504	-	-	-	-

APPENDIX B – Scanning Electron Microscopy (SEM) Micrographs

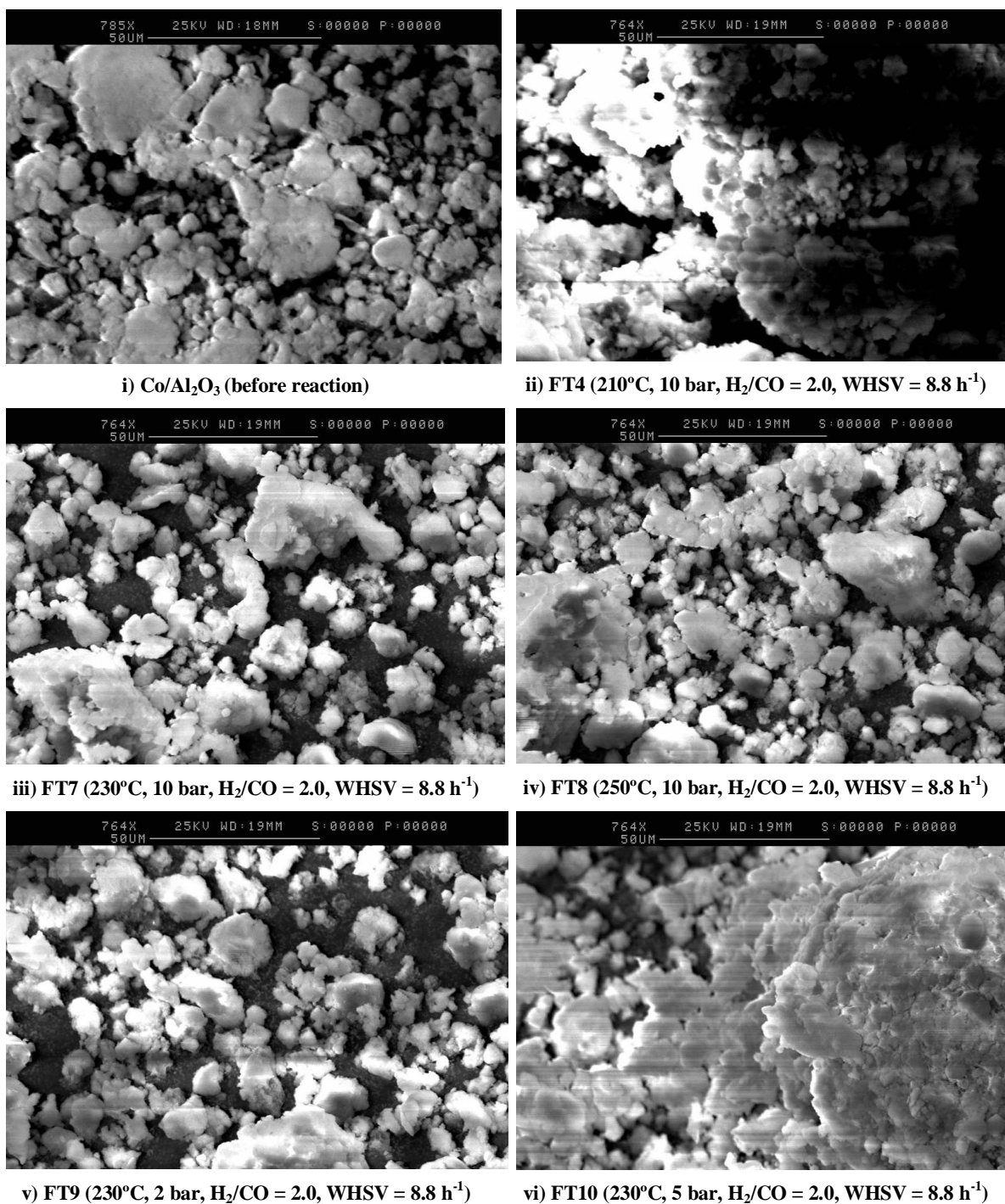
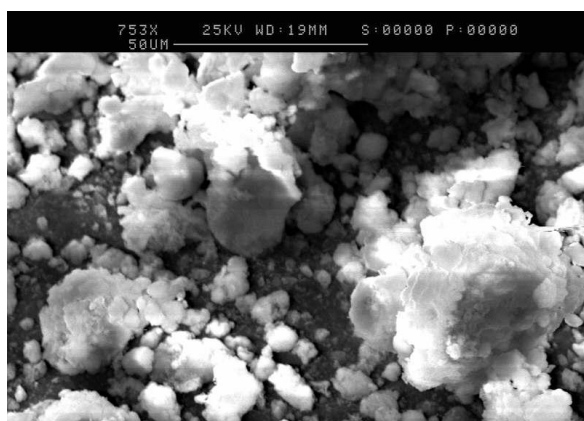
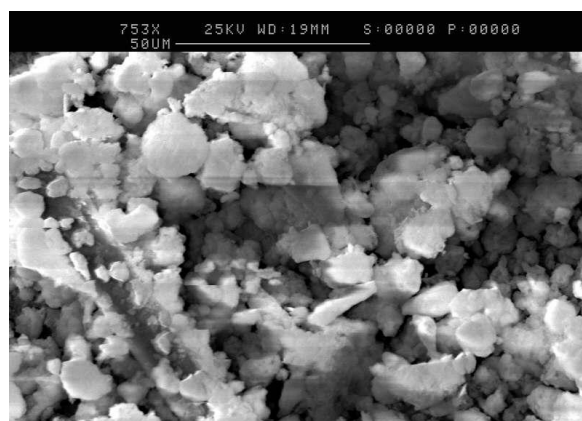


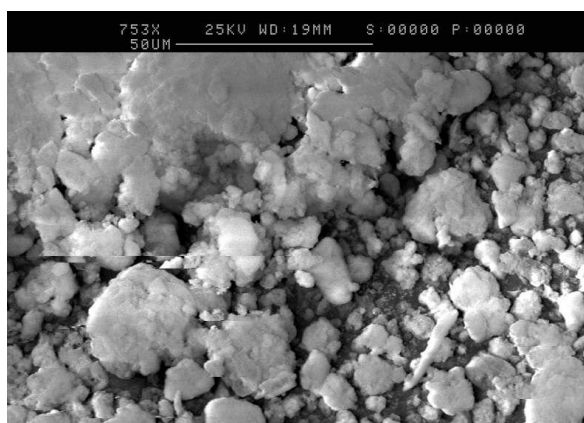
Figure B1 – SEM micrographs of Co/Al₂O₃ catalyst i) before FT synthesis reaction, and ii-xi) after FT synthesis parameter study test runs (FT4-FT15)



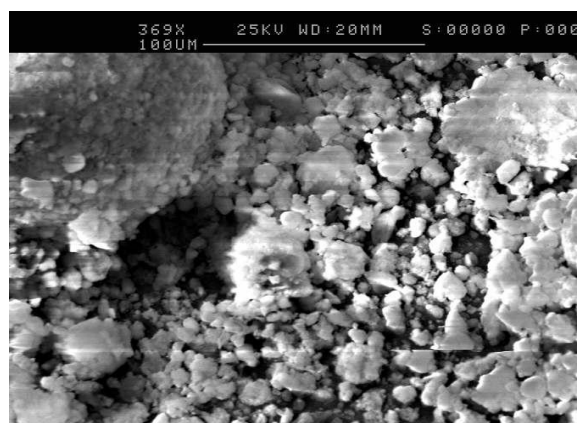
vii) FT11 (230°C, 8 bar, H₂/CO = 2.0, WHSV = 8.8 h⁻¹)



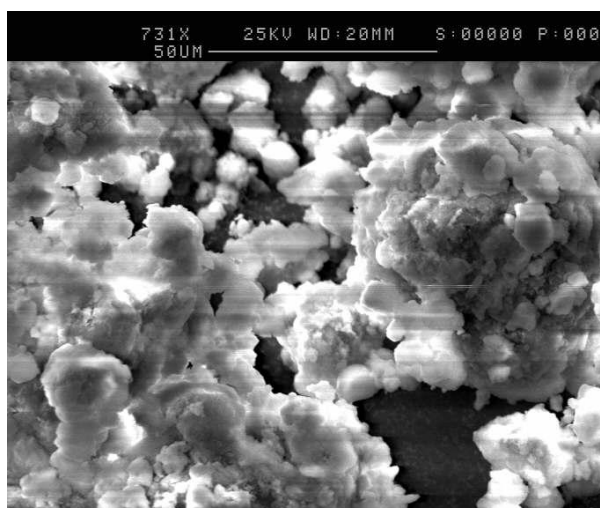
viii) FT12 (230°C, 10 bar, H₂/CO=2.0, WHSV= 11.5 h⁻¹)



ix) FT13 (230°C, 10 bar, H₂/CO = 2.0, WHSV= 10.5 h⁻¹)



x) FT14 (230°C, 10 bar, H₂/CO = 1.6, WHSV = 9.8 h⁻¹)



xi) FT15 (230°C, 10 bar, H₂/CO = 1.8, WHSV = 8.8 h⁻¹)

Figure B1 (continued) – SEM micrographs of Co/Al₂O₃ catalyst i) before FT synthesis reaction, and ii-xi) after FT synthesis parameter study test runs (FT4-FT15)

APPENDIX C – Catalyst Preparation Methods

C1 – Preparation Method for the Co/Al₂O₃ Catalyst

This catalyst was prepared under the supervision of the Chemical Engineering Department at the Federal University of Rio de Janeiro (UFRJ), in Brazil. This was done using an incipient wet impregnation technique [157], giving a catalyst with a final composition of 10wt.%Co/Al₂O₃. The method used is described below:

Ingredients: i) Alumina 214 (Degussa Lote: 99SX1152), ii) Cobalt nitrate hexahydrate P.A. – Co(NO₃)₂.6H₂O, iii) Deionised water

Apparatus: spatula, round-bottom flask, 3 glass beakers, ceramic deep dish, vacuum rotary evaporator. Note: clean all apparatus with sodium free (neutral) soap detergent and deionised water, and then dry in an oven at 105°C.

Method:

1. Weigh 5.0g of Co(NO₃)₂.6H₂O in a small beaker
2. Add 10mL of deionised water to the beaker and mix
3. Then add another 10mL of deionised water to the beaker and continue mixing
4. Weigh 10.0g Alumina 214
5. In the conical round-bottom flask:
 - First, add the alumina powder, then add the cobalt nitrate hexahydrate and de-ionised water to the alumina in the flask
 - Then add another 20mL of deionised water to the flask
 - Then add a small amount of deionised water to rinse the powder off the sides of the flask.
6. Place the flask in a vacuum rotary evaporator (with silica oil bath) for 2 hours at room temperature to achieve a homogeneous mixture.
7. Then increase the bath temperature gradually to 90°C until water evaporates.
8. Once temperature reaches 90°C, initiate the vacuum slowly (so as not to lose any catalyst).
9. Once fully dried (after approximately 4-6 hours), a pink powder should be observed. Stop the vacuum, but continue rotation for 30 minutes.
10. Then turn off the heat, and continue rotating the flask (while out of the silicon oil bath). Clean/dry the flask with tissue paper as it rotates.
11. Remove the flask from the rotary evaporator and dry off the water in the neck of the flask.
12. Empty contents of the flask into a deep ceramic dish. Remove contents stuck in the flask with a clean, long glass spatula.
13. Grind/press the catalyst powder with clean glass spatula into uniform fine powder (until no lumps are present).
14. Place dish in a drying oven and set to 105°C for 20 hours.
15. Then place the dish in a muffle oven, and set the temperature ramp to 5°C/min and raise the temperature up to 400°C. Maintain at this final temperature for 3 hours, in order to calcine the catalyst sample.
16. Remove the dish and catalyst from the muffle oven and place in a vacuum for storage.

C2 – Preparation Method for the Co/TiO₂ Catalyst

This catalyst was externally prepared by CATAL International Ltd using pore volume impregnation (precipitation), according to a method available in the literature by Jinlin Li *et al.* [163], which is outlined as follows: A 9.8wt.%Co-0.22wt.%Ru/TiO₂ catalyst was prepared by impregnation of the calcined 9.8wt.%Co/TiO₂ catalyst with a ruthenium nitrosyl nitrate (Alfa) solution. The titania (Degussa P-25 TiO₂) support contained 72% anatase, and had a surface area of 45m²/g. This support was calcined at 400°C, then boron-modified by pore volume impregnation with boric acid (Sigma-Aldrich) solution, and dried at 120°C for 16 hours. This was then calcined in air for 6 hours at 400°C.

Cobalt (9.80 wt.%) was then deposited on the boron-modified titania carrier by pore volume impregnation with cobalt nitrate (Alfa) solution. The sample was then dried at 120°C for 16 hours and then calcined at 300°C for 6 hours. The catalyst sample was promoted with ruthenium by impregnating the pretreated 9.8wt.%Co/TiO₂ with a ruthenium nitrosyl nitrate (Alfa) solution. Finally, the sample was dried at 120°C for 16 hours and then calcined at 300°C for 6 hours. The boron and ruthenium contents were 0.05 and 0.22wt.%, respectively.

C3 – Preparation Method for the Fe/Al₂O₃ Catalyst

This catalyst, comprised of a multi metal promoted precipitated iron oxide on cobalt aluminate 1.6mm spheres (which were then crushed to an average particle size of <350µm), was also externally prepared by CATAL International Ltd using a procedure that entailed successive impregnations (precipitation), as outlined below [160]. The final composition by weight of the catalyst was 60% iron oxide phase and 40% alumina support. The composition by wt.% of the iron oxide phase was 91.9 Fe₂O₃/2.6 La/3.2 Re/1.5 Ru/0.8 Cr.

1. The 1.6 mm promoted alumina base/support was calcined at 620°C in air.
2. Impregnation 1 – Iron nitrate solution containing urea was impregnated onto the alumina spheres and calcined at 350°C.
3. Impregnation 2 - Iron nitrate solution containing urea was again impregnated onto the alumina spheres and calcined at 350°C.
4. Impregnation 3 – Iron nitrate solution containing urea was impregnated for a third time onto the alumina spheres and calcined at 350°C.
5. Impregnation 4 – Iron nitrate solution containing urea and 25% total ruthenium (iron nitrate/urea/+25% total Ru) was then impregnated onto the alumina spheres and calcined at 350°C.
6. Impregnation 5 - Iron nitrate solution containing urea, 25% total ruthenium and 20% total Re (iron nitrate/urea/25% total Ru/20 % total Re solution) was then impregnated onto the alumina spheres and calcined at 350°C.
7. Impregnation 6 – Iron nitrate solution containing urea, 50% total ruthenium and 80% total Re (iron nitrate/urea/50% total Ru/80% total Re solution) was then impregnated onto the alumina spheres and calcined at 400°C.

APPENDIX D – GC-MS: Liquid Hydrocarbon Product Analysis Method Development

Initially, two standard saturated alkane solutions were acquired from Sigma Aldrich; 1) a mixture of C₈-C₂₀ in hexane, and 2) a mixture of C₂₁-C₄₀ in toluene. During preliminary investigations, two separate methods were developed for analysing the two sets of hydrocarbon standards, outlined in Tables D1 and D2, below.

Table D1 – GC-MS method for analysis of standard C₈-C₂₀ saturated alkane in hexane solution

Step	Temp. (°C)	Heat Rate (°C/min)	Hold (min)	Total Time (min)
1	45	0.0	2.00	2.0
2	260	5.0	7.50	52.5

Table D2 – GC-MS method for analysis of standard C₂₁-C₄₀ saturated alkane in toluene solution

Step	Temp. (°C)	Heat Rate (°C/min)	Hold (min)	Total Time (min)
1	50	0.0	2.0	2.0
2	180	2.0	5.0	72.0
3	330	3.0	5.0	127.0

Both of these standard solutions were injected in the GC/MS using the above methods and resulted in chromatograms that had high peak resolutions. However, the results could not be directly compared with the liquid hydrocarbon samples collected from the FT synthesis experiments, as these samples contained hydrocarbons that ranged from C₆-C₄₀. Two separate chromatogram standards, therefore, would require a split analysis of the FT hydrocarbon samples. A method encompassing the wider hydrocarbon range (C₆-C₄₀) was therefore developed, which combined the GC-MS temperature programs of the C₈-C₂₀ and C₂₁-C₄₀ method. A standard C₇-C₄₀ saturated alkane solution in hexane was acquired from Sigma Aldrich, and the suitable GC-MS method that was developed is given in Table D3 below.

Table D3 – GC-MS analysis method for C₇-C₄₀ saturated alkane in hexane solution (standard)

Step	Temp. (°C)	Heat Rate (°C/min)	Hold (min)	Total Time (min)
1	40	0.0	5.0	5.0
2	180	2.0	5.0	80.0
3	260	2.0	5.0	125.0
4	330	2.0	10.0	170.0

The slow heating rate was maintained because it was observed that while the heating programme gave a relatively clean chromatogram for the hydrocarbon standards, the same was not observed with the FT liquid hydrocarbon samples. In the case of the samples, it was observed that around the main saturated alkane hydrocarbon peak, other peaks (representing isomers of the compound as well as other compounds such as alkenes and alcohols) with lower intensities were also eluting. A higher heating rate would have resulted in a loss of resolution and co-elution of peaks.

In order to ascertain that all the hydrocarbons in the standard solution had eluted and that the saturated hydrocarbon peaks were assigned correctly, a few tests were performed. A sample of pure dodecane (C₁₂) was dissolved in hexane (3 wt.% solution) and injected into the GC-MS and the retention time matched with the dodecane in the standard. The NIST library was also used for identifying the hydrocarbon peaks. The retention time of the solvent peak (hexane) also matched the retention time of the standard solution. This allowed the method to be further modified by putting in a solvent delay of four minutes.

APPENDIX E – Calculations

E1 – Capital Cost Estimation

- For plant capacities above 4500 t/y, temperature and pressure above ambient, petrochemical-type processes:

$$C (\text{£}_{2000}) = 7470 * N * Q^{0.6} * 10^X \quad (\text{Zevnik and Buchanan [94, 96]})$$

$$\text{Where: } X = (0.1 * \log_{10}P_{\max}) + [1.80 * 10^{-4} (T_{\max} - 300)] + F_m$$

C = fixed capital cost (£, mid-2000)

Q = plant capacity (tons per year product)

N = number of process steps

P_{max} = maximum process pressure (atm)

T_{max} = maximum process temperature (K)

F_m = materials of construction factor (= 0.2 for stainless steel)

- For plant capacities below 4500 t/y, the equation becomes:

$$C (\text{£}_{2000}) = 17280 * N * Q^{0.5} * 10^X \quad (\text{Zevnik and Buchanan [94, 96]})$$

Table E1.1 – Capital cost estimation for operation at pressures of 5 and 25 bar [94, 96]

Plant	1	2	3	4	5	6
Q (t/y)	10000	10000	10000	2000	2000	2000
N	15	15	14	10	10	9
P _{max} (atm)	25	5	5	25	5	5
T _{max} (K)	503	503	503	503	503	503
F _m	0.2	0.2	0.2	0.2	0.2	0.2
Log ₁₀ (Pmax)	1.398	0.699	0.699	1.398	0.699	0.699
X	0.376	0.306	0.306	0.376	0.306	0.306
C (£ ₂₀₀₀)	66,949,272	56,996,588	53,196,816	18,381,999	15,649,330	14,084,397
Cost Reduction (%)	-	14.87	20.54	-	14.87	23.40

E2 – Pressure Drop Calculations

Table E2.1 – 20cm³ Reactor Dimensions

I.D.	0.765 cm
O.D.	1.406 cm
Height (L)	43.5 cm
A _x (cross-sectional area)	0.4596 cm ²
Volume ($\pi D^2 L/4$)	20 cm ³

Table E2.2 – Densities of Catalysts and Packing Materials

Material	Bulk Density (ρ_B) (g/cm ³)	Voidage (ϵ_B) [*]	Particle Density (ρ_P) (g/cm ³)
Co/TiO ₂ catalyst	0.6711	0.4	1.1185
Co/Al ₂ O ₃ catalyst	0.2779	0.4	0.4632
Fe/Al ₂ O ₃ catalyst	1.2488	0.4	0.7493
Borosilicate glass beads (1mm)	1.2205	-	-

^{*} where $\epsilon_B = 1 - \rho_B/\rho_P$

(ϵ_B is assumed to be 0.4 for spherical particles)

- Pressure Drop, $(-\Delta P) = (f u^2 \rho_f L) / d_p$

Where: d_p is the particle diameter

ρ_f is the fluid density

L is the catalyst bed height,

u is the superficial velocity = volumetric flow rate / column cross-sectional area

f is the friction factor defined by the Ergun correlation:

$$f = [1.75 + 150(1 - \epsilon_B) / Re] (1 - \epsilon_B) / \epsilon_B^3$$

and Reynold's Number, $Re = (d_p u \rho_f) / \mu_f$

where μ_f is the fluid/syngas viscosity

Table E2.3 – Typical Syngas Properties [171]

Syngas viscosity, μ_f	$1.8 \times 10^{-5} \text{ kgm}^{-1}\text{s}^{-1}$
Syngas density, ρ_f	1.20 kg/m^3

E2.1 – Pressure Drop across Co/Al₂O₃ Catalyst Bed (using 0.5g)

$$d_p = 50\mu\text{m or } 5 \times 10^{-5}\text{m (assuming spherical particle)}$$

$$\rho_f = 1.20 \text{ kg/m}^3$$

$$L = 3.91 \text{ cm or } 0.0391 \text{ m}$$

$$u = (2.353 \times 10^{-3} \text{ m}^3/\text{s}) / (4.596 \times 10^{-3} \text{ m}^2) = 0.512 \text{ m/s}$$

$$\mu_f = 1.8 \times 10^{-5} \text{ kgm}^{-1}\text{s}^{-1}$$

$$\text{Re} = (5 \times 10^{-5}\text{m})(0.512 \text{ m/s}) (1.20 \text{ kg/m}^3) / (1.8 \times 10^{-5} \text{ kgm}^{-1}\text{s}^{-1}) = \mathbf{1.71}$$

$$f = [1.75 + 150(1 - 0.4) / 1.71] (1 - 0.4) / 0.4^3 = \mathbf{509.83}$$

$$(-\Delta P) = (509.83) (0.512^2) (1.20) (0.0391) / (5 \times 10^{-5})$$

$$= 125416.11 \text{ Pa or } \mathbf{1.25 \text{ bar}}$$

E2.2 – Pressure Drop across Co/Al₂O₃ Catalyst Bed (using 2.0g)

$$d_p = 50\mu\text{m or } 5 \times 10^{-5}\text{m (assuming spherical particle)}$$

$$\rho_f = 1.20 \text{ kg/m}^3$$

$$L = 15.65 \text{ cm or } 0.1565 \text{ m}$$

$$u = (2.353 \times 10^{-3} \text{ m}^3/\text{s}) / (4.596 \times 10^{-3} \text{ m}^2) = 0.512 \text{ m/s}$$

$$\mu_f = 1.8 \times 10^{-5} \text{ kgm}^{-1}\text{s}^{-1}$$

$$\text{Re} = (5 \times 10^{-5}\text{m})(0.512 \text{ m/s}) (1.20 \text{ kg/m}^3) / (1.8 \times 10^{-5} \text{ kgm}^{-1}\text{s}^{-1}) = \mathbf{1.71}$$

$$f = [1.75 + 150(1 - 0.4) / 1.71] (1 - 0.4) / 0.4^3 = \mathbf{509.83}$$

$$(-\Delta P) = (509.83) (0.512^2) (1.20) (0.1565) / (5 \times 10^{-5})$$

$$= 501985.18 \text{ Pa or } \mathbf{5.02 \text{ bar}}$$

E3 –Energy Balance Calculations

Energy balance calculations, for experiment FT16 (Table 5.1 in section 5.1.6) at the following conditions: (230°C, 10 bar, H₂/CO = 2.0, WHSV = 8.8 h⁻¹, m_{cat} = 2.0 g), were carried out as follows:

$$\text{Energy IN (Q}_{\text{IN}}) = \text{Energy OUT (Q}_{\text{OUT}})$$

$$(\text{Calorific Value}_{\text{reactants}} + \text{Heat Capacity}_{\text{reactants}}) = (\text{Calorific Value}_{\text{products}} + \text{Heat Capacity}_{\text{products}})$$

Energy IN

$$Q_{\text{IN}} = Q_{\text{CO, in}} + Q_{\text{H}_2, \text{ in}} + Q_{\text{N}_2, \text{ in}}$$

$$Q_{\text{IN}} = [(\dot{m}_{\text{CO in}} * CV_{\text{CO}}) + (\dot{m}_{\text{CO in}} * C_{\text{P CO}} * \Delta T)] + [(\dot{m}_{\text{H}_2 \text{ in}} * CV_{\text{H}_2}) + (\dot{m}_{\text{H}_2 \text{ in}} * C_{\text{P H}_2} * \Delta T)] \\ + (\dot{m}_{\text{N}_2 \text{ in}} * C_{\text{P N}_2} * \Delta T)$$

Energy OUT

$$Q_{\text{OUT}} = Q_{\text{CO, out}} + Q_{\text{H}_2, \text{ out}} + Q_{\text{N}_2, \text{ out}} + Q_{\text{CO}_2} + Q_{\text{CH}_4} + Q_{\text{C}_2\text{-C}_5} + Q_{\text{OIL}} + Q_{\text{H}_2\text{O}}$$

$$Q_{\text{OUT}} = [(\dot{m}_{\text{CO out}} * CV_{\text{CO}}) + (\dot{m}_{\text{CO out}} * C_{\text{P CO}} * \Delta T)] \\ + [(\dot{m}_{\text{H}_2 \text{ out}} * CV_{\text{H}_2}) + (\dot{m}_{\text{H}_2 \text{ out}} * C_{\text{P H}_2} * \Delta T)] \\ + [(\dot{m}_{\text{C}_2\text{-C}_5} * CV_{\text{C}_2\text{-C}_5}) + (\dot{m}_{\text{C}_2\text{-C}_5 \text{ out}} * C_{\text{P C}_2\text{-C}_5} * \Delta T)] \\ + [(\dot{m}_{\text{OIL}} * CV_{\text{OIL}}) + (\dot{m}_{\text{OIL}} * C_{\text{P OIL}} * \Delta T)] \\ + [(\dot{m}_{\text{N}_2 \text{ out}} * C_{\text{P N}_2 \text{ out}} * \Delta T) + (\dot{m}_{\text{H}_2\text{O}} * C_{\text{P H}_2\text{O}} * \Delta T) + (\dot{m}_{\text{CO}_2} * C_{\text{P CO}_2} * \Delta T)]$$

E3.1 – Assumptions

The assumptions made in order to carry out the above calculations were the following:

1. Steady-state operation over 48.38 hour duration of experiment run
2. No reactant or product losses
3. T_{ambient} = 25°C, T_{IN} = 200°C, T_{OUT} = 230°C
4. ΔT_{IN} = 200 – 25 = 175; ΔT_{OUT} = 230 – 25 = 205
5. Calorific value (CV) of reactants and products calculated at the average temperature of 215°C

APPENDIX F – GC/MS Chromatograms of Standard Saturated C₇-C₄₀ Alkane Solution versus FT Liquid Hydrocarbons

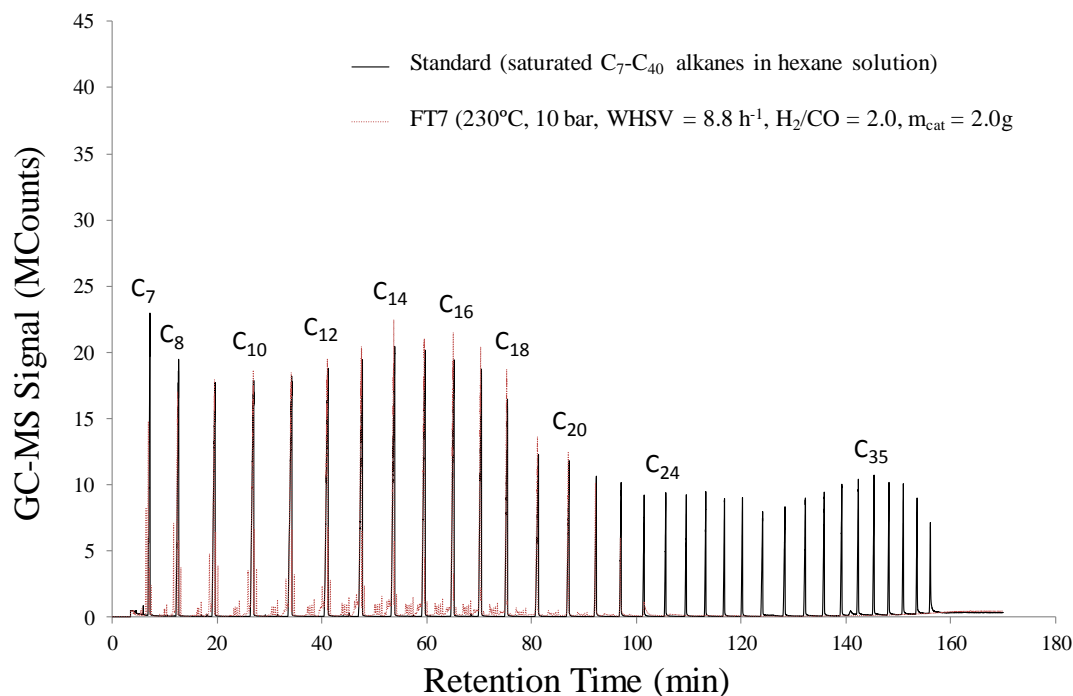


Figure F1 – GC-MS chromatogram: comparison of standard versus liquid hydrocarbon product from FT synthesis test FT7

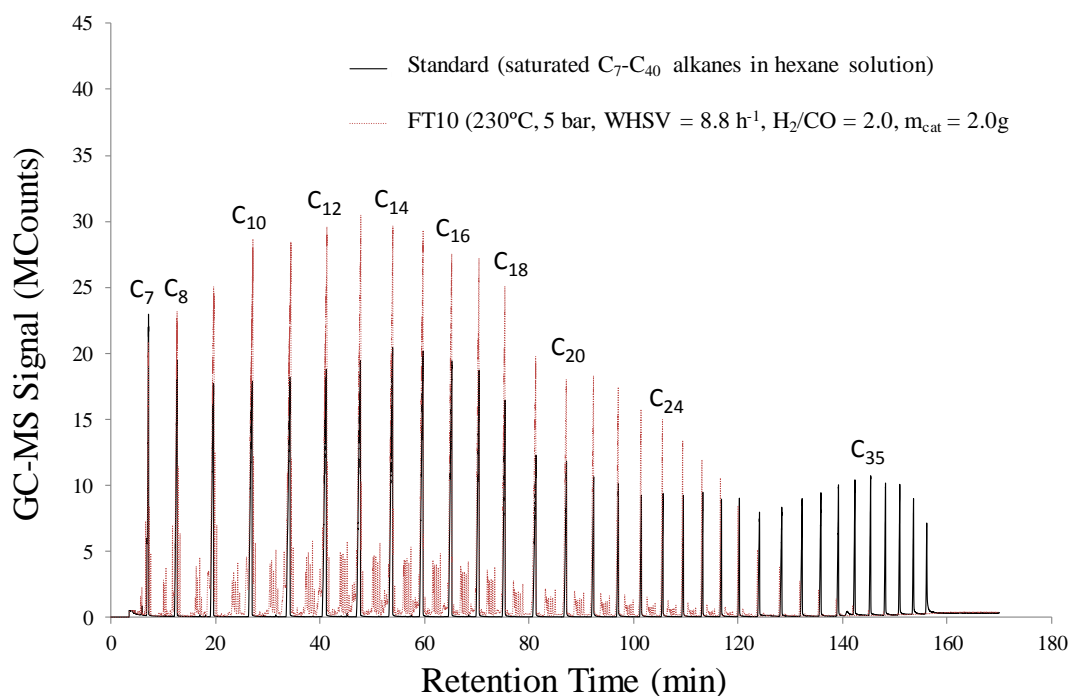


Figure F2 – GC-MS chromatogram: comparison of standard versus liquid hydrocarbon product from FT synthesis test FT10

APPENDIX H – FT Synthesis Experiments Lab Record Sheet

Date: _____ Test Number: _____

Catalyst: _____ Catalyst Mass: _____

Activation Conditions:

DRYING: _____

Drying Start Time: _____ Drying End Time: _____

REDUCTION:

Reduction Start Time: _____ Reduction End Time: _____

PRE-REACTION: _____

Time of first GC injections (to begin tracking CO conversion): _____

Injection frequency: _____

Feed Gas Composition Analysis (Reactor Bypass Mode)

Time	Feed Injection 1		Time	Feed Injection 2		Time	Feed Injection 3	
	N ₂			N ₂			N ₂	
	CO			CO			CO	
CO Composition			H₂ Composition			N₂ Composition		

REACTION: _____

Start Time: _____ End Time: _____

Instrument	Flowrates (ml/min)				H ₂ /CO
	H ₂	CO	N ₂	Total	
<i>MFC Set Point (SCCM)</i>				-	-
<i>MFC Actual (SCCM)</i>				-	-
<i>External Flow Meter</i>					

System Set Points						
Reactor Pressure	Reactor Temp°	Reactor Temp° ramp	Oven Temp°	GLS-1 Temp°	GLS-2 Temp°	GC Transfer Line Temp°

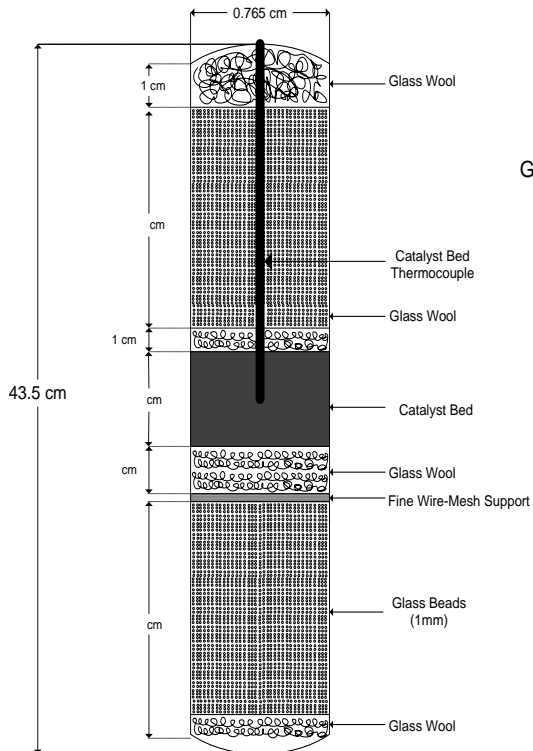
FT Synthesis Experiments Lab Record Sheet (continued)

Observations: _____

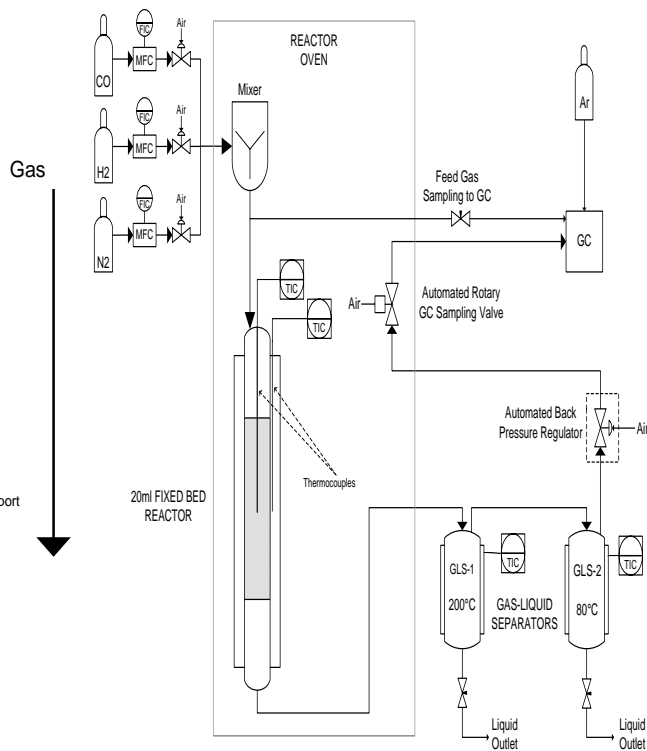
LIQUIDS/WAX COLLECTED

SAMPLE ORIGIN	Temperature (°C)	VIAL LABEL	VIAL MASS	
			EMPTY	AFTER REACTION
a				
GLS-1 (PV-P11)				
GLS-2 (PV-P21)				
b				
GLS-1 (PV-P11)				
GLS-2 (PV-P21)				

REACTOR PACKING METHOD



REACTOR SET-UP SCHEMATIC



APPENDIX I – Publications

- I.** *P. Doss, and A. V. Bridgwater, “Synthesis of Hydrocarbons via the Fischer-Tropsch Process”. In “Proceedings of the Bioten Conference on Biomass Bioenergy, and Biofuels 2010”.Ed. A. V. Bridgwater, (2011), CPL Press.*